

CRANFIELD UNIVERSITY

JACINTO CARRASCO-MUÑOZ Y GUERRA

DESIGN EXPLORATION METHODOLOGY FOR ULTRA THICK
LAMINATED COMPOSITES

SCHOOL OF ENGINEERING
Department of Applied Mechanics and Astronautics

PhD Thesis
Academic Year: 2007-2012

Supervisors: Prof Rade Vignjevic and Dr Kevin Hughes
January 2012

CRANFIELD UNIVERSITY

SCHOOL OF ENGINEERING
Department of Applied Mechanics and Astronautics

PhD Thesis

Academic Year 2007-2012

JACINTO CARRASCO-MUÑOZ Y GUERRA

DESIGN EXPLORATION METHODOLOGY FOR ULTRA THICK
LAMINATED COMPOSITES

Supervisors: Prof Rade Vignjevic and Dr Kevin Hughes
January 2012

© Cranfield University 2012. All rights reserved. No part of this
publication may be reproduced without the written permission of the
copyright owner.

Abstract

Existing test and analytical methods (theoretical and numerical) are normally restricted to thin laminate components, which cannot accurately represent the 3D stress state behaviour of the so called Ultra Thick Laminates (UTL) structures. Thus, it is necessary to expand the scope of application of the current numerical methods to accurately predict the out-of-plane delamination failure associated with these types of structures (mainly due to the transverse shear stresses and interlaminar stresses).

The overall objective of this work is to address the following research objectives:

- To assess the functionality, advantages and limitations of different solid element formulations, including layered solid elements that are available in commercial Finite Element codes, applied to the mechanical response prediction of UTL composite components (thicknesses up to 30 mm are considered).
- To perform a design exploration and optimisation of constant thickness UTL composite component in terms of the orientation of a varying and repeatable stacking sequence of an eight ply Non-Crimped Fabric, in order to assess the design implications on performance.

In order to achieve the above stated objectives a standard, flexible and expandable FE based design exploration methodology (at a ply level) for UTL composite components is proposed, which considers a commercial FE tool (ANSYS), and a data management system and optimisation tool (ISIGHT), through the use of layered solid elements (SOLID186 and SOLID191, 20-node layered solid elements). Application of manufacturing design rules (for reducing the number of feasible stacking sequences to be evaluated) is also considered, in order to reduce the computational cost of such a study, as well as to present a practical solution from the manufacturing point of view.

Initially, in-plane and out-of-plane capabilities of various layered element formulations and modelling strategies were evaluated for thin and thick laminate applications against known analytic solutions (CLT, etc), in order to understand the key parameters and the accuracy limitations of each formulation. This led to practical recommendations for pre and post processing of thick laminate FE models, such as for the number of layered solid elements required as a function of the thickness of the UTL component to effectively predict the magnitude and variation in transverse shear stress across the thickness.

The application of this research was demonstrated on the design exploration and performance optimisation of a UTL composite specimen (with constant thickness) under a 3-point bending test (linear static analysis), for which experimental results were available. The individual ply orientations are the design variables considered, and the performance was assessed through the vertical displacement of the component and the maximum transverse shear stress value.

This exploration of the design space did identify other possible configurations that may have a better performance than the baseline (Biax), considering only the maximum transverse shear stress values as directly responsible for the delamination failure. However, these improved designs may present a higher number of plies failed or a higher failure index (Tsai-Wu failure criteria). Further experimental studies are required to further explore the design space, but this work represents the starting point and possible approaches for development of robustness and weight optimisation of UTL composites are proposed.

Acknowledgements

I would really like to thank Prof. Rade Vignjevic, who offered me the unique opportunity of this PhD, which has revealed as one of the most important experiences of my life, and who always believed in me. Also, to Dr Kevin Hughes, for providing me technical and personal support, especially in the difficult times, and for guiding me in order to develop my critical thinking and a more autonomous, systematic and creative way of working.

To Prof. J.P. Fielding, my former supervisor, for sharing his knowledge and for his kindness.

To the ALCAS project, Airbus UK and Messier Dowty and the Worshipful Company of Coachmakers and Coach Harness Makers that sponsored this PhD financially. I would like to express my gratitude to Sir Tim Laurence, Mr Marcus Wills, Prof. Colin Kirk and Prof. Ian Poll.

Also, I would like to express my acknowledgments to Dr. Enrique Herencia, and to my colleagues at INGENIBER S.A., Dr. Miguel Ángel Moreno, Mr Emilio Baños and Mr Jorge Vázquez, as their technical advice and support were really important.

To all staff members of the Crashworthiness, Impact, and Structural Mechanics Group of the School of Engineering at Cranfield University, with a special mention to Mr Jason Brown, for being so passionate about his work and for assisting me almost at any time, and to Mrs Marion Bastable, who was a wonderful departmental administrator.

I also would like to have a word of gratitude to all my colleagues in the office, especially to Mao Chedid and Alexis Kalogerakos.

To Dr. Tayeb Zeguer, my line manager at Jaguar Land Rover, not only for giving the opportunity of having my dreamt job, but also for his passion, support and encouragement to get the best out of me.

To all the staff members at Cranfield University that offered me generous help and advice when most needed, with special mention to the staff members of the Registry, the Library and the IT Department.

To my dear friend Dr Ramón Fernando Colmenares Quintero for the invaluable experiences lived together. To Wilson Vesga for his encouragement and patience, to Dr. Leticia Chico Santamarta, Dr. Diogenes Antille, Solange Baena, Jorge Almazan and Dr Mattia Padulo for their values and the great time we spent together. To my dear friend Fco. Javier Aparicio and his family.

To my family, without whom all this would have been impossible, with all my love for them.

To all the people I have learnt from, and the list does not stop growing.

To the memory of my beloved Mother, wherever she may be and to my dear Father.

Table of Contents

Abstract	i
Acknowledgements.....	iii
List of Figures	ix
List of Tables	xvii
Nomenclature	xix
1 Introduction.....	1
1.1 Composite Materials	1
1.2 The need for this research	2
1.2.1 The ALCAS Project	2
1.2.1.1 Cranfield University contribution	2
1.2.1.2 Current approach.....	4
1.2.2 Nature of the Problem	6
1.3 Project objectives and scope.....	7
1.4 Contribution to knowledge.....	8
1.5 Organization of the thesis.....	9
2 Literature Review	11
2.1 Introduction	11
2.2 Three-axes of complexity	11
2.3 FE modelling of thick laminated composite components	15
2.4 Design optimisation of laminated composites.....	17
2.4.1 Design optimisation	17
2.4.2 Optimisation of laminated composites	18
2.5 Multi-level optimisation analysis	20
2.5.1 Manufacturing constraints	22
2.5.2 Summary.....	25
3 Analysis of Laminated Composite Structures	27
3.1 Introduction	27
3.2 Classic Lamination Theory (CLT)	27
3.3 Stiffness and Strength of laminated composites.....	27
3.3.1 Micromechanics – Stiffness analysis	28
3.3.2 Macromechanics of a lamina – Stiffness analysis.....	29
3.3.2.1 Specially orthotropic ply.....	29
3.3.2.2 Generally orthotropic ply.....	31
3.3.2.3 Invariant forms of stiffness and compliance matrix.....	32
3.3.3 Strength analysis of an orthotropic lamina.....	33
3.3.3.1 Maximum-stress theory	33
3.3.3.2 Maximum-strain theory	34
3.3.3.3 Tsai-Hill theory	34
3.3.3.4 Tsai-Wu stress theory.....	35
3.3.4 Macromechanics of a Laminate.....	37
3.3.4.1 Constitutive equation	37
3.3.5 Strength analysis of a laminate.....	43
3.3.5.1 Procedure for laminate strength analysis.....	43

3.4	Limitations to CLT	44
3.4.1	Interlaminar shear stresses and free edge effects	44
3.5	Deformations due to transverse shear.....	46
3.5.1	First-Order shear deformation theory.....	46
3.5.2	Higher-order shear deformation theory.....	48
3.5.3	Layerwise theory	48
3.5.4	Laminate constitutive equations including TSD	50
3.6	Summary.....	51
4	FE Analysis of Laminated Composite Structures	53
4.1	Sublaminates	54
4.2	Modelling composites.....	56
4.2.1	FE tools benchmark	56
4.2.2	Main areas of interest.....	56
4.3	Available element formulation	57
4.3.1	Layered shell elements	58
4.3.2	Layered solid elements	59
4.4	Layered configuration definition.....	60
4.4.1	Constitutive matrices definition.....	60
4.4.2	Individual layer properties.....	61
4.4.3	Ply drop-off laminates and node offset	63
4.4.4	Modelling solid elements	65
4.5	Element coordinate system	66
4.6	Failure criteria specification.....	67
4.6.1	Failure criteria analysis via FC Commands.....	70
4.6.2	Failure criteria analysis via TB command	71
4.6.3	User-written failure criteria.....	74
4.7	Composite modelling and postprocessing best practice	74
4.7.1	Coupling effects	74
4.7.2	Interlaminar shear stresses	74
4.7.3	Input data verification	75
4.7.4	Specifying results file data.....	76
4.7.5	Selecting elements with a specific layer number	76
4.7.6	Specifying a layer for results post-processing.....	76
4.7.7	Transforming results to another coordinate system	77
4.8	Summary.....	77
5	Verification – Element Formulation vs CLT	79
5.1	Settings and assumptions	79
5.2	CLT	82
5.3	FE Analysis	83
5.3.1	Geometry	84
5.3.2	Mesh	85
5.3.3	Constraints.....	88
5.3.4	Loads	93
5.3.5	Postprocessing.....	100
5.4	Results.....	103
5.5	Conclusions	115

6	Verification – Ultra Thick Laminate	117
6.1	Accuracy vs CPU time	117
6.1.1	Analytic solution	118
6.1.2	FE Analysis	121
6.1.2.1	Model Description	121
6.1.2.2	Geometry	123
6.1.2.3	Mesh	124
6.1.2.4	Element coordinate system	124
6.1.2.5	Boundary conditions	125
6.1.3	Results	126
6.1.4	Conclusions	131
6.2	3-Points bending test	132
6.2.1	Settings and assumptions	133
6.2.2	Analytic solution	135
6.2.3	FE Analysis	137
6.2.4	Results	139
6.2.5	Conclusions	142
7	UTL Composites: Design Exploration	143
7.1	FE-Based optimisation methodology	143
7.1.1	Introduction	143
7.1.2	Composite design optimisation	143
7.1.3	Smeared properties vs individual ply definition approach	144
7.1.3.1	Layered configuration definition	144
7.1.4	FE-Based optimisation methodology	146
7.1.5	Framework requirements and simulation tools	147
7.1.6	Main Modules	148
7.1.6.1	Setup Study	148
7.1.6.2	Design of Experiments	149
7.1.6.3	Approximation Method: Response Surface Method	150
7.1.6.4	Optimisation	151
7.1.7	Scope of application	153
7.1.8	Stacking sequence design exploration	154
7.1.8.1	Stacking sequence: Methodology	154
7.1.9	Conclusions	157
7.2	Stacking sequence: Case study	158
7.2.1	Settings and assumptions	158
7.2.2	Results	160
7.2.3	Conclusions	163
8	Conclusions and Future Work	165
8.1	Conclusions	165
8.1.1	Plate deformations due to transverse shear	165
8.1.2	FEA of UTL composite components	166
8.1.3	Case studies for thin and thick composite components	167
8.1.4	Design exploration methodology	170
8.1.5	Design exploration methodology: case study	170
8.2	Recommendations for Future Work	172

8.2.1 Layered solid element orientation analysis	172
8.2.2 3D analytical results	173
8.2.3 Geometric design variables	173
8.2.4 Experimental test validation.....	173
8.2.5 Ply drop off	173
8.2.6 User defined failure criteria.....	174
8.2.7 Edge effects: Stress concentration due to bolts.....	174
8.2.8 Weight Optimisation methodology of UTL composites.....	175
8.2.8.1 Approach 1: Constant number of plies per sub-assembly	175
8.2.8.2 Approach 2: Constant number of subassemblies through the thickness	178
REFERENCES	179
BIBLIOGRAPHY	183
Appendix A Laminate strength analysis	187
Appendix B ANSYS parametric input file.....	190
Appendix C Mesh Refinement	201
Appendix D ANSYS parametric input file	210
Appendix E Pressure due to Bending Moment.....	217
Appendix F 3 Point bending test	221
Appendix G First ply failure.....	235
Appendix H Design Rules	249
Appendix I Element Orientation	260
Appendix J ANSYS Layered element formulation	275

List of Figures

Figure 1-1 Composite introduction on Airbus aircrafts. Source: Assler, 2006.	1
Figure 1-2 Typical DOC's for a long range airliner. Source: Watson, 2007.....	2
Figure 1-3 Critical components of the ALCAS lateral wing box assembly, with MLG SSF detailed CAD model. Source: Mahmood, 2007.....	3
Figure 1-4 Final lug thickness of the manufacture MLG SSF (EADS). Source: Siemetzki et al., 2007.	4
Figure 1-5 3D stress state.....	4
Figure 1-6 Delamination failures in a T-section test model due to normal through thickness stresses σ_{33} . $F_{pull,max}=110kN$ (left), $F_{axial,max}=42kN$ (right). Source: Siemetzki et al., 2007.....	5
Figure 1-7 MLG SSF reinforced with CFRP ribs. CAD design. Source: Siemetzki et al., 2007.....	5
Figure 1-8 CAD model of the MLG SSF considering manufacturing constraints (l). Manufactured central laminate (r). Source: Siemetzki et al., 2007.....	7
Figure 2-1 Evolution of structural model complexity. Source: Venkataraman and Haftka, 2002.....	12
Figure 2-2 Evolution of analysis complexity. Source: Venkataraman and Haftka, 2002.	12
Figure 2-3 Evolution of optimisation complexity. Source: Venkataraman and Haftka, 2002.....	13
Figure 2-4 Three-axes of complexity. Source: Venkataraman and Haftka, 2002.	14
Figure 2-5 Transverse shear stress distribution across a short beam under bending. Solid element (l), layered solid element (r). Source: Czichon et al., 2011.	16
Figure 2-6 Laminate definition in a torque link assembly. Source: Thuis, 1999.	16
Figure 2-7 Schematic representation of a bioengineering application. Source: Chen et al., 2000.	17
Figure 2-8 2-Level optimisation analysis of an anisotropic composite panel. Source: Herencia et al., 2008.	20
Figure 2-9 FE-based optimisation framework. Source: Chen et al., 2000.....	22
Figure 2-10 Composite wing rib designable patches. Source: Toporov et al., 2005. ...	23
Figure 2-11 Ply blocking. Source: Toporov et al, 2005.....	24
Figure 2-12 Ply percentage for each orientation. Source:Toporov et al., 2005.	24
Figure 2-13 Thickness ratio of 2:1 between patches. Source: Toporov et al., 2005.....	24
Figure 2-14 Continuity between plies. Source: Toporov et al., 2005.....	25

Figure 3-1 Material axes of a single unidirectional ply. Source: Baker et al., 2004.	29
Figure 3-2 Global or laminate axes for a single ply. Source: Baker et al., 2004.....	29
Figure 3-3 Tsai-Wu failure curves obtained for three different interaction terms F_{12} . For $F_{12}=0.0$ (blue), for $F_{12}=0.5$ (green), for $F_{12}=-0.5$ (brown). Source: Abbey, 2010. ...	36
Figure 3-4 In-plane forces and moments acting on a laminate reference plane. Source: Barbero, 1999.	37
Figure 3-5 Distance from each layer top and bottom planes to the laminate reference plane. Source: Barbero, 1999.....	37
Figure 3-6 Coupling terms within a lamina considered in the constitutive stiffness matrix ABD. Source: Kollár, 2003.	41
Figure 3-7 Design guidelines affecting the coupling phenomena in laminated composite plates. Source: Marsden and Irving, 2002.	42
Figure 3-8 Stress distribution across the laminate thickness of a balanced symmetric laminate. Source: Abbey, 2010.	45
Figure 3-9 Free edge delamination mechanism. Source: Agarwal et al., 2006.	45
Figure 3-10 Plate geometry deformation in the x-z plane. Source: Barbero, 1999.....	47
Figure 3-11 Assumed in-plane displacement field $u\alpha$ through the laminate thickness for a layerwise theory. Source: Zhang et al., 2010.....	49
Figure 4-1 Modelling approaches at a (a) Micromechanics, (b) Meso-scale and (c) Macro-scale. Source: Barbero, 2008.....	53
Figure 4-2 Thick laminated component (top), represented by layered shell elements (left), or solid elements (right). Source: Kollár, 2003.....	54
Figure 4-3 Thick laminated component (left), sublaminates (middle), and the FE mesh (right). Source: Kollár, 2003.	54
Figure 4-4 Illustration of a sublaminate. Source: Kollár, 2003.	55
Figure 4-5 Layered Model Showing Dropped Layer. Source: ANSYS help manual.....	63
Figure 4-6 Layered shell with nodes at midplane. Source: ANSYS help manual.....	64
Figure 4-7 Layered shell with nodes at bottom surface. Source: ANSYS help manual.....	64
Figure 4-8 Typical thick laminate ply drop off.	65
Figure 4-9 Plate modelled with different volumes stacked together (l), and their finite elements mesh using one layer of layered solid elements per volumen (r).....	66
Figure 4-10 Element coordinate system default orientation in shell elements: (a) ANSYS, (b) MSC-MARC. Source: Barbero, 2008.....	66
Figure 4-11 Reorientation of the element coordinate system for a curve plate.....	67
Figure 4-12 T-axial FE model (l) and peeling failure at $F_{axial}=42kN$ on tension side (r). Source: Siemetzki et al., 2007.....	75

Figure 5-1 Thin plate under in-plane forces (N_x , N_y , N_{xy}).	80
Figure 5-2 Thin plate under bending moments (M_x , M_y).	80
Figure 5-3 Schematic representation of different element types available for modelling laminates.	83
Figure 5-4 Plate geometry and 2D dimensions.	84
Figure 5-5 Plate geometry modelled as volumes: (a), two volumes (b), three volumes (c), and a volume per layer (d).	85
Figure 5-6 Mesh size (2D).	85
Figure 5-7 Different layered solid element used, colour coded by Real Constant (for the laminate definition). With one element through the thickness (a), with two elements (b), with three (c), and with one element per layer (d).	86
Figure 5-8 Stacking sequence $[45/0/0/0/0/45/90]_S$ (1 layered element through the thickness).	87
Figure 5-9 Nodes located at MID surface ($Z=0$). Layered shell elements.	88
Figure 5-10 Boundary conditions applied on a thin plate under in-plane axial load N_x modelled with layered shell elements.	89
Figure 5-11 Boundary conditions of the plate under N_x modelled with SOLID186, SOLID191 (with one element through the thickness).	90
Figure 5-12 Boundary conditions of the plate under N_x modelled with SOLID191 (with one element per ply).	90
Figure 5-13 Boundary conditions applied on a thin plate under in-plane shear load N_{xy} modelled with layered shell elements.	91
Figure 5-14 Boundary conditions of the plate under N_{xy} modelled with SOLID191 (with two elements through the thickness).	91
Figure 5-15 Boundary conditions of the plate under N_{xy} modelled with SOLID191 (with three elements through the thickness).	92
Figure 5-16 Boundary conditions applied on a thin plate under out-of-plane moment M_x modelled with layered shell elements.	92
Figure 5-17 Constraints on the plate under M_x modelled with SOLID191 (with one element through the thickness).	93
Figure 5-18 Boundary conditions applied on a thin plate under in-plane axial load N_x modelled with layered shell elements.	93
Figure 5-19 Example of consistent nodal loading for 4-node and 8-node elements.	95
Figure 5-20 Boundary conditions applied on a thin plate under in-plane shear load N_{xy} , modelled with SHELL181 (4-node shell element).	96
Figure 5-21 Boundary conditions applied on a thin plate under in-plane shear load N_{xy} , modelled with SHELL99, or SHELL281 (8-node shell elements).	97

Figure 5-22 Boundary conditions of the plate under N_{xy} modelled with SOLID191 (with one element per ply).	98
Figure 5-23 Boundary conditions applied on a thin plate under out-of-plane bending moment load M_x , modelled with SHELL181 (4-node shell element).....	98
Figure 5-24 Boundary conditions of the plate under M_x modelled with SOLID46, SOLID186 SOLID191, and SOLSH190 (with two elements through the thickness).	100
Figure 5-25 Boundary conditions of the plate under M_x modelled with SOLID191 (with one element per ply).	100
Figure 5-26 Results are requested in the centre node location. Thin plate under in-plane N_x axial load modelled with layered shell elements.....	101
Figure 5-27 Element results are requested in the top centre element (approximately). Thin plate under in-plane N_x axial. One solid element through the thickness or shell elements (left). Two solid elements through the thickness (centre). Three solid elements through the thickness or one solid element per ply (right).	103
Figure 5-28 ϵ_x per ply comparison. Thin plate under in-plane load $N_x=1000$ N/m.	104
Figure 5-29 ϵ_y per ply comparison. Thin plate under in-plane load $N_x=1000$ N/m.	104
Figure 5-30 ϵ_{xy} per ply comparison. Thin plate under in-plane load $N_x=1000$ N/m.	105
Figure 5-31 ϵ_1 per ply comparison. Thin plate under in-plane load $N_x=1000$ N/m.	105
Figure 5-32 ϵ_2 per ply comparison. Thin plate under in-plane load $N_x=1000$ N/m.	106
Figure 5-33 ϵ_{12} per ply comparison. Thin plate under in-plane load $N_x=1000$ N/m.....	106
Figure 5-34 σ_1 per ply comparison. Thin plate under in-plane load $N_x=1000$ N/m.....	107
Figure 5-35 σ_2 per ply comparison. Thin plate under in-plane load $N_x=1000$ N/m.....	107
Figure 5-36 τ_{12} per ply comparison. Thin plate under in-plane load $N_x=1000$ N/m.....	108
Figure 5-37 Maximum Stress Failure Index per ply comparison. Thin plate under in-plane load $N_x=1000$ N/m.	108
Figure 5-38 Tsai-Wu Failure Index per ply comparison. Thin plate under in-plane load $N_x=1000$ N/m.....	109
Figure 5-39 Maximum Stress Failure Index per ply comparison. Thin plate under in-plane load $N_y=1000$ N/m.	109
Figure 5-40 Tsai-Wu Failure Index per ply comparison. Thin plate under in-plane load $N_y=1000$ N/m.....	110
Figure 5-41 Maximum Stress Failure Index per ply comparison. Thin plate under in-plane shear load $N_{xy}=1000$ N/m.	110
Figure 5-42 Tsai-Wu Failure Index per ply comparison. Thin plate under in-plane shear load $N_{xy}=1000$ N/m.....	111
Figure 5-43 Maximum Stress Failure Index per ply comparison (except SOLID46). Thin plate under out-of-plane bending moment $M_x=1000$ Nm/m.....	111

Figure 5-44 Tsai-Wu Failure Index per ply comparison (except SOLID46). Thin plate under out-of-plane bending moment $M_x=1000$ Nm/m.	112
Figure 5-45 Maximum Stress Failure Index per ply comparison (except SOLID46). Thin plate under out-of-plane bending moment $M_y=1000$ Nm/m.....	112
Figure 5-46 Tsai-Wu Failure Index per ply comparison (except SOLID46). Thin plate under out-of-plane bending moment $M_y=1000$ Nm/m.	113
Figure 6-1 T-junction specimen under bending moment ($F_{axial,max}=42$ kN). Simulation model (l), and correlation test (r) showing delamination due to radial stress, σ_{33} . Source: Siemetzki et al., (2007).	117
Figure 6-2 Curved beam under bending moment. Source: Nguyen, 2010.....	118
Figure 6-3 Analytic radial (σ_{33}) and tangential (σ_{22}) stresses (Pa) across the thickness of a curved beam under applied out-of-plane bending moment $M=100$ Nm/m...	121
Figure 6-4 Iso view of the curved plate and the material axes directions. Source: Nguyen, 2010.....	122
Figure 6-5 Curved plate geometry model. Geometry is defined different for each model: 1 element through the thickness (l) to four elements through the thickness (r). .	123
Figure 6-6 Curved plate geometry model. Geometry is defined with 12 volumes to be meshed with one solid element per ply.....	124
Figure 6-7 Reorientation of the elements coordinate system, ESYS. Initial ESYS orientation (l), modified ESYS orientation (r).	124
Figure 6-8 BCs applied on the curved beam modelled with one solid element per layer. Bending moment applied as a linear varying pressure over the end section.....	125
Figure 6-9 Comparison of radial stress (σ_{33}) (Pa) across the curved plate thickness (m). One layered solid element through the thickness with 12 plies (at 0°). Curved plated (0.06 m thick) under $M=100$ Nm/m.	126
Figure 6-10 Comparison of radial stress (σ_{33}) (Pa) across the curved plate thickness (m). Three layered solid element through the thickness with 4layers per element (12 layers in total at 0°). Curved plated (0.06 m thick) under $M=100$ Nm/m.	127
Figure 6-11 Comparison of radial stress (σ_{33}) (Pa) across the curved plate thickness (m). Four layered solid element through the thickness with 3 layers per element (12 in total at 0°). Curved plated (0.06 m thick) under $M=100$ Nm/m.	127
Figure 6-12 Comparison of radial stress (σ_{33}) (Pa) across the curved plate thickness (m). One solid element per layer (12 layers in total at 0°). Curved plated (0.06 m thick) under $M=100$ Nm/m.....	128
Figure 6-13 Comparison of tangential stress (σ_{22}) (Pa) across the curved plate thickness (m). Results represent the behaviour of four different cases, 1 to 4 layered solid elements through the thickness (12 layers in total at 0°). Curved plated (0.06 m thick) under $M=100$ Nm/m.	128
Figure 6-14 Comparison of tangential stress (σ_{22}) (Pa) across the curved plate thickness (m). 1 solid element per layer(12 layers in total at 0°). Curved plated (0.06 m thick) under $M=100$ Nm/m.....	129

Figure 6-15 Level of through thickness integration accuracy based on the element shape. Source: ANSYS help manual.....	129
Figure 6-16 Number of nodes in the curved plate FEM. Different modelling strategies, with 1 to 4 layered solid elements through the thickness or 1 solid element per ply.	130
Figure 6-17 Processor characteristics	131
Figure 6-18 CPU time (seconds) required to run a single analysis of curved plate under bending. 5 different modelling strategies with 1 to 4 layered solid elements through the thickness or 1 solid element per ply.....	131
Figure 6-19 Crack propagations modes according to the fracture mechanics approach. Source: Swanson et al., 1997.....	132
Figure 6-20 Non-Crimped Fabric. Source: Baker et al., 2004.....	133
Figure 6-21 Simply supported beam dimensions. Source: Czichon et al., 2011.	133
Figure 6-22 Delamination on a sample specimen ($F_{crit, Biax} = 43$ kN). Source: Czichon et al., 2011.....	135
Figure 6-23 3-points bending experimental test setup. Source: Czichon et al., 2011.	138
Figure 6-24 3-points bending FEM. UTL component with 15 layers of elements (SOLID191 20-node layered solid elements), under $F_{crit, Biax} = 43$ kN.....	139
Figure 6-25 Transverse shear stress distribution (Pa) across the thickness, for a 30 mm specimen at 43 kN.	139
Figure 6-26 Transverse shear stress distribution (Pa) for layers 33 to 80, for a 30 mm specimen at 43 kN.	140
Figure 6-27 Location of the section where τ_{13} requested (outer surface along the transverse direction). Source: Czichon et al., 2011.	140
Figure 6-28 Transverse shear stress (τ_{13}) distribution comparison (MPa), for a 30mm specimen at 43 kN. Source (left): Czichon et al, 2011.	141
Figure 6-29 Transverse shear stress (τ_{13}) distribution (MPa), for a 30mm specimen at 43 kN. Two solid elements per ply (Biax). Source: Czichon et al., 2011.....	141
Figure 6-30 Nodal / Element (averaged) transverse shear stress (τ_{13}) distribution (MPa), for a 30mm specimen at 43 kN. 15 stacked SOLID191 (Biax).	142
Figure 7-1 Schematic description of a generic FE-based optimisation methodology.	146
Figure 7-2 Design exploration interdigitation. Source: Koch et al., 2002.....	148
Figure 7-3 Design space exploration of a parametric MLG SSF geometric model.....	149
Figure 7-4 Optimisation techniques available in ISIGHT. Source: Koch et al., 2002..	152
Figure 7-5 Stacking sequence design exploration methodology.....	155
Figure 7-6 Manufacturing design rules spreadsheet.....	156

Figure 7-6 Maximum vertical displacement (mm) vs maximum shear stress (MPa). .	162
Figure 7-7 Maximum shear stress (MPa) vs maximum number of plies failed (in-plane).	162
Figure 8-1 Parametric MLG SSF FE model (only geometry shown), alongside with available geometric design variables (l). CAD model (r). Source (r): Siemetzki et al., 2007.	167
Figure 8-2 Element coordinate system of half of the laminate elements. Design variables.	172
Figure 8-3 Vertical displacement u_z (m) of a metallic plate due to pretension bolts. ..	174
Figure 8-4 Proposed weight optimisation methodology for UTL composites.	175
Figure 8-5 Schematic representation of a reinforced thick curved plate under pure bending moment.	176
Figure 8-6 Reinforce curved plate geometry, with various sub-assemblies across the thickness.	177
Figure 8-7 Reinforce curved plate FE model, with various layered solid elements across the thickness.	177
Figure C-1 Maximum Stress Failure Index per ply comparison. Thin plate under in- plane load $N_x=1000$ N/m.	203
Figure C-2 Maximum Stress Failure Index per ply comparison. Thin plate under in- plane load $N_x=1000$ N/m.	204
Figure C-3 Tsai-Wu Failure Index per ply comparison. Thin plate under in-plane load $N_x=1000$ N/m.	204
Figure C-4 Tsai-Wu Failure Index per ply comparison. Thin plate under in-plane load $N_x=1000$ N/m.	205
Figure C-5 Maximum Stress Failure Index per ply comparison. Thin plate under in- plane load $N_x=1000$ N/m.	205
Figure C-6 Tsai-Wu Failure Index per ply comparison. Thin plate under in-plane load $N_x=1000$ N/m.	206
Figure C-7 Maximum Stress Failure Index per ply comparison. Thin plate under out-of- plane load $M_x=1000$ Nm/m.	206
Figure C-8 Maximum Stress Failure Index per ply comparison. Thin plate under out-of- plane load $M_x=1000$ Nm/m.	207
Figure C-9 Tsai-Wu Failure Index per ply comparison. Thin plate under out-of-plane load $M_x=1000$ Nm/m.	207
Figure C-10 Tsai-Wu Failure Index per ply comparison. Thin plate under out-of-plane load $M_x=1000$ Nm/m.	208
Figure C-11 Maximum Stress Failure Index per ply comparison. Thin plate under out- of-plane load $M_x=1000$ Nm/m.	208

Figure C-12 Tsai-Wu Failure Index per ply comparison. Thin plate under out-of-plane load $M_x=1000$ Nm/m.....	209
Figure E-1 Schematic representation of a bending moment applied on a plane section.	217
Figure E-2 Schematic representation of a linearly varying surface load on a surface.....	217
Figure G-1 Schematic description of the analysis. Source: Abbey, 2010.....	235
Figure G-2 FE model general view.....	237
Figure G-3 End constraint applied to avoid locking due to Poisson's ratio.....	237
Figure G-4 Load applied at a middle plane of the shell elements.	238
Figure G-5 Constant stress state (in the fibre direction).	238
Figure G-6 Transverse contraction due to the applied load and the BCs applied.	238
Figure G-7 Inverse of Tsai-Wu strength ratio index failure criterion.....	239
Figure G-8 Unity check value for ply angle equal to 0°	240
Figure G-9 Constant stress state (in the fibre direction).	240
Figure G-10 Inverse of Tsai-Wu strength ratio index failure criterion.....	241
Figure G-11 Total failing load (due to Tsai-Wu failure criteria) against ply angle.	242
Figure G-12 In-plane stresses (S_1 , S_2 , S_{12}) against ply angle.	243
Figure G-13 Tsai-Wu failure index terms against ply angle.	244
Figure J-1 SHELL99 geometry. Source: ANSYS help manual.	275
Figure J-2 SOLID46 geometry. Source: ANSYS help manual.	277
Figure J-3 Level of through thickness integration accuracy based on the element shape. Source: ANSYS help manual.....	278
Figure J-4 SOLID191 geometry. Source: ANSYS help manual.	279
Figure J-5 SOLID186 geometry. Source: ANSYS help manual.	284

List of Tables

Table 2-1 Summary of decomposition levels: Source: Fu et al., 1998.	21
Table 4-1 Element types available in ANSYS with layered option to model layered composite.....	57
Table 4-2 Element types available in ANSYS with layered option to model layered composite.....	58
Table 4-3 Constant values to define certain failure criteria using TB commands. Source: Barbero, 2008.	71
Table 4-4 Lists of failure index output available through the ETABLE command using the Sequence Number method.....	73
Table 5-1 Plate dimensions (in SI units).....	80
Table 5-2 2D orthotropic material properties (in SI units).	81
Table 5-3 Strengths levels (in SI units).....	81
Table 5-4 Laminate definition.....	82
Table 5-5 Load cases (in SI units).....	82
Table 6-1 Parameters description of curved beam dimensions.	119
Table 6-2 Curved plate dimensions (in SI units).....	119
Table 6-3 Radial and tangential stresses from exact solution obtained at different radial location (from inner to outer every 5mm) (in SI units).	120
Table 6-4 2D orthotropic material properties (in SI units).	122
Table 6-5 Laminate definition.....	122
Table 6-6 Specimen dimensions. Source: Czichon et al., 2011.....	134
Table 6-7 Laminate definition. Source: Czichon et al., 2011.....	134
Table 6-8 3D material properties (in SI units). Source: Czichon et al., 2011.....	134
Table 6-9 Strength properties (in SI units). Source: Czichon et al., 2011.	134
Table 6-10 Crack position (measured from the bottom of the specimen) for several tests. Source: Czichon et al., 2011.....	135
Table 6-11 Input parameters. Source: Czichon et al., 2011.....	136
Table 6-12 Analytic shear stress distribution τ_{13} across the thickness of an isotropic beam.....	137
Table 6-13 FEM comparison (between Czichon et al., 2011, and author's).....	138
Table 7-1 Simulation tools.....	147
Table 7-2 DOE techniques provided in ISIGHT. Source: Koch et al., 2002.	150

Table 7-3 Optimisation techniques implemented in ISIGHT. Source: Koch et al., 2002.	152
Table 7-4 Matrix of experiments.....	159
Table 7-5 DOE results.	161
Table 7-6 Performance comparison between the baseline Biax configuration and an improved configuration.....	163
Table G-1 Coupon test dimensions. Source: Abbey, 2010.....	235
Table G-2 Material properties.	236
Table G-3 Strength values.	236
Table G-4 Failing load factor (obtained with ANSYS) and failing load for a range of ply angles.	241
Table H-1 Matrix of experiments of 3 variables with 3 levels.	250
Table J-1 Number of integration points	275
Table J-2 Number of integration points	277
Table J-3 Number of integration points	279
Table J-4 Number of integration points	284

Nomenclature

Acronyms

ALCAS	Advanced Low-Cost Aircraft Structures
ANSYS	Finite Element Software
APDL	ANSYS Parametric Design Language
BC	Boundary Condition
CAD	Computer Aided Design
CFRP	Carbon Fibre Reinforced Plastic
CLT	Classic Lamination Theory
DOC	Direct Operating Cost
DOE	Design of Experiments
DOF	Degree of Freedom
EADS	The European Aeronautic Defence and Space Company N.V.
FEM	Finite Element Model
FEA	Finite Element Analysis
FSDT	First-order Shear Deformation Theory
GA	Genetic Algorithm
ISIGHT	Data Management System and Optimisation Commercial Code
IW	Innovation Works
LSS	Laminate Stacking Sequence
MIT	Massachusetts Institute of Technology
MLG	Main Landing Gear
MTOW	Maximum Take-Off Weight

NCF	Non-Crimped Fabric
RS	Response Surface
SMAX	Maximum stress failure criterion (ANSYS)
SME	Society of Manufacturing Engineering
SSF	Side Stay Fitting
TSD	Transverse Shear Deformation
TT	Through Thickness
TWSI	Tsai-Wu strength index failure criterion (ANSYS)
TWSR	Inverse of Tsai-Wu strength ratio index failure criterion (ANSYS)
UD	Uni Directional (ply)
UTL	Ultra Thick Laminates
VBA	Visual Basic

Symbols

a	Panel length
$[A]$	Membrane (or extensional) stiffness matrix
A_{ij}	Terms of the membrane stiffness matrix, $i=j=1,2,6$
b	Panel width
$[B]$	Membrane-bending coupling stiffness matrix
B_{ij}	Terms of the coupling stiffness matrix, $i=j=1,2,6$
$[D]$	Bending stiffness matrix
D_{ij}	Terms of the bending stiffness matrix, $i=j=1,2,6$
E_i	Young's modulus (stiffness) in i direction, $i=1,2,3$ (1=fibre, 2=matrix, 3=out of plane)

E_{ij}	Stiffness of j, j=f,m (f=fibre, m=matrix) in the i, i=1,2 (fibre or matrix direction)
f_{12}	Interaction factor
FI	Failure Index
F_{ij}	laminate strength, i=1,2,3; j=t,c (t=tension, c=compression)
F_{12}, F_{23}, F_{13}	Shear strength
G_{ij}	Shear modulus i=1,2; j=2,3
G_i	Shear modulus of i, i=f,m (f=fibre, m=matrix)
h	Laminate thickness
$[H]$	Transverse shear matrix
H_{ij}	Terms of the transverse shear matrix, i=j=4,5
$K = K(z)$	Shear correction factor
k	Ply number
M_i	Bending moments (per unit width), i=x,y,xy
N_i	Resultant force (per unit width), i=x,y,xy
p	Pressure distribution
Q_i	Transverse shear resultants, i=x,y
$[Q]$	Reduced stiffness matrix
Q_{ij}	Terms of the reduced stiffness matrix, i=j=1,2,6
$\{Q\}$	Transverse shear vector
$[\bar{Q}]$	Transformed reduce stiffness matrix
\bar{Q}_{ij}	Terms of the transformed reduced stiffness matrix, i=j=1,2,6
s	Symmetric
S	Shear strength

t	Panel thickness
$[T]$	Transformation matrix
t_{ply}	Ply thickness
U_i, U_j^*	material invariants, $i=1..5; j=1,2$
V_i	Volume fraction of $i=f,m$ (fibre or matrix)
X_i	Strength under $i=t,c$ (tension, compression) in the fibre direction
Y_i	Strength under $i=t,c$ (tension, compression) in the transverse fibre direction
$\{\gamma^0\}$	Transverse shear strain vector
γ_i	Transverse shear strain, $i=xy,xz,yz$ (global XY axes), or $i=12$ in the 12 axes
γ_{ij}^u	laminate ultimate shear strain, $i=12,23,13; j=t,c$ (t =tension, c =compression)
$\{\varepsilon_{x-y}\}$	Strain vector (global xy axes)
$\{\varepsilon_{1-2}\}$	Strain vector (1,2 axes)
ε_i	Normal strain $i=x,y$ (global XY axes) or $i=1,2$ in the 12 axes
$\{\varepsilon^0\}$	Mid-plane strain vector
ε_{ij}^u	laminate ultimate strain, $i=1,2,3; j=t,c$ (t =tension, c =compression)
θ	Angle between the global x-axis and the fibre direction
k	Middle surface curvatures
ν_i	Poisson's ration in i direction, $i=12,21$ (also 23,31)
v_i	Volume of $i=f,m$ (fibre, matrix)
ξ_i^j	Lamination parameters, $i=1,2,3; j=A,D$
ρ	Density

$\{\sigma_{x-y}\}$	Stress vector (global XY axes)
$\{\sigma_{1-2}\}$	Stress vector (1,2 axes)
σ_i	Normal stress $i=x,y$ (global XY axes), or $i=1,2,3$ or $i=11,22,33$ (1,2,3 axes)
τ_i	Transverse shear stress $i=xy,xz,yz$ (global XY axes), $i=12,23,31$ (12 axes)
φ_c	Position of the crack from the bottom surface
ϕ_i	Rotation about the i axis, $i=x,y$

1 Introduction

1.1 Composite Materials

Weight saving, due to their high specific strength and stiffness ratios (Jones, 1999; Baker et al., 2004) alongside their corrosion and fatigue resistance, has made composite materials to be nowadays applied in a wide range of sectors, such as civil engineering, medical instrumentation, sport equipment, as well as in all means of transport to some extent (marine, automotive, rail system and aerospace).

In the aerospace industry the implementation of laminated composite structures has been slower than expected, not only due to their high certification and manufacturing costs, but also to their low impact damage resistance and through-thickness strength compared with their metallic counterparts (Baker et al., 2004), among others.

Over the last decade, the lower cost of manufacturing technologies for composite structures has increased their use for commercial aircraft applications (Figure 1-1). Various civil aircraft manufacturers, have not just restricted the use of composite materials to secondary structures, as they did in the past (flaps, ailerons, spoilers, etc), but they have also applied them in primary structures. As an example, for the Airbus A380 program, the amount of composite material utilised represents more than 20% of the total airframe weight. Moreover, for the Airbus A350 and Boeing B787 programs, the use of composite materials comprise around 50% of the total airframe weight.

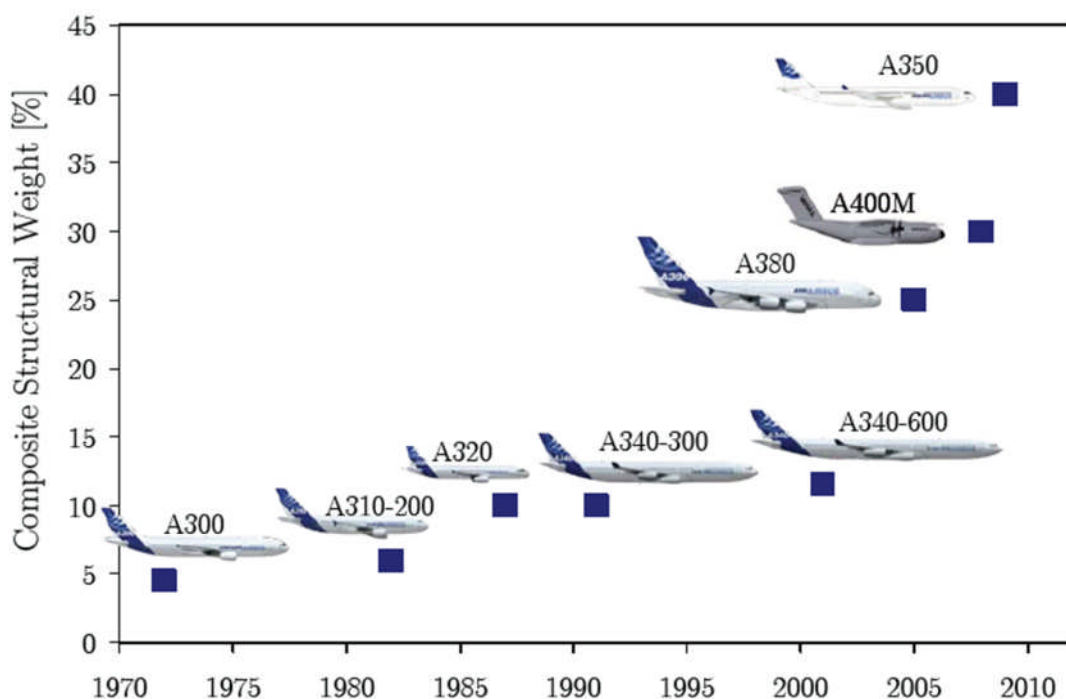


Figure 1-1 Composite introduction on Airbus aircrafts. Source: Assler, 2006.

A main driver for this increment has been the fact that, unlike metallic components, the stiffness of composite structures can be tailored. By influencing the component design and the manufacturing process applied (laminates stacking sequence, material properties, etc) the load applied to a component can be transferred to the rest of the structure in a more controlled manner. Current practical applications are generally limited to symmetric or mid-symmetric laminates with 0° , 90° , 45° and -45° layer angles, due to the manufacturing constraints (Herencia et al., 2008).

1.2 The need for this research

1.2.1 The ALCAS Project

ALCAS (Advanced Low-Cost Aircraft Structure) is a European Union project which aim is to offer improved aircraft performance by enhancing its structural efficiency; applying, where possible, composite materials on aircraft primary and secondary structures; making use of novel design concepts as well as of low-cost manufacturing technologies, which implies a significant reduction on the DOCs of the operators (Watson, 2007).

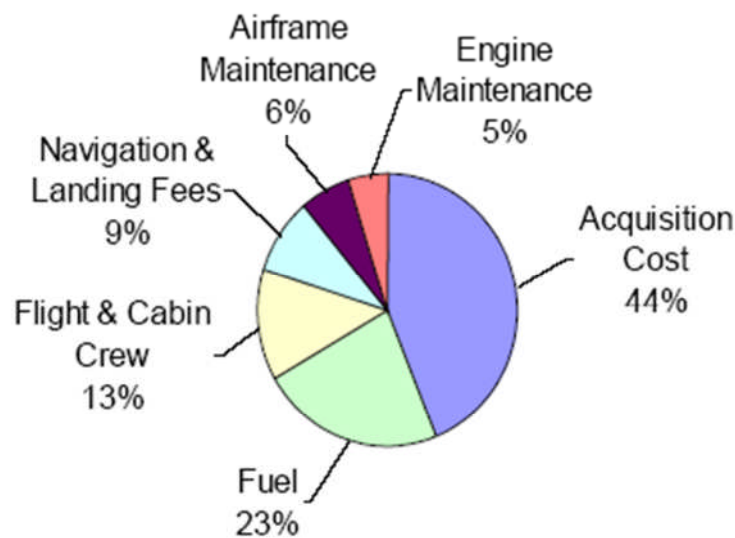


Figure 1-2 Typical DOC's for a long range airliner. Source: Watson, 2007.

For a general description of the ALCAS project refer to Watson (2007).

1.2.1.1 Cranfield University contribution

There are 60 partners involved in the project, among aerospace industry manufacturers, research institutes, SME, test houses and universities, within which Cranfield University is found. Cranfield University main contribution concerns the development of a design exploration and optimisation methodology for thick composites applications, which can evaluate a wide range of design alternatives, in order to improve the structural performance.

This research forms part of a work package that implied the collaboration with AIRBUS UK and MESSIER DOWTY in the design of the Main Landing Gear Side Stay Fitting (MLG SSF) that integrates the main landing gear with the aircraft composite wing.

The whole assembly represents a 70% scaled down model of the Airbus A320. The MLG SSF has already been developed by EADS IW in Ottobrunn (München), responsible of its design, tests and manufacturing processes (using the Vacuum Assisted Process (Barbero, 1999; Agarwal et al., 2006; Baker et al., 2004). The final bracket configuration includes lugs of 90 mm thick (Figure 1-4), manufactured as a constant thickness curved and plane plates made up of a stack up of Non-Crimped Fabric, which is a type of through-thickness reinforced laminate used in the aerospace industry (Baker et al., 2004). The analysis of these kinds of structures, typically referred to as Ultra Thick Laminates (UTL), should account for a 3D stress state, in order to predict and characterise the out-of-plane delamination failure, associated with transverse shear stresses and interlaminar stresses, or with normal through-thickness stresses in thick curved plates.

Existing tests and analytical methods (theoretical and numerical) are normally restricted to thin laminate applications. The mechanical behaviour of thick components cannot be accounted using thin shell element formulations, but with solid formulation that can accurately predict and characterise the out-of-plane delamination failure, in order to deliver a fail-safe design (Baker et al., 2004).

Figure 1-3 shows the CAD models provided by both companies. A CATIA model of the lateral wing box along with the main landing gear attachments was supplied by AIRBUS UK, and a CATIA model of the main landing gear test leg was obtained from MESSIER DOWTY.

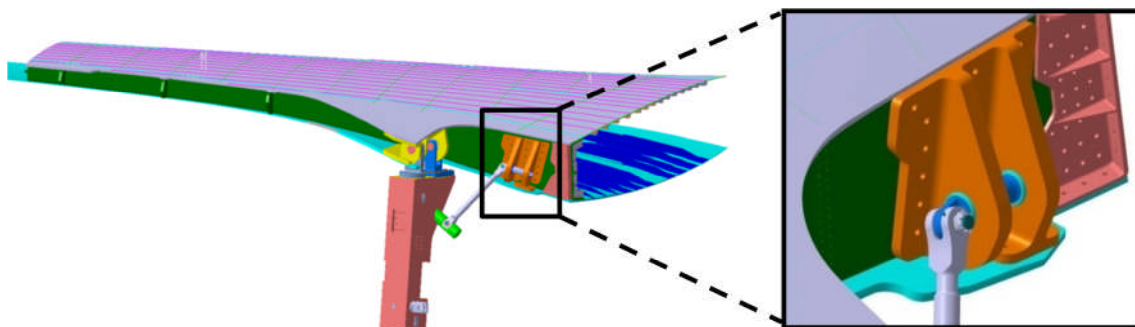


Figure 1-3 Critical components of the ALCAS lateral wing box assembly, with MLG SSF detailed CAD model. Source: Mahmood, 2007.

Despite the significant reduction in mould cost of the Vacuum Assisted Process (VAP) compared with the conventional Resin Transfer Moulding process (RTM) (Baker et al., 2004), there are some important parameters to consider when manufacturing this kind of UTL structures; for instance, the difficulties of component repeatability (influenced by

a homogeneous resin distribution and curing process), high certification costs, and the difficulties of simulating the complex behaviour of 3D reinforced laminated composites, used to improve the low through thickness strength associated with laminated composite components, just to name a few.

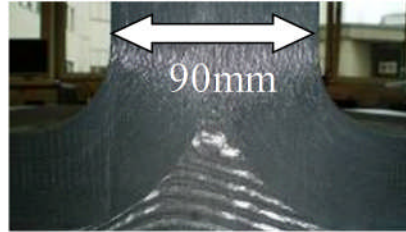


Figure 1-4 Final lug thickness of the manufacture MLG SSF (EADS). Source: Siemetzki et al., 2007.

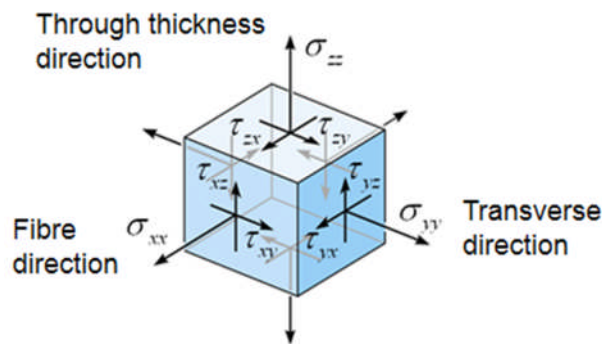


Figure 1-5 3D stress state.

1.2.1.2 Current approach

The “black metal” approach is the design method used by EADS IW for the bracket development, by which the composite bracket layout is the same as the standard metallic bracket. A series of batch tests, based on few sub assembly sections of the bracket subjected to in-plane and out-of-plane load (with thicknesses ranging between 60-90 mm), were performed for a certain laminate configuration (only two laminate configurations were finally evaluated). Its final proposal includes a series of countermeasures that prevent the main failure mechanisms from occurring, including through thickness delamination (Siemetzki et al., 2007).

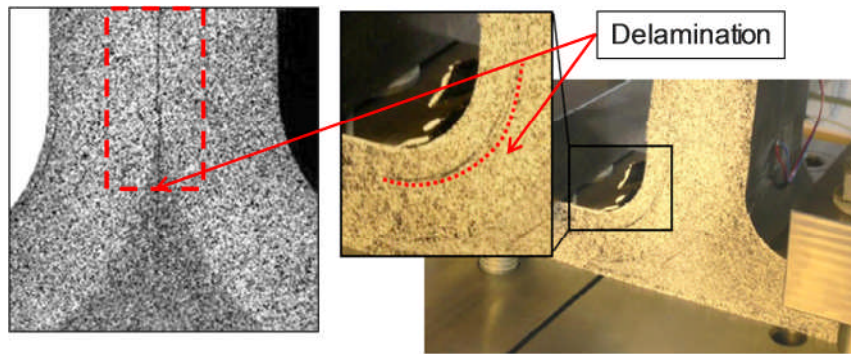


Figure 1-6 Delamination failures in a T-section test model due to normal through thickness stresses σ_{33} . $F_{\text{pull,max}}=110\text{kN}$ (left), $F_{\text{axial,max}}=42\text{kN}$ (right). Source: Siemetzki et al., 2007.

The “black metal” approach can potentially lead to a lighter design, but may introduce a whole range of potential problems, including delamination, additional stresses due to bolts, weight penalty due to use of reinforcing metallic plates or due to the need of thicker composite plates (in order to avoid through thickness delamination), etc.

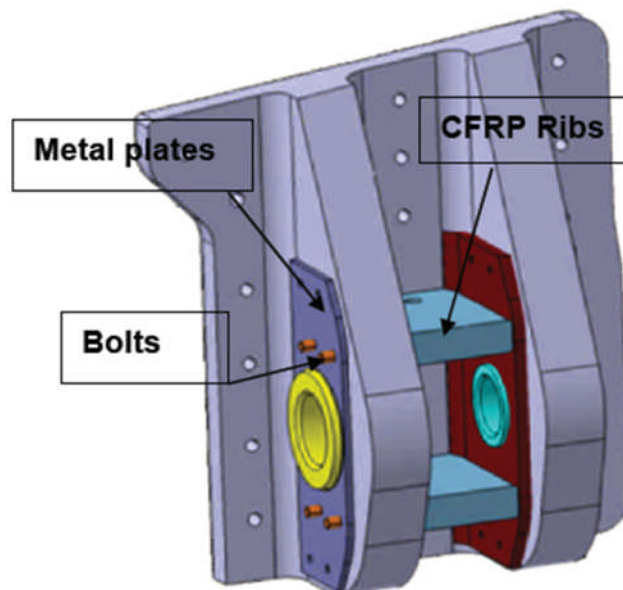


Figure 1-7 MLG SSF reinforced with CFRP ribs. CAD design. Source: Siemetzki et al., 2007.

Furthermore, as this approach is based on the previous metallic layout, it may not fully benefit from one of the main advantages of using fibre reinforced composite laminates, by which the structural stiffness can be tailored (Baker et al., 2004), which if not accounted may result in a poor load transfer capability (not ideal for composites).

Making use of the orthotropic nature of laminated composite, the component performance could be optimised. Since delamination initiation at an edge may

significantly affect the laminate performance, it is required to consider edge-delamination-suppression concepts (Agarwal et al., 2006; Jones, 1999) at an early stage in the design process.

Hence, the need of a design methodology for thick laminated components that can explore a broad design space, enabling to evaluate different layup configuration, a wider range of bracket geometric layouts and dimensions, and various laminate stacking sequences and material properties, is justified.

The proposed optimisation methodology represents an industry oriented systematic procedure for designing more efficient Ultra Thick Laminated composite structures.

1.2.2 Nature of the Problem

The complexity behind the design analysis and optimisation of thick laminated components depends on many factors, some of which are listed below:

- Lack of experimental data of thick laminated components available in literature.
- Limited number of analytic theories which can accurately describe the laminate through thickness behaviour. For instance, the Classic Lamination Theory, based on plane stress theory, cannot be used to characterise the laminate through thickness behaviour of UTL, as it neglects the through thickness stresses.
- More complex FEM, involving:
 - Lack of element formulations in commercial FE tools that represent 3D reinforced laminate behaviour.
 - Parametric definition of the FE models, for a robust and flexible design space definition. Furthermore, the geometry created must respect the way in which the laminates are manufactured (Figure 1-8), and more important, the material axes definition should be coherently updated for each new geometry considered.
 - The use of layered solid elements is required in order to reduce the computational cost associated with the analysis of these types of structures, and yet accurately calculate the interlaminar (transverse) shear stresses and direct through thickness stresses, directly responsible for the delamination failure of these structures. A clear understanding of the functionalities, advantages and limitations of the current element formulations available is vital.
 - Large number of design variables, i.e. laminate variables (number of plies, ply orientation, stacking sequences, etc), geometric entities, etc.
 - Large amount of results generated to post-process.
- Non-linear nature of the optimisation analysis, as the ply orientation, for instance, is regarded as a discrete variable (due to the current manufacturing

limitations in industry). This may result in very expensive computational analysis.

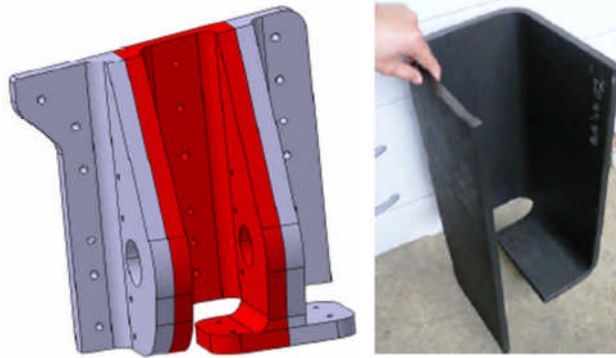


**Figure 1-8 CAD model of the MLG SSF considering manufacturing constraints (l).
Manufactured central laminate (r). Source: Siemetzki et al., 2007.**

1.3 Project objectives and scope

The overall objective of this work is to address the following research questions:

- To assess the functionality advantages and limitations of layered solid element formulations, available in commercial Finite Element codes, applied to the mechanical response prediction of Ultra Thick Laminate (UTL) composite components.
- Perform a design exploration and optimisation of a constant thickness UTL composite component, in order to improve its performance (considering the manufacturing limitations).

Prior to tackling these aims, a series of activities need to be undertaken:

1. Perform a systematic and detailed assessment of the capabilities of existing commercial finite element code, for determining their suitability in modelling UTL. The main requirements and limitation are evaluated.
2. However, before this can be done, enough confidence in practical experience for modelling and postprocessing FEA of laminated composites need to be developed. A Classic Lamination Theory (CLT) simple example under in-plane and out-of-plane loads will be used as a starting point to perform a laminate strength analysis (linear static), to determine the level of accuracy of the different element formulations available and modelling strategies.
3. This is then extended to consider thicker applications owing a 3D stress state. Effects of tangential and normal stresses are evaluated for a curved thick plate and the transverse shear stress distribution across the thickness is evaluated for an UTL composite specimen (with a constant thickness of 30 mm) under 3-

points bending. Linear static analysis is considered in both cases; results are compared against analytic and experimental data found in literature.

4. A critical assessment of different FE-based optimisation methodologies available in literature, used for both, thin and thick laminated applications (in industry and academia), will be done.
5. A design exploration and / or optimisation methodology for improving the performance of UTL applications will be justified. The computational requirements for an accurate data transfer among all software packages used are considered. Various analysis approaches are evaluated and discussed, and a selection of effective input and output variables are defined for each of the analyses proposed. The utilization of manufacturing design rules is considered in order to reduce the number of feasible stacking sequences to be evaluated.
6. Some of the previous FE models created will be used for verification and evaluation purposes of the proposed methodology.
7. The proposed methodology should be validated in the future with real experimental test results, both to improve and expand its applicability.
8. Additionally, guidelines for future weight optimisation of UTL composite components making use of layered solid elements is also presented as future work.

1.4 Contribution to knowledge

The main contribution to knowledge of this research is:

- To assess the functionality, advantages and limitations of different solid element formulations, including layered solid elements that are available in commercial Finite Element codes, applied to the mechanical response prediction of UTL composite components (thicknesses up to 30 mm are considered).
- To perform a design exploration and optimisation of constant thickness UTL composite component in terms of the orientation of a varying and repeatable stacking sequence of an eight ply Non-Crimped Fabric, in order to assess the design implications on performance.

In order to achieve these objectives a standard, flexible and expandable FE based optimisation methodology for UTL composite components was developed, which accounts for the following requirements:

- Commercial FE tool and data management system and optimisation tool
- Parametric Finite Element Models definition
- Layered solid elements
- Application of manufacturing design rules

1.5 Organization of the thesis

In summary, the present chapter introduces the importance of composite materials in the aerospace industry. The need of this research is justified based on the fact that current design approach of thick laminated structures (“black metal”) may not fully exploit the benefits of tailoring the component stiffness. The main difficulties associated with the design optimisation of thick laminated composites are highlighted. The project objectives and contribution to knowledge of this research were presented, as well as the list of actions required in order to accomplish them.

In chapter 2, the computational cost associated with the design optimisation analysis of UTL composite structures have been quantified in terms of three main parameters, model, analysis and optimisation costs. Several ways of improving the efficiency of this type of analysis by understanding the problematic behind each one of them, and the design optimisation methods currently available conforms the rest of the section.

Chapter 3 provides a general description of the main theories developed for modelling laminated composite plates, some of them implemented in the element formulation of most of the commercial FE codes; focusing on their suitability and limitations for accurately represent the through thickness stresses, as the failure mechanisms of thick laminated plates are highly affected by the transverse shear and normal stresses through the plate thickness. Interlaminar shear stresses and free edge effects are also discussed due to their influence in delamination failure mechanism of thick laminates.

In chapter 4, the main characteristics of a FE Analysis of composite structures are described, as the methodology proposed is based on this analysis. FE commercial tool requirements are discussed, in terms of design space definition of thick laminates via parametric model generation, and in terms of analysis accuracy and efficiency via layered solid formulations. The analysis steps involved in a laminate FE Analysis are particularised for ANSYS, the FEA commercial tool used in this research. A general description of the layered element formulations available and best modelling and post-processing practice are given, including the layered configuration definition, element coordinate system transformation, and the available 3D failure criteria definition, focussing on thick laminate applications.

The main purpose of chapter 5 is to get practical experience with ANSYS for modelling thin laminated composite plates, as a previous step before tackling the UTL composite structural analysis. Different layered element formulations and modelling strategies (with different number of layered solid element through the thickness) were benchmarked against analytical results obtained from CLT analysis performed on a particular configuration of a laminated plate under in-plane and out-of-plane load cases, by comparing several in-plane.

In chapter 6, the verification analyses presented in chapter 5 are extended for the case of thick laminates. Simulation solutions are compared against analytical and experimental results available.

Chapter 7 presents the bulk of the research. A generic, standard and flexible FE based design optimisation methodology, along with its modules is described in section 7.1. The proposed framework is particularised for the effective and practical design exploration and local optimisation of constant thickness UTL in terms of the laminate stacking sequence.

In Section 7.2 alternative design configurations of the short beam model used in Section 6.2 are evaluated in order to find a stacking sequence(s) that improve the component performance.

Chapter 8 presents the conclusions and future work, discussing some guidelines to the weight optimisation analysis with layered solid elements.

2 Literature Review

2.1 Introduction

This chapter will review and discuss the main concepts involved in the design optimisation analysis of laminated composite structures, with particular emphasis in UTL composite applications. Ultimately, the current limitations in the design optimisation of UTL composite will be highlighted, as a justification for the design exploration methodology proposed in this research. The areas of interest that are going to be introduced are listed below:

- Three-axes of complexity
- FE modelling of thick composite laminates
- Optimisation of laminated composites
- Multi-level optimisation analysis
- Manufacturing constraints

2.2 Three-axes of complexity

The main complexities associated with the optimisation of composite structures are going to be identified, in order to justify a FE-based optimisation methodology approach which could provide accurate, yet affordable solutions.

Venkataraman and Haftka (2002) proposed that the level of complexity of the design optimisation of composite structures could be measured in terms of the following parameters:

- Model
- Analysis
- Optimisation

According to these authors, the complexity of structural analysis could be measured by its computational cost, which accounts for both, modelling and analysis costs.

It has been determined that generally there are two main parameters that significantly affect the modelling cost; these are the number of Degrees of freedom (DOF) of a Finite Element Model (FEM), and the topology of the structural component. Generally, for the same number of nodes, it is more efficient to analyse a beam type structure than a three-dimensional one (Chedid, 2009).

Figure 2-1 shows an evolution of the structural optimisation analysis complexity via various composite laminates applications, alongside the research papers in which each of those optimisation analyses have been published. With regards to the main area of interest of this research it worth mentioning that, according to the diagram, design

optimisation of 3D structures are considered as the most complex structures (in terms of the abovementioned drivers) (Venkataraman and Haftka, 2002).

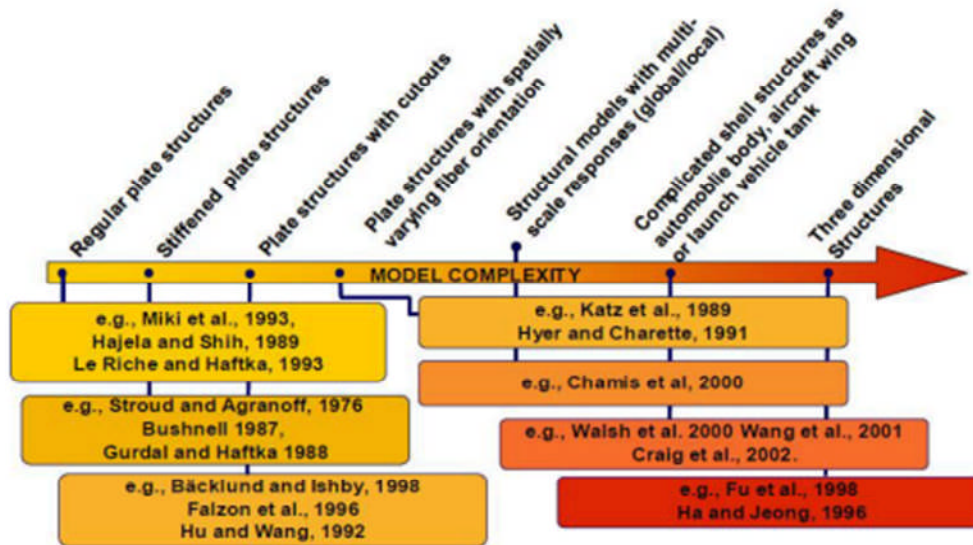


Figure 2-1 Evolution of structural model complexity. Source: Venkataraman and Haftka, 2002.

Regarding the analysis complexity, linear elastic analyses (the only one applied in this research) are considered the simplest type of analysis. Thus, the cost of a more complex analysis is always referred as relative to the linear one (Venkataraman and Haftka, 2002).

Figure 2-2 depicts the complexity increment for various types of analysis. Non-linear transient analyses, required for crash simulation represents the highest level of analysis complexity.

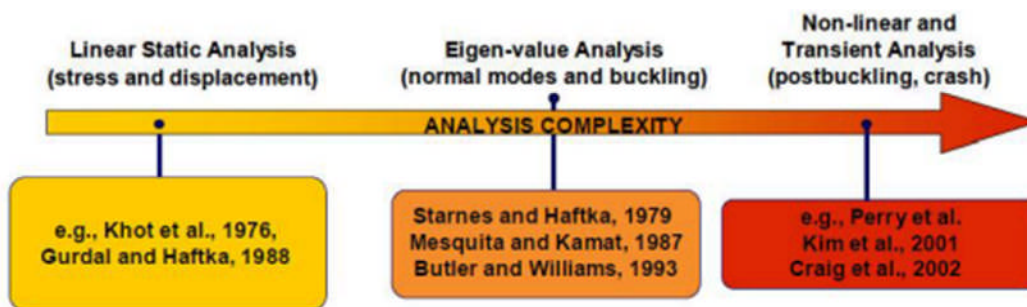


Figure 2-2 Evolution of analysis complexity. Source: Venkataraman and Haftka, 2002.

Finally, the optimisation cost is measured by three parameters, the number of analysis required, the number of design variables and the optimisation type (Venkataraman and

Haftka, 2002). Generally, the simplest type of optimisation analyses is the Graphical optimisation with lamination parameters, and the numerical gradient-based local optimisation. Global optimisation with discrete design variables and probabilistic optimisation, which may results in highly non-linear problem formulation, are classified as the most complex analyses.

The figure below shows the optimisation techniques organized by the level of complexity.

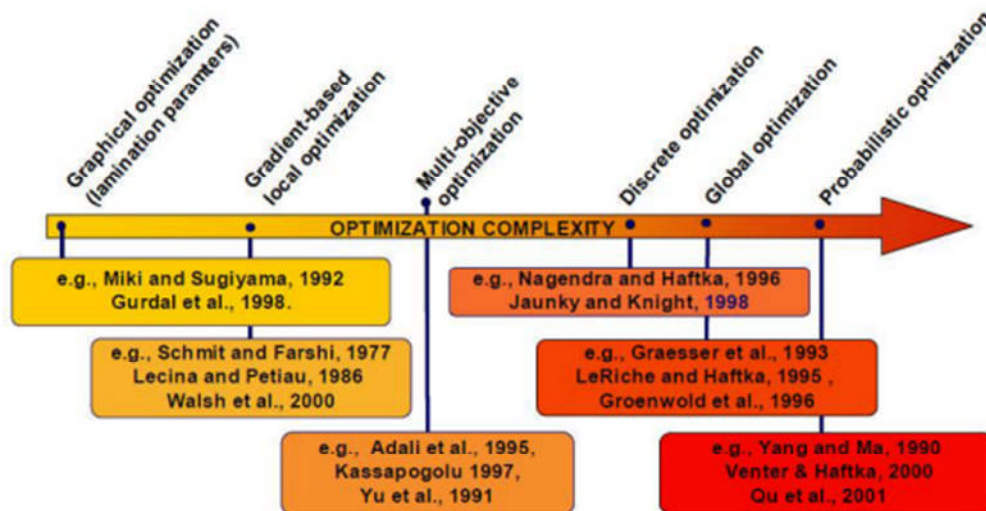


Figure 2-3 Evolution of optimisation complexity. Source: Venkataraman and Haftka, 2002.

Uncertainty is another factor proposed by Venkataraman and Haftka (2002) to evaluate the analysis complexity, that when considered in the optimisation result in a much more expensive analysis than the deterministic optimisation analysis proposed in this research.

A schematic representation of the three-axes of complexity is depicted in Figure 2-4. Point P determines the optimisation problems with the highest level of complexity. State of the art optimisation problems will rely upon the surface confined within the cubic region, which represents the relation among the three parameters. Thus, the maximisation on the level of complexity of two parameters will have a significant effect on the complexity of the third.

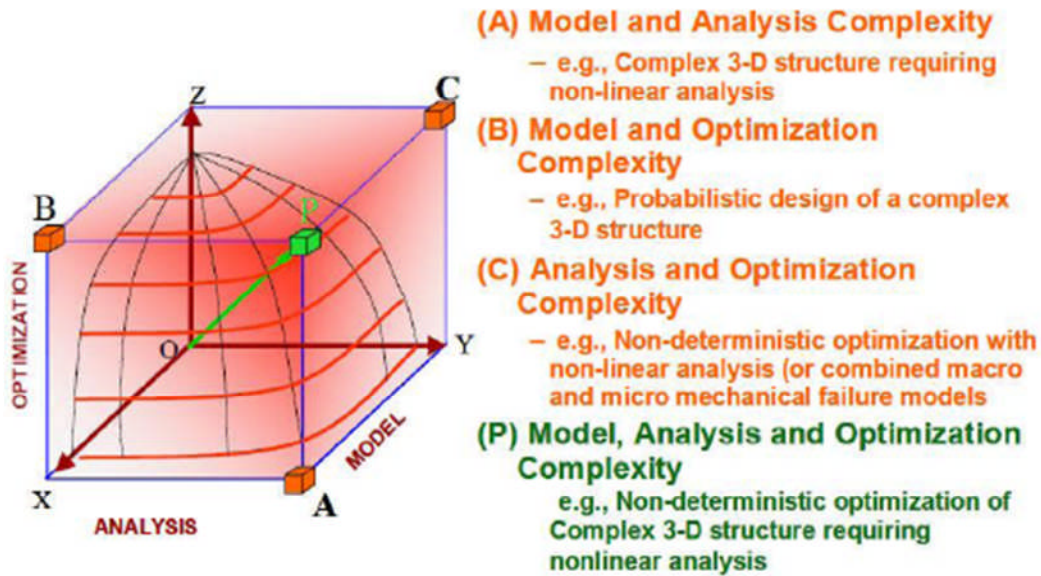


Figure 2-4 Three-axes of complexity. Source: Venkataraman and Haftka, 2002.

The high level of complexity associated with the design optimisation analysis of thick laminated composite components is due to the following reasons:

- *High modelling cost:* In order to characterise the 3D stress state behaviour of these types of structures, high fidelity finite element models are required with the subsequent penalty in the analysis cost. Different modelling approaches for thick laminated structures are available, which significantly affect the computational cost of these analyses. For further discussion on this matter refer to Section 2.x and Section 4.
- *High analysis cost:* For the present case, only linear static analysis is considered, although the flexible nature of the methodology proposed enables to use of more complex type of analysis. For instance, non-linear transient explicit analysis to evaluate the energy absorption capabilities of the main landing gear bracket in a Foreign Impact Damage analysis, or the investigation of progressive failure with non-linear material model and interactive criterion (Czichon et al., 2011).
- *High optimisation cost:* When defined at a ply level, the number of design variables required to describe the laminated nature of thick composite structure can become quite significant, only by just considering the ply orientation, thickness and stacking sequence. The different nature of these design variables, i.e, continuous, discrete and integer may require the use of expensive global search genetic algorithms, or the use of a multi-level optimisation approach employing different non-linear optimisation techniques.

By considering the parameters affecting the high level of complexity inherent to the design optimisation analysis of UTL composite structures, possible ways to reduce their impact need to be identified.

2.3 FE modelling of thick laminated composite components

The complex three dimensional stress state that characterise the behaviour of UTL structures can only be represented by using various solid element per ply, considering 3D equilibrium equations (Khandan et al., 2012). However, due to the large number of DOF and design variables considered, related to the number of plies modelled, the analysis becomes impractical for engineering applications.

There are several examples in literature that describe element formulations developed for an accurate transverse stress prediction. For instance a three dimensional finite element analysis that can accurately represent the 3D stress state of thick laminated composites under bending was developed by Barker et al. (1972) in which each laminate ply was modelled with one or more solid elements through the thickness.

More effective element formulations as the layered solid elements have been developed to overcome this problem. This approach reduces significantly the computation cost of running high fidelity analysis of thick laminated composites, providing also enough level of accuracy to evaluate the through thickness stresses.

There are various plate deformation theories formulated in order to predict accurately the transverse stress distribution in moderately thick plates, some of these theories, as the High Order Shear Deformation Theory is normally embedded in the layered solid element formulation of some commercial FE codes. For a more detailed description of these theories refer to Section 3.5.

A layered solid element suitable for modelling thick laminated composites was developed by Kuhlmann and Rolfes, 2004. The full stress tensor is calculated in two steps and its behaviour was compared with elements available in commercial codes, i.e. MSC MARC. The element provides an accurate and efficient way of analysing thick laminated composites.

Czichon et al. (2011) performed a comparison of the efficiency that two different solid element formulations have for predicting the transverse shear stress distribution across a 30 mm short beam under bending application. One of the modelling approaches consider that each lamina is represented with two solid elements per layer (Figure 2-5 left), and the other considers a stack up of sublaminates modelled with layered solid elements (Figure 2-5 right).

Results demonstrated that the computational cost of running expensive high fidelity analysis is significantly superior in the case of using two solid elements per layer. Furthermore, the difference in terms of the shear stress distribution across the beam

thickness, only present variations at a ply level. The fact that the only parameter sought in these analysis was the maximum shear stress value, obtained in both cases with reasonable accuracy, represents that the use of layered solid elements is justified for this type of analysis.

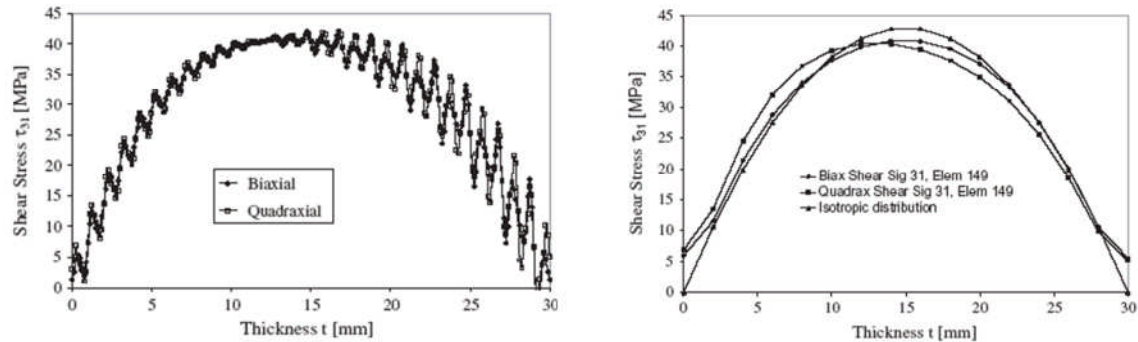


Figure 2-5 Transverse shear stress distribution across a short beam under bending. Solid element (l), layered solid element (r). Source: Czichon et al., 2011.

Another parameter that affects the computational cost of the optimisation analysis of laminated structures is the laminate configuration, which can be defined by smaller number continuous smeared homogeneous properties as design variables, instead of using the discrete nature of the plies orientation when the laminate is defined at a ply level. The FE model of the torque link assembly depicted below (Figure 2-6) was modelled with eight-node brick elements (MARC element type 7) (Thuis, 1999) and smeared properties.

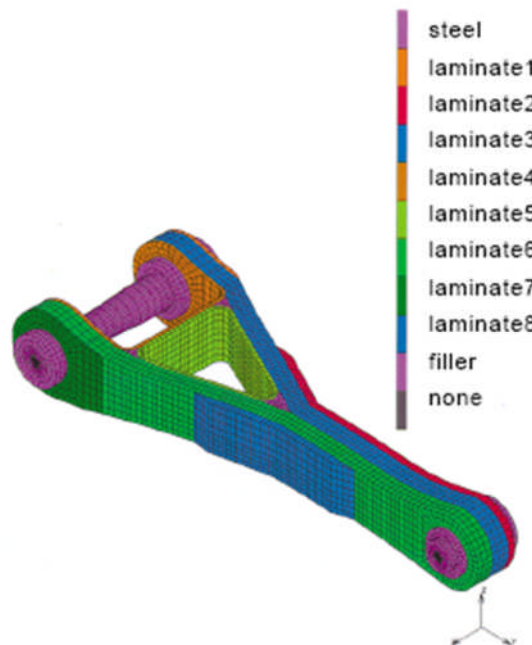


Figure 2-6 Laminate definition in a torque link assembly. Source: Thuis, 1999.

Other applications in which the laminate properties are smeared could be found in the bioengineering area, due to the high anisotropy of the structures under investigation (Figure 2-7).

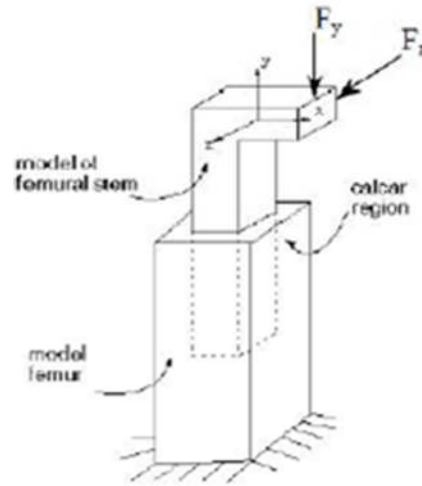


Figure 2-7 Schematic representation of a bioengineering application. Source: Chen et al., 2000.

From what has been presented in this section, it is clear that for an efficient yet accurate representation of the triaxial stress state required for the characterisation of the thick laminated composites behaviour, layered element formulations should be considered.

Following a description of the main concepts related to the design optimisation analysis of composite laminates is presented.

2.4 Design optimisation of laminated composites

The large number of design variables available that could be considered in the design of a laminated composite structure represents a challenge for the structural engineers, who have to determine not only which of those variables have a significant impact in the component behaviour, but also the range of values for which those design variables provide the best design in terms of its performance. The aim of achieving the best component performance that delivers a fail safe design, under various failure mechanisms, considering a large number of design variables and their range of variation represents a suitable problem definition for the application of mathematical optimisation in the design process of laminated composites (Gürdal et al., 1999).

2.4.1 Design optimisation

The standard form of a single objective optimisation problem is presented in the following mathematical statement:

$$\begin{aligned}
 & \text{minimise } f(\mathbf{x}) && \mathbf{x} \in X && \text{(2-1)} \\
 & \text{such that } h(\mathbf{x}) = 0 \\
 & && g(\mathbf{x}) \leq 0 \\
 & && \mathbf{x}^L \leq \mathbf{x} \leq \mathbf{x}^U
 \end{aligned}$$

Generally, the purpose of the optimisation is to optimise (maximise or minimise) the *objective function*, represented by $f(\mathbf{x})$, which measures then the efficiency of the design. This process is normally carried out within certain limits determined by the *constraints*, $g(\mathbf{x})$ (inequality), and $h(\mathbf{x})$ (equality). The optimisation design space is defined by the design variables, represented by a n-dimensional vector \mathbf{x} ; these are the parameters that vary, between their lower and upper bounds, during the optimisation process. Design variables can be regarded as *continuous*, *discrete* or *integer*, which is a special case of discrete variables (Gürdal et al., 1999).

The techniques employed to solve the non-linear optimisation problem stated in Eq (2-1) are called non-linear mathematical programming (MP). There are various gradient based algorithms available for analysing these non-linear optimisation problems, their suitability and efficiency is largely dependent on the shape of the design space, which is also determined by the definition of the objective function and the constraints (Gürdal et al., 1999). The evaluation of a design space with design variables of different nature (continuous, discrete and integer) may deliver an undesired local optimum as the best solution, and has to be considered carefully. More recently, the increasing interest in developing new optimisation techniques has resulted in the implementation of global search algorithms, such as the genetic algorithms (GAs). GAs are based on natural selection and natural genetics laws (Goldberg, 1989, cited in Herencia et al., 2008), and are quite popular for the evaluation of design spaces that present many local optima (Coley, 1999, cited in Herencia et al., 2008).

2.4.2 Optimisation of laminated composites

As stated in Section 1.2.1.2 one of the main benefits of using composite materials is due to the fact that the structural stiffness of the component can be tailored, which can be interpreted as a performance objective function optimisation. In general, there are two possible objectives when dealing with laminated composite performance optimisation, which are the minimisation of the structure weight subjected to certain stiffness limits, or the maximisation of the component stiffness under strengths constraints (which is the case of the present research) (Gürdar et al., 1999). In both cases, the ply thickness, the fibre orientation, the number of plies and the stacking sequence are the design variables commonly considered in a laminated composite design optimisation.

Initially the application of optimisation analysis of composite laminates considered only design variables with continuous nature. In that sense, Schmit and Farshi (1973, 1977) (cited in Herencia et al., 2008) performed an optimisation analysis of homogeneous orthotropic symmetric laminates, by defining ply thicknesses as the continuous design variables.

The discrete nature of the composite design variables is justified due to the fact that the laminate should account for an integer number of plies, and also due to the manufacturing limitations that restrict the ply orientation to certain fixed angles (Gürdal et al., 1999). As a consequence of the discrete nature of the design variables, a limited number of laminate stacking sequences should be evaluated when performing a design optimisation.

For thin application Gürdal et al. (1999) propose an exhaustive enumeration strategy of the stacking sequences in order to evaluate the different design alternatives. For thicker applications considering a design optimisation of a non-repetitive stacking sequence may become challenging.

In that sense, a reduced number of laminate properties, called lamination parameters were introduced by Tsai and Pagano (1968) and Tsai and Hahn (1980) (both authors cited in Herencia et al., 2008) for characterising the laminate constitutive stiffness matrix.

Miki and Suiyama (1991) (cited in Gürdal et al., 1999) determined an alternative to the discrete nature of the plies orientation by using the optimisation of continuous lamination parameters.

Herencia et al. (2008) cited several sources in which lamination parameters have been optimised using mathematical programming techniques for achieving best structural performance in different applications (Fukunaga and Vanderplaats, 1991; Haftka and Walsh, 1992; Nagendra et al. 1992).

More recently, GAs has been applied for the optimisation of laminated structures with discrete design variables (Le Riche and Haftka 1993, cited in Herencia et al. 2008).

With regards to thick laminates optimisation, there are not many examples available in literature, due to the large number of variables defined. For instance, the assembly of the torque link introduced in Section 2.3 was optimised for minimum weight. The design variables considered were the laminate thicknesses of the different sections in which the component was divided, and the application presented two fixed stacking sequence configurations. The thicknesses obtained from the optimisation were rounded up for in order to deliver a practical design.

There are alternative methods to reduce the complexity of the optimisation analysis with large number of design variables, next section discuss one of these approaches.

2.5 Multi-level optimisation analysis

Multi-level optimisation schemes were developed to manage the level of complexity found in structural design optimisation problems (Chen et al., 2000). There are several sources in literature that discuss the application of decomposition method in optimisation analysis (Sobieski and James, 1985; Watkis and Morris, 1987; Conti and Cella, 1992; all cited in Chen et al., 2000).

A two-level optimisation approach for the optimisation of anisotropic composite panels was presented by Herencia, et al (2008). A novel transverse shear stiffness formulation was considered in the laminate constitutive matrix. In the first step the optimum laminate thickness and lamination parameters of a smeared laminate were obtained, by performing a gradient-based optimisation analysis, as both design variables are continuous. As a result, the percentages of each ply orientation within the lamina are determined by the optimum lamination parameter, but the optimum stacking sequence is not known. A second optimisation with a genetic algorithm is required then to calculate an optimum laminate stacking sequence which behaviour is similar to the one obtained in the first optimisation analysis. A fitness function was created to evaluate the differences between both laminates. A schematic representation of the two-level optimisation process is depicted in Figure 2-8.

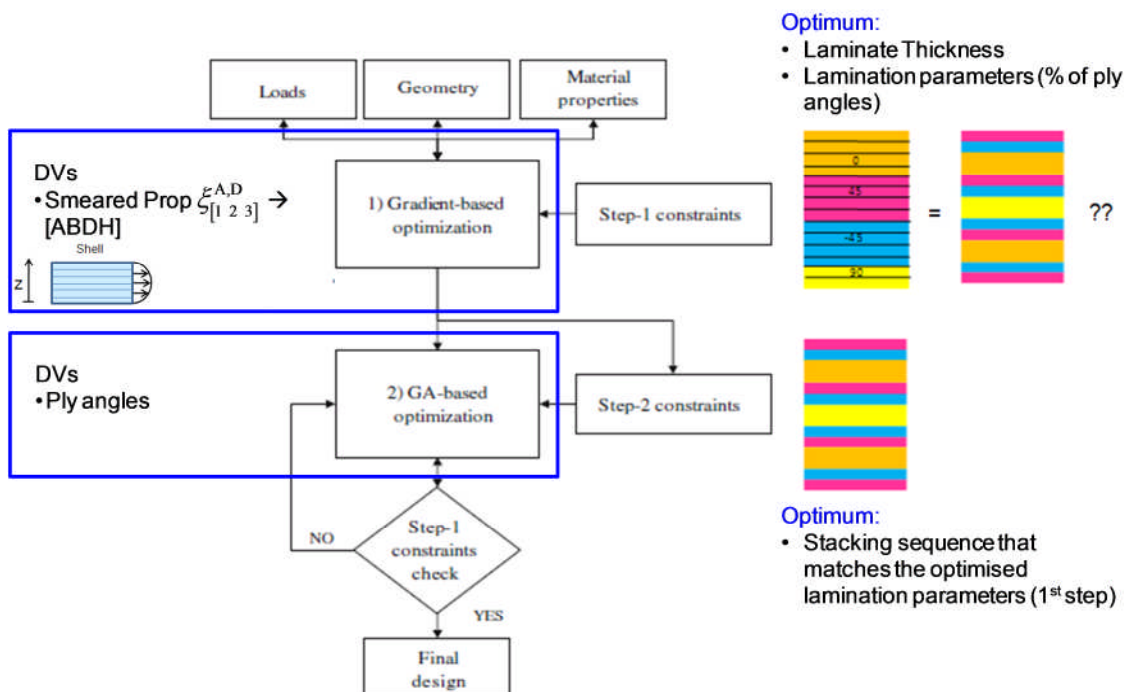


Figure 2-8 2-Level optimisation analysis of an anisotropic composite panel.

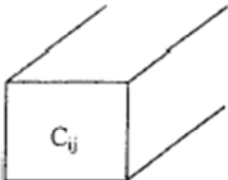
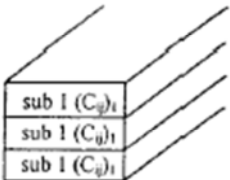
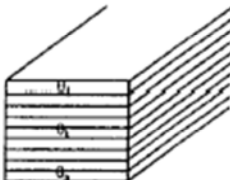
Source: Herencia et al., 2008.

The interest of using lamination parameters for the optimisation process is because they represent less parameter to characterise the stiffness of a laminate than when using a detailed laminate definition (meso-level). Furthermore they have a continuous nature.

A hierarchical multi-level decomposition approach was proposed by Chen et al. (2000) for reducing the complexity of the optimisation of a thick composite structure due to the large number of design variables considered. The authors try to manage the complexity of the optimisation analysis by decomposing the problem into sub-problems with less design variables, adopting the approach developed by Fu (1998) and Fu et al. (1998), and imposing stiffness and strength level constraints. Table 2-1 shows the optimisation levels considered in this analysis.

It can be seen that in decomposition levels 1 and 2 the laminate configuration of the laminate and sublaminates respectively are defined using smeared homogeneous properties.

Table 2-1 Summary of decomposition levels: Source: Fu et al., 1998.

Optimization level:	Level 1 (laminate)	Level 2 (sublaminate)	Level 3 (ply)
Structural model:	Global model, homogeneous stem and surrounding bone, in-plane loading, 3-D	Global model, piece-wise homogeneous stem and surrounding bone, in-plane & out-of-plane loading, 3-D	Local model, individual plies, 3-D
Objective:	Strain energy in the calcar region of the femur	Interfacial shear stress between of the femur and the stem	Stem strength
Design variables:			
Constraints:	Interfacial shear stress between the bond and the stem	In-plane stiffness	In-plane stiffness and out-of-plane stiffness

As part of the methodology presented by the authors (Chen et al., 2000), the FE-based design optimisation framework shown in Figure 2-9 was used, which in order to reduce the computation cost associated to high fidelity design analysis relies on the use of Design of Experiments (DOE) techniques and Response Surface Models (RSM).

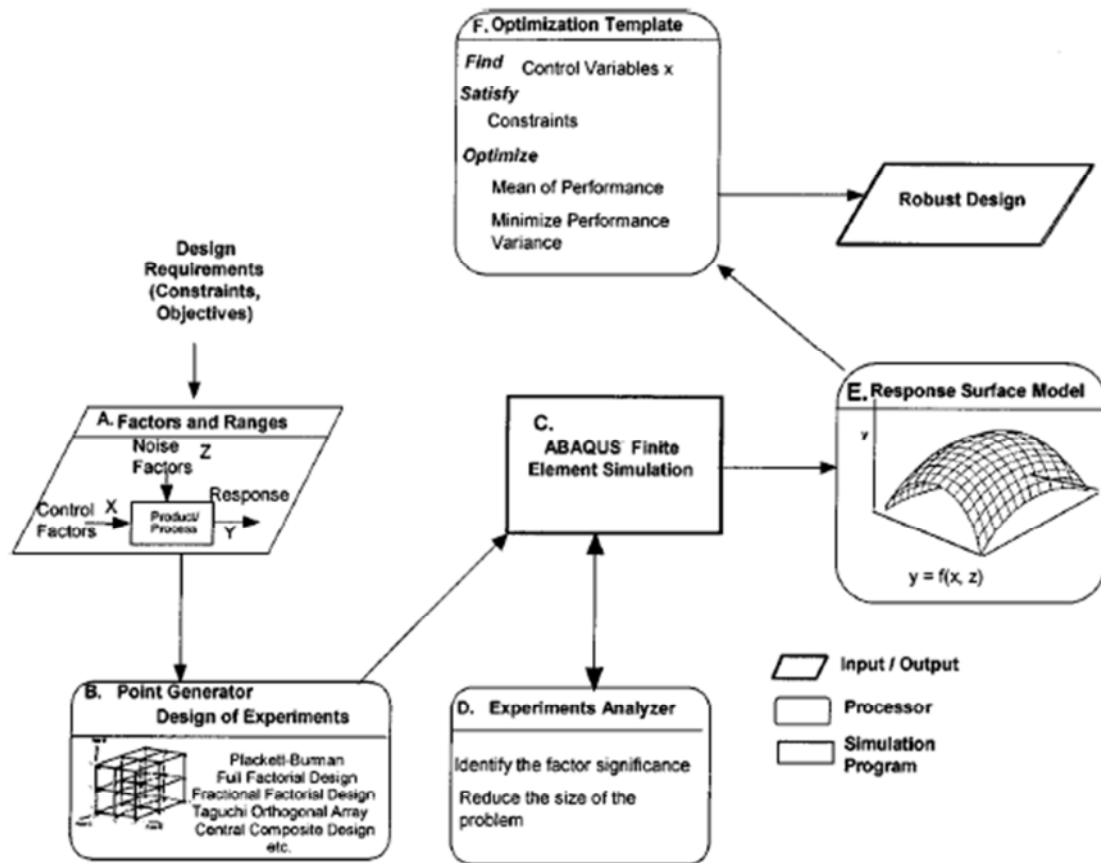


Figure 2-9 FE-based optimisation framework. Source: Chen et al., 2000.

The requirements and implications of a multi-level decomposition approach for the optimisation analysis of thick laminated structures is discussed in Section 7.1.3. The FE-based optimisation approach framework adopted for this research is based in the framework presented by Chen et al. (2000) (Figure 2-9).

2.5.1 Manufacturing constraints

In the past, optimisation techniques were oriented to the application in the design of structures made of isotropic materials, lacking then in capabilities which are unique to the analysis of laminated composite components. For instance, the definition of continuous design variables has no longer interest in composite structures design, which requires the use of discrete nature design variables (ply orientation) in order to provide a practical solution (Gürdal et al., 1999).

The number of ways in which a composite structure is manufactured affects the component performance. In order to obtain the best practical solution the integration of manufacturing constraints within the design optimisation process should be considered (Gürdal et al., 1999).

There are a meaningful number of optimisation analyses available in literature that considers manufacturing constraints in order to provide optimum practical design solutions, limiting also the number of analyses to evaluate.

Ghiasi et al. (2009) applied a Multi-Objective Optimisation (MOO) approach for an optimisation analysis which simultaneously considers structural performance and manufacturing process; finding the optimised design solutions of the Pareto optimal set.

A multi-constraint optimisation methodology using GA was applied by Park et al. (2003) in the design of composite laminated plates manufactured by Resin Transfer Moulding (RTM). The constraints considered were not only structural strength requirements, but also manufacturing process requirements.

Herencia et al, 2008 also included practical manufacturing constraints in the optimisation analysis of anisotropic composite panels with T-shaped stiffeners. The ply contiguity (blocking) were approximated as function of the structure membrane lamination parameters, in order to ensure practical laminates.

A commercial application of manufacturability optimisation was presented by Toporov et al (2005), who applied GA for reducing the mass of a particular aircraft composite component while considering certain manufacturing lay-up rules and the level of structural integrity of the component. This was done by adding or removing plies at certain discrete orientation from the patches, which can vary in location, size and number.



Figure 2-10 Composite wing rib designable patches. Source: Toporov et al., 2005.

This represents an example of application of manufacturing constraints in optimisation problem, to limit the number of feasible design.

The manufacturing constraints considered in this case were the following:

- The number plies grouped together is constrained (ply blocking condition).

- Ensuring a minimum percentage of plies in each direction, for instance 10%.
- Thickness ratio of two adjacent patches is also constrained.

The application of the last manufacturing constraint for the case of weight optimisation of layered solid elements would force that for every patch considered both thickness, the patch volume thickness and the layered element thickness (determined by the number of plies per element times their thickness) should be linked, in order for them to be modified simultaneously, which introduce a high level of complexity to the analysis. Regarding, a constant ply thickness that would represent a modification of the laminate definition within the FE code, either for adding or removing plies.

A schematic representation of the manufacturing design rules considered is depicted below:

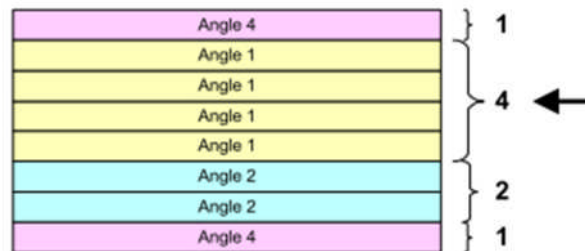


Figure 2-11 Ply blocking. Source: Toporov et al, 2005

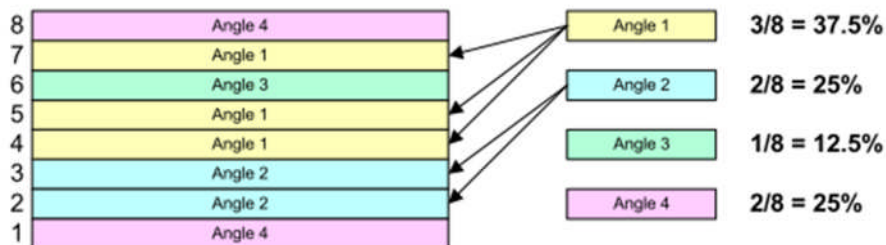


Figure 2-12 Ply percentage for each orientation. Source:Toporov et al., 2005.

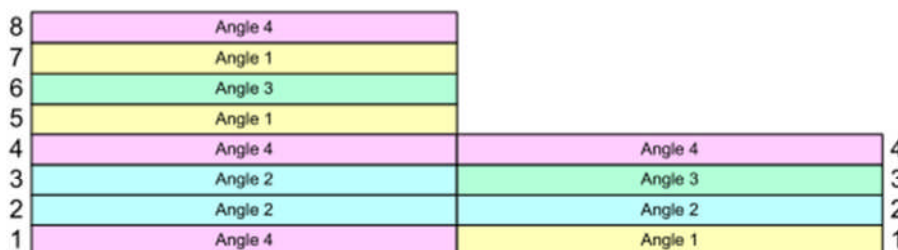


Figure 2-13 Thickness ratio of 2:1 between patches. Source: Toporov et al., 2005.

Additionally, a measure of discontinuity between plies was considered in the objective function.

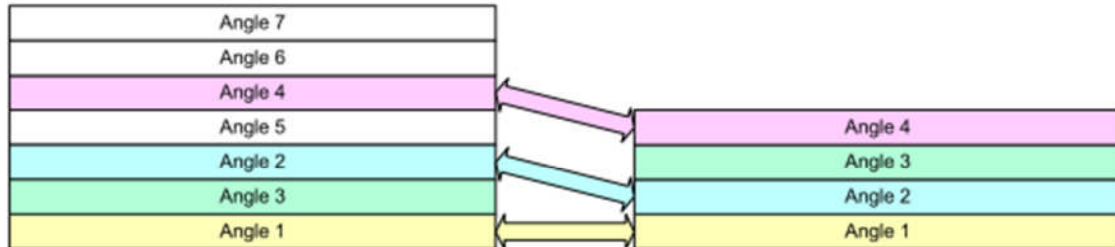


Figure 2-14 Continuity between plies. Source: Toporov et al., 2005.

The level of continuity between patches is measured counting the number of continuous layers (Toporov et al, 2005).

This research does not consider at this stage weight optimisation analysis of UTL composites. However, for thick laminates the application of patches continuity constraint needs to be considered carefully, as the addition and subtraction of the laminate plies would require consistent variation between the volume thicknesses and the layered solid elements thicknesses that represents the laminate, which may result a cumbersome task.

2.5.2 Summary

In this chapter the computational cost associated with the design optimisation analysis of UTL composite structures have been quantified in terms of three main parameters, model, analysis and optimisation costs. Several ways of improving the efficiency of this type of analysis by understanding the problematic behind each one of them, and the design optimisation methods currently available conforms the rest of the section.

Different modelling techniques for computing the 3D stress state inherent to thick laminated structures have been discussed in terms of accuracy and computational cost. Layered solid element formulation, with implemented transverse shear order deformation theories (described in Section 3.5) has proved to be an efficient way of modelling this type of structures, which requires the whole laminate to be divided into sublaminates.

The main concepts related with the optimisation analysis of composite laminates have been introduced. The main problem associated with the optimisation of laminates is the discrete nature of some of its design variables, which result in a non-linear optimisation formulation. Several alternatives to overcome this limitation are discussed, as the use of continuous lamination parameters, the use of genetic algorithms that are useful in the evaluation of a design space with multiple local minimum, or the multi-level

decomposition approach that divide the optimisation problem into sub problems with fewer design variables.

Also, as the ultimate intention of this research is to propose a design exploration methodology that could be applied in industry applications, various examples in which manufacturing constraints have been applied to the design optimisation analysis of laminated structures have been discussed.

3 Analysis of Laminated Composite Structures

3.1 Introduction

Stress induced failure mechanisms of thick laminated plates are highly affected by the transverse shear and normal stresses through the plate thickness, therefore it is vital to understand and accurately characterise these stresses. This chapter presents different theories developed for modelling laminated composite plates, providing a general description of each one of them, focusing on the discussion of their advantages and limitations for accurately represent the through thickness stresses, as well as their suitability for each application. Interlaminar shear stresses and free edge effects are also discussed due to their influence in delamination failure mechanism of thick laminates.

3.2 Classic Lamination Theory (CLT)

Classic Lamination Theory is developed on the assumption of a plane stress state, $\sigma_z = 0$, by which the sections originally plane and normal to the plate midplane remain plane and normal after deformation (Agarwal et al., 2006; Baker et al., 2004; Kollár, 2003; Swanson, 1997; Jones, 1999). This assumption limits its scope of application mainly to thin laminated plates (thickness-to-width ratios < 10) under pure bending or pure tension. The assumption considered may introduce an error in the free edges of the plate by neglecting the effect of transverse shear stresses (see Section 3.4). Also, as the theory neglects the effects of transverse shear strain (γ_{xz} and γ_{yz}) under the 2D laminate deformation, the through thickness behaviour of thick plates may differ significantly from the predicted by the CLT (especially on the free edges), which normally presumes a stiffer out-of-plane deflection of the plate (Khandan et al., 2012).

The discontinuous through-thickness response of composite laminated plates, as well as their anisotropic nature, results in the need to consider transverse shear and normal stresses if a more precise response of the component want to be achieved. Section 3.5 presents some developed theories that account for the transverse shear effects in moderately thick plates.

3.3 Stiffness and Strength of laminated composites

This section presents the main equations considered in Classic Lamination Theory to characterise and analyse a thin laminated plate made of unidirectional plies, as they are required in the analyses performed in Section 5.

3.3.1 Micromechanics – Stiffness analysis

The stiffness and strength of a unidirectional fibre reinforced laminae are determined by the ones of their constituents, fibre and matrix, and the relative amount in which they are present. Thus, a micromechanics study is required for their analytical prediction.

Considering a representative ply element, consisting on a single fibre embedded in a matrix, and assuming a perfect bonding between them, the strains of both constituents remain the same when subjected to a stress in the fibre direction. Under this assumption, it is possible to determine the stiffness in the fibre direction E_1 by applying the *Rules of Mixture*.

$$E_1 = V_f E_{1f} + (1 - V_f) E_m \quad (3-1)$$

Being V_f the fibre volume fraction, and E_{1f} and E_m the stiffness of the fibre and matrix in the fibre direction respectively. The longitudinal module E_1 , is normally determined by the fibre properties. Under the same loading conditions, the major Poisson's ratio is:

$$v_{12} = v_f V_f + v_m V_m \quad (3-2)$$

Where v_f and v_m are the volumes of the fibre and matrix respectively, and V_m is the matrix volume fraction.

Considering now the representative element subjected to a transverse stress, the stresses in fibre and matrix are the same, assuming that the Poisson's effect in the fibre direction can be neglected. According to this, the stiffness in the transverse fibre direction E_2 is defined as:

$$E_2 = \frac{1}{\left(\frac{V_f}{E_{2f}}\right) + \left(\frac{1-V_f}{E_m}\right)} \quad (3-3)$$

which is normally determined by the matrix properties. Being E_{2f} and E_m the stiffness of the fibre and matrix in the transverse fibre direction respectively.

The in-plane shear modulus is determined from a representative elements subjected to shear stress:

$$G_{12} = \frac{1}{\left(\frac{V_f}{G_f}\right) + \left(\frac{1-V_f}{G_m}\right)} \quad (3-4)$$

as well normally determined by the matrix properties.

3.3.2 Macromechanics of a lamina – Stiffness analysis

For the development of the stress-strain relation of a FRP of lamina, a study of macromechanics is required, which assumes a homogeneous orthotropic material definition and a plane stress state (as the layer is regarded as a thin-walled), among others.

3.3.2.1 Specially orthotropic ply

An especially orthotropic ply is a type of orthotropic ply in which the material axes (Figure 3-1) coincide with the global axes (Figure 3-2).

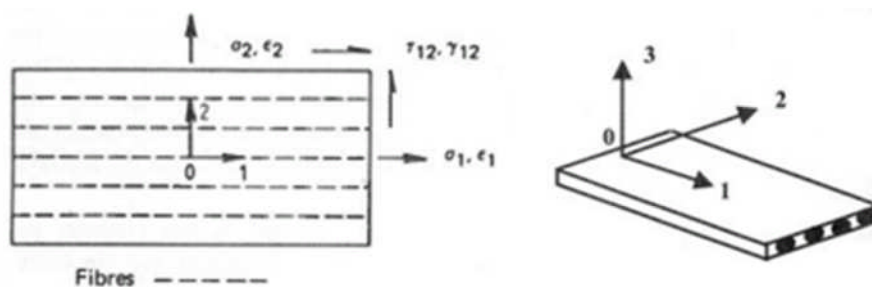


Figure 3-1 Material axes of a single unidirectional ply. Source: Baker et al., 2004.

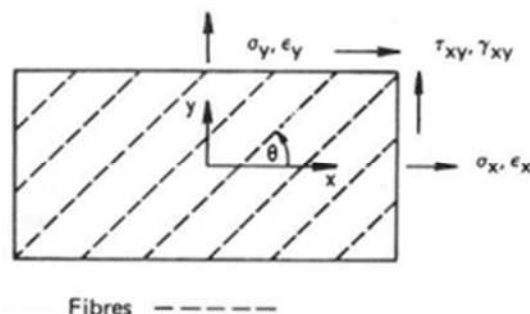


Figure 3-2 Global or laminate axes for a single ply. Source: Baker et al., 2004.

The in-plane stress-strain relationship, for an especially orthotropic ply, in matrix form is

$$\begin{Bmatrix} \sigma_1 \\ \sigma_2 \\ \tau_{12} \end{Bmatrix} = \begin{bmatrix} \frac{E_1}{1 - \nu_{12}\nu_{21}} & \frac{\nu_{21}E_1}{1 - \nu_{12}\nu_{21}} & 0 \\ \frac{\nu_{12}E_2}{1 - \nu_{12}\nu_{21}} & \frac{E_2}{1 - \nu_{12}\nu_{21}} & 0 \\ 0 & 0 & G_{12} \end{bmatrix} \begin{Bmatrix} \varepsilon_1 \\ \varepsilon_2 \\ \gamma_{12} \end{Bmatrix} \quad (3-5)$$

or

$$\begin{Bmatrix} \sigma_1 \\ \sigma_2 \\ \tau_{12} \end{Bmatrix} = \begin{bmatrix} Q_{11} & Q_{12} & 0 \\ Q_{12} & Q_{22} & 0 \\ 0 & 0 & Q_{66} \end{bmatrix} \begin{Bmatrix} \varepsilon_1 \\ \varepsilon_2 \\ \gamma_{12} \end{Bmatrix} \quad (3-6)$$

or in abbreviated form:

$$\{\sigma_{1-2}\} = [Q]\{\varepsilon_{1-2}\} \quad (3-7)$$

Where $[Q]$ is the reduced stiffness matrix, which is symmetric about its leading diagonal, thus:

$$\nu_{12}E_2 = \nu_{21}E_1 \quad (3-8)$$

For an orthotropic ply in 2D there are four independent elastic constants. In practice E_1 , E_2 , ν_{12} , and G_{12} are required, as ν_{21} is determined from the above equation.

9 independent elastic constants are required to fully characterise the stress-strain relationship of an especially orthotropic ply in 3D (E_1 , E_2 , E_3 , G_{12} , G_{23} , G_{31} , ν_{12} , ν_{23} , ν_{31}).

Transversally isotropic ply or laminate (in the 2-3 plane) requires 5 independent elastic constants though:

$$\begin{aligned} E_1 & \quad E_2 & (E_3 = E_2); \\ \nu_{12} & \quad \nu_{23} & (\nu_{13} = \nu_{12}); \\ G_{12} & \quad G_{23} = E_2/2(1 + \nu_{23}) & G_{13} = G_{12} \end{aligned}$$

3.3.2.2 Generally orthotropic ply

The stress-strain relationship of a generally orthotropic ply, in which the fibres are oriented at an angle θ to the global axis, expressed in the global XY axes, can be determined by the transformation of the reduced stiffness matrix $[Q]$ of an especially orthotropic ply to the XY axes.

$$\begin{Bmatrix} \sigma_x \\ \sigma_y \\ \tau_{xy} \end{Bmatrix} = \begin{bmatrix} \bar{Q}_{11} & \bar{Q}_{12} & \bar{Q}_{16} \\ \bar{Q}_{12} & \bar{Q}_{22} & \bar{Q}_{26} \\ \bar{Q}_{16} & \bar{Q}_{26} & \bar{Q}_{66} \end{bmatrix} \begin{Bmatrix} \varepsilon_x \\ \varepsilon_y \\ \gamma_{xy} \end{Bmatrix} \quad (3-9)$$

Or in abbreviated form:

$$\{\sigma_{x-y}\} = [\bar{Q}]\{\varepsilon_{x-y}\} \quad (3-10)$$

The $[\bar{Q}]$ is known as the transformed reduced stiffness matrix, which terms can be defined as

$$\begin{Bmatrix} \bar{Q}_{11} \\ \bar{Q}_{22} \\ \bar{Q}_{66} \\ \bar{Q}_{12} \\ \bar{Q}_{16} \\ \bar{Q}_{26} \end{Bmatrix} = \begin{bmatrix} m^4 & n^4 & 2m^2n^2 & 4m^2n^2 \\ n^4 & m^4 & 2m^2n^2 & 4m^2n^2 \\ m^2n^2 & m^2n^2 & -2m^2n^2 & (m^2 - n^2)^2 \\ m^2n^2 & m^2n^2 & m^4 + n^4 & -4m^2n^2 \\ m^3n & -mn^3 & mn^3 - m^3n & 2(mn^3 - m^3n) \\ mn^3 & -m^3n & m^3n - mn^3 & 2(m^3n - mn^3) \end{bmatrix} \begin{Bmatrix} Q_{11} \\ Q_{22} \\ Q_{12} \\ Q_{66} \end{Bmatrix} \quad (3-11)$$

Where $m = \cos\theta$ and $n = \sin\theta$

From Eq (3-5) and Eq (3-6):

$$Q_{11} = \frac{E_1}{(1 - \nu_{12}\nu_{21})} \quad (3-12)$$

$$Q_{22} = \frac{E_2}{(1 - \nu_{12}\nu_{21})} \quad (3-13)$$

$$Q_{12} = \frac{\nu_{12}E_2}{(1 - \nu_{12}\nu_{21})} \quad (3-14)$$

$$Q_{66} = G_{12} \quad (3-15)$$

3.3.2.3 Invariant forms of stiffness and compliance matrix

Another way of expressing the terms of the transformed reduced stiffness matrix is as follows:

$$\bar{Q}_{11} = U_1 + U_2 \cos 2\theta + U_3 \cos 4\theta \quad (3-16)$$

$$\bar{Q}_{22} = U_1 - U_2 \cos 2\theta + U_3 \cos 4\theta \quad (3-17)$$

$$\bar{Q}_{12} = U_4 - U_3 \cos 4\theta \quad (3-18)$$

$$\bar{Q}_{16} = \frac{1}{2} U_2 \sin 2\theta - U_3 \sin 4\theta \quad (3-19)$$

$$\bar{Q}_{26} = \frac{1}{2} U_2 \sin 2\theta - U_3 \sin 4\theta \quad (3-20)$$

$$\bar{Q}_{66} = U_5 - U_3 \cos 4\theta \quad (3-21)$$

Where

$$\begin{bmatrix} U_1 \\ U_2 \\ U_3 \\ U_4 \\ U_5 \end{bmatrix} = \frac{1}{8} \begin{bmatrix} 3 & 2 & 3 & 4 \\ 4 & 0 & -4 & 0 \\ 1 & -2 & 1 & -4 \\ 1 & -6 & 1 & -4 \\ 1 & -2 & 1 & 4 \end{bmatrix} \begin{bmatrix} Q_{11} \\ Q_{12} \\ Q_{22} \\ Q_{66} \end{bmatrix} \quad (3-22)$$

Where the parameters U_1 to U_5 are called the material invariants.

3.3.3 Strength analysis of an orthotropic lamina

Due to the difficulties associated with determining all failure strengths of an orthotropic ply in all directions at a point, it has been agreed that under a multi-axial stress state, the number of failure strengths measured from a specially orthotropic ply in the principal material axes is limited to X_t , Y_t , (tension) X_c , Y_c , (compression), and S (shear). For comparison purposes, the applied stresses must be transformed into the same coordinate system (σ_1 , σ_2 , τ_{12}).

In order to determine the ply failure various failure criteria have been established, each of them represents a different way of comparing the applied stress with the allowable stress values. Some of the most commonly applied failure criteria are presented here.

3.3.3.1 Maximum-stress theory

Failure occurs if any of the following conditions is not satisfied.

Tensile stresses:

$$\sigma_1 \leq X_t \quad (\text{Fibre break}) \quad \text{and} \quad \sigma_2 \leq Y_t \quad (\text{Matrix crack})$$

$$\text{or} \quad FI1 = \frac{\sigma_1}{X_t} \leq 1 \quad \text{and} \quad FI2 = \frac{\sigma_2}{Y_t} \leq 1$$

Compressive stresses:

$$|\sigma_1| \leq |X_c| \quad (\text{Fibre break}) \quad \text{and} \quad |\sigma_2| \leq |Y_c| \quad (\text{Matrix crack})$$

$$\text{or} \quad FI1 = \left| \frac{\sigma_1}{X_c} \right| \leq 1 \quad \text{and} \quad FI2 = \left| \frac{\sigma_2}{Y_c} \right| \leq 1$$

Shear stresses:

$$|\tau_{12}| \leq S \quad \text{Shear crack}$$

$$\text{or } FI12 = \frac{|\tau_{12}|}{S} \leq 1$$

By this criterion, ply failure would occur if:

- $FI1 \geq 1$ (failure in direction 1 under tension or compression)
- $FI2 \geq 1$ (failure in direction 2 under tension or compression)
- $FI12 \geq 1$ (failure in direction 1-2 under shear)

3.3.3.2 Maximum-strain theory

Failure occurs if any of the following conditions is not satisfied.

Tension strain:

$$\varepsilon_1 \leq \varepsilon_{1t}^u \quad \text{and} \quad \varepsilon_2 \leq \varepsilon_{2t}^u$$

$$\text{or } FI1 = \frac{\varepsilon_1}{\varepsilon_{1t}^u} \leq 1 \quad \text{and} \quad FI2 = \frac{\varepsilon_2}{\varepsilon_{2t}^u} \leq 1$$

Compression strain:

$$|\varepsilon_1| \leq |\varepsilon_{1c}^u| \quad \text{and} \quad |\varepsilon_2| \leq |\varepsilon_{2c}^u|$$

$$\text{or } FI1 = \left| \frac{\varepsilon_1}{\varepsilon_{1c}^u} \right| \leq 1 \quad \text{and} \quad FI2 = \left| \frac{\varepsilon_2}{\varepsilon_{2c}^u} \right| \leq 1$$

Shear strain:

$$|\gamma_{12}| \leq \gamma_{12}^u \quad \text{or} \quad FI12 = \left| \frac{\gamma_{12}}{\gamma_{12}^u} \right| \leq 1$$

By this criterion, ply failure would occur if

- $FI1 \geq 1$ (failure in direction 1 under tension or compression)
- $FI2 \geq 1$ (failure in direction 2 under tension or compression)
- $FI12 \geq 1$ (failure in direction 1-2 under shear)

3.3.3.3 Tsai-Hill theory

Failure would occur if the following condition is not satisfied:

$$\left[\frac{\sigma_1}{X} \right]^2 + \left[\frac{\sigma_2}{Y} \right]^2 + \left[\frac{\tau_{12}}{S} \right]^2 - \frac{\sigma_1 \sigma_2}{X X} < 1 \quad (3-23)$$

Where $X = X_t$ or X_c (in absolute value) and $Y = Y_t$ or Y_c (in absolute value)

It is an interactive criterion that considers all stress components. It would determine the ply failure, but not the mode of failure.

3.3.3.4 Tsai-Wu stress theory

The Tsai-Wu failure criteria can be expressed as:

$$FI = F_1\sigma_1 + F_2\sigma_2 + F_{11}\sigma_1^2 + F_{22}\sigma_2^2 + F_{66}\tau_{12}^2 + 2F_{12}\sigma_1\sigma_2 \quad (3-24)$$

where

$$F_1 = \frac{1}{X_t} - \frac{1}{X_c} \quad F_{11} = \frac{1}{X_t X_c}$$

$$F_2 = \frac{1}{Y_t} - \frac{1}{Y_c} \quad F_{22} = \frac{1}{Y_t Y_c}$$

$$F_{66} = \frac{1}{S^2}$$

The absolute values of X_c , Y_c are considered, and

$$F_{12} \cong f_{12} \sqrt{F_{11} F_{22}} = f_{12} \sqrt{\frac{1}{X_t X_c Y_t Y_c}}$$

It is an interactive criterion, considering all stress components, and it determines the ply failure, but not the failure mode.

Interaction terms (like F_{12}) are difficult to measure and may affect significantly the shape of the failure curve (Figure 3-3). It is desired in order to assign a suitable interaction term value to check the finite element code recommendations (normally $F_{12}=0$).

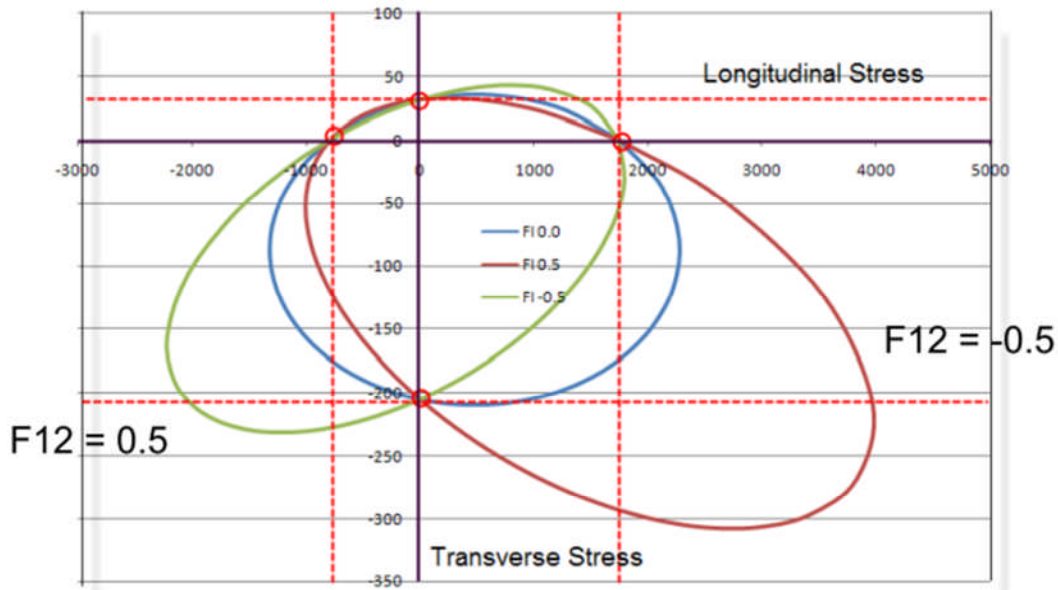


Figure 3-3 Tsai-Wu failure curves obtained for three different interaction terms F_{12} . For $F_{12}=0.0$ (blue), for $F_{12}=0.5$ (green), for $F_{12}=-0.5$ (brown). Source: Abbey, 2010.

The fact that the failure index is represented by quadratic terms restricts the possibility of scaling the design by means of the FI (Abbey, 2010). For instance, a FI of 7.8 does not represent a laminate that is 7.8 times weaker. Most commercial finite element codes provide the option to output the Tsai-Wu failure index as an alternative index called the Strength Ratio (S.R.).

The S.R. is a linear scale factor relating the allowable stress and the induced stress, which could be used to not only to predict the laminate failure, but to determine the design modifications required to achieve the desired stress levels. The Margin of Safety (M.S.) = S.R. - 1 thus the S.R. is equivalent to the Reserve Factor (R.F.). A value of S.R. < 1.0 means then the laminate failure.

The failure theory used to obtain the F.I. will determine the expression by which the S.R is derived. For the case of the Tsai-Wu failure criteria, factoring all terms of its expression by the Strength Ratio (S.R.) in order to achieve the failure boundary (FI=1.0), a second order linear equation is determined, which roots determine the SR.

$$0.0 = \left[\frac{\sigma_1^2}{X_T X_C} + \frac{\sigma_2^2}{Y_T Y_C} + \frac{\tau_{12}^2}{S^2} + 2F_{12}\sigma_1\sigma_2 \right] SR^2 + \left[\sigma_1 \left[\frac{1}{X_T} - \frac{1}{X_C} \right] + \sigma_2 \left[\frac{1}{Y_T} - \frac{1}{Y_C} \right] \right] SR - 1.0 \quad (3-25)$$

3.3.4 Macromechanics of a Laminate

3.3.4.1 Constitutive equation

The resultant in-plane forces and moments intensity (per unit length) acting on each layer, say ply- k , of a small laminate element are:

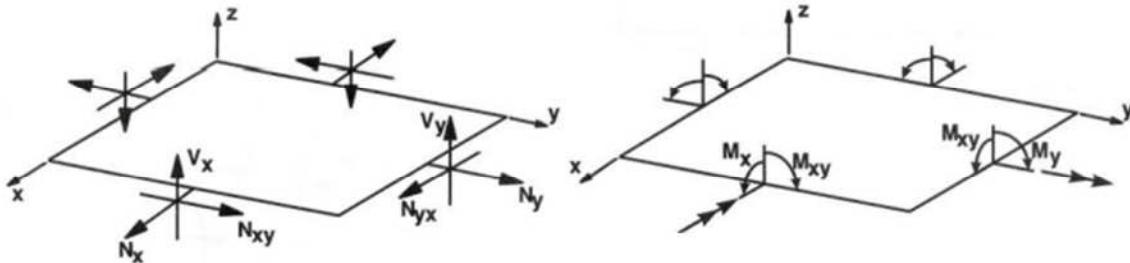


Figure 3-4 In-plane forces and moments acting on a laminate reference plane.

Source: Barbero, 1999.

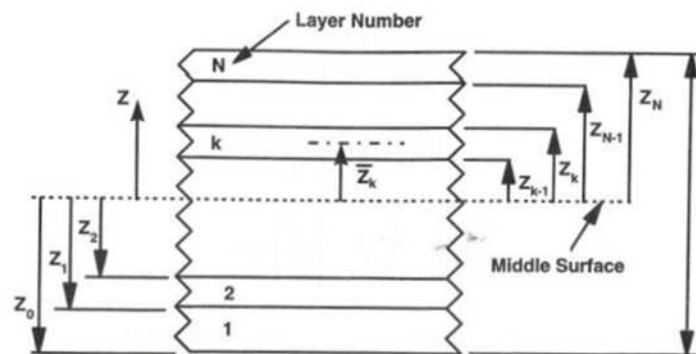


Figure 3-5 Distance from each layer top and bottom planes to the laminate reference plane. Source: Barbero, 1999.

$$N_x = \int_{z_{k-1}}^{z_k} \sigma_x dz \quad (3-26)$$

$$N_y = \int_{z_{k-1}}^{z_k} \sigma_y dz$$

$$N_{xy} = \int_{z_{k-1}}^{z_k} \tau_{xy} dz$$

$$M_x = \int_{z_{k-1}}^{z_k} \sigma_x z dz \quad (3-27)$$

$$M_y = \int_{z_{k-1}}^{z_k} \sigma_y z dz$$

$$M_{xy} = \int_{z_{k-1}}^{z_k} \tau_{xy} z dz$$

Substituting the integral in the previous expressions with the summation of the contribution of each layer for a laminate made up of n layers:

$$\begin{Bmatrix} N_x \\ N_y \\ N_{xy} \end{Bmatrix} = \int_{z_{k-1}}^{z_k} \begin{Bmatrix} \sigma_x \\ \sigma_y \\ \tau_{xy} \end{Bmatrix} dz = \sum_{k=1}^n \int_{z_{k-1}}^{z_k} \begin{Bmatrix} \sigma_x \\ \sigma_y \\ \tau_{xy} \end{Bmatrix} dz \quad (3-28)$$

and

$$\begin{Bmatrix} M_x \\ M_y \\ M_{xy} \end{Bmatrix} = \int_{z_{k-1}}^{z_k} \begin{Bmatrix} \sigma_x \\ \sigma_y \\ \tau_{xy} \end{Bmatrix} z dz = \sum_{k=1}^n \int_{z_{k-1}}^{z_k} \begin{Bmatrix} \sigma_x \\ \sigma_y \\ \tau_{xy} \end{Bmatrix} z dz \quad (3-29)$$

Which represents the resultant system of forces and moments acting at the laminate midplane.

From Eq (3-10) $\{\sigma_{x-y}\} = [\bar{Q}]_k \{\varepsilon_{x-y}\}$. Expressing the strains in terms of midplane strains and plate curvatures (Kollár, 2003):

$$\{\sigma_{x-y}\} = [\bar{Q}]_k \{\varepsilon^0 + z k_{x-y}\} \quad (3-30)$$

By replacing the stresses in (3-28) and (3-29) with the equation (3-30)

$$\begin{aligned} \begin{Bmatrix} N_x \\ N_y \\ N_{xy} \end{Bmatrix} &= \sum_{k=1}^n \left\{ \int_{z_{k-1}}^{z_k} \begin{bmatrix} \bar{Q}_{11} & \bar{Q}_{12} & \bar{Q}_{16} \\ Q_{12} & \bar{Q}_{22} & \bar{Q}_{26} \\ \bar{Q}_{16} & \bar{Q}_{26} & \bar{Q}_{66} \end{bmatrix} \begin{Bmatrix} \varepsilon_x^0 \\ \varepsilon_y^0 \\ \gamma_{xy}^0 \end{Bmatrix} \right. \\ &\quad \left. + z \begin{Bmatrix} k_x \\ k_y \\ k_{xy} \end{Bmatrix} \right\} dz \end{aligned} \quad (3-31)$$

$$\begin{aligned} \begin{Bmatrix} M_x \\ M_y \\ M_{xy} \end{Bmatrix} &= \sum_{k=1}^n \left\{ \int_{z_{k-1}}^{z_k} \begin{bmatrix} \bar{Q}_{11} & \bar{Q}_{12} & \bar{Q}_{16} \\ Q_{12} & \bar{Q}_{22} & \bar{Q}_{26} \\ \bar{Q}_{16} & \bar{Q}_{26} & \bar{Q}_{66} \end{bmatrix} \begin{Bmatrix} \varepsilon_x^0 \\ \varepsilon_y^0 \\ \gamma_{xy}^0 \end{Bmatrix} \right. \\ &\quad \left. + z \begin{Bmatrix} k_x \\ k_y \\ k_{xy} \end{Bmatrix} \right\} z dz \end{aligned} \quad (3-32)$$

Considering not only that the midplane strains and plate curvatures are constant at a layer level, but also that the transformed reduced stiffness matrix $[\bar{Q}]$ remains constant within a laminate, they all can be extracted from the integration. By using the definition of three new matrices, the previous equations can finally be expressed as:

$$\begin{Bmatrix} N_x \\ N_y \\ N_{xy} \end{Bmatrix} = \begin{bmatrix} A_{11} & A_{12} & A_{16} \\ A_{12} & A_{22} & A_{26} \\ A_{16} & A_{26} & A_{66} \end{bmatrix} \begin{Bmatrix} \varepsilon_x^0 \\ \varepsilon_y^0 \\ \gamma_{xy}^0 \end{Bmatrix} + \begin{bmatrix} B_{11} & B_{12} & B_{16} \\ B_{12} & B_{22} & B_{26} \\ B_{16} & B_{26} & B_{66} \end{bmatrix} \begin{Bmatrix} k_x \\ k_y \\ k_{xy} \end{Bmatrix} \quad (3-33)$$

$$\begin{Bmatrix} M_x \\ M_y \\ M_{xy} \end{Bmatrix} = \begin{bmatrix} B_{11} & B_{12} & B_{16} \\ B_{12} & B_{22} & B_{26} \\ B_{16} & B_{26} & B_{66} \end{bmatrix} \begin{Bmatrix} \varepsilon_x^0 \\ \varepsilon_y^0 \\ \gamma_{xy}^0 \end{Bmatrix} + \begin{bmatrix} D_{11} & D_{12} & D_{16} \\ D_{12} & D_{22} & D_{26} \\ D_{16} & D_{26} & D_{66} \end{bmatrix} \begin{Bmatrix} k_x \\ k_y \\ k_{xy} \end{Bmatrix} \quad (3-34)$$

Where:

$$[A_{ij}] = \sum_{k=1}^n [\bar{Q}_{ij}]_k (z_k - z_{k-1}) \quad (3-35)$$

$$[B_{ij}] = \frac{1}{2} \sum_{k=1}^n [\bar{Q}_{ij}]_k (z_k^2 - z_{k-1}^2)$$

$$[D_{ij}] = \frac{1}{3} \sum_{k=1}^n [\bar{Q}_{ij}]_k (z_k^3 - z_{k-1}^3)$$

The laminate constitutive equation is then:

$$\begin{Bmatrix} N \\ M \end{Bmatrix} = \begin{bmatrix} A & B \\ B & D \end{bmatrix} \begin{Bmatrix} \varepsilon^0 \\ \kappa \end{Bmatrix} \quad (3-36)$$

The A , B , D matrices are known as the *extensional stiffness matrix*, *coupling stiffness matrix*, and *bending stiffness matrix*, respectively. The extensional stiffness matrix relates the resultant in-plane forces to the in-plane strains, and the bending stiffness matrix relates the resultant out-of-plane moments to the plate curvatures.

The coupling stiffness matrix $[B]$ accounts for the coupling between bending and extension of the laminate, by which the normal and shear in-plane forces generates plate curvatures (twisting and bending) accompanied by in-plane strains. Equivalently, bending and twisting moments produce not only curvatures but also in-plane deformations.

Figure 3-6 illustrates some coupling terms (third column) of the constitutive ABD matrix. Whenever any of these terms is zero there is no corresponding coupling effect. Similarly, the remaining coupling terms (A_{26} , D_{26} , B_{26} , B_{22}) can be depicted by applying an in-plane force N_y and a moment M_y in the y - z plane (Kollár, 2003). For a more detail description of each coupling effect associated with each ABD matrix term refer to Kollár (2003).

Coupling	No Coupling	Element
Extension–shear 		A_{16}
Bending–twist 		D_{16}
Extension–twist 		B_{16}
In-plane–out-of-plane 		B_{11}
		B_{12}
		B_{66}
Extension–extension 		A_{12}
Bending–bending 		D_{12}

Figure 3-6 Coupling terms within a lamina considered in the constitutive stiffness matrix ABD. Source: Kollár, 2003.

The laminate stiffness can be tailored by altering the laminate definition (i.e. stacking sequence, material properties, layers' orientations), in order to eliminate or minimise unwanted coupling effects, so as to meet certain specific requirements. A series of well know laminate constructions, which have a direct effect on specific ABD matrix stiffness factors (reducing them to zero), are presented below,

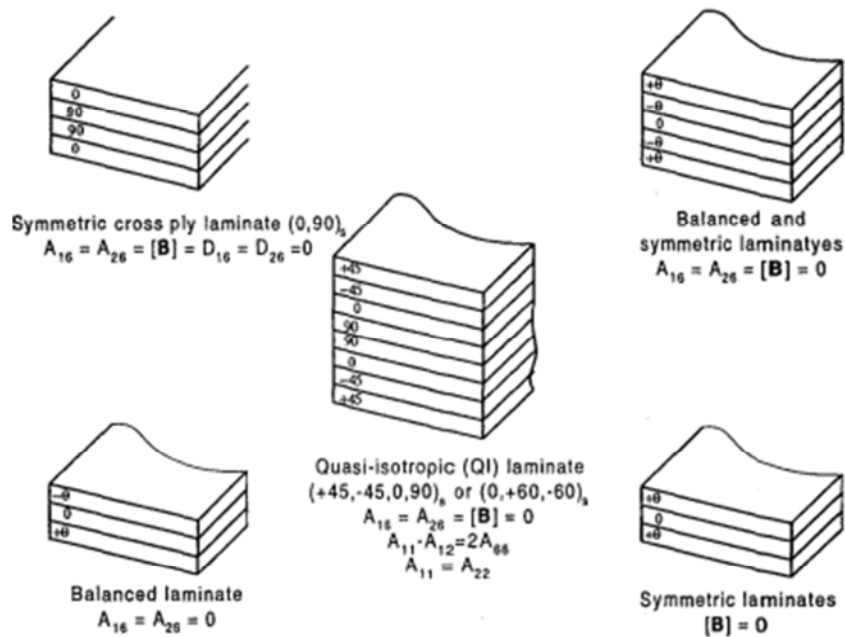


Figure 3-7 Design guidelines affecting the coupling phenomena in laminated composite plates. Source: Marsden and Irving, 2002.

- Symmetric laminates, in which the layers are symmetrically placed with respect to the midplane, have no bending-extension coupling, thus the corresponding $[\mathbf{B}]$ matrix is zero.
- A_{16} and A_{26} account for the coupling between in-plane forces and in in-plane shear strains. They can be reduced to zero by using any of the three following laminate constructions (1) UD laminates with all its layers oriented in the same direction, (2) cross-ply laminates, containing only layers oriented at 0° and 90° , and (3) balanced laminates, which are those with equal number of layers oriented at $\pm\theta$ angle. These laminates can also be symmetric.
- D_{16} and D_{26} represent the bending-twisting coupling. This effect is cancelled in cross-ply laminates. Another alternative to minimise its effects is by using balanced anti-symmetric laminates, which can be improved by increasing the number of layers. The use of this type of laminate construction is not common, mainly due to its non-symmetric nature.
- A particular type of construction that worth mentioning is the quasi-isotropic. In this type of laminate the extensional stiffness matrix $[\mathbf{A}]$ is isotropic (orientation independent). As for the case of isotropic plates, the following equations are satisfied: $A_{11} = A_{22}$, $A_{11} - A_{12} = 2A_{66}$, and $A_{16} = A_{26} = 0$. The design requirements for a laminate to be quasi-isotropic are:

- The laminate should have three or more layers.
- All layers must have the same thickness and reduced stiffness matrix $[Q]$ (material properties).
- The angle between consecutive plies remains constant.

Other coupling phenomena to consider are:

- B_{11} , B_{12} and B_{22} accounts for the in-plane forces-bending moments coupling. When these factors are zero the applied direct forces will generate no plate curvatures and applied bending moments will not have any effect on the axial strains.
- B_{66} is the in-plane shear force-torque coupling.

3.3.5 Strength analysis of a laminate

3.3.5.1 Procedure for laminate strength analysis

- a) Determine the $[ABD]$ and then its inverse $[abd]$ matrices for the laminate concerned
- b) Calculate the mid-plane strains in the laminate, from:

$$\begin{Bmatrix} \varepsilon^0 \\ k \end{Bmatrix} = \begin{bmatrix} a & b \\ b & d \end{bmatrix} \begin{Bmatrix} N \\ M \end{Bmatrix} \quad (3-37)$$

- c) Work out the total strain for each ply

$$\begin{Bmatrix} \varepsilon_x \\ \varepsilon_y \\ \gamma_{xy} \end{Bmatrix} = \begin{Bmatrix} \varepsilon_x^0 \\ \varepsilon_y^0 \\ \gamma_{xy}^0 \end{Bmatrix} + z \begin{Bmatrix} k_x \\ k_y \\ k_{xy} \end{Bmatrix} \quad (3-38)$$

And then transform it to the principal material axes by

$$\begin{Bmatrix} \varepsilon_1 \\ \varepsilon_2 \\ \gamma_{12} \end{Bmatrix} = [T_\varepsilon] \begin{Bmatrix} \varepsilon_x \\ \varepsilon_y \\ \gamma_{xy} \end{Bmatrix} \quad (3-39)$$

where

$$\begin{Bmatrix} \varepsilon_1 \\ \varepsilon_2 \\ \gamma_{12} \end{Bmatrix} = \begin{bmatrix} \cos^2\theta & \sin^2\theta & \sin\theta\cos\theta \\ \sin^2\theta & \cos^2\theta & -\sin\theta\cos\theta \\ -2\sin\theta\cos\theta & 2\sin\theta\cos\theta & \cos^2\theta - \sin^2\theta \end{bmatrix} \begin{Bmatrix} \varepsilon_x \\ \varepsilon_y \\ \gamma_{xy} \end{Bmatrix} \quad (3-40)$$

d) Calculate the stresses in the layer coordinate system for each ply

$$\begin{Bmatrix} \sigma_1 \\ \sigma_2 \\ \tau_{12} \end{Bmatrix} = \begin{bmatrix} Q_{11} & Q_{12} & 0 \\ Q_{21} & Q_{22} & 0 \\ 0 & 0 & Q_{66} \end{bmatrix} \begin{Bmatrix} \varepsilon_1 \\ \varepsilon_2 \\ \gamma_{12} \end{Bmatrix} \quad (3-41)$$

And apply the desired failure criteria for a ply strength evaluation.

3.4 Limitations to CLT

3.4.1 Interlaminar shear stresses and free edge effects

The general plane stress assumption that the CLT is based on enables to predict in-plane stresses in a laminated plate under constant forces and moments applied, but may cause inaccurate stresses prediction in certain regions of the model, such as at the free-edges. In this case, the through thickness stresses σ_z , τ_{xz} , and τ_{yz} need to be considered in order to ensure the boundary condition equilibrium (despite CLT does not consider them). These stresses, called the interlaminar shear stresses, may appear as a result of Poisson's ratios mismatch or due to coupling coefficients of adjacent plies (Agarwal et al., 2006; Baker et al., 2004; Barbero, 2008; Matthews et al., 2000; Swanson, 1997), and they are present in the contact surfaces between plies, as well as within the ply interface.

The interlaminar stresses are then largest at the lamina interface, but may be quite significant also in the region close to the free edges (laminated side edges, cutouts, holes, etc.), within a distance from the edge approximately equal to the laminate thickness, and their effects decrease rapidly as soon as they move away from the boundaries. They have a major influence on the free edge of thick plates under bending applications (thickness-to-width ratios > 10), regardless of the fact that in regions away from the edges the laminate theory provides quite accurate in-plane stress results.

Figure 3-8 (Abbey, 2010) depicts the free edge effects on the stress distribution across the width of a four-ply balanced symmetric laminate, with plies oriented at $\pm 45^\circ$ (Pipes and Pagano, 1970). The results were obtained by the finite-difference method. In regions away from the edges the stresses remain constant and its values correspond

to the predicted by the classic lamination theory. However, in the vicinity of the laminate free edges, τ_{xz} increases significantly, while σ_x decreases and τ_{xy} tends to zero. The other three through thickness stresses increase their values although not as much as τ_{xz} . It has been observed by carrying out analyses with different laminate geometries, that the region of influence of the free edge effects is approximately equal to the laminate thickness, in which the stresses present a different value from the one predicted by the lamination theory.

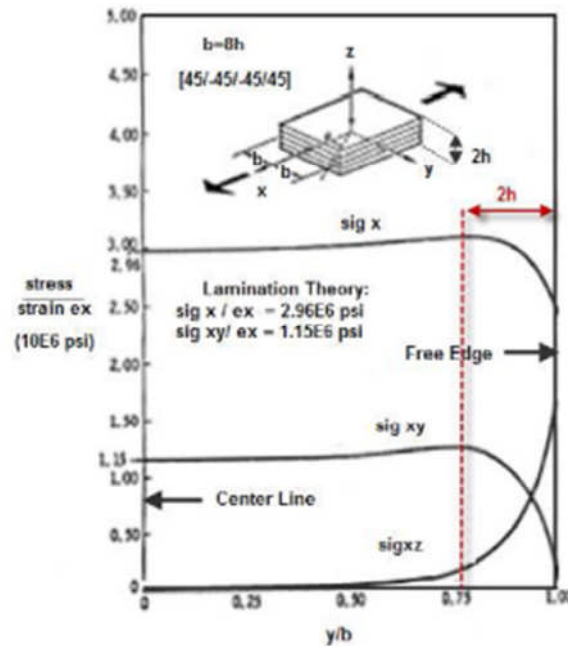


Figure 3-8 Stress distribution across the laminate thickness of a balanced symmetric laminate. Source: Abbey, 2010.

Large interlaminar shear stresses between adjacent plies may generate matrix cracks on the free edge. In some cases these cracks may lead to a laminate delamination failure mechanism (Figure 3-9), which under fatigue loading conditions significantly affects the fatigue life and fatigue strength of the component.

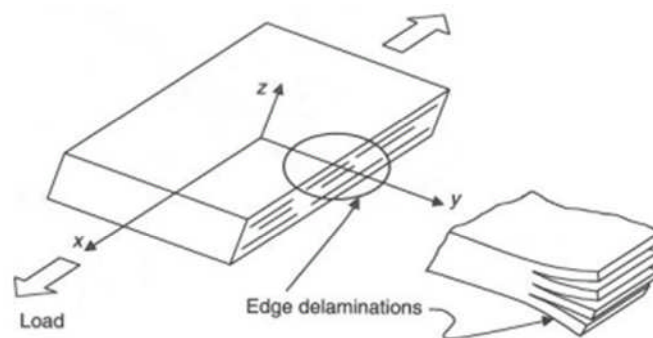


Figure 3-9 Free edge delamination mechanism. Source: Agarwal et al., 2006.

According to Agarwal et al. (2006) the magnitude and nature of the interlaminar shear stresses is influenced by the laminate stacking sequence. Thus in order to avoid delamination failure efforts should be made at the early stage of the design process to minimise the interlaminar shear effects. Generally, stacking sequences that give the lower values of D_{16} and D_{26} without influencing any other terms of the laminate stiffness matrix should be selected (Agarwal et al., 2006).

3.5 Deformations due to transverse shear

Following, various theories that account for the transverse shear effects in moderately thick plates are presented.

3.5.1 First-Order shear deformation theory

CLT and classical laminated-plate theory were developed under the assumption that the out-of-plane shear strains γ_{xz} and γ_{yz} are zero. This assumption is derived from the premise that plane sections remain plane and normal to the plate midplane during deformation. In order to consider the shear strains γ_{xz} and γ_{yz} this last assumption needs to be modified (Agarwal et al, 2006).

First-order shear deformation theory (FSDT) assumes that sections originally plane and normal to the plate midplane remain plane, but not normal after deformation. The displacement field for the FSDT is given by (Agarwal et al., 2006) (see Figure 3-10):

$$u(x, y, z) = u_0(x, y) + z\phi_x(x, y) \quad (3-42)$$

$$v(x, y, z) = v_0(x, y) + z\phi_y(x, y)$$

$$w(x, y, z) = w_0(x, y)$$

Where ϕ_x and ϕ_y are the rotations about the y and x axes, respectively. For the displacement field proposed, the following shear strains are generated:

$$\gamma_{xz}^0 = \phi_x + \frac{\partial w_0}{\partial x} \quad (3-43)$$

$$\gamma_{yz}^0 = \phi_y + \frac{\partial w_0}{\partial y}$$

As the shear strains are constant across the thickness (Barbero, 1999; Agarwal et al, 2006), FSDT predicts uniform through-thickness shear stress across each lamina thickness. The assumption proposed gives accurate results for the case of thin laminates but induces some errors for thick laminates and for when analysing laminates which layers have very different shear stiffness (Barbero, 1999). Also, this assumption introduces an inaccuracy in the formulation, as the transverse shear stresses τ_{xz} and τ_{yz} must be zero on the top and bottom surfaces of the plate (boundary condition).

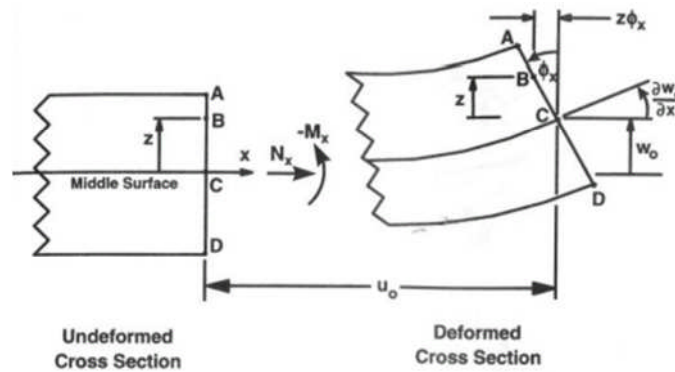


Figure 3-10 Plate geometry deformation in the x-z plane. Source: Barbero, 1999.

The shear-force resultants Q_{xz} and Q_{yz} are related to the shear strains γ_{xz} and γ_{yz} by the transverse shear matrix $[H]$, according to:

$$\begin{Bmatrix} Q_{xz} \\ Q_{yz} \end{Bmatrix} = \begin{bmatrix} H_{55} & H_{45} \\ H_{45} & H_{44} \end{bmatrix} \begin{Bmatrix} \gamma_{xz} \\ \gamma_{yz} \end{Bmatrix} \quad (3-44)$$

Where:

$$H_{ij} = K(z) \int_{z_{k-1}}^{z_k} \bar{Q}_{ij} dz \quad (3-45)$$

In which \bar{Q}_{ij} are the transformed stiffness coefficients, and $K(z)$ is the shear correction coefficient to introduce the transverse shear stresses variation across the plate thickness. Normally $K = 5/6$.

This theory has been implemented within the element formulation of layered shell elements, and is available in almost all commercial Finite Element codes for stress calculation of thin laminated composite applications.

3.5.2 Higher-order shear deformation theory

A higher-order shear deformation theory has been developed to satisfy the zero shear stresses condition at the top and bottom surfaces of the plate, not accounted in FSDT. The displacement field for this theory is given by (Agarwal et al., 2006):

$$u(x, y, z) = u_0(x, y) + z\phi_x(x, y) - \frac{4}{3h^2}z^3 \left(\phi_x + \frac{\partial w}{\partial x} \right) \quad (3-46)$$

$$v(x, y, z) = v_0(x, y) + z\phi_y(x, y) - \frac{4}{3h^2}z^3 \left(\phi_y + \frac{\partial w}{\partial y} \right)$$

$$w(x, y, z) = w_0(x, y)$$

The introduction of cubic terms in u and v displacements enables to satisfy the transverse shear-stress boundary condition at the top and bottom surfaces of the plate. Thus, no shear correction factor is required for this formulation.

Higher-order theory assumes a parabolic transverse shear stress distribution through the thickness of each lamina, whereas the first-order theory assumes a constant transverse shear stress distribution.

3.5.3 Layerwise theory

More recently, layerwise theories (multi-layer theory) have been developed to predict laminate global response and 3d stress distribution more accurately.

Consider a constant thickness laminate made up of uniform thickness layers with arbitrary orientation. The laminate can be divided, in the through thickness direction, into a series of numerical layers (kinematic layers), which can be greater than, equal to, or less than the number of physical laminate plies (Zhang et al., 2010).

Layerwise theory main idea is to assume a certain in-plane displacement field through the laminate thickness (Figure 3-11) or stress model for each numerical layer, and then apply equilibrium and compatibility equations at the layers interface to reduce the number of the unknown variables (Khandan et al., 2012).

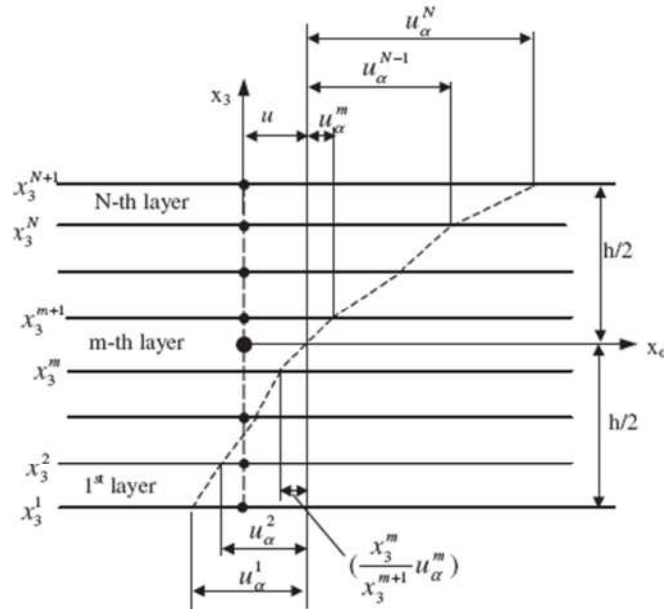


Figure 3-11 Assumed in-plane displacement field u_α through the laminate thickness for a layerwise theory. Source: Zhang et al., 2010.

For the case of thick laminate plates, the number of unknown variables required increases significantly with the number of layers, resulting in computationally expensive study (Khandan et al., 2012). Some authors (Cho and Parmenter, 1993) though developed models in which the number of unknown variables is independent of the number of layers.

The principal limitation of the Equivalent Single Layer (ESL) theories described in Section 3.5 is the lack of accuracy for describing the through thickness behaviour of thick laminates, especially in the vicinity of the free edges, where interlaminar shear effect become significant. Layerwise theory tries to overcome such deficiencies by proposing more accurate layerwise field equations are required.

Zig-zag theories (ZZ) are developed to account for the piece-wise behaviour of the displacement and stress fields in the through-thickness direction (Khandan et al., 2012). In this case, in order to ensure the equilibrium condition at the layer interface, the transverse stresses must be continuous. *“The compatibility of the displacements and the interlaminar equilibrium of the transverse stresses in the thickness direction are assured by defining a new stiffness matrix called $C0z$ ”* (Khandan et al., 2012).

For a more detail discussion of the laminate theories refer to Khandan et al. (2012).

3.5.4 Laminate constitutive equations including TSD

By considering the transverse shear deformation (TSD), the laminate constitutive equation, Eq. (3-36), can be expressed as (Herencia et al., 2008):

$$\begin{Bmatrix} N \\ M \\ Q \end{Bmatrix} = \begin{bmatrix} A & B & 0 \\ B & D & 0 \\ 0 & 0 & H \end{bmatrix} \begin{Bmatrix} \varepsilon^0 \\ k \\ \gamma^0 \end{Bmatrix} \quad (3-47)$$

Where $\{Q\}$ is the transverse shear vector, $[H]$ is the transverse shear matrix, and $\{\gamma\}$ is the transverse shear strain vector.

The stiffness properties presented in Eq. (3-47) can be expressed in terms of material stiffness invariants (U, U^*) and 12 lamination parameters (the expressions for the U stiffness invariants are given in Eq. (3-22)). For symmetric laminates ($[B]=0$) the number of lamination parameters are reduced to 8. Moreover, considering only orthotropic plies at $0^\circ, 90^\circ, +45^\circ$ and -45° , the lamination parameters are finally reduce to 6 (Herencia et al, 2008). Thus, the $[ABD]$ stiffness matrix terms can be expressed as:

$$\begin{Bmatrix} A_{111} \\ A_{112} \\ A_{222} \\ A_{666} \\ A_{166} \\ A_{266} \end{Bmatrix} = h \begin{bmatrix} 1 & \xi_1^A & \xi_2^A & 0 & 0 \\ 0 & 0 & -\xi_2^A & 1 & 0 \\ 0 & -\xi_1^A & \xi_2^A & 0 & 0 \\ 1 & 0 & \xi_2^A & 0 & 0 \\ 0 & \xi_3^A & -\xi_2^A & 0 & 1 \\ 0 & \frac{\xi_3^A}{2} & 0 & 0 & 0 \\ 0 & \frac{\xi_3^A}{2} & 0 & 0 & 0 \end{bmatrix} \begin{Bmatrix} U_1 \\ U_2 \\ U_3 \\ U_4 \\ U_5 \end{Bmatrix} \quad (3-48)$$

$$\begin{Bmatrix} D_{111} \\ D_{112} \\ D_{222} \\ D_{666} \\ D_{166} \\ D_{266} \end{Bmatrix} = \frac{h^3}{12} \begin{bmatrix} 1 & \xi_1^D & \xi_2^D & 0 & 0 \\ 0 & 0 & -\xi_2^D & 1 & 0 \\ 0 & -\xi_1^D & \xi_2^D & 0 & 0 \\ 1 & 0 & \xi_2^D & 0 & 0 \\ 0 & \xi_3^D & -\xi_2^D & 0 & 1 \\ 0 & \frac{\xi_3^D}{2} & 0 & 0 & 0 \\ 0 & \frac{\xi_3^D}{2} & 0 & 0 & 0 \end{bmatrix} \begin{Bmatrix} U_1 \\ U_2 \\ U_3 \\ U_4 \\ U_5 \end{Bmatrix} \quad (3-49)$$

$$\begin{Bmatrix} H_{55} \\ H_{45} \\ H_{44} \end{Bmatrix} = \frac{5h}{6} \begin{bmatrix} 1 & -\frac{1}{2}(3\xi_1^A - \xi_1^D) \\ 0 & -\frac{1}{2}(3\xi_3^A - \xi_3^D) \\ 1 & \frac{1}{2}(3\xi_1^A - \xi_1^D) \end{bmatrix} \begin{Bmatrix} U_1^* \\ U_2^* \end{Bmatrix} \quad (3-50)$$

Where the material stiffness invariant U^* are given by:

$$\begin{Bmatrix} U_1^* \\ U_2^* \end{Bmatrix} = \begin{bmatrix} \frac{1}{2} & \frac{1}{2} \\ \frac{1}{2} & -\frac{1}{2} \end{bmatrix} \begin{Bmatrix} Q_{44} \\ Q_{55} \end{Bmatrix} \quad (3-51)$$

The ply stiffness properties $Q_{44} = G_{23}$ and $Q_{55} = G_{13}$

The membrane and bending lamination parameters are obtained by:

$$\xi_{[1\ 2\ 3]}^A = \frac{1}{h} \int_{-h/2}^{h/2} (\cos 2\varphi \cos 4\varphi \sin 2\varphi) dz \quad (3-52)$$

$$\xi_{[1\ 2\ 3]}^D = \frac{12}{h^3} \int_{-h/2}^{h/2} (\cos 2\varphi \cos 4\varphi \sin 2\varphi) z^2 dz \quad (3-53)$$

As already mentioned at the end of Section 3.5.1, in order to determine the transverse shear resultants $\{Q\}$, a shear correction coefficient $K(z)$ need to be considered for assuming a transverse shear stresses variation across the plate thickness (to fulfil the boundary condition). Normally this correction coefficient adopts a constant value of 5/6, but it may be accounted by a parabolic distribution (Herencia et al., 2008).

3.6 Summary

The present chapter provides a general description of the main theories developed for modelling laminated composite plates, some of them implemented in the element formulation of most of the commercial FE codes; focusing on their suitability and limitations for accurately represent the through thickness shear effects, as delamination failure mechanisms of thick laminated plates are highly influenced by them.

CLT and FSDT do not allow an accurate description of the transverse shear stresses for the case of thick and moderately thick laminated plates. However, a reasonable representation of their behaviour can be obtained by the HSDT, currently adopted by several layered solid elements, some of them described in Section 4 of this thesis.

The layerwise theory is also unable to accurately define transverse shear stresses despite it allows their interlaminar continuity at the plies interface.

An accurate computation of transverse shear stresses can only be achieved then by adopting 3D equilibrium equations (Khandan et al., 2012), using one or various solid elements per layer for describing the laminate behaviour, with the associated penalty in computational cost due to the large number of variables considered (directly related to the number of layers), which makes this approach impractical for engineering applications.

4 FE Analysis of Laminated Composite Structures

As already mentioned throughout this report, the analysis of laminated components is somehow more difficult than its metallic counterpart, mainly due to the orthotropic nature of its layers' properties. Thus, especial care must be taken when modelling a laminated composite component. The desired level of post-processing and the computational cost of the analysis will determine the way in which the structure and material properties of the component should be described. Generally three possible modelling strategies are available (Figure 4-1).

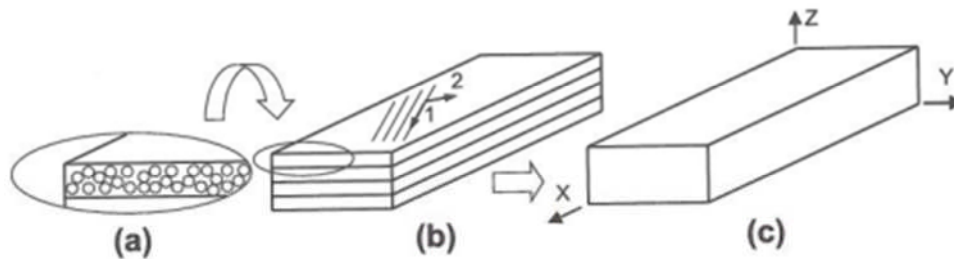


Figure 4-1 Modelling approaches at a (a) Micromechanics, (b) Meso-scale and (c) Macro-scale. Source: Barbero, 2008.

The component should be considered at its constituents' level, i.e. fibre and matrix, when seeking a great level of detail. It is then necessary to model a representative laminate unit cell, accounting for the required number of fibres, their shape, dimension and distribution; this may include fibres at different orientation (woven), for instance. Anisotropic material properties of both constituents need to be applied. This approach enables to study the microstructure of a component; some of the possible results may include not only the fibre or matrix failure, but also at their interfaces.

On the other hand, in the macro-scale level approach (see Figure 4-1 c), which is the least detailed one, the laminate can be considered as a homogeneous equivalent material. Thus, the mechanical behaviour of the composite component can be accounted by using orthotropic smeared material properties. This laminate definition however, disables the possibility of obtaining the stress distribution at a ply level, thus regardless of the element type used the plies cannot be evaluated individually. Despite that, a simple laminate definition is enough when displacement, buckling loads or modes, or vibration frequencies and modes are required (Barbero, 2008), for which only the laminate stiffness is needed.

When the component is modelled this way, only the generic strains and curvatures can be analysed, in response to the applied forces and moments.

If what required is either the stress or strain components of each lamina or the lamina failure index determination, a more detail definition of the component laminate should be provided. It is then necessary to input the elastic material properties of each lamina, their thicknesses and orientations, as well as to define the corresponding laminate stacking sequences (LSS) and regions of application. This method, usually referred to as the meso-scale level approach (see Figure 4-1 b), is the one used in this research.

Depending on the level of accuracy and efficiency sought when applying the meso-scale level approach, different element formulations are available, and the consequences of choosing each one of them are described in the next section.

4.1 Sublaminates

A laminated composite component may be represented by either layered shell elements or solid elements (Figure 4-2). For thick applications none of these is practical. Layered shell elements provide inaccurate through thickness results. When employing solid elements, each ply must be at least modelled by one layer of element (as the material throughout the element must remain uniform), which, considering the large number of plies that some of this laminates may consist of, result in an infeasible analysis for engineering purposes.

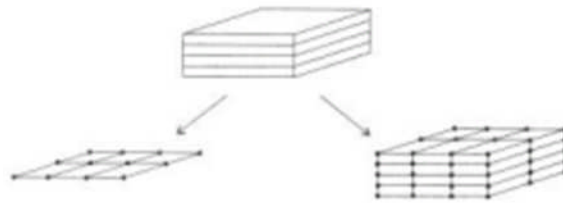


Figure 4-2 Thick laminated component (top), represented by layered shell elements (left), or solid elements (right). Source: Kollár, 2003.

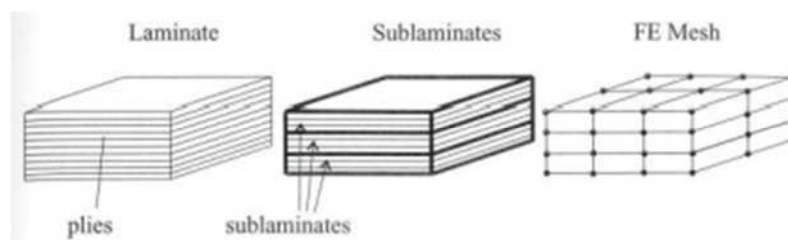


Figure 4-3 Thick laminated component (left), sublaminates (middle), and the FE mesh (right). Source: Kollár, 2003.

Layered solid elements were developed to overcome these limitations, and to provide accurate and efficient through thickness laminate behaviour. The laminate can be then divided into sublaminates or subassemblies, each one of them being represented by a

layer of layered solid elements (Figure 4-3) with the same sublaminates thickness. Each element could account for more than 100 layers in some cases, which can be defined individually in terms of material definition, thickness and orientation, as in subsequent sections will be more in detailed described. A generic compliance matrix $[S]$ of the sublaminates is defined by the relationship (Kollár, 2003):

$$\begin{Bmatrix} \bar{\epsilon}_x \\ \bar{\epsilon}_y \\ \bar{\epsilon}_z \\ \bar{\gamma}_{yz} \\ \bar{\gamma}_{xz} \\ \bar{\gamma}_{xy} \end{Bmatrix} = \underbrace{\begin{bmatrix} S_{11} & S_{12} & S_{13} & S_{14} & S_{15} & S_{16} \\ S_{21} & S_{22} & S_{23} & S_{24} & S_{25} & S_{26} \\ S_{31} & S_{32} & S_{33} & S_{34} & S_{35} & S_{36} \\ S_{41} & S_{42} & S_{43} & S_{44} & S_{45} & S_{46} \\ S_{51} & S_{52} & S_{53} & S_{54} & S_{55} & S_{56} \\ S_{61} & S_{62} & S_{63} & S_{64} & S_{65} & S_{66} \end{bmatrix}}_{[S]} \begin{Bmatrix} \bar{\sigma}_x \\ \bar{\sigma}_y \\ \bar{\sigma}_z \\ \bar{\tau}_{yz} \\ \bar{\tau}_{xz} \\ \bar{\tau}_{xy} \end{Bmatrix} \quad (4-1)$$

Where the stiffness matrix $[E]$ is equivalent to the inverse of the compliance matrix, and the bar represents average stresses and strains.

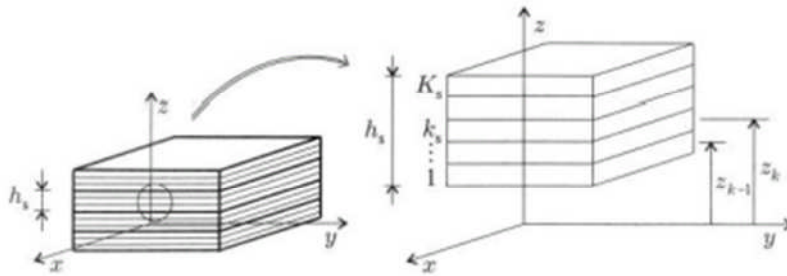


Figure 4-4 Illustration of a sublaminates. Source: Kollár, 2003.

Eq (4-1) may be particularised for the case of composite materials (Kollár, 2003):

$$\begin{Bmatrix} \bar{\epsilon}_x \\ \bar{\epsilon}_y \\ \bar{\epsilon}_z \\ \bar{\gamma}_{yz} \\ \bar{\gamma}_{xz} \\ \bar{\gamma}_{xy} \end{Bmatrix} = \begin{bmatrix} S_{11} & S_{12} & S_{13} & 0 & 0 & S_{16} \\ S_{21} & S_{22} & S_{23} & 0 & 0 & S_{26} \\ S_{31} & S_{32} & S_{33} & 0 & 0 & S_{36} \\ 0 & 0 & 0 & S_{44} & S_{45} & 0 \\ 0 & 0 & 0 & S_{54} & S_{55} & 0 \\ S_{61} & S_{62} & S_{63} & 0 & 0 & S_{66} \end{bmatrix} \begin{Bmatrix} \bar{\sigma}_x \\ \bar{\sigma}_y \\ \bar{\sigma}_z \\ \bar{\tau}_{yz} \\ \bar{\tau}_{xz} \\ \bar{\tau}_{xy} \end{Bmatrix} \quad (4-2)$$

$$[S] = [E]^{-1}$$

The compliance matrices for some of the element formulation used in this research, alongside the main equations that characterise each one of them are presented in 8.2.8.2 Appendix J.

4.2 Modelling composites

4.2.1 FE tools benchmark

Once the research objectives were clearly defined and the analysis and disciplines involved were identified a software benchmark had been done, in order to determine which commercial FE tool gives response to all project needs. The main requirements are listed below:

- Parametric modelling definition capability
- Layered solid elements
- Licence availability within the Crashworthiness, Impacts and Structural Mechanics Group (CISM) at Cranfield University.

Most commercial codes can be parametrised to some extent. Regarding the layered element formulation, the only commercial tools that provide this capability are ABAQUS, ANSYS and MSC MARC, the latter not available within the department. ANSYS v11 (Classic environment not the Workbench) has been finally the CAE simulation tool chosen to perform all FE analyses, due to the number of licenses available in the School of Engineering and the author's previous experience with the code.

4.2.2 Main areas of interest

Depending on the element type used, as well as on the modelling strategy results obtained can differ significantly from the true component behaviour. Therefore, a broad and detailed description of laminate modelling with ANSYS is presented below, in order to have a clear idea of the FE software capacities and limitations. Its main topics are grouped in the following sections:

- Available element formulations
- Layered configuration definition
- Failure criteria specification
- Best practice: Preprocessing
- Best practice: Postprocessing

4.3 Available element formulation

The element types available in ANSYS with layered option to model layered composite materials are listed in Table 4-1. The elements are grouped in three different element type categories, ie, shells, solids and solid-shells:

Table 4-1 Element types available in ANSYS with layered option to model layered composite.

<i>Element Type</i>	<i>ANSYS Element</i>
Shell	SHELL91; SHELL99; SHELL181; SHELL281
Solid	SOLID46; SOLID185; SOLID186; SOLID191
Solid-Shell	SOLSH190

The element formulation to choose depends upon the type of analysis to perform, the level of accuracy sought and the type of results available for each formulation. A brief description of each element is presented below.

Table 4-2 summarizes the main characteristics of each layered element type. The table second column refers to the way in which the laminate properties can be specified; two ways are available, either defining the constitutive matrices (macro-scale level) or specifying individual layer properties (meso-scale level). Refer to Section 4.4 for a more detailed description of the layered configuration definition and the implications of each way at a results level. As it can be seen, only two elements offer the constitutive matrix input option, which are SHELL99 and SOLID46.

Third column refers to the family of commands required to define the failure criteria. Refer to Section 4.6 for a detailed description of failure criteria using ANSYS.

Finally, fourth column summarizes the non-linearities capabilities available for each formulation. The full list of the available non-linear options can be found for each element in the *ANSYS help manual*.

The 3D shell elements and have six degrees of freedom (DOF) at each node (translations in the x, y, and z directions and rotations about the x, y, and z axes). Solid elements as well as the solid-shell element have three degrees of freedom (DOF) at each node (translations in the nodal x, y, and z directions).

Table 4-2 Element types available in ANSYS with layered option to model layered composite.

<i>Element Type</i>	<i>Layer Input Data</i>	<i>Failure Criteria</i>	<i>Non Linearities</i>
SHELL91	R,RMORE	TB,FAIL (at SOLU) FCxxx (at POST1)	Some material and geometrical nonlinearities
SHELL99	R,RMORE + Const. Matrix	TB,FAIL (at SOLU) FCxxx (at POST1)	Large deflection
SHELL181	SECxxx rather than real constants	FCxxx (at POST1)	Full nonlinear capabilities
SHELL281	SECxx.x Real constants for single layer shell	FCxxx (at POST1)	Full nonlinear capabilities
SOLSH190	SECxxx	FCxxx (at POST1)	Full nonlinear capabilities
SOLID46	R,RORE + Constant. Matrix	TB, FAIL (at SOLU) FCxxx (at POST1)	Nonlinear capabilities
SOLID185	SECxxx	FCxxx (at POST1)	Full nonlinear capabilities
SOLID186	SECxxx	FCxxx (at POST1)	Full nonlinear capabilities
SOLID191	R,RMORE	TB,FAIL (at SOLU) FCxxx (at POST1)	No nonlinear capabilities

4.3.1 Layered shell elements

A brief description of the layered element types available in ANSYS is presented below (ANSYS help manual; Barbero, 2008).

SHELL91 – 8-node nonlinear layered structural shell elements

This element may be used for modelling either layered shell structures, or thick laminates and sandwich structures. It allows a maximum of 100 different layers.

When more than three layers are defined SHELL99 is more efficient than SHELL91. However, unlike SHELL99, this element has non-linear and large strain capabilities, and it is more robust for large-deflection behaviour.

SHELL99 – 8-node linear layered structural shell element

This element type may be used to model thin to moderately thick layered plate and shell structures with a side-to-thickness ratio of roughly 10 or greater. Up to a total of 250 different uniform-thickness layers can be defined, if more layers are required a user-input constitutive matrix is available. It also has the option to offset the nodes to the top, middle or bottom surface. The element does not support non-linear capabilities. See Appendix 0 for a more detailed description of the element formulation.

SHELL181 – 4-node finite strain shell

This element is suitable for analyzing thin to moderately-thick shell structures. It may be used for layered applications for modelling laminated composite shells (using FSDT) or sandwich construction. The element has full nonlinear capabilities. It allows up to 250 different layers. The laminate definition is input by means of the section definitions (SECxxx) rather than real constants set.

SHELL281 – 8-node finite strain shell

This element is suitable for analyzing thin to moderately-thick shell structures. It may be used for layered applications for modelling laminated composite shells (using FSDT) or sandwich construction. The element has full nonlinear capabilities. It allows up to 250 different layers. The laminate definition is input by means of the section definitions (SECxxx) rather than real constants set.

SOLSH190 – 8-node 3D layered structural solid shell

The element can be used for simulating shell structures with a wide range of thickness (from thin to moderately thick). It is defined by a solid element topology. The element has full nonlinear capabilities including large strain. It allows up to 250 different layers. The laminate definition is input by means of the section definitions (SECxxx) rather than real constants set. The accuracy when modelling layered shells is governed by the FSDT (Section 3.5.1). The element can be stacked to model through-the-thickness discontinuities.

4.3.2 Layered solid elements

Despite most laminated structures can be analysed using the thin plates assumptions describe in Section 3.2 (plane stress state), sometimes it is not possible to assume it. For example, when the composite material is studied at a micro-scale level, i.e., for the case of a woven fabric, or the laminate is very thick and it's behaviour is described by 3D stress state, or when studying localized phenomena such as free edges effects

(Section 3.4.1). In these cases, the composite should be analysed with solid elements. ANSYS offers a series of layered solid elements, which are less computationally expensive than solid element formulations, yet with a good level of accuracy (ANSYS help manual, and Barbero, 2008).

SOLID46 – 8-node 3D layered structural solid element

It is a low order solid element, which can be used to model thick layered shells or solid structures. Two laminate definition options are available: it allows up to 250 layers per element, and in case more layers are required a user-input constitutive matrix option is also available. Several elements can be stacked as an additional alternative, as well as for improving the solution accuracy. See Appendix 8.2.8.2J.2 for a more detailed description of the element formulation.

SOLID185 layered solid – 8-node 3D layered structural solid element

Low order version of SOLID186.

SOLID186 layered solid – 8-node 3D layered structural solid

The element has full nonlinear capabilities and allows 250 different layers. The laminate definition is input by means of the section definitions rather than real constants set. See Appendix 8.2.8.2J.4 for a more detailed description of the element formulation.

SOLID191 – 20-node layered structural solid element

It is designed to model thick layered shells or layered solids and allows up to 100 layers per element. As with SOLID46, this element can be stacked to model through-the-thickness discontinuities. The element does not support nonlinear materials or large deflections. See Appendix 8.2.8.2J.3 for a more detailed description of the element formulation.

4.4 Layered configuration definition

The main driver characterizing the behaviour of a laminated composite structure is its layered configuration. ANSYS offers two methods for defining a composite laminate:

- By specifying the constitutive matrices coefficients (only available for elements SOLID46 and SHELL99).
- By means of the individual definition of the ply properties alongside with the laminate stacking sequence.

4.4.1 Constitutive matrices definition

This method offered to characterise the laminate behaviour is suited for macro-scale level analysis. It is an alternative mean to specify the accurate laminate stiffness for the

case of having laminates with an unknown LSS definition, or for the case of laminates with a huge number of different plies, avoiding in the latest the tedious process of input a great amount of data. Therefore, no detailed stress results at a ply level can be requested, as the change in lamina material properties is not specified, but only the component displacement, or the buckling and vibrations modes.

The main benefit of this option is that the laminate, which could be made-up of an unlimited number of layers, is finally represented by few constitutive matrices coefficients (A, B, D and H matrices) that relate the generalized forces and moments with the generalized strains and curvatures, as stated in Eq. (3-36). The matrices should be calculated though outside ANSYS, and the resulting coefficients are defined in the input file as real constants. By the same manner, a thermal load vector could be as well supplied.

This approach is available as an option for elements SOLID46 and SHELL99 (KEYOPT(2)). For these elements, the non-zero values of the constitutive matrix coefficients should be input using R and RMODIF commands.

For further documentation regarding its definition, etc, refer to the *ANSYS help manual*.

4.4.2 Individual layer properties

As stated several times throughout this chapter, the computation of strain and stress at a ply level (meso-scale approach) requires an accurate definition of the multidirectional laminate. This includes not only the elastic material properties of each laminae and their thicknesses, but also the LSS description, which specifies the angle of each lamina with respect to the laminate x-axis (global coordinates). The software is then able to compute internally the laminate stiffness by means of the A,B,D and H matrix.

In this method, the layer configuration is specified layer-by-layer from bottom to top. The bottom layer then is designated as layer 1, and additional layers are stacked from bottom to top in the positive Z (normal) direction of the element coordinate system. In case of having a symmetric laminate only half of the layers have to be defined.

There are two possible ways to input the layer properties. They can either be defined as real attributes using real constant commands (R, RMORE, RMODIF), or as attributes of a section definition via the section commands (SECTYPE, SECDATA).

Both ways are not available for all ANSYS layered elements; Table 4-2 summarizes the method available for each element type.

A complete list of all real constant available and their number is defined for each element type (see the *Element Reference*). The real constant LSYM allows to account for laminate symmetry. If the properties of the layers are symmetric about the midthickness of the element (LSYM = 1), only half the properties, up to and including

those of the middle layer (if any), need to be entered. Otherwise (LSYM = 0), the properties of all layers should be entered.

Laminate defined with SECDATA commands need to be fully defined, regardless of being midplane symmetric.

For each layer the following properties have to be defined:

- *Material Properties* – Each layer can have a different material definition assigned via the material reference number. The material can be defined as a linear (MP command) or non linear (TB command). Refer to Table 4-2 for a general description of the non-linearities available for each layered element type (plasticity is available only for elements SOLID191 and SHELL91). Layers' material properties, when defined as linear, could be either isotropic or orthotropic. For when orthotropic material properties are defined, Poisson's ratio is most often supplied in its major form. Furthermore, the material directions are parallel to the layer coordinate system.
- *Layer Orientation Angle* -- Defines the orientation of the layer coordinate system with respect to the element coordinate system. It is the angle (in degrees) between X-axes of the two systems. By default, the layer coordinate system is parallel to the element coordinate system. All elements have a default coordinate system which can be changed using the element attribute (element coordinate system ESYS).
- *Layer Thickness* – It can either be defined as a constant thickness, in which case only the thickness at one node (I) needs to be specified, or it can be tapered, where the thickness is assumed to vary bilinearly over the area of the layer, in this case the thickness must be input in all four corners. Dropped layers may be represented with zero thickness.
- *Number of integration points per layer* – Determine the level of accuracy of the results. The default is three points. This attribute applies only to sections defined via the section commands.

As an example, the same 8 plies symmetric laminate is created using both alternatives, i.e. by real constants or as section definition. The laminate is made of the same material ID (mat1), and all eight plies have the same thickness (tply). The orientation of each ply is represented by the parameter Theta%II%, being II the ply number.

```
! USING REAL CONSTANTS
R,1,8,1           ! 8=total number of plies; Symmetric Stacking
RMORE
RMORE,mat1,Theta1,tply,mat1,Theta2,tply
```

```

RMORE,mat1,Theta3,tply,mat1,Theta4,tply

! USING SECDATA
SECTYPE,1,SHELL
SECDATA,tply,mat1,Theta1,9           ! TK,MAT,THETA,NUMPT
SECDATA,tply,mat1,Theta2,9
SECDATA,tply,mat1,Theta3,9
SECDATA,tply,mat1,Theta4,9
!====Symmetry====
SECDATA,tply,mat1,Theta4,9
SECDATA,tply,mat1,Theta3,9
SECDATA,tply,mat1,Theta2,9
SECDATA,tply,mat1,Theta1,9
SECOFFSET,MID

```

4.4.3 Ply drop-off laminates and node offset

Laminate thickness reduction is achieved by layer drop-off, where some layers only extend over only part of the model. For all laminate layers to be modelled as continuous, the dropped layers' thicknesses are set to zero in the appropriate regions of the model. Thus, there must be defined as many real constants sets (or section data sets), containing different laminate configuration, as regions are defined in the model, to be then assigned as corresponds. Figure below shows a model with four layers, the second of which is dropped over part of the model.



Figure 4-5 Layered Model Showing Dropped Layer. Source: ANSYS help manual.

When modelling laminates with shell elements it is necessary to consider two more concepts which affect the laminate definition:

- The surface normal vector, which determines the position of the top and bottom surfaces of the laminate.
- And the node offset, which determines the relative position of the shell surface through the real laminate thickness (at the bottom, at the middle, or at the top)

For element SHELL181 and SHELL281, whose laminate configuration are define as shell sections by means of section commands, nodes can be offset to the bottom, midplane or top of the section using the SECOFFSET command. For elements SHELL91 and SHELL99, the node offset option (KEYOPT(11)) can be used instead. The figures below illustrate several ply drop-off examples.

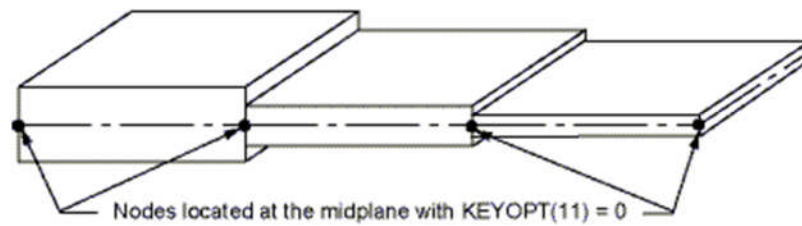


Figure 4-6 Layered shell with nodes at midplane. Source: ANSYS help manual.

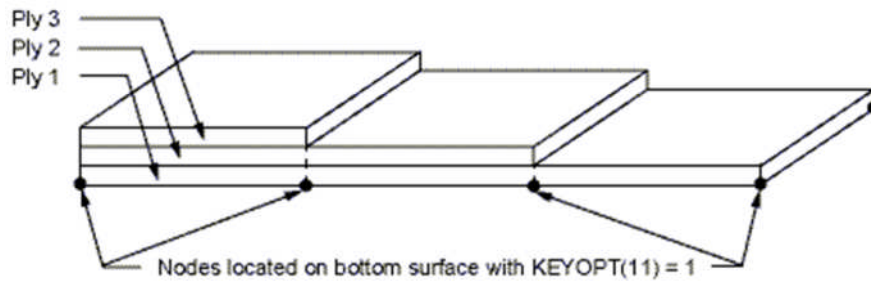


Figure 4-7 Layered shell with nodes at bottom surface. Source: ANSYS help manual.

In case a detailed 3D stress analysis of a ply drop-off laminate is required, a precise geometry definition needs to be modelled.

Ply drop-off description using layered solid elements is far more complex than for the case of layered shell elements. Consider a thick laminate that is divided in three sublaminates (Figure 4-8); each one of them can be modelled with a layer of layered solid elements. However, the ply drop-off pocket (laminated wedge at the right end of laminate 2) cannot be modelled using the same element type, but modelling each individual layer with at least one solid element through its thickness, which force sublaminates 2 and 3 to be modelled the same way to satisfy node compatibility (instead of using solid layered formulation); increasing significantly the model complexity as well as the analysis cost. This should be taken into account when planning to perform a weight optimisation using layered solid elements. For this research ply drop-off have not been considered.

Alternative ways of modelling ply drop-off in thick laminates should consider the use of 3D layerwise element (Zinno and Barbero, 1994), capable of representing a variable number of layers and thicknesses (Section 3.5.3).

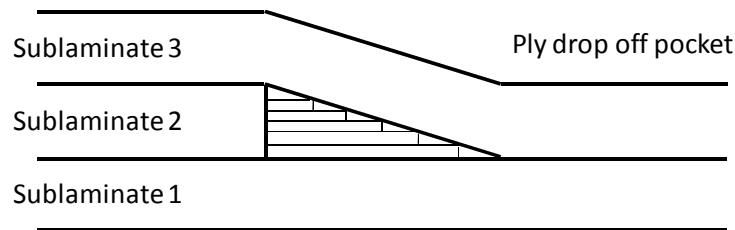


Figure 4-8 Typical thick laminate ply drop off.

4.4.4 Modelling solid elements

When solid elements are going to be used, the plate (or component) should be modelled as a volume for the case of having only one layered element through the thickness, or a series of volumes stacked on top of each other for the case of having more than one layered element through the thickness.

The reason behind this is related with postprocessing, as when the component has many layers of elements through the thickness, the same ply ID (i.e. ply 1) is repeated throughout all stacked layers of elements. Thus, when a particular ply is wanted to be processed it is difficult to isolate it. A real constant element attribute should be associated then with the unmeshed volumes. To overcome this problem, an element component (by the ANSYS command definition `CM,name,ELEM`) for each layer (of elements) could be created or it could be used a different real constant for each layer (which requires volume edition as it is explained in the previous paragraph). In this case, the real constants are used as layer of elements identifier (apart from defining the laminate configuration of certain layered elements). Thus, when a particular layer want to be selected, the layer of elements that contain the layer of interest is first selected, by issuing the real constant number associated with that layer of elements. Subsequently the ply number can be selected, within the selected layer of elements, for which data is going to be processed (Figure 4-9).

If, for instance, the layer of elements 5 want to be isolated (containing various plies itself), it can be simply issued `ESEL,S,REAL,,5`. Something similar could also be done with element types (in case of having various formulations within the same model) or other value, but REALs are probably easiest. Subsequent command `LAYER` specifies the element layer (within the already selected layer of elements, i.e. 5) for which data is going to be processed.

For layered solid elements `SOLID185/186` and `SOLSH190` both, real constants and section data need to be used, but only the section data will be used for the laminate definition, so the real constants here again will be used just as a layer of elements identifier.



Figure 4-9 Plate modelled with different volumes stacked together (I), and their finite elements mesh using one layer of layered solid elements per volumen (r).

Needless to say that each volume thickness should match the layer of element thickness (equal to the number of plies per element times the ply thickness).

4.5 Element coordinate system

A very important task when modelling a laminate is to define its coordinate system properly. Relative lamina orientation with respect to the laminate axis and other parameters and properties are defined based on the laminate orientation. The results (strains and stresses) are also computed in these directions. The laminate coordinate system is determined in FEA by the element coordinate system, represented by a right-handed orthogonal system, which orientation is defined by each element type.

For solid elements the element coordinate system is normally parallel to the global coordinate system. For shell elements the x and y axes are defined on the element surface, and the z axis is always normal to the surface, according to the right-hand rule. The way in which the x and y axes are determined may be different for each commercial code; in ANSYS the x-axis for each element is assigned to the element edge that connects the first and second nodes.

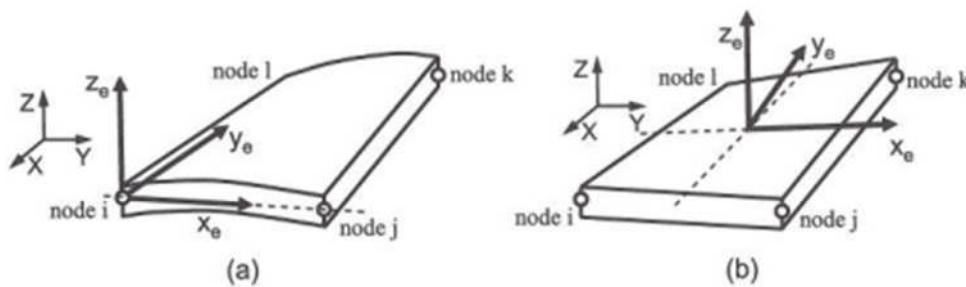


Figure 4-10 Element coordinate system default orientation in shell elements: (a) ANSYS, (b) MSC-MARC. Source: Barbero, 2008.

In case of meshing a flat rectangular surface, with rectangular elements (for both, shells or solids), the laminate coordinate system is parallel to the global one, as all elements have the first and second node aligned with the global X-axis. In some other cases though, the element coordinate system needs to be modified, in order to

represent the laminate orientation precisely. Section 6.1.2.4 describes how to modify the element coordinate system orientation in a solid curved plate laminate.

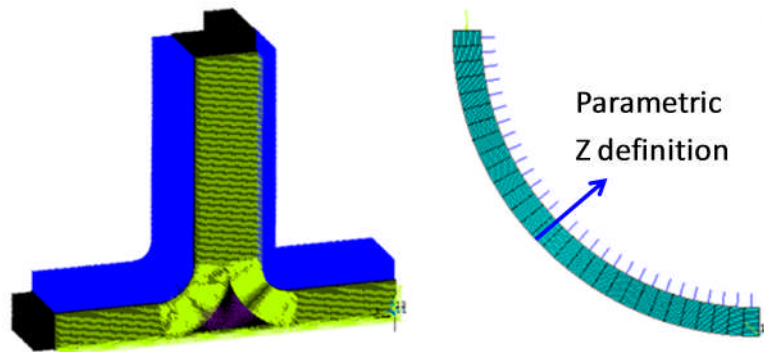


Figure 4-11 Reorientation of the element coordinate system for a curve plate

4.6 Failure criteria specification

All failure criteria presented in this section are used to determine if a layer has failed under the applied loads. They are unable though to track the failure propagation leading to total laminate failure. Damage mechanisms derived in continuum mechanics represent an alternative in order to do so.

The failure appearance can be predicted by means of the failure index, which is defined as (Barbero, 2008):

$$I_F = \frac{\text{stress}}{\text{strength}} \quad (4-3)$$

Failure occurs whenever $I_F \geq 1$. The inverse of the failure index is called strength ratio

$$R = \frac{1}{I_F} = \frac{\text{strength}}{\text{stress}} \quad (4-4)$$

Failure is predicted when $R \leq 1$.

ANSYS offers three available predefined failure criteria, and the user can specify up to six failure criteria more. The predefined criteria are the following:

- Maximum Strain Failure Criterion, which allows up to nine failure strains.

- Maximum Stress Failure Criterion, which allows up to nine failure stresses.
- Tsai-Wu Failure Criterion, which allows up to nine failure stresses and three additional coupling coefficients.

All equations below are expressed in the layer coordinate system, where the subscripts denote the fibre direction (1), the in-plane transverse to the fibres direction (2), and the through the thickness direction (3). Failure is evaluated where corresponds under tension (t) or compression (c).

Maximum Strain Criterion

The failure index is defined as

$$I_F = \max \left\{ \begin{array}{ll} \varepsilon_1 / \varepsilon_{1t}^u & \text{if } \varepsilon_1 > 0 \text{ or } -\varepsilon_1 / \varepsilon_{1c}^u \text{ if } \varepsilon_1 < 0 \\ \varepsilon_2 / \varepsilon_{2t}^u & \text{if } \varepsilon_2 > 0 \text{ or } -\varepsilon_2 / \varepsilon_{2c}^u \text{ if } \varepsilon_2 < 0 \\ \varepsilon_3 / \varepsilon_{3t}^u & \text{if } \varepsilon_3 > 0 \text{ or } -\varepsilon_3 / \varepsilon_{3c}^u \text{ if } \varepsilon_3 < 0 \\ \text{abs}(\gamma_{12}) / \gamma_{12}^u \\ \text{abs}(\gamma_{23}) / \gamma_{23}^u \\ \text{abs}(\gamma_{13}) / \gamma_{13}^u \end{array} \right. \quad (4-5)$$

The quantities in the denominator are the ultimate strains. Note that compression ultimate strains have positive values.

Maximum Stress Criterion

The failure index is defined as

$$I_F = \max \left\{ \begin{array}{ll} \sigma_1 / F_{1t} & \text{if } \sigma_1 > 0 \text{ or } -\sigma_1 / F_{1c} \text{ if } \sigma_1 < 0 \\ \sigma_2 / F_{2t} & \text{if } \sigma_2 > 0 \text{ or } -\sigma_2 / F_{2c} \text{ if } \sigma_2 < 0 \\ \sigma_3 / F_{3t} & \text{if } \sigma_3 > 0 \text{ or } -\sigma_3 / F_{3c} \text{ if } \sigma_3 < 0 \\ \text{abs}(\sigma_{12}) / F_{12} \\ \text{abs}(\sigma_{23}) / F_{23} \\ \text{abs}(\sigma_{13}) / F_{13} \end{array} \right. \quad (4-6)$$

The parameter F represents a strength value. Note that compression strengths have a positive value.

Tsai-Wu Criterion

Using the Tsai-Wu criterion the failure index is defined as

$$I_F = \frac{1}{R} = \left[-\frac{B}{2A} + \sqrt{\left(\frac{B}{2A}\right)^2 + \frac{1}{A}} \right]^{-1} \quad (4-7)$$

with

$$A = \frac{\sigma_1^2}{F_{1t}F_{1c}} + \frac{\sigma_2^2}{F_{2t}F_{2c}} + \frac{\sigma_3^2}{F_{3t}F_{3c}} + \frac{\sigma_{12}^2}{F_{12}^2} + \frac{\sigma_{23}^2}{F_{23}^2} + \frac{\sigma_{13}^2}{F_{13}^2} \quad (4-8)$$

$$+ C_{12} \frac{\sigma_1 \sigma_2}{\sqrt{F_{1t}F_{1c}F_{2t}F_{2c}}} + C_{23} \frac{\sigma_2 \sigma_3}{\sqrt{F_{2t}F_{2c}F_{3t}F_{3c}}} + C_{13} \frac{\sigma_1 \sigma_3}{\sqrt{F_{1t}F_{1c}F_{3t}F_{3c}}}$$

and

$$B = (F_{1t}^{-1} - F_{1c}^{-1})\sigma_1 + (F_{2t}^{-1} - F_{2c}^{-1})\sigma_2 + (F_{3t}^{-1} - F_{3c}^{-1})\sigma_3 \quad (4-9)$$

where C_{12} , C_{23} , C_{13} are the Tsai-Wu coupling coefficients, that by default are taken to be -1 (values between -1 and 0 are recommended). Note that compression strengths have a positive value.

In case the through-the-thickness strength values F_{3t} and F_{3c} are not available, they can be assumed to be equal to the in-plane transverse strength values. For the case of a non-available interlaminar strength F_{13} , the in-plane shear strength value is assigned. And for the remaining interlaminar strength F_{23} , the matrix shear strength value can be assumed (Barbero, 2008).

As it can be summarized in Table 4-2, failure criteria can be analyzed either in postprocessing module (POST1) for all shell and solid structural elements, using the FC commands, or in the solution phase for SHELL91, SHELL99, SOLID46 and SOLID191, by means of the TB,FAIL command.

Following, a description of the two alternative ways of evaluating the failure criteria in ANSYS is presented.

For both of them, it is defined that compression strength values must be introduced in ANSYS using negative numbers. In case any of these compression strength values is not available, ANSYS will assign it the negative value of the corresponding tensile strength.

If there is no interest in computing the failure in a particular direction, a large strength value must be input in that direction.

For 2D analysis, set the strength values with indexes 3, 13 and 23 to a value several orders of magnitude larger than the values with 1, 2 and 12 indexes, and set C_{13} and C_{23} to zero.

4.6.1 Failure criteria analysis via FC Commands

When postprocessing failure criteria results specified via the FC command the active coordinate system must be the coordinate system of the material being analyzed.

As abovementioned, failure criteria analysis performed via the FC commands (FC, FCDEL, FCLIST, etc) is defined and calculated in the postprocessing phase (POST1), once the model is solved. Prior to the failure criteria parameters definition, solution (or layer) coordinate system must be the active one, using RSYS,SOLU. Then, the layer where the failure criterion is going to be evaluated is selected using the LAYER command.

Failure criteria can be evaluated at an element or nodal level (PLESOL, PRESOL, PLNSOL, PRNSOL, etc). The results available include the maximum stress or strain failure index MAXF, defined by Eqs (4-6) and (4-5) respectively. The inverse of Tsai-Wu strength ratio index TWSR, define in Eq (4-7), and the Tsai-Wu strength index (TWSI), which is defined by $TWSI=A+B$, being A and B defined in Eqs (4-8) and (4-9) respectively. This index does not have engineering interpretation and it is recommended not to be used.

A generic APDL sequence of commands for defining the failure criteria via the FC commands is shown below (Barbero, 2008)

```

/POST1                ! Postprocessing module
RSYS,LSYS             ! Layer coordinate system

FC,1,S,XTEN,1500e6    ! F1t strength. F1t=F1c
FC,1,S,YTEN,40e6     ! F2t strength
FC,1,S,YCMP,-246e6   ! F2c strength
FC,1,S,ZTEN,10e13    ! Z value set to a large number
FC,1,S,XY,68e6       ! F12 strength
FC,1,S,YZ,10e13     ! YZ value set to a large number
FC,1,S,XZ,10e13     ! XZ value set to a large number
FC,1,S,XYCP,-1       ! C12 coeff (defaults to -1)
FC,1,S,YZCP,-1       ! C23 coeff (defaults to -1)
FC,1,S,XZCP,-1       ! C23 coeff (defaults to -1)
!FCLIST

LAYER,1              ! Results for layer 1

```

```

PRNSOL,S,FAIL          ! Print nodal solution FAIL index, where
                        ! MAXF is Maximum stress failure criteria index
                        ! TSWI is Tsai-Wu 'strength index' (recommended
                        ! not be used)
                        ! TWSR is the Tsai-Wu index (inverse of strength ratio)
                        ! Plot nodal solution
PLNSOL,S,MAXF          ! Maximum stress FC index
PLNSOL,S,TWSR         ! Tsai-Wu strength ratio index
FINISH

```

4.6.2 Failure criteria analysis via TB command

In this option the failure criteria is defined in the preprocessing module (/PREP7) using the TB, FAIL command, which enables to define up to six failure criteria. These include three predefined failure criteria are available (maximum strain failure criteria, maximum stress failure criterion, and Tsai-Wu criterion), and up to three more user defined failure criteria.

Failure criteria definition requires the commands TB,FAIL and TBTEMP,,CRIT. Followed by TBDATA command, which allows to activate any of the six failure criteria available using a “key” value from the options presented in Table 4-3.

Table 4-3 Constant values to define certain failure criteria using TB commands.

Source: Barbero, 2008.

KEY	Value	Meaning
#key1	0	Do not include this predefined criterion
	1	Predefined maximum strain failure criterion (uses constants 1-9 in TBDATA). Output as FC1
	-1	Include user-defined criterion with subroutine USRFC1
#key2	0	Do not include this predefined criterion
	1	Predefined maximum stress criterion (uses constants 10-18 in TBDATA). Output as FC2
	-1	Include user-defined criterion with subroutine USRFC2
#key3	0	Do not include this predefined criterion
	2	Predefined Tsai-Wu failure criterion, using failure index (uses constants 10-21 in TBDATA). Output as FC3
	-1	Include user-defined criterion with subroutine USRFC3

#key4 to		User-defined failure criteria – Output as FC4 to FC6
#key6	0	Do not include this criterion
	-1	User-defined criteria with subroutines USRFC4, USRFC5, USRFC6, respectively

A generic APDL sequence of commands for defining the failure criteria via the TB commands is shown below (Barbero, 2008)

```

! In /PREP7)          ! Defined in the preprocessing module
TB,FAIL,#mat,1      ! Data table for failure criterion, material ID #mat
TBTEMP,,CRIT
TBDATA,1,#key1,#key2,#key3,#key4,#key5,#key6      ! Failure criterion
                                                    ! "key" values
                                                    ! (from table 4-3)
    ! #key1 - Maximum strain FC (uses constants 1-9 in TBDATA)
    ! #key2 - Maximum stress FC (uses constants 10-18 in TBDATA)
    ! #key3 - Tsai-Wu FC (uses constants 10-21 in TBDATA)
    ! #key4 ... #key6 user defined FC

! Definition of the all possible failure criteria constants using
! TBDATA
! For maximum strain FC (constants 1-9)
TBDATA,1,#e1t,#e1c,#e2t,#e2c,#e3t,#e3c      ! Ultimate normal strains
TBDATA,7,#e12u,#e23u,#e13u      ! Ultimate shear strains
! For maximum stress & Tsai-Wu FC (constants 1-18)
TBDATA,10,#F1t,#F1c,#F2t,#F2c,#F3t,#F3c      ! Normal strengths
TBDATA,16,#F12,#F23,#F13      ! Shear strengths
! For Tsai-Wu FC (additional constants 19-21)
TBDATA,19,#C12,#C23,#C13      ! Tsai-Wu coupling coeff

```

Once the model is solved, the available results for the failure criteria are stored in the element miscellaneous records, summarized in Table 4-4 (created from the ANSYS *Element Reference* of SHELL91, SHELL99, SOLID46 and SOLID191). These can be retrieved during postprocessing using the ETABLE command (table of elements' values).

Table 4-4 Lists of failure index output available through the ETABLE command using the Sequence Number method.

<i>Output quantity name</i>	<i>Item</i>	<i>Sequence number</i>
FCMAX (over all layers), Failure criterion number where maximum occurs	NMISC	1
VALUE, Value for this criterion	NMISC	2
LN, Layer number where maximum occurs	NMISC	3
FC, Failure criterion number	NMISC	$(4NL) + 8 + 15(N-1) + 1$
VALUE, Maximum number for this criterion	NMISC	$(4NL) + 8 + 15(N-1) + 2$

Where, FC is the failure criterion number (1=maximum strain, 2=maximum stress and 3=Tsai-Wu criterion), and VALUE, as described in the table, is the maximum failure index for this failure criteria. These two output variables depend on the maximum layer number NL, and N is the failure number as stored on the results file in compressed form. When only the maximum stress and the Tsai-Wu failure criteria are included, the maximum stress criteria will be stored first (N=1) and the Tsai-Wu failure criteria will be stored second (N=2). In addition, if more than one criterion is requested, the maximum value over all criteria is stored last (N=3 for this example).

PRETABLE or PLETABLE commands enable to print or display non-averaged contour plots of these miscellaneous element results.

```

/POST1
RSYS,LSYS      ! Layer coordinate system

LAYER,1        ! Results obtained for layer 1

ETABLE,ERASE           ! Erase previous data stored in ETABLE
ETABLE,FCMAX,NMISC,1  ! FC values and maximum at
                       ! each integration point
ETABLE,VALUE,NMISC,2  ! Maximum value for this criterion
ETABLE,LN,NMISC,3     ! Layer number where maximum occurs

PRETAB,FCMAX          ! Print all element values for FCMAX
FINISH                ! Exit the /POST1

```

4.6.3 User-written failure criteria

ANSYS allows specifying up to six user-written failure criteria by means of user subroutines, which should be linked with it beforehand. For a brief description of user-programmable features refer to the *Advanced Analysis Techniques Guide*.

4.7 Composite modelling and postprocessing best practice

This section includes useful practical recommendation for modelling and postprocessing composite layered elements:

- Coupling effects
- Interlaminar shear stresses
- Input data verification
- Specifying results file data
- Selecting elements with a specific layer number
- Specifying a layer for results processing
- Transforming results to another coordinate system

4.7.1 Coupling effects

As a resultant of stacking layers, with different material properties, in different orientations, the composite laminates exhibit various types of coupling interactions (see Section 3.3.4.1). For this reason, model symmetry may not be able to use in case of having not symmetric laminate, despite the geometry and loading are symmetric, because the output stresses or strains may not be symmetric.

4.7.2 Interlaminar shear stresses

As already stated in Section 3.4.1, in many cases the interlaminar shear stresses are quite significant near the free edge, which may cause subsequent free-edge delamination. In order to increase accuracy of the interlaminar shear stresses and the through thickness normal stresses through the laminate thickness when working with fully integrated layered solid elements, various elements should be stacking in the thickness direction, with the corresponding increased meshing complexity and the penalty in the computation time. For the case of layered shell elements, the shear stress distribution law through the thickness is assumed to be parabolic, with no shear carried at the top and bottom surfaces of the element.

As illustrated below, t-axial bending loads acting on a T-shape bracket representative of the MSG SSF experienced peeling failure due to a combination of through thickness

stresses across the curved plate thickness. The use of full integrated layered solid elements to represent this effect is required (Siemetzki et al., 2007).

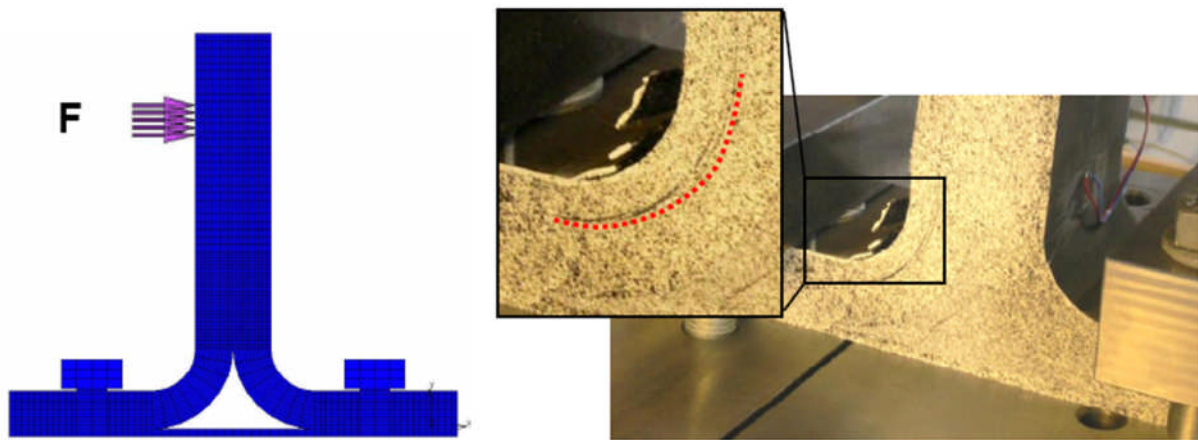


Figure 4-12 T-axial FE model (l) and peeling failure at $F_{axial}=42\text{kN}$ on tension side (r). Source: Siemetzki et al., 2007.

4.7.3 Input data verification

Several commands are available in order to check the large amount of input data required to model a laminated composite prior to the solution phase:

- SLIST – Summarizes the laminate properties when defined as a section (using SECxxx). When *Full* argument is requested (*Details*), the ABD matrix is printed.
- RLIST – List the laminate properties when defined using R, RMORE commands.
- ELIST – Lists the nodes and attributes (material type, element type, real constant, coordinate system, section number) of all selected elements.
- EPLOT – Displays all selected elements. By using the /ESHAPE,1 command before EPLOT, the layered shell elements are displayed as solids, representing its layers and their thicknesses, which values are obtained from the real constant or section definition. For the case of layered solid elements the layers are represented.
- /PSYMB,LAYR,*n* followed by EPLOT -- Displays layer number *n* for all selected layered elements. This method can be used to display and verify the angle, thickness and material of each individual layer across the model.
- /PSYMB,ESYS,1 followed by EPLOT -- Displays the element coordinate system triad of the selected elements. This method can be used to display and verify the orientation of the transformed element coordinate systems. (use /VSCALE,,2 to double the size of the triad)

- LAYLIST – Lists all layers stacking sequence (or a range of layers) defined using real constants (SHELL99, SHELL91, SOLID46, and SOLID191 elements).
- LAYPLOT and SECPLLOT – Displays the laminate stacking sequence defined as real constants (R, RMODIF commands) or as sections (SECDATA command) respectively (see the figure above). All layers defined in a specific section or real constant set or a range of layers are plotted, representing for each layer its layer angle (THETA) and its material number (MAT), which is colour coded.
- /ESHAPE,1 to view the layers comprising laminate. Layered shell elements will be shown as 3D elements.
- /PNUM,REAL,1 followed by VPLOT could be used when creating a solid model with various layers of elements through, in order to identify each layer of elements.

4.7.4 Specifying results file data

There are only three data available in the results file by default, which corresponds to the bottom of the first (bottom) layer, the top of the last (top) layer, and the layer with the maximum failure criteria value.

In order to write all data for all layers, the element option KEYOPT(8)=1 need to be set, although this lead to a very large results file. For this case, only the TOP and BOT results for a specified layer are stored, where MID values are averaged from the other two.

However, for certain elements (SHELL181, SHELL281), all three locations TOP, BOT and MID can be stored for each layer.

4.7.5 Selecting elements with a specific layer number

The command ESEL,S,LAYER allows to select elements that contain the requested layer number or range of layers' numbers. Elements with a nonzero thickness requested layers are the only one selected.

4.7.6 Specifying a layer for results post-processing

For specifying the layer number for which results should be computed use the command LAYER.

When working with layered shell elements, to specify the location within the layer to request the results, MID, TOP and BOT, issue the SHELL command.

However, despite requesting the results for a specific layer (regardless of the output location), they are plotted in the entire element, even for the case of layered solid elements.

For the particular case of requesting the results of a particular layer of a layered solid element when various layers of elements are stacked together refer to Section 5.3.1.

4.7.7 Transforming results to another coordinate system

By default, all layers results are postprocessed (POST1 postprocessor) in the global Cartesian coordinate system. However, the RSYS command allows transforming the results to another coordinate system. In order to printout or display results in the layer coordinate system, both RSYS,SOLU or RSYS,LSYS can be used, alongside with LAYER command.

4.8 Summary

The methodology proposed is based on FE analysis of thick laminates. This section gives an overview of the main characteristics of FE analysis of laminated composite, particularised for this kind of structures. Depending on the level of post-processing sought, possible modelling strategies were presented, and meso-scale approach was proposed for this research, as the through thickness stress, the main variable for evaluating delamination, is required at a ply level.

The use of layered solid elements was justified, providing benefits in terms of accuracy and efficiency of the analysis of thick laminates, which requires the division of the laminate into sublaminates, each one of them represented by a layer of elements of the same thickness.

ANSYS was the FEA commercial tool used in this research, and its election was based on the fact of having parametric model definition capabilities, by means of the Ansys Parametric Design Language. It also offers several layered solid formulations, and licences were available in the School of Engineering at Cranfield University.

The analysis steps involved in a laminated structure FE Analysis are particularised for ANSYS. A general description of the layered element formulations available (for theoretical description of various element formulations refer to 8.2.8.2Appendix J) and best parametric modelling and post-processing practice are given, including the layered configuration definition, element coordinate system transformation (defining the laminate coordinate system), and the available 3D failure criteria definition.

Special emphasis is given to solid modelling generation and postprocessing, and to discuss the limitations of ply drop off for solids elements applications, which finally have not been considered in this study.

In summary, the main aim of this section was to present the FE commercial tool requirements, capabilities and limitations, in terms of design space definition of thick laminates via parametric model generation, and analysis accuracy and efficiency via layered solid formulations.

5 Verification – Element Formulation vs CLT

Due to the limited amount of testing data available in the literature on UTL, the functionalities of different element formulations were initially assessed against simple benchmark examples for thin laminates.

The main aim of the following series of analyses is to get practical experience in using ANSYS for parametrically modelling thin laminated composite plates with different layered element formulations and modelling strategies, as well as for getting a clear understanding of the main in-plane output parameters, and how to postprocess them.

A simple FE model of a laminated plate subjected to in-plane and out-of-plane loading conditions was created for several layered element types, in order to compare the in plane results (failure index ultimately) obtained from the FE analysis, with the results obtained using the Classic Lamination Theory (plane stress assumption $\sigma_z = 0$), for the same laminate definition.

A series of input files created in APDL (ANSYS Parametric Design Language) were created, making use of the Pre / Post processing best practice definition for each layered element type used.

5.1 Settings and assumptions

For verification purposes, a fictitious *thin* plate and laminate definition has been used in this section (based on an exercise extracted from the MSc lecture notes of *Design and analysis of composite materials*, Cranfield University, 2006), in which a plane stress state can be assumed (despite of its non-realistic dimensions).

A 1 by 1 (m²) thin plate with 14 plies of carbon fibre, epoxy resin, each one with a ply thickness of 5 mm was created. The laminate definition was: [45/0/0/0/0/45/90]_s. The plate was constrained for not having rigid body motion, and care was taken for not to have stress concentration due to Poisson's effect. The plate was subjected to various loads, each of them applied independently: Three in-plane forces (per unit width), tensions in the x and y directions, and pure shear N_x , N_y , N_{xy} (1000 N/m); and bending moments (per unit width) in the x and y directions M_x , M_y (1000 Nm/m). A schematic representation of the loads applied to the thin plate is shown in Figure 5-1 and Figure 5-2.

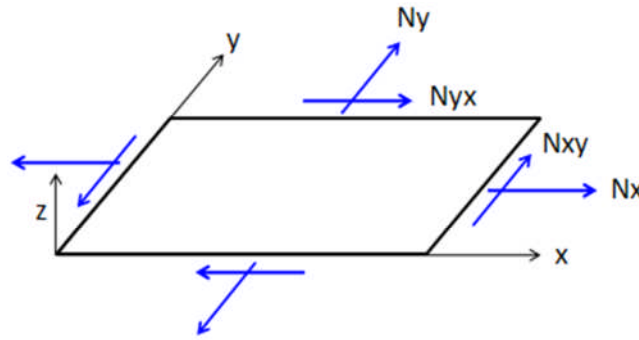


Figure 5-1 Thin plate under in-plane forces (N_x , N_y , N_{xy}).

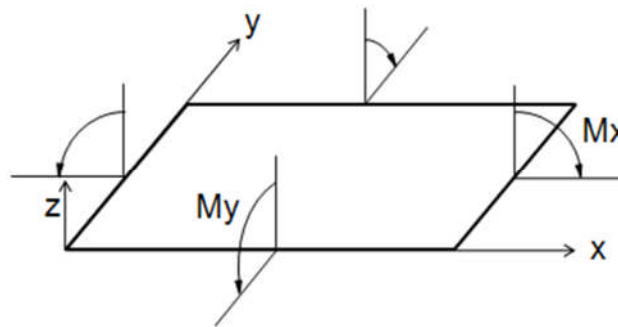


Figure 5-2 Thin plate under bending moments (M_x , M_y).

Find a summary of all plate dimensions, laminate definition and material properties (all in SI units) used in the following tables:

Table 5-1 Plate dimensions (in SI units).

<i>Dimension</i>	<i>Value (m)</i>
Length	1.00
Width	1.00
Total thickness	0.07

As already mentioned the laminate is made of carbon fibre, epoxy resin composite material, defined as a 2D orthotropic material, which requires then four independent elastic constants to be characterised (Eqs. (3-1) to (3-4)):

Table 5-2 2D orthotropic material properties (in SI units).

<i>Elastic Constant</i>	<i>Definition</i>	<i>Value</i>
E_1 (Pa)	Young's modulus in the fibre direction	1.81E+11
E_2 (Pa)	Young's modulus in the transverse direction	1.03E+10
ν_{12}	Major Poisson's ratio	0.28
G_{12} (Pa)	Shear modulus	7.17E+09

The stress limits are defined as:

Table 5-3 Strengths levels (in SI units).

<i>Strength</i>	<i>Definition</i>	<i>Value</i>
X_t (Pa)	Strength under tension in the fibre direction	1.50E+09
X_c (Pa)	Strength under compression in the fibre direction	1.50E+09
Y_t (Pa)	Strength under tension in the transverse fibre direction	4.00E+07
Y_c (Pa)	Strength under compression in the transverse fibre direction	2.46E+08
S (Pa)	Shear strength	6.80E+07

The laminate definition is described below:

Table 5-4 Laminate definition.

<i>Laminate Parameter</i>	<i>Value</i>
Total number of plies	14
Ply thickness (m)	5.00E-03
Stacking sequence	[45/0/0/0/0/45/90] _s
Mid plane location	Z=0

And the loads, which are applied independently, are presented in the following table:

Table 5-5 Load cases (in SI units).

<i>Independent load case</i>	<i>Value</i>
In-plane axial load per unit length – N_x (N/m)	1000
In-plane axial load per unit length – N_y (N/m)	1000
In-plane shear load per unit length – N_{xy} (N/m)	1000
Out-of-plane bending load per unit length – M_x (Nm/m)	1000
Out-of-plane bending load per unit length – M_y (Nm/m)	1000

5.2 CLT

The main steps involved in the strength analysis of a laminate at a ply level, using Classic Lamination Theory (Sections 3.3.2 and 3.3.4), are:

1. Determine the compliance matrix $[ABD]$ and its inverse, the $[abd]$ matrix.
2. Knowing the in-plane and out-of-plane loads applied, calculate the mid-plane strains in the laminate: $\{\varepsilon_{x-y}^0, k_{x-y}\} = [abd]\{N, M\}$
3. Obtain the total strain $\{\varepsilon_{x-y}\}$ for each layer and then transform it to the layer coordinate system $\{\varepsilon_{1-2}\} = [T_\varepsilon]\{\varepsilon_{x-y}\}$

4. Work out the stresses $\{\sigma_{1-2}\} = [Q]\{\varepsilon_{1-2}\}$ for each ply in the layer coordinate system and apply the failure criteria for ply strength evaluation. The two criteria evaluated are the Tsai-Wu failure criteria and the maximum stress failure criteria.

In order to account for all these calculations an Excel spreadsheet has been used. This was initially provided by NAFEMS in the Composites e-Learning Training Course (Abbey, 2010), being afterwards customised and expanded by the author, including the results calculations at a different location within each ply: bottom, middle and top of each ply.

For a detail description of the analytical expression used in the spreadsheet refer to Appendix A.

5.3 FE Analysis

The plate was created making use of different element formulation, both layered shells (4 and 8 nodes) and layered solid elements (8 and 20 nodes), as well as an intermediate layered solid-shell formulation (8 nodes).

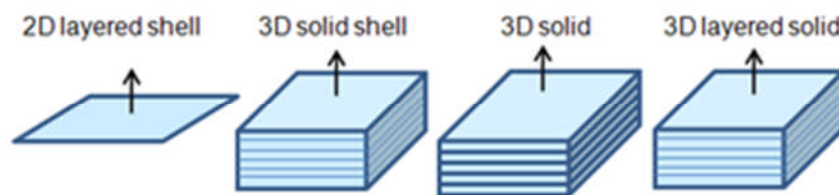


Figure 5-3 Schematic representation of different element types available for modelling laminates.

Despite the ultimate purpose of the thesis is to deal with the FEA of UTL composites, the current analysis involves the modellisation of a thin plate not only using layered shell elements, which are the most suited elements for these types of applications, but also using layered solid elements. The idea behind it is to understand the functionalities, capabilities and limitations of each formulation at an in-plane level.

For the case of solid elements, different modelling strategies were evaluated, modifying the number of layered elements through the thickness, in order to evaluate the effects that, not only the element formulation, but also the modellisation technique has on the accuracy of the results at a layer in-plane level.

A summary of the ANSYS element formulations and the different modelling strategies (in the case of solid elements) used is summarised below:

- *Shells*: SHELL99, SHELL181, SHELL281

- *Solids*: SOLID46 and SOLID185 (2 elements through the thickness), SOLID186, SOLID191 (1, 2, 3 elements through the thickness; 1 element per layer)
- *Solid-shell*: SOLSH190 (2 elements through the thickness)

A general description of these layered elements can be found in Section 4.3.

Despite there are two formulations, SHELL99 and SOLID46, that offer the possibility of input the laminate definition as smeared properties, all laminates evaluated in this thesis has been defined at a ply level.

Following, a description of the plate FE model generation is presented.

5.3.1 Geometry

The geometry generated is driven by the type of element formulation to be used. For shell elements the plate is modelled as a $1 \times 1 \text{ m}^2$ area. When using solid, the plate is modelled as a volume for the case of having only one layered element through the thickness, or a series of volumes stacked on top of each other for the case of having more than one layered element through the thickness (Figure 5-5), as discussed in Section 4.4.4.

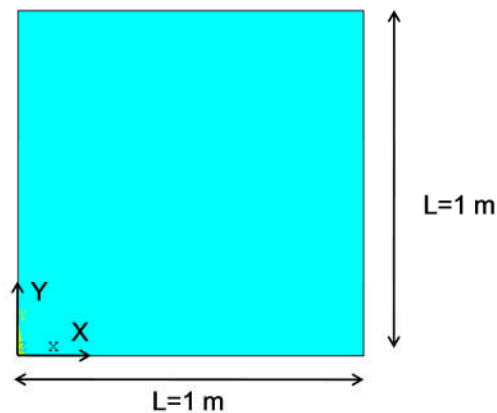


Figure 5-4 Plate geometry and 2D dimensions.

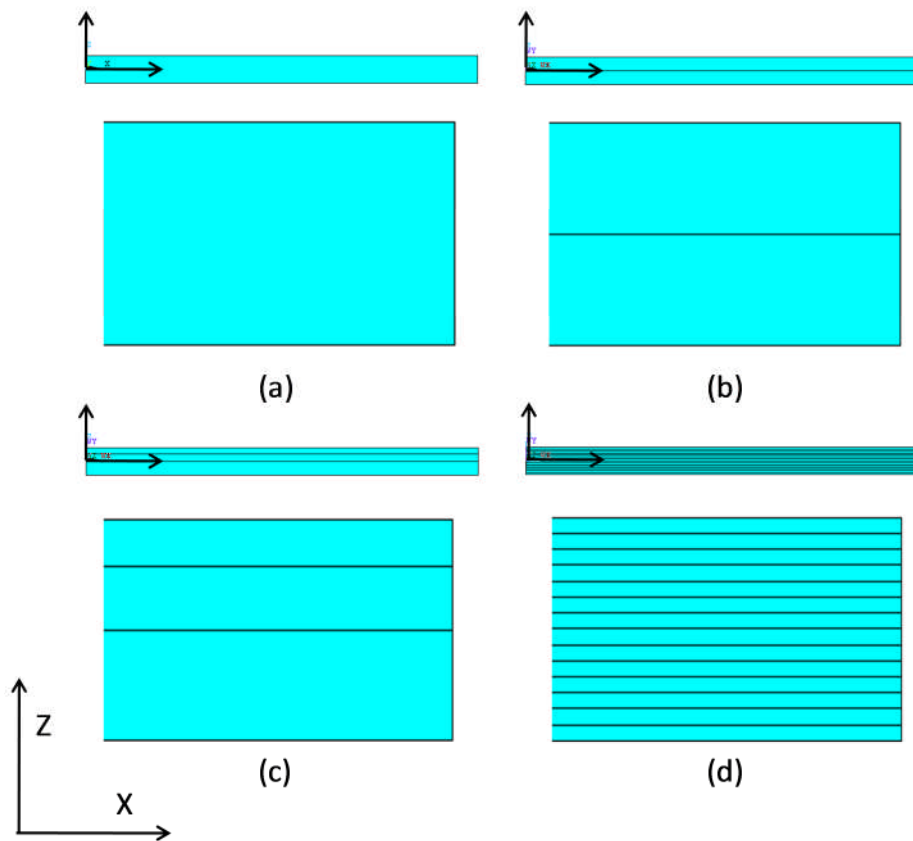


Figure 5-5 Plate geometry modelled as volumes: (a), two volumes (b), three volumes (c), and a volume per layer (d).

5.3.2 Mesh

A mesh of 12x12 elements (x and y directions respectively) was initially created for all formulations.

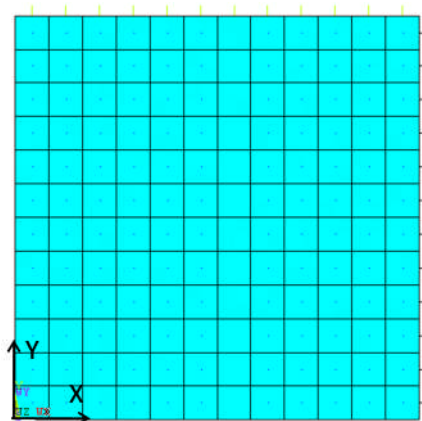


Figure 5-6 Mesh size (2D).

Throughout the thickness though, the number of layered element used varies.

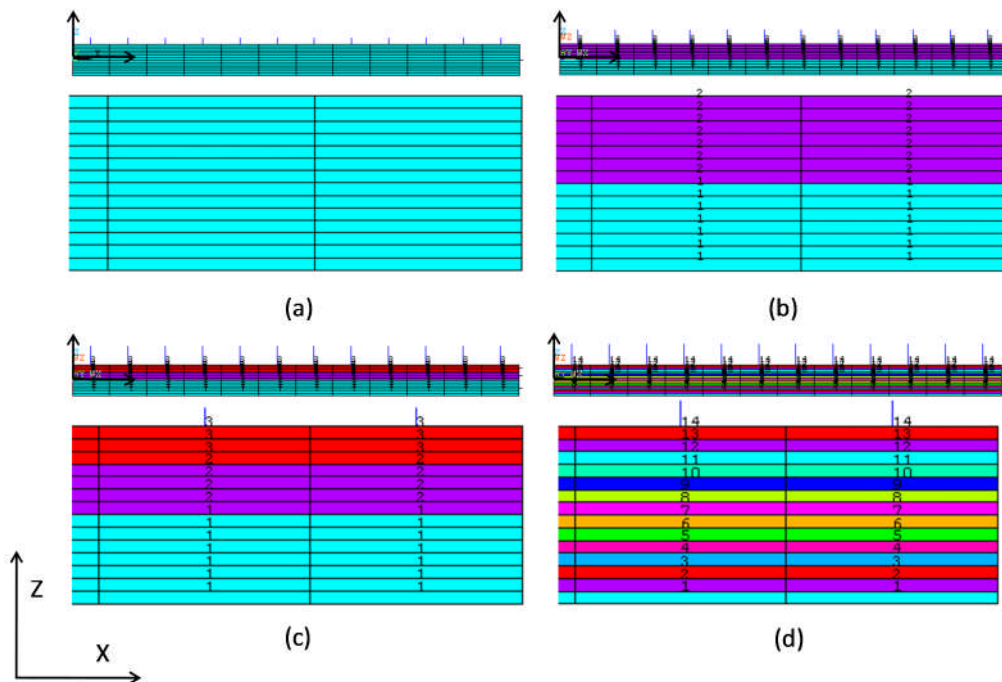


Figure 5-7 Different layered solid element used, colour coded by Real Constant (for the laminate definition). With one element through the thickness (a), with two elements (b), with three (c), and with one element per layer (d).

The figure above represents the plate meshes through the thickness with layered solid elements according to the different modelling strategies. Each volume shown in Figure 5-5 has been meshed with layers of elements. The different colours correspond to the different real constant set used as layer elements identifiers.

In this example, the reference axes (structural loading axes) have the same direction definition as the material axes, defined by the element coordinate system (Section 4.5). Both, Figure 5-6 and Figure 5-7 depict the reference axes in the bottom left corner of each capture.

In order to select a certain layer of elements the following real constant assignation need to be accounted. In all cases the plies have been defined from bottom to top:

- Two volumes through the thickness
 - ESEL,S,REAL,,1 (bottom layer of elements) → Plies 1 to 7 (1 to 7)
 - ESEL,S,REAL,,2 (top layer of elements) → Plies 8 to 14 (1 to 7)
- Three volumes through the thickness
 - ESEL,S,REAL,,1 (bottom layer of elements) → Plies 1 to 7 (1 to 7)
 - ESEL,S,REAL,,2 (top-middle layer of elements) → Plies 8 to 11 (1 to 4)

- ESEL,S,REAL,,3 (top layer of elements) → Plies 12 to 14 (1 to 3)
- One solid element per layer
 - ESEL,S,REAL,,1 (bottom layer of elements) → Ply 1
 - ESEL,S,REAL,,2 → Ply 2
 - ...
 - ESEL,S,REAL,,14 (top layer of elements) → Ply 14

Once a certain layer of elements is selected, a ply can be selected within it by issuing the command LAYER (use the layer number within the parentheses in the above definition as corresponds).

Laminate stacking sequence can be checked at this stage:

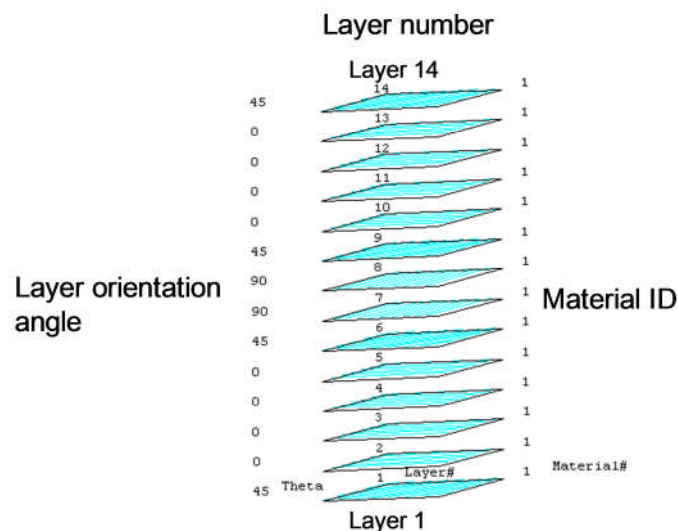


Figure 5-8 Stacking sequence $[45/0/0/0/0/45/90]_s$ (1 layered element through the thickness).

The capture is extracted from an ANSYS plot by means of the following code:

```
LAYPLOT,1           ! Layer stacking sequence of the plate (element 1)
/GROPTS,VIEW,1
```

For the element SHELL99 the node offset option (KEYOPT(11)) locates the element nodes at the bottom, middle, or top surface of the shell, in this case the nodes are located at MID surface of the shell ($Z=0$) (the same way it has been defined in the CLT spreadsheet). Figure 5-9 depicts a node offset to the middle of the surface:

```
KEYOPT,1,11,0
```

For elements SHELL181, and SHELL281 where the laminate is defined as sections defined via the section commands (SEC_{xxx}), nodes can be offset to the middle of the shell using the command:

```
SECOFFSET,MID
```

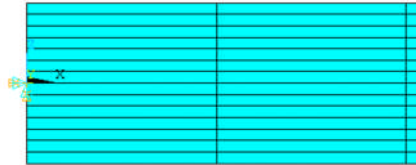


Figure 5-9 Nodes located at MID surface (Z=0). Layered shell elements.

5.3.3 Constraints

a) Axial tension load per unit length in the longitudinal direction N_x (or in the transverse direction N_y)

The axial load is created applying a tension in one side of the plate while the opposite side is constrained.

When modelling the end constraint, the main idea behind it is to avoid locking in Poisson's ratio. Thus, in case of having that end fully built-in, that will lock in the transverse direction, locking all the strains, which will produce a stress concentration in the transverse direction. Best way to avoid that is to have a roller support that allows transverse direction translation, apart from one central node.

Shell element formulations (either with 4 or 8 nodes per elements) have all in ANSYS six DOFs per node (3 translations and 3 rotations) which should be constrained in order not to have rigid body motion. The constraints must be applied in the way so that $\sum F = 0$, $\sum M = 0$.

A summary of the boundary conditions applied to layered shell elements is presented here:

- $X=0 \rightarrow 1, 5, 6 \rightarrow$ Avoiding translation in the X direction and rotation in the complementary directions (Y and Z).
- Centre node (at $X=0$) \rightarrow Fully clamped.

Where the numbers represents the direction in which the corresponding DOF has been constraint:

1. Translation in the X direction
2. Translation in the Y direction

3. Translation in the Z direction
4. Rotation in the X direction
5. Rotation in the Y direction
6. Rotation in the Z direction

So when pulling in the X direction, the specimen will stretch in the longitudinal direction and shrink in the transverse direction due to Poisson's ratios effect without locking any strains in Y; that way a constant stress state is achieved.

```

NSEL, S, LOC, X, 0
DSYM, SYMM, X           ! Line X=0 → 1,5,6

NSEL, S, LOC, X, 0
NSEL, R, LOC, Y, L/2
D, ALL, ALL

```

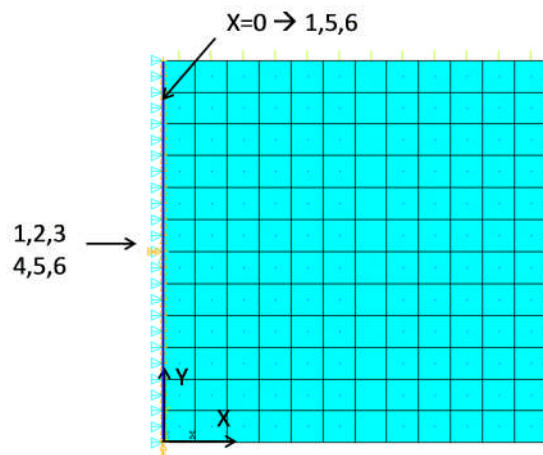


Figure 5-10 Boundary conditions applied on a thin plate under in-plane axial load N_x modelled with layered shell elements.

Solid elements are 8 or 20 node elements with 3 DOFs per node (3 translations). For this case as well, in order not to have rigid body motion, $\sum F = 0$, $\sum M = 0$ should apply.

Regardless of the layered solid element formulation used (including solid-shell element), and regardless of the number of elements through the thickness, the following boundary conditions apply to the plate subjected to axial load N_x :

- Area in $X=0 \rightarrow 1$ (constraining indirectly rotation 5, 6)
- In the same area $X=0$, constraint:
 - Centre vertical line $Y=L/2 \rightarrow 2$ (constraining indirectly rotation 4)

- Centre horizontal line $Z=0 \rightarrow 3$ (Mid side nodes applied at the Mid surface (as in the spreadsheet))

The following figures depict the previous constraints applied to the different element formulation / modelling strategy.

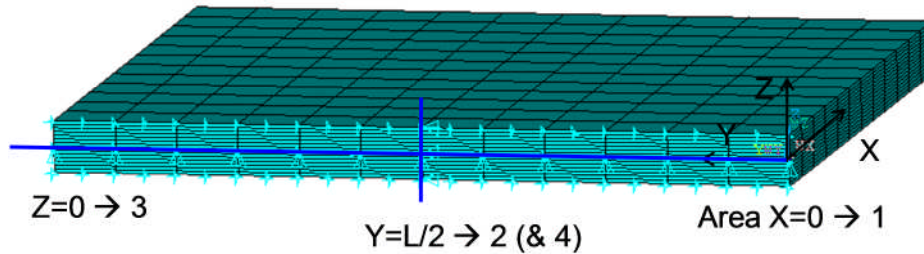


Figure 5-11 Boundary conditions of the plate under N_x modelled with SOLID186, SOLID191 (with one element through the thickness).

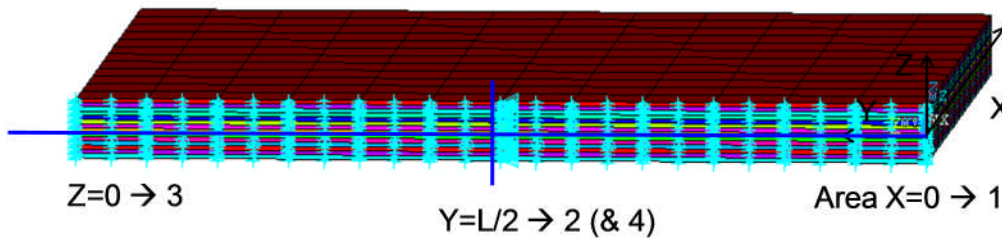


Figure 5-12 Boundary conditions of the plate under N_x modelled with SOLID191 (with one element per ply).

b) Shear load per unit length N_{xy}

For shell elements the plate is constrained with the following supports:

- Origin: 1,2,3,4,5
- Corner at $(L/2, L/2)$: inclined support in 2 (which indirectly constraint the 6th DOF).

In order to avoid rigid body motion and stress concentration in the supports location under the applied shear load.

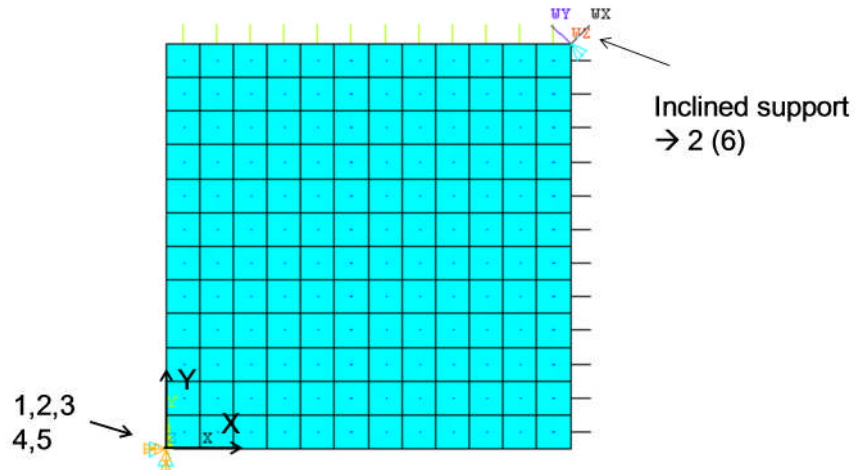


Figure 5-13 Boundary conditions applied on a thin plate under in-plane shear load N_{xy} modelled with layered shell elements.

The equivalent boundary conditions applied for the solid elements model is:

- Vertex at (0, 0): 1,2 (which indirectly constraint rotations 4, 5)
- Origin: 3
- Vertex at ($L/2$, $L/2$): inclined support 2

The 6th DOF is constrained between the inclined support and the constraint 2 at the origin.

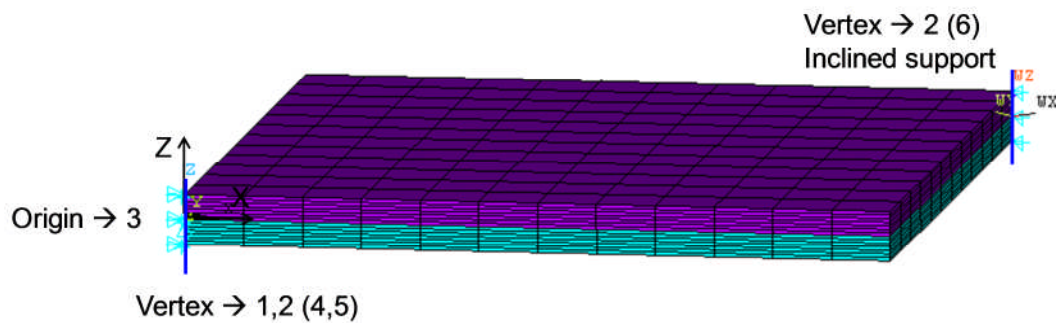


Figure 5-14 Boundary conditions of the plate under N_{xy} modelled with SOLID191 (with two elements through the thickness).

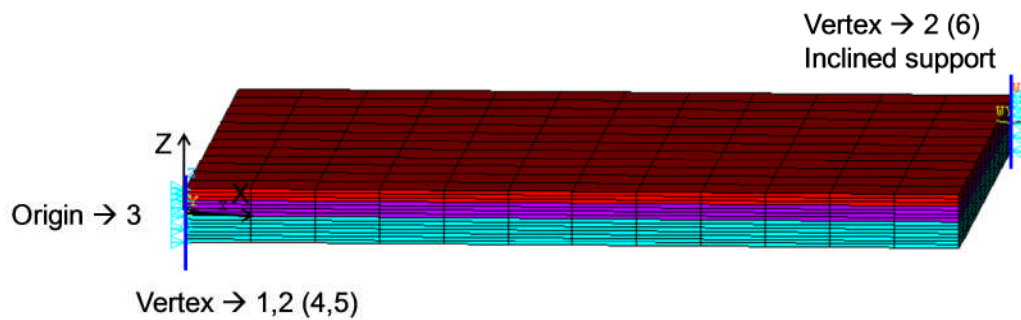


Figure 5-15 Boundary conditions of the plate under N_{xy} modelled with SOLID191 (with three elements through the thickness).

c) Out-of-plane bending moment per unit length M_x (or M_y)

For shell elements the plate is constrained with the following supports:

- Corners at $(0, 0)$ and $(0, L) \rightarrow 1$ (which indirectly constraint 6)
- Node at $(0, L/2) \rightarrow 2, 3$
- Nodes at $(L/2, 0)$ and $(L/2, L) \rightarrow 3$ (which indirectly constraint 4)

Note: constraint 5 created due to 3 between nodes with X in 0 and L/2

In order to avoid rigid body motion and stress concentration in the supports location under the applied bending moment, M_x .

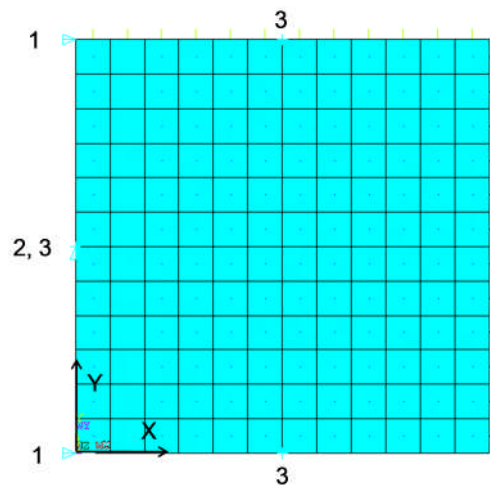


Figure 5-16 Boundary conditions applied on a thin plate under out-of-plane moment M_x modelled with layered shell elements.

For all solid elements models the constraints applied are:

- Node at $(0, L/2, 0) \rightarrow 2, 3$

- Nodes at $(L/2, 0, 0)$ and $(L/2, L, 0) \rightarrow 1, 3$

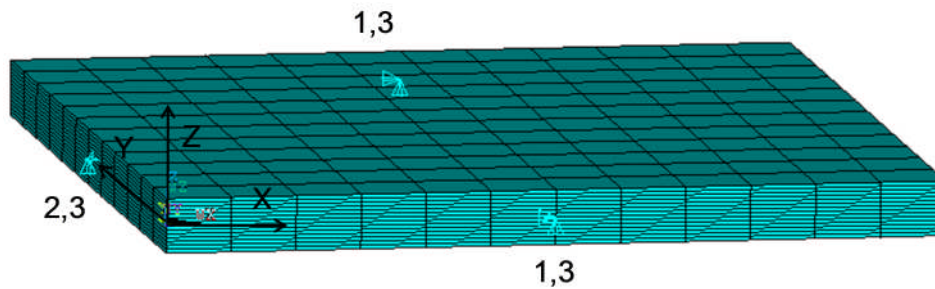


Figure 5-17 Constraints on the plate under M_x modelled with SOLID191 (with one element through the thickness).

5.3.4 Loads

a) N_x (or N_y)

For shell elements, the axial tensile load N_x (or N_y) is applied as a force per unit width using the command SFL (surface loads on lines of an area). The ANSYS code in this case for the load definition is:

```
! NX
LSEL,S,LOC,X,L           ! Select line at X=L
SFL,ALL,PRES,-Nx        ! Surface loads on lines of an area

/PSF,PRES,NORM,2,0,1    ! Display load as arrows
```

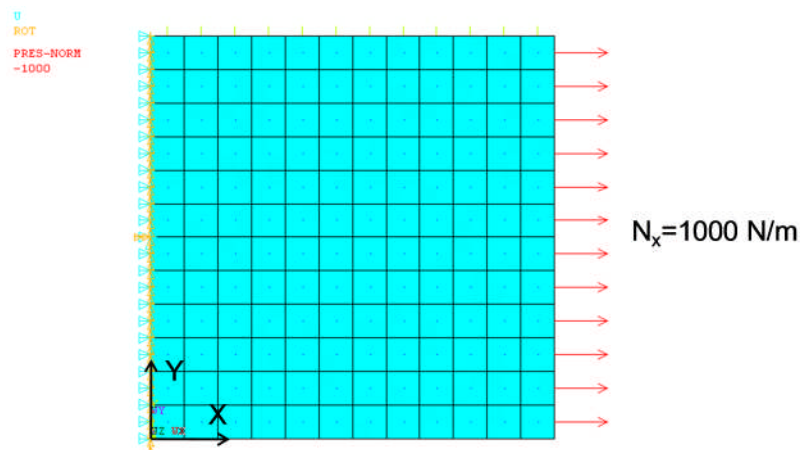


Figure 5-18 Boundary conditions applied on a thin plate under in-plane axial load N_x modelled with layered shell elements.

For solid modelling there are two ways of applying the axial tension load. Either using surface effect elements (SURF154) for the load application, which are elements that

may be overlaid on a face area of the solid elements (face 1 in this case); or by direct application of the load on a face area of the solid element (on face 3 in this case).

In both cases, the load is applied as a pressure, defined as N_x/t , being t the total plate thickness, using the command SFE (surface loads on elements). The ANSYS code of both approaches is presented below.

Using surface effect elements, SURF154 (on face 1):

```

! NX
ASEL,S,LOC,X,L      ! Select area at X=L
NSLA,,1            ! Select the nodes associated with that area
NPLLOT

TYPE,2             ! Select the element type 2 (SURF154)
REAL,2            ! REAL,3 → for when 2 elements through thickness.
                  ! REAL,4 → for when 3 elements tt
                  ! REAL,15 → for when one solid per ply
ESURF,ALL         ! Generates SURF154 elements overlaid on the free
                  ! faces of existing selected solid elements

ESEL,S,TYPE,,2    ! Select this elements, and...
EPLLOT

CM,e_surf_nx,ELEM !... create a component with the selected elements
CMSEL,S,e_surf_nx

SFE,e_surf_nx,1,PRES,,-Nx/t      ! Apply the pressure on the component

/PSF,PRES,NORM,2,0,1            ! display the pressure as arrows

```

By direct application (Face 3):

```

! NX
ASEL,S,LOC,X,L      ! Select the area at location X=L
NSLA,,1            ! Select the nodes associated with that area
NPLLOT
ESLN               ! Select the elements associates with that nodes

SFE,ALL,3,PRES,,-Nx/t      ! Apply the pressure on face 3 of
                           !those elements

/PSF,PRES,NORM,2,0,1      ! Plot the pressure as arrows

```

d) Shear load per unit length N_{xy}

One possible way of applying shear loads on shells can be directly created using *consistent nodal loading*.

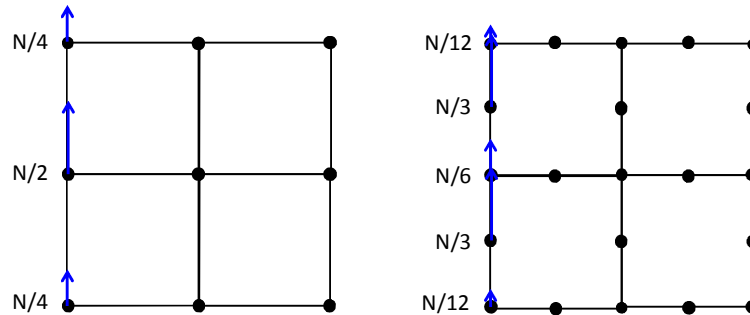


Figure 5-19 Example of consistent nodal loading for 4-node and 8-node elements.

Extending the same principle to the case under concern, shear load N_{xy} , for the 4-node shell element (SHELL181), the loads to be applied at a nodal level are:

- Edge nodes (except edge end nodes):

$$\frac{\pm N_{xy}}{(Num_Nodes + 1)}$$

- Edge end nodes:

$$\frac{\pm N_{xy}}{2(Num_Nodes + 1)}$$

- Total load (per unit length):

$$\left[Num_Nodes \frac{\pm N_{xy}}{(Num_Nodes + 1)} \right] + \left[2x \frac{\pm N_{xy}}{2(Num_Nodes + 1)} \right] = \pm N_{xy}$$

Where Num_Nodes is the total number of nodes of the plate edge where load is applied.

$$Num_Nodes = Edge_Nodes - Edge_End_Nodes$$

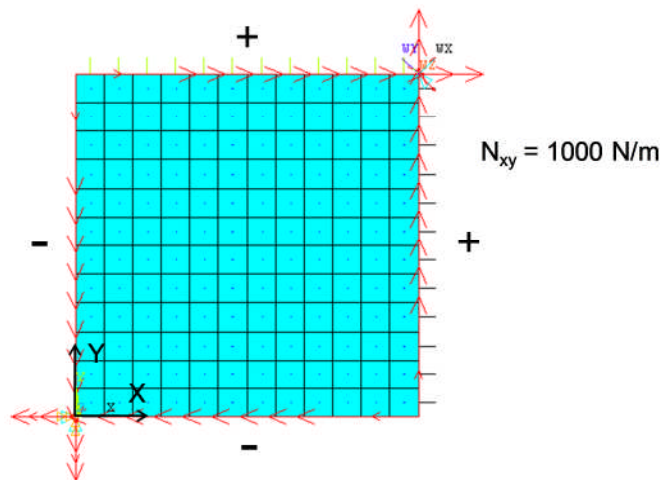


Figure 5-20 Boundary conditions applied on a thin plate under in-plane shear load N_{xy} , modelled with SHELL181 (4-node shell element).

And for the 8-node shell element (SHELL99, SHELL281), the loads to be applied at a nodal level are:

- Element corner nodes on edge (except edge end nodes):

$$\frac{\pm N_{xy}}{3(\text{Num_Nodes} + 1)}$$

- Mid-side nodes:

$$\frac{\pm 2N_{xy}}{3(\text{Num_Nodes} + 1)}$$

- Edge end nodes:

$$\frac{\pm N_{xy}}{6(\text{Num_Nodes} + 1)}$$

- Total load (per unit length):

$$\left[\text{Elem_Corner_Nodes} \frac{\pm N_{xy}}{3(\text{Num_Nodes} + 1)} \right] + \left[\text{Num_Mid_Nodes} \frac{\pm 2N_{xy}}{3(\text{Num_Nodes} + 1)} \right] + \left[2x \frac{\pm N_{xy}}{6(\text{Num_Nodes} + 1)} \right] = \pm N_{xy}$$

Where

$$\text{Num_Nodes} = \text{Elem_Corner_Nodes} - \text{Edge_End_Nodes}$$

Figure 5-20 and Figure 5-21 depict the shear load applied on the plate modelled with 4-node shell elements and 8-node shell elements, respectively. Both plots include the sign applied on every plate boundary.

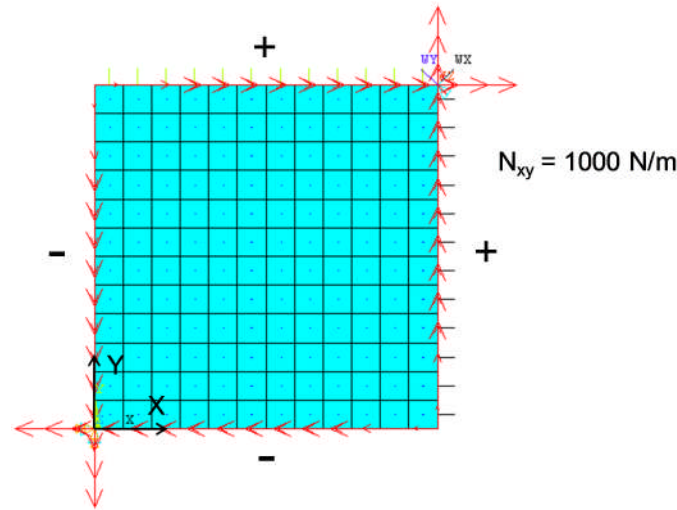


Figure 5-21 Boundary conditions applied on a thin plate under in-plane shear load N_{xy} , modelled with SHELL99, or SHELL281 (8-node shell elements).

For solid modelling there is only one way of applying shear load, this is by using surface effect elements (SURF154) for the load application, which are elements that may be overlaid on a face area of the solid elements (face 2 in this case), as previously explained.

The load is applied as a pressure, defined as N_{xy}/t , being t the total plate thickness, using the command SFE (surface loads on elements). The ANSYS code the load application in the plate sections at $X=0$ and $X=L$ is described below. The complete pure shear load includes the shear application at $Y=0$ and $Y=L$ plate sections.

Using surface effect elements, SURF154 (on face 2):

```

! NXY (X=0)
ASEL,S,LOC,X,L      ! Select the areas at X=0 and X=L
ASEL,A,LOC,X,0
NSLA,,1            ! Select the nodes associated with that areas
NPLOT

TYPE,2             ! Select the element type 2 (SURF154)
REAL,2             ! REAL,3 → for when 2 elements through thickness
                  ! REAL,4 → for when 3 elements tt
                  ! REAL,15 → for when one solid per ply
ESURF,ALL          ! Generates SURF154 elements overlaid on the free
                  ! faces of existing selected solid elements

ESEL,S,TYPE,,2    ! Select this elements, and...
EPLLOT

```

```

CM,e_surf_nxy_xL,ELEM      !... create a component with the selected
                           ! elements

CMSEL,S,e_surf_nxy_xL

SFE,e_surf_nxy_xL,2,PRES,,Nxy/t  ! Apply the pressure on the component

/PSF,PRES,TANX,2,0,1      ! Display the pressure as arrows

```

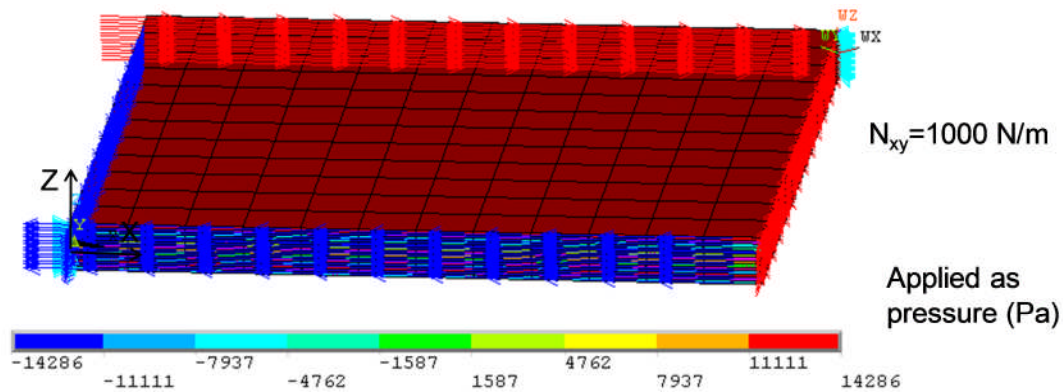


Figure 5-22 Boundary conditions of the plate under N_{xy} modelled with SOLID191 (with one element per ply).

Figure above depicts the shear load applied on the plate modelled with solid elements.

e) Out-of-plane bending moment per unit length M_x (or M_y)

Pure bending moments on plate have been applied in this case as well using the *consistent nodal loading* approach.

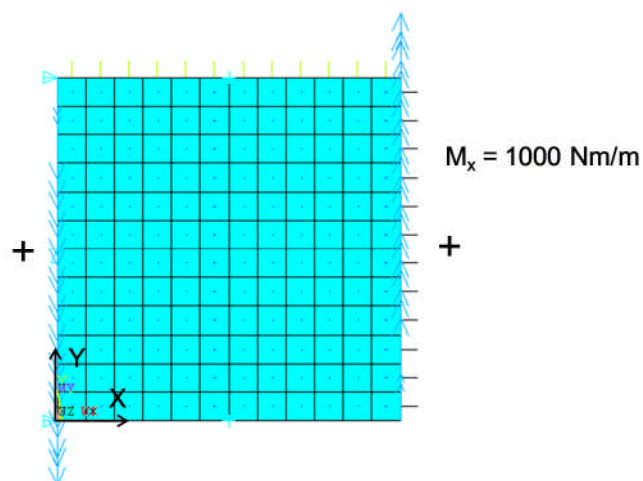


Figure 5-23 Boundary conditions applied on a thin plate under out-of-plane bending moment load M_x , modelled with SHELL181 (4-node shell element).

For solid modelling the easiest way of applying bending moment load is to specify it as a linear varying surface load (gradient) by means of the SFGRAD command. The pressure distribution on a beam with thickness t (along the z normal direction), when a moment M_x is applied on the extreme sections at $X=0$ and $X=L$ is described as:

$$p = \frac{6}{t^2} M_x - \frac{12}{t^3} M_x \left(z + \frac{t}{2} \right) \quad (5-1)$$

The analytical explanation to obtain this expression is described in Appendix E.

```

! MX (X=L)
SLOPE1=12*Mx/(t**3)
SFGRAD,PRES,0,Z,-t/2,-SLOPE1      ! Z slope of -SLOPE in global
                                   ! Cartesian
NSEL,S,LOC,X,L                    ! Select nodes for pressure applicat.
SF,ALL,PRES,6*Mx/(t**2)           ! Pressure at selected nodes
                                   ! 6*Mx/(t**2) at Z=-t/2
                                   ! 0 at Z=0
                                   ! -6*Mx/(t**2) at Z=t/2
                                   ! According to the -SLOPE1 definition

ALLSEL,ALL
EPlot

!=====

! MX (X=0)
SLOPE2=12*Mx/(t**3)
SFGRAD,PRES,0,Z,-t/2,-SLOPE2
NSEL,S,LOC,X,0
SF,ALL,PRES,6*Mx/(t**2)

ALLSEL,ALL
EPlot

/PSF,PRES,NORM,2,0,1              ! Display pressure as arrows

```

Figure 5-24 to Figure 5-25 depict the bending moment M_x applied on the plate modelled with solid elements.

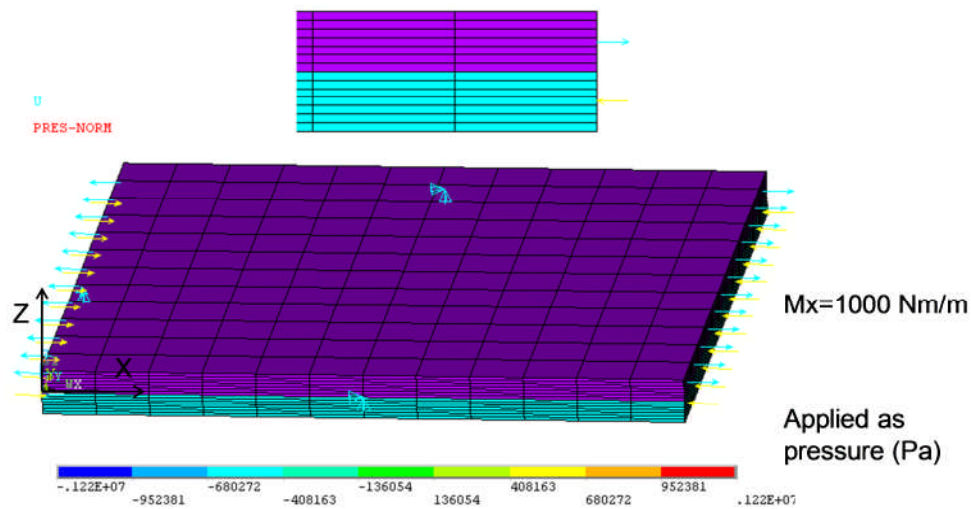


Figure 5-24 Boundary conditions of the plate under M_x modelled with SOLID46, SOLID186, SOLID191, and SOLSH190 (with two elements through the thickness).

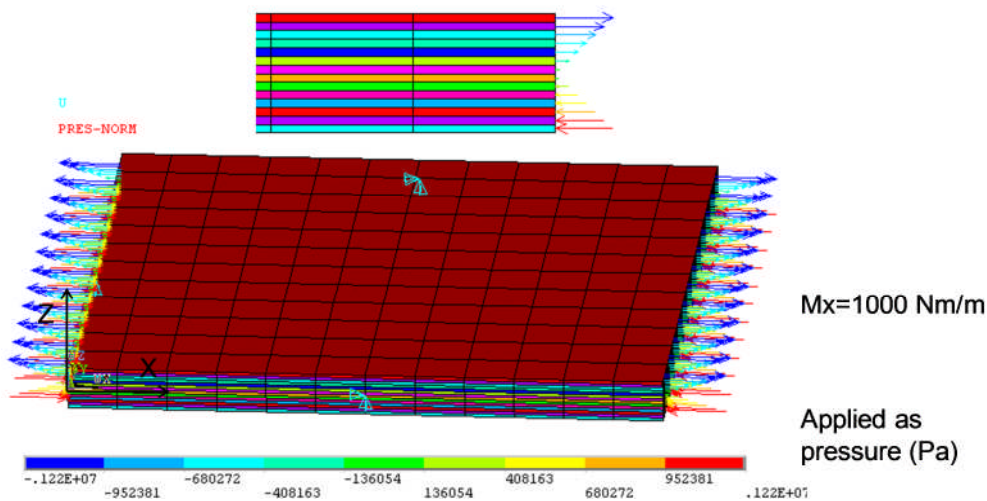


Figure 5-25 Boundary conditions of the plate under M_x modelled with SOLID191 (with one element per ply).

5.3.5 Postprocessing

Various in-plane results were requested (either as nodal or element results) from the FE model in the top centre location of each ply, which were extracted in the same order as the strength analysis steps presented in Section 5.2:

- Strains in the global coordinate system: $\varepsilon_x, \varepsilon_y, \gamma_{xy}$
- Strains in the laminate coordinate system: $\varepsilon_1, \varepsilon_2, \gamma_{12}$
- Stresses in the laminate coordinate system: $\sigma_1, \sigma_2, \tau_{12}$

- Failure index:
 - Maximum stress failure index
 - Tsai-Wu failure index (that for the purpose of this analysis is determined, despite it doesn't have an engineering interpretation (Section 4.6.1))

All results obtained are compared against Classic Lamination Theory results obtained with the Excel Spreadsheet (Appendix A).

All nodal results are obtained in the centre node of the plate. The centre node ID is stored in a variable (Centre_Node), which will then be referred to when requesting the corresponding results. The results are as well requested at the top of each ply (as calculated in the Classic Lamination Theory spreadsheet):

For shell elements, the ANSYS code created to store the centre node ID and request the results in the top location is the following:

```
SHELL, TOP                ! Results requested at the top of the shell
NSEL, S, LOC, X, L/2      ! Select the centre node (L/2, L/2)
NSEL, R, LOC, Y, L/2
*GET, Centre_Node, NODE, , NUM, MAX ! Store the Centre Node ID for
                                ! postprocessing purposes
```

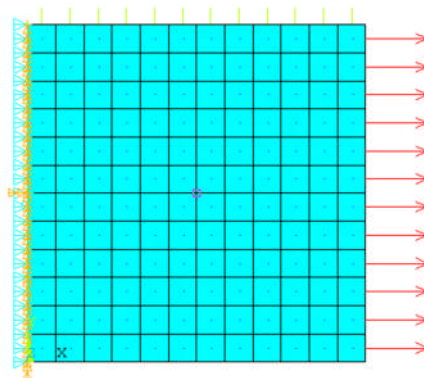


Figure 5-26 Results are requested in the centre node location. Thin plate under in-plane N_x axial load modelled with layered shell elements.

For the solid elements modelling with one element through the thickness (SOLID186, SOLID191) the centre top node ID is stored by means of:

```
NSEL, S, LOC, X, L/2      ! Select the top centre node
                            ! (L/2, L/2, t/2)
NSEL, R, LOC, Y, L/2
NSEL, R, LOC, Z, t/2
*GET, Centre_Node, NODE, , NUM, MAX ! Store the Centre Node ID for
                                ! postprocessing purposes
```

When modelling with two solid elements through the thickness (SOLID46, SOLID185, SOLID191, SOLSH190), the nodal results are obtained in the centre top node of each layer of elements, associated with each real constant identifier, which means:

- For bottom layer elements (REAL,1 (containing plies from 1 to 7)) select the centre node at $Z=0$.

```
NSEL,S,LOC,X,L/2
NSEL,R,LOC,Y,L/2
NSEL,R,LOC,Z,0
*GET,Ctr_Nd_elem1,NODE,,NUM,MAX

ALLSEL,ALL
```

- For top layer elements (REAL,2 (containing plies from 8 to 14)) select the centre node at $Z=h/2$.

```
NSEL,S,LOC,X,L/2
NSEL,R,LOC,Y,L/2
NSEL,R,LOC,Z,h/2
*GET,Ctr_Nd_elem2,NODE,,NUM,MAX
```

When modelling with three solid elements through the thickness (SOLID191):

- For bottom layer elements (REAL,1 (containing plies from 1 to 7)) select the centre node at $Z=0$.
- For top-middle layer elements (REAL,2 (containing plies from 8 to 11)) select the centre node at the corresponding layer thickness.
- For top layer elements (REAL,3 (containing plies from 12 to 14)) select the centre node at $Z=h/2$.

For the case of modelling the plate with one solid element per ply (SOLID191), a different Centre Node parameter should be created for the centre top of each ply:

```
*DO,II,1,14
  NSEL,S,LOC,X,L/2
  NSEL,R,LOC,Y,L/2
  NSEL,R,LOC,Z,-(h/2)+(II*tply)
  *GET,Ctr_Nd_elem%II%,NODE,,NUM,MAX

ALLSEL,ALL
*ENDDO
```

All element results are obtained in the centre element (approximately). For the case of modelling the plate with various solid elements through the thickness, the element

results are requested in the centre element (approximately) of each layer of elements, associated with each real constant.

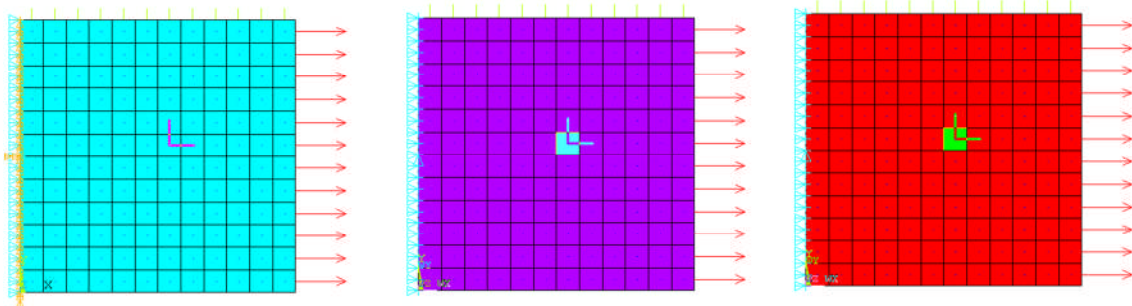


Figure 5-27 Element results are requested in the top centre element (approximately). Thin plate under in-plane N_x axial. One solid element through the thickness or shell elements (left). Two solid elements through the thickness (centre). Three solid elements through the thickness or one solid element per ply (right).

5.4 Results

Results comparison among all different formulations and CLT calculations are presented in the form of radar charts. The deviation of the *Simulation* results from the *CLT* results is given by the following expression:

$$Deviation [\%] = \frac{Simulation - CLT}{CLT} \times 100 \quad (5-2)$$

The radar charts represent the deviation according to the following expression.

$$Deviation = 1 + \frac{Deviation [\%]}{100} \quad (5-3)$$

Each radar chart axis represents a ply. Thus, a comparison of all 14 laminate layers is done; consistently, ply number 1 is located at the bottom of the laminate and ply number 14 is located at the top.

Due to the large amount of data generated for this analysis only few results comparison are going to be presented.

For the in-plane axial loading case, N_x , all intermediate results required in CLT to evaluate the failure index of the plate are going to be compared (Section 5.3.5). But for

the rest of the loading cases, as the ultimate interest is to evaluate the failure index, only this is going to be compared (for the two failure criteria evaluated, Tsai-Wu and Maximum stress criteria).

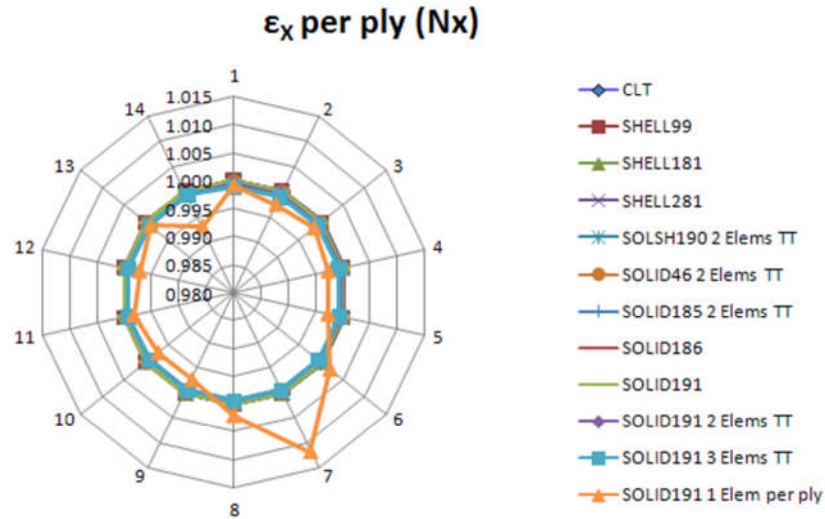


Figure 5-28 ϵ_x per ply comparison. Thin plate under in-plane load $N_x=1000$ N/m.

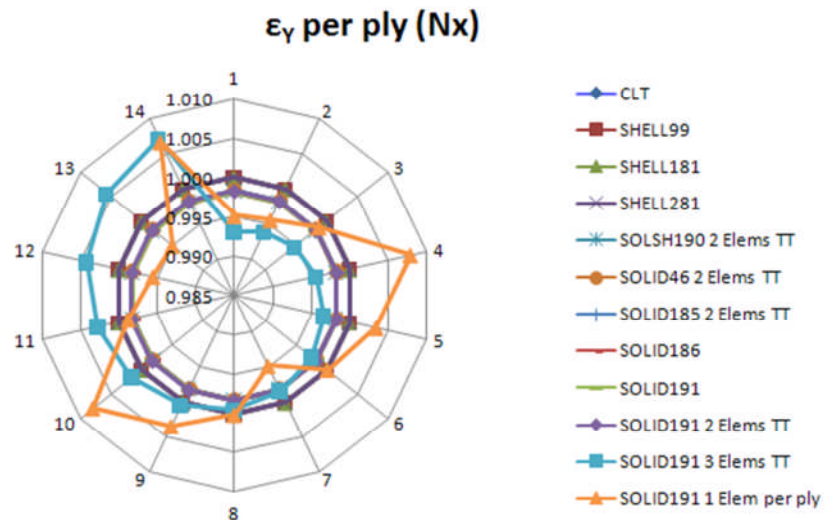


Figure 5-29 ϵ_y per ply comparison. Thin plate under in-plane load $N_x=1000$ N/m.

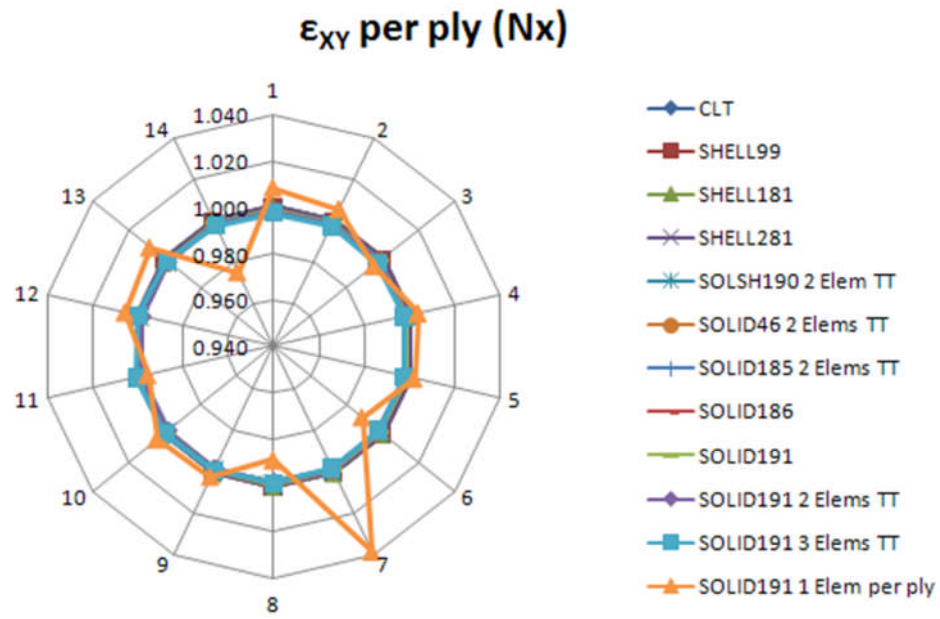


Figure 5-30 ϵ_{xy} per ply comparison. Thin plate under in-plane load $N_x=1000$ N/m.

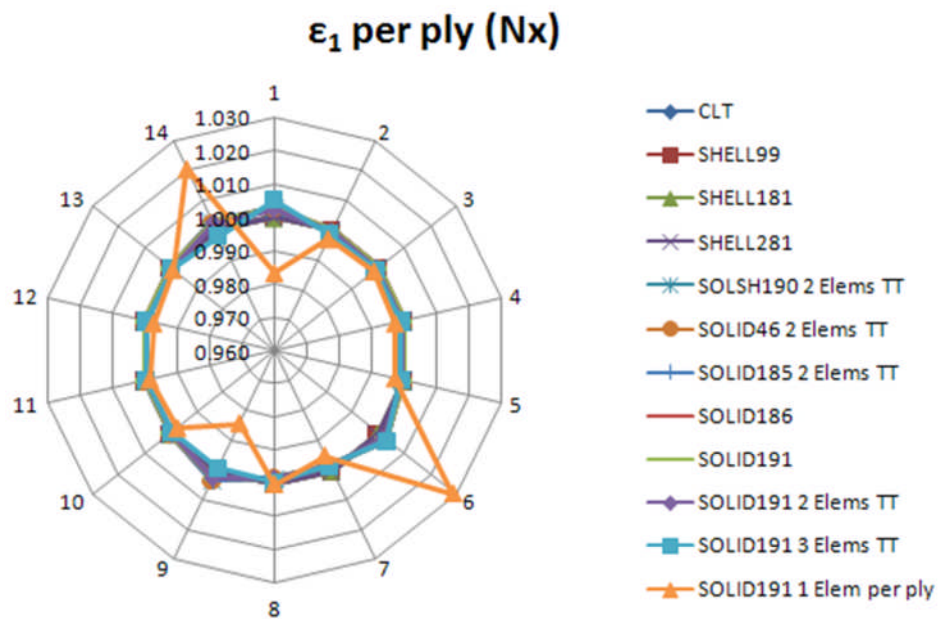


Figure 5-31 ϵ_1 per ply comparison. Thin plate under in-plane load $N_x=1000$ N/m.

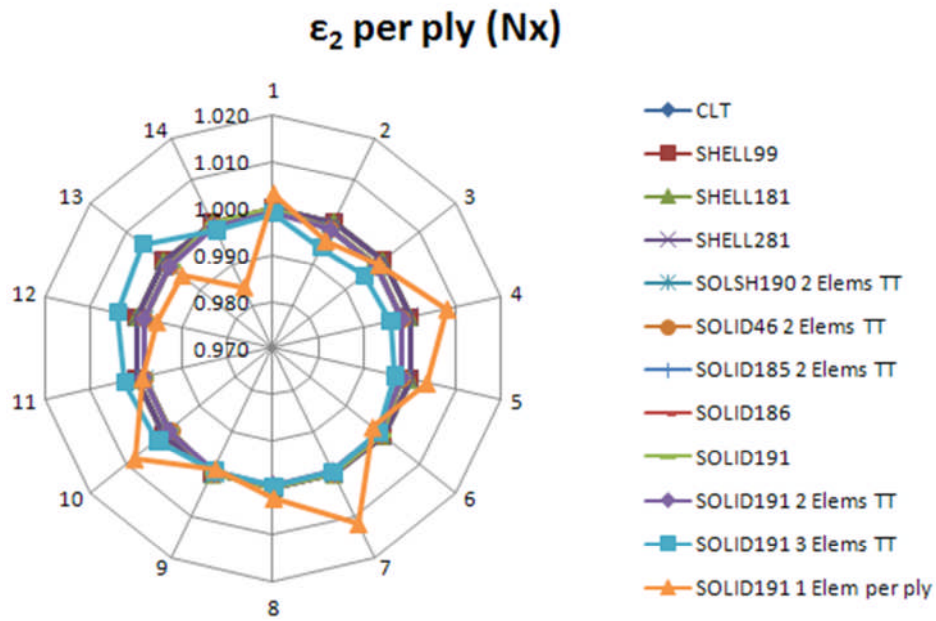


Figure 5-32 ϵ_2 per ply comparison. Thin plate under in-plane load $N_x=1000$ N/m.

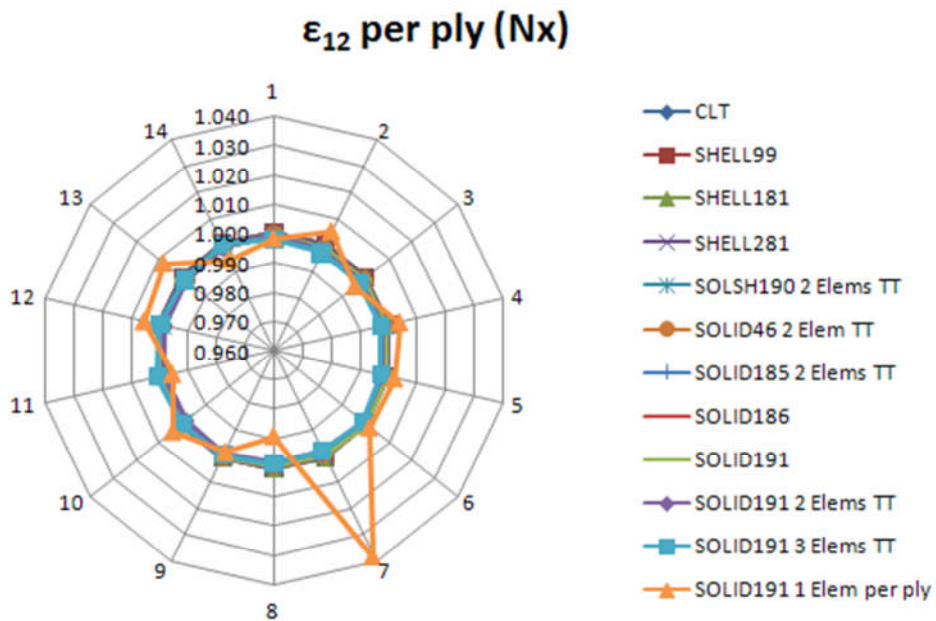


Figure 5-33 ϵ_{12} per ply comparison. Thin plate under in-plane load $N_x=1000$ N/m.

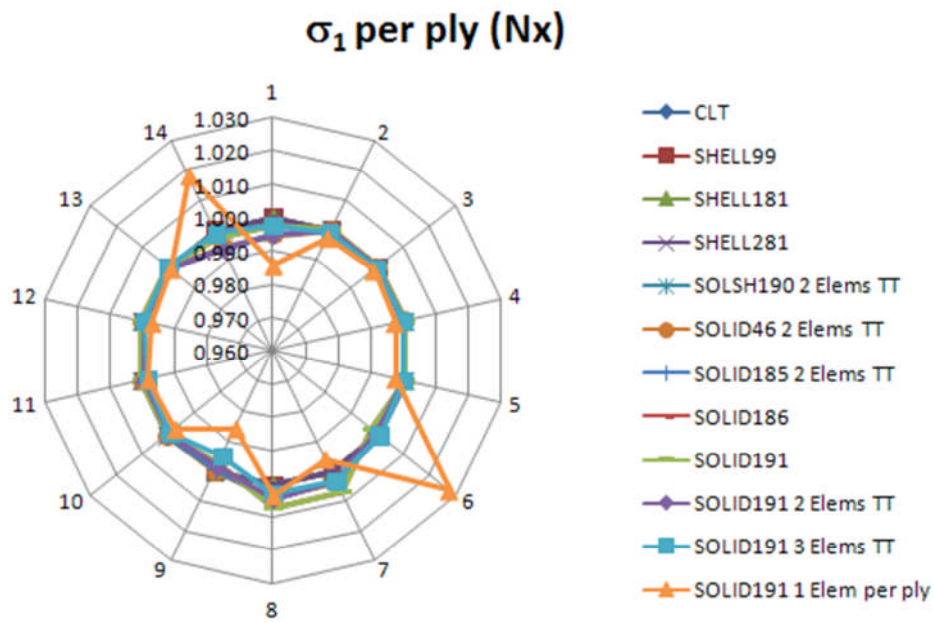


Figure 5-34 σ_1 per ply comparison. Thin plate under in-plane load $N_x=1000$ N/m.

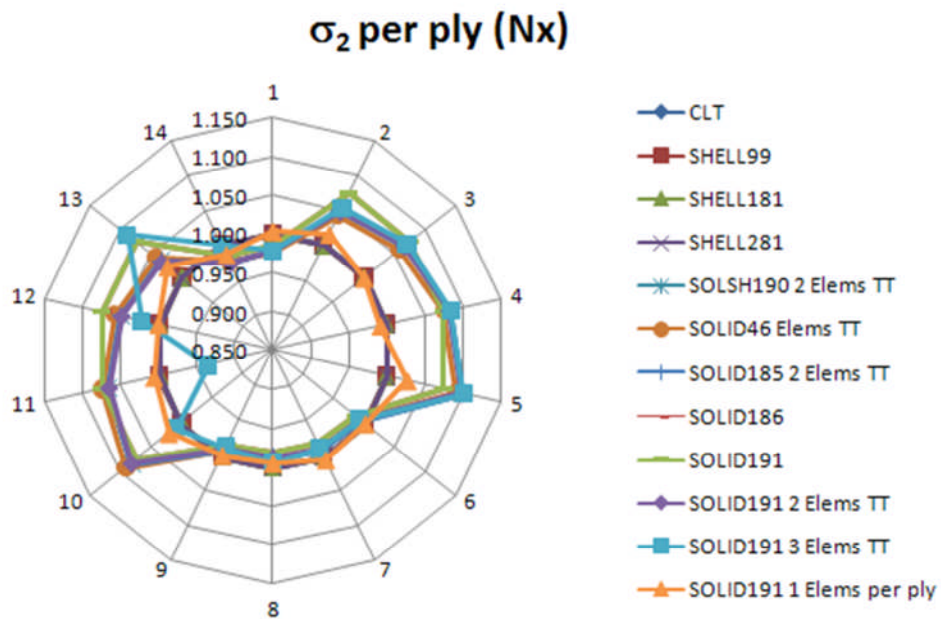


Figure 5-35 σ_2 per ply comparison. Thin plate under in-plane load $N_x=1000$ N/m.

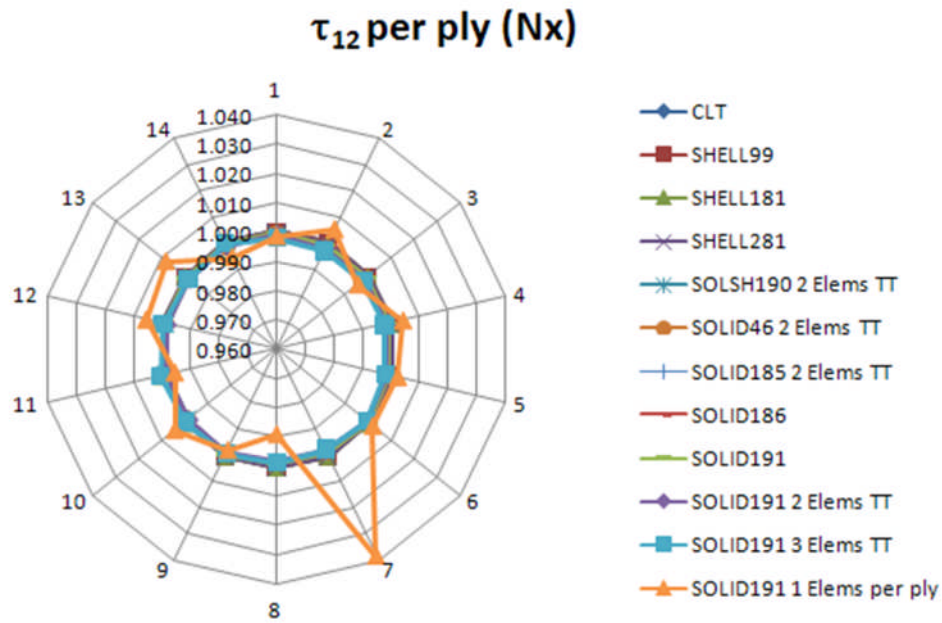


Figure 5-36 τ_{12} per ply comparison. Thin plate under in-plane load $N_x=1000$ N/m.

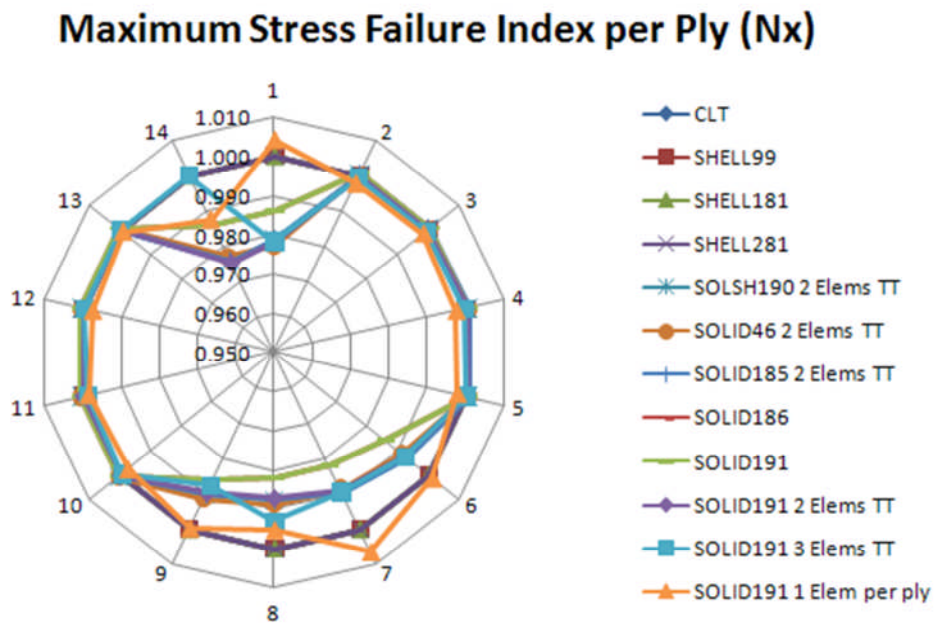


Figure 5-37 Maximum Stress Failure Index per ply comparison. Thin plate under in-plane load $N_x=1000$ N/m.

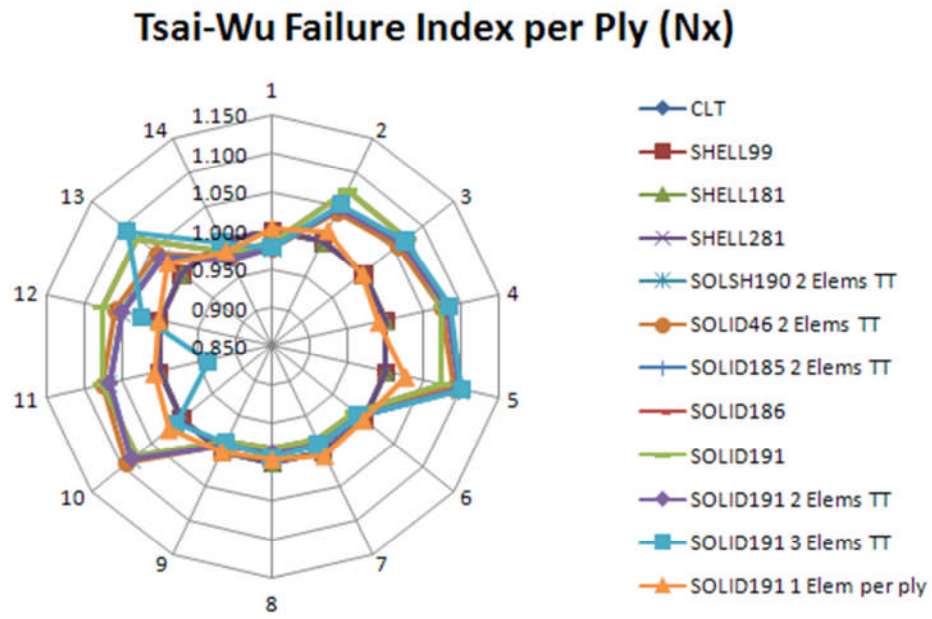


Figure 5-38 Tsai-Wu Failure Index per ply comparison. Thin plate under in-plane load $N_x=1000$ N/m.

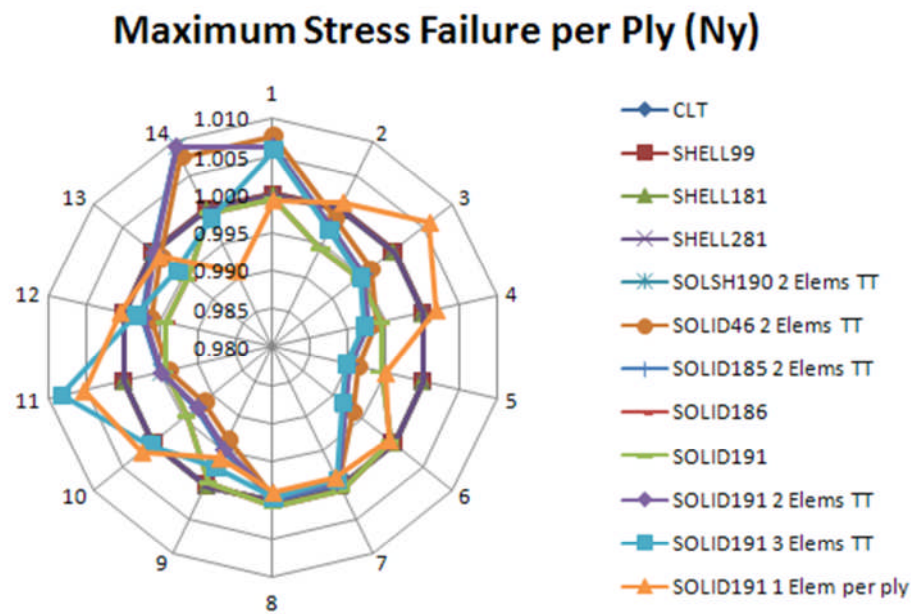


Figure 5-39 Maximum Stress Failure Index per ply comparison. Thin plate under in-plane load $N_y=1000$ N/m.

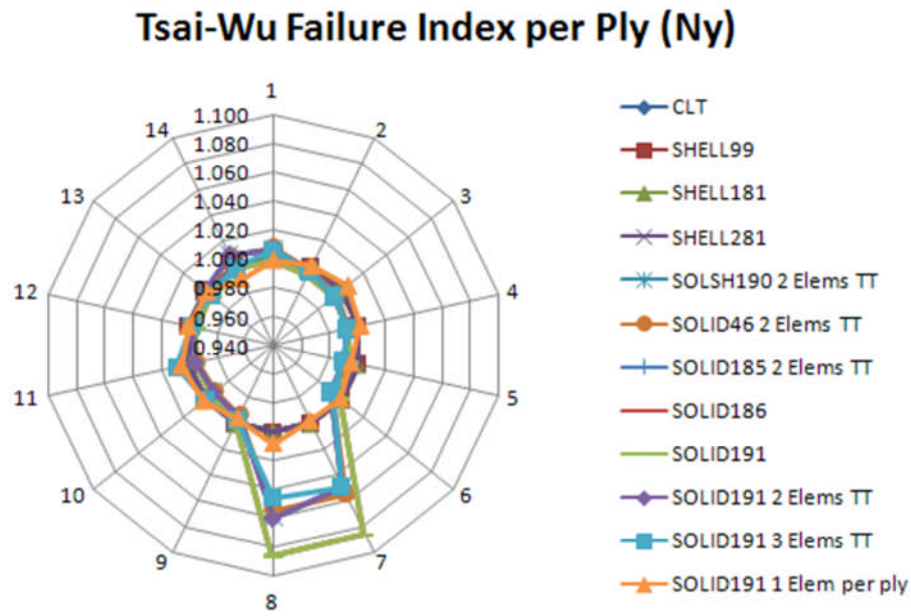


Figure 5-40 Tsai-Wu Failure Index per ply comparison. Thin plate under in-plane load $N_y=1000$ N/m.

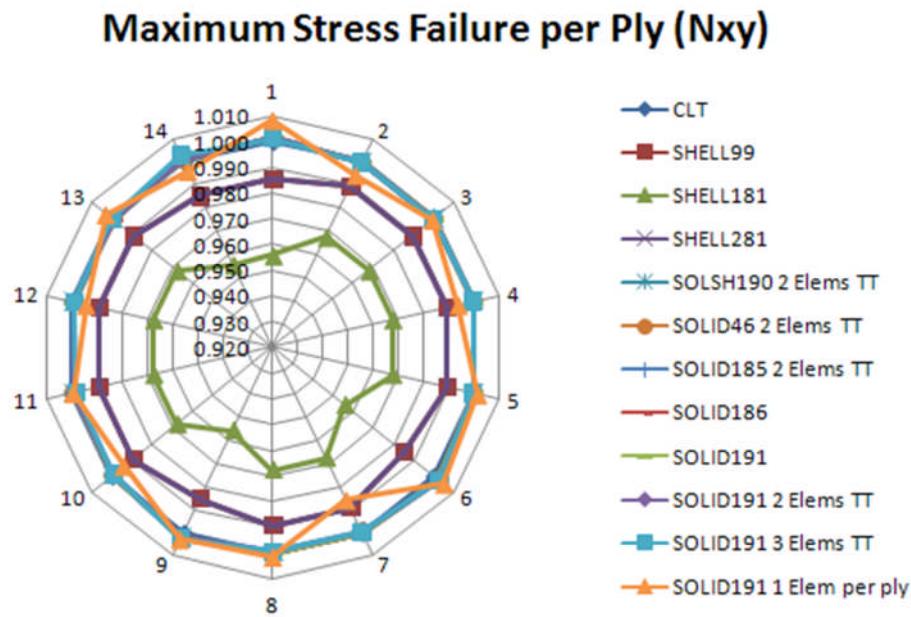


Figure 5-41 Maximum Stress Failure Index per ply comparison. Thin plate under in-plane shear load $N_{xy}=1000$ N/m.

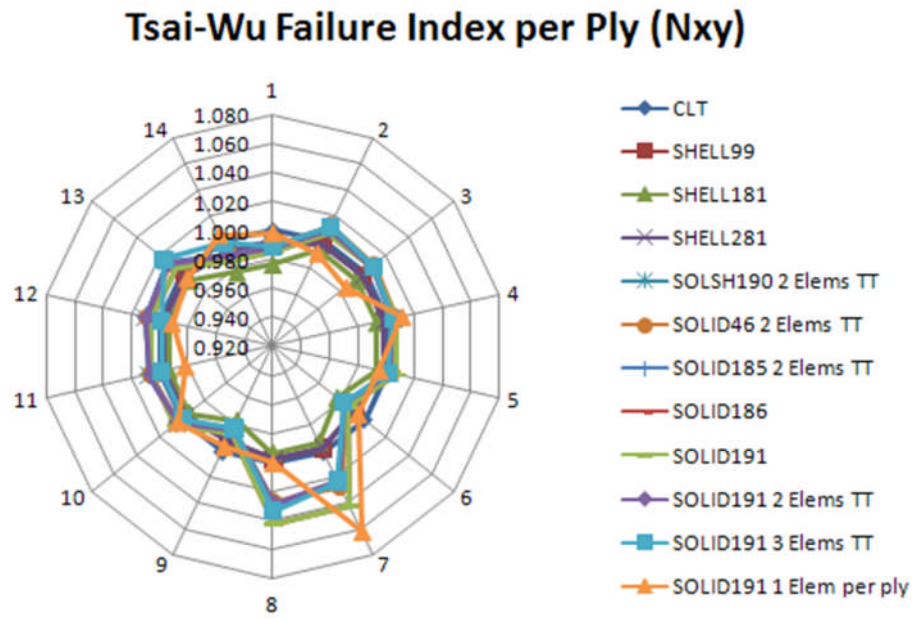


Figure 5-42 Tsai-Wu Failure Index per ply comparison. Thin plate under in-plane shear load $N_{xy}=1000$ N/m.

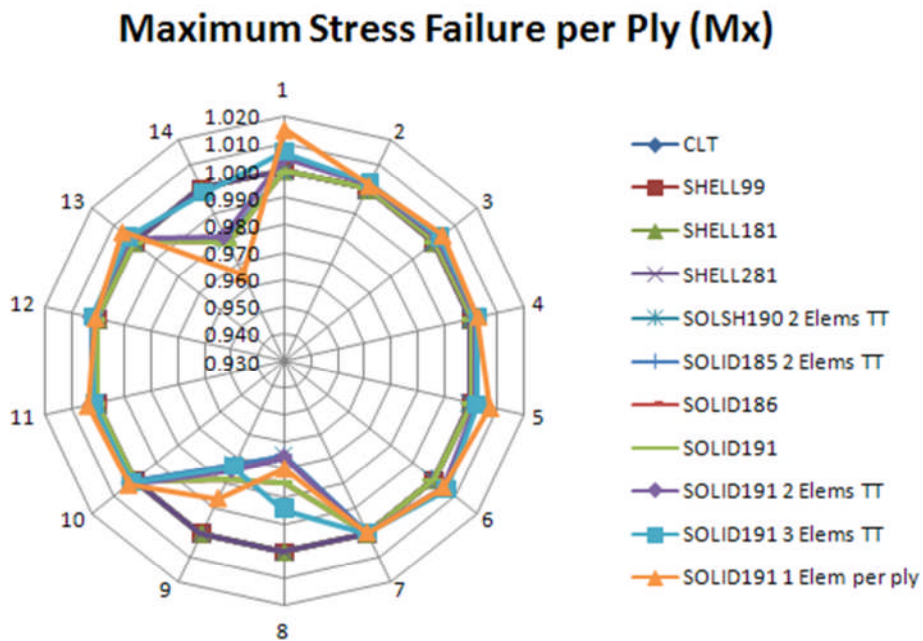


Figure 5-43 Maximum Stress Failure Index per ply comparison (except SOLID46). Thin plate under out-of-plane bending moment $M_x=1000$ Nm/m.

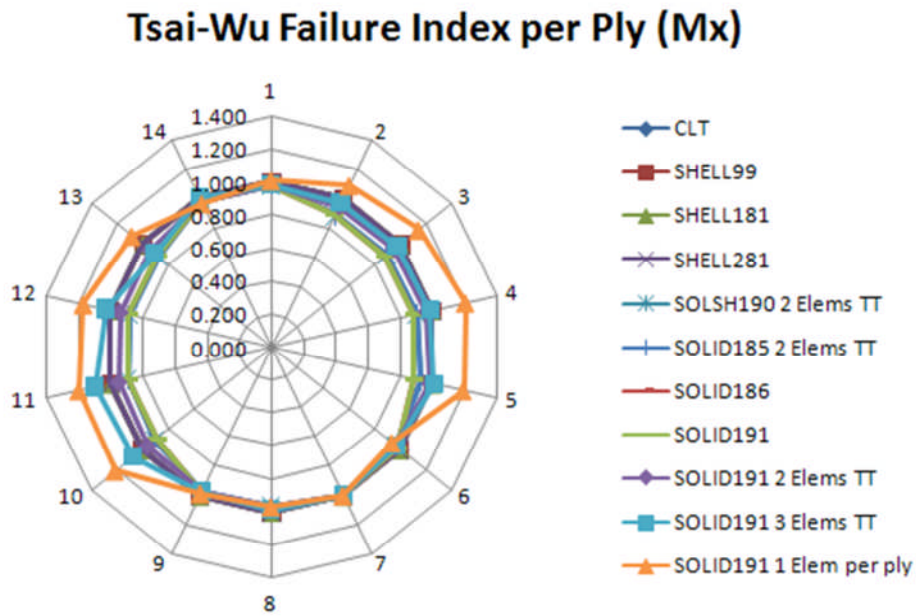


Figure 5-44 Tsai-Wu Failure Index per ply comparison (except SOLID46). Thin plate under out-of-plane bending moment $M_x=1000$ Nm/m.

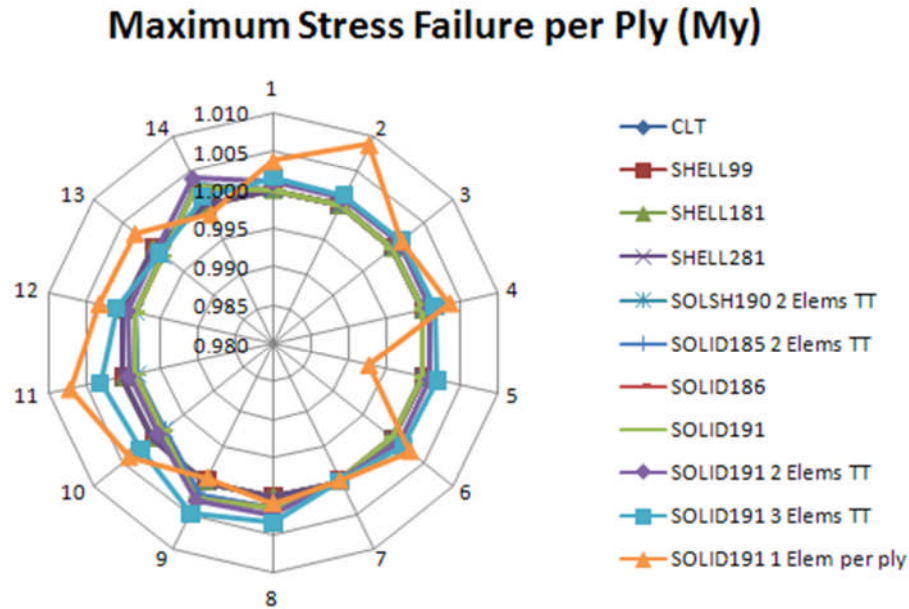


Figure 5-45 Maximum Stress Failure Index per ply comparison (except SOLID46). Thin plate under out-of-plane bending moment $M_y=1000$ Nm/m.

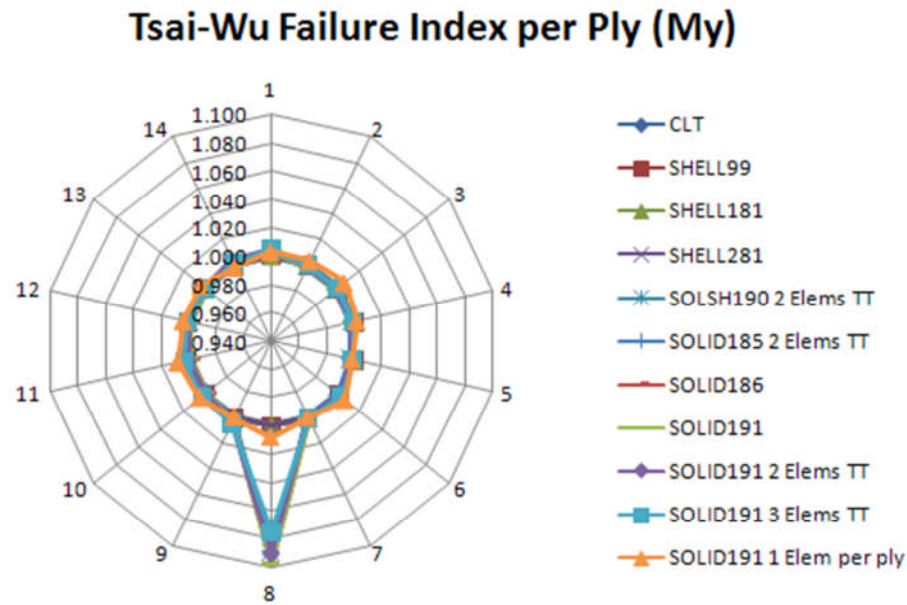


Figure 5-46 Tsai-Wu Failure Index per ply comparison (except SOLID46). Thin plate under out-of-plane bending moment $M_y=1000$ Nm/m.

The main steps involved in a finite element analysis can be found in Kollár (2003). The strain vector at the integration points within the element are determined from the displacement subvector δ , accounting for the integration points displacement, and the strain-displacement matrix $[B]$, according to the following expression:

$$\boldsymbol{\varepsilon} = [B]\boldsymbol{\delta} \quad (5-4)$$

These strains are transformed from the global axis (element coordinate system (Section 4.5)) to the layer coordinates. Finally, the stresses at the element integration points are computed by

$$\boldsymbol{\sigma} = [E]\boldsymbol{\varepsilon} \quad (5-5)$$

Being $[E]$ the stiffness matrix of the laminated composite characterising the material. This matrix has a different definition for each element formulation. The stiffness matrices for some of the layered elements used in this analysis are presented in 8.2.8.2 Appendix J.

On the other hand, the determination of the failure indices by means of the CLT (excel spreadsheet) has revealed that the Tsai-Wu failure index is primarily defined by its second term (Eq (3-24)), ruled by the stresses in the transverse fibre direction, being the other terms several orders of magnitude smaller. No interaction term has been considered ($F_{12}=0$) for this case. Despite this failure criterion does not have an engineering interpretation (Section 4.6.1), it predicts the ply failure although not the mode of failure (tension or compression).

Maximum stress failure criterion has shown more conservative than Tsai-Wu, with higher failure indices at a ply level. It is a non-interactive criterion, which not only predicts the ply failure but its mode of failure.

In general, all layered shell elements provide very accurate results for both, in-plane and out-of-plane loads. The only deviation with regards the analytical results (CLT) are found for the shear load case N_{xy} , with less than 3% of deviation for SHELL181 (4-node layered shell), and less than 1% for the other two formulations. This may be due to the fact that shear loads were applied using *consistent nodal loading* in an inclined support (Section 5.3.4 d), instead of pressure loads in lines (SFL), and some inaccuracy might have been caused. SHELL99 and SHELL281, for which FSDT has been considered, give the same results, as and the latter is an improved shell formulation that can be used instead of SHELL99 for most problems (ANSYS help manual). SHELL181 provides slightly more inaccurate results for this load case, possibly due to its under integrated element formulation definition. Tsai-Wu failure indices are predicted more accurately than the maximum stress ones, and in terms of orientation, failure indices of plies at 45° present the highest deviations.

Regarding the layered solid formulations, for the case of the axial load in the fibre direction (N_x), all results give a good agreement with the analytical ones, but the SOLID191 with one element per ply diverges in general more than the other element formulations (with a deviation ranging between 1%-4%), presenting variations at a ply level. Maximum stress failure indices are more accurately described by the layered solid formulations than the Tsai-Wu failure indices. For the latter (as well as for σ_2 responsible for the second term of the Tsai-Wu failure index expression), most layered solid formulations overestimate the failure index for the plies defined in the direction where load is applied (fibre direction in this case), presenting up to 10% of deviation.

As already mentioned, for the rest of the loading cases the two failure indices are the only results considered. For N_y , again all layered solid formulations give more accurate results for the case of maximum stress criterion (with less than 1% of deviation) than for the Tsai-Wu criterion. Also, as with the previous load case, solid formulations (except SOLID191 with one element per ply, which shows less variation) overestimate the Tsai-Wu failure indices in the load application direction (transverse fibre direction in this case), presenting up to 10% of deviation

For the shear load case N_{xy} , all solid formulations give very good agreement, with less than 1% of deviation with regards to the maximum stress failure index, and with less than 4%-6% for the case of Tsai-Wu failure index, particularly for the plies oriented along the fibre and transverse fibre direction.

For the bending moment loading cases (M_x , M_y) the worst results are the obtained for SOLID46 (8-node) with exaggerated deviations from analytic results (more than 50%), thus they have been excluded from the charts. For M_x , all formulations provide deviations smaller than 3% for the maximum stress failure index, but quite significant for all plies at 0° , with maximum deviations of nearly 20% for the SOLID191 with one element per ply. This fact is not yet well understood and needs further investigation with other laminate configurations.

For M_y , all formulations present deviations smaller than 2% for the maximum stress failure, and a good agreement as well for the Tsai-Wu failure index, except for the 8th ply (90°) with less than 10%. Again, other laminate configurations need to be considered for a better understanding of the in-plane response of layered solid elements under bending applications.

5.5 Conclusions

The principal purpose of the present section was to get practical experience with ANSYS for modelling thin laminated composite plates, as a previous step before tackling the UTL composite structural analysis. Different layered element formulations were benchmarked against analytical results obtained from CLT analysis performed on a particular configuration of a laminated plate under in-plane and out-of-plane load cases, by comparing several in-plane results (ultimately the ply failure index for Tsai-Wu and Maximum stress criteria).

For the case of layered solid formulations, different modelling strategies were also evaluated, modifying the number of layered elements through the thickness for a fixed number of plies; in order to evaluate the effects that, not only the element formulation, but also the modellisation technique has on the accuracy of the results at a layer in-plane level.

This analysis has helped also to develop the author skills for creating and postprocessing parametric models using the Ansys Parametric Design Language, which could represent a wide range of different laminate configurations, with the idea of using such capability in future applications.

The plate was modelled with layered shell elements (4 and 8 nodes), layered solid elements (8 and 20 nodes), and intermediate layered solid-shell formulation (8 nodes), defining all laminates at a ply level, and not by using smeared properties.

All layered shell formulations give a very good agreement with the analytical results, for both, in-plane and out-of-plane. The only deviations are found in the under integrated formulation (SHELL181) when in-plane shear is applied.

The higher deviation values obtained for layered solid formulations demonstrate that, in general, they are not suited for thin applications, although in some cases they have a very good agreement with the analytical results (as for the case of in-plane shear load).

For Maximum stress criterion, which has shown to be a more conservative failure criterion than Tsai-Wu's, its ply failure indices are more accurately predicted by layered solid formulations than Tsai-Wu failure indices. For the latter, most layered solid formulations overestimate the failure index for the plies defined in the direction where load is applied, presenting up to 10% of deviation in some cases.

The results obtained for SOLID191 modelled with one element per ply showed more variability at a ply level than the rest of the formulations, and considering the deviations obtained for this element formulation for all different modelling strategies thicker applications are required to extract more solid conclusions.

For a fixed number of plies and a fixed plate thickness, as the number of layered elements through the thickness is increased their aspect ratio is distorted, possibly affecting the quality of the results. For this reason a mesh sensitivity analysis was carried out. Results are presented in Appendix C. Various meshes were compared (14x14, 28x28, 50x50). From the results obtained it can be concluded that in-plane failure indexes results are not really mesh depended, for the element size considered.

6 Verification – Ultra Thick Laminate

6.1 Accuracy vs CPU time

Ansys layered solid element formulations were extended to consider more complex examples, such as a moderately thick curved plate under pure bending moment (to which an analytical solution is available), which could partially represent a simplified model of one half of the main side stay fitting flange. This natural extension to the complexity of the problem provided another opportunity to assess the applicability of layered solid formulations for analysing and predicting the mechanical response of UTL components.

Laminated curved plates are vulnerable to out-of-plane delamination failure when bending moments are applied on them, resulting in tensile or compressive radial stresses in the fillet region at the component edge. By this failure mechanism, plies tend to separate from each other, producing a significant reduction of the plate mechanical properties (strength and stiffness), which eventual will cause the structure to collapse.

The main parameters affecting delamination are either the interlaminar shear stresses (τ_{13}) between adjacent layers, or the tensile radial stress (σ_{33}) across the laminate thickness. From these two, the latest is the principal cause of delamination of laminated curved plates.

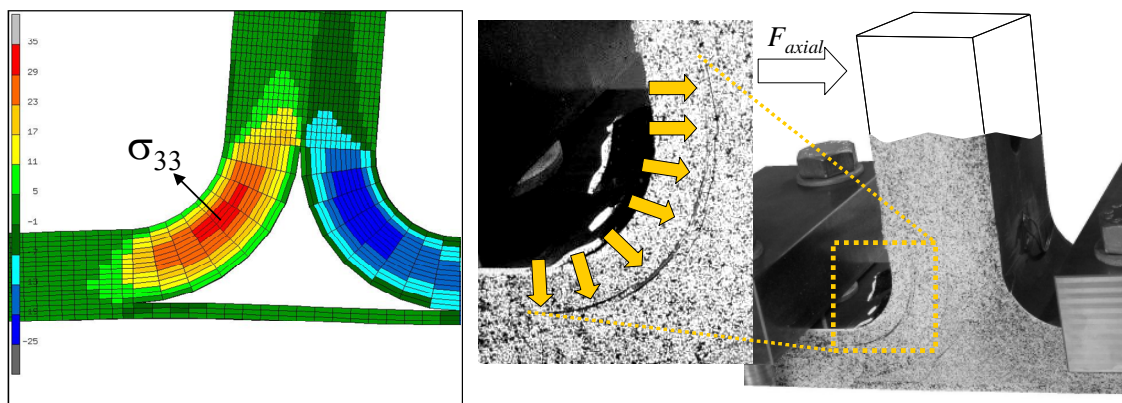


Figure 6-1 T-junction specimen under bending moment ($F_{axial,max}=42kN$).

Simulation model (l), and correlation test (r) showing delamination due to radial stress, σ_{33} . Source: Siemetzki et al., (2007).

The aim for this second analysis is to determine the Pre / Post processing best practice, and the required element formulation and number of elements through the thickness to accurately represent the radial stress (σ_{33}), and the tangential stress (σ_{22}) of a moderately thick laminated curved plate subjected to an out-of-plane bending moment, at a low computational cost.

6.1.1 Analytic solution

The exact analytical expressions for the radial (σ_{33}) and tangential (σ_{22}) stresses across the thickness of an isotropic curved beam under bending moment M are available in literature (Ugural et al., 2003).

$$\sigma_{33} = \frac{4M}{tb^2N} \left[\left(1 - \frac{a^2}{b^2}\right) \left(\ln \frac{r}{a}\right) - \left(1 - \frac{a^2}{r^2}\right) \left(\ln \frac{b}{a}\right) \right] \quad (6-1)$$

$$\sigma_{22} = \frac{4M}{tb^2N} \left[\left(1 - \frac{a^2}{b^2}\right) \left(1 + \ln \frac{r}{a}\right) - \left(1 + \frac{a^2}{r^2}\right) \left(\ln \frac{b}{a}\right) \right] \quad (6-2)$$

with,

$$N = \left(1 - \frac{a^2}{b^2}\right)^2 - 4 \frac{a^2}{b^2} \ln^2 \left(\frac{b}{a}\right) \quad (6-3)$$

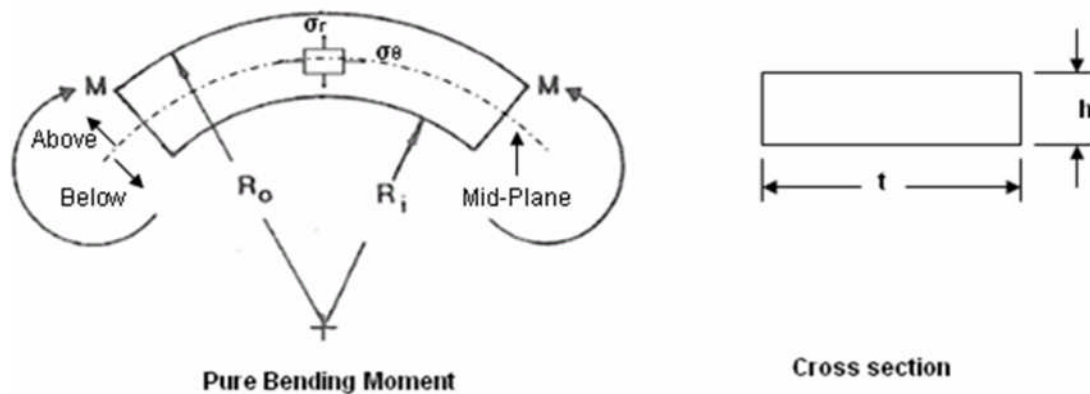


Figure 6-2 Curved beam under bending moment. Source: Nguyen, 2010.

The parameters involved in the expressions are described in the following table, and represented in Figure 6-2.

Table 6-1 Parameters description of curved beam dimensions.

<i>Parameter</i>	<i>Description</i>
$a=R_i$	Inner radius
$b=R_o$	Outer radius
R	Radial location across beam thickness ($R_i < r < R_o$)
T	Plate width
H	Cross section height

The dimensions in metric units used to calculate the radial and tangential stresses of this curved beam are shown in Table 6-2.

Table 6-2 Curved plate dimensions (in SI units).

<i>Dimension</i>	<i>Parameter</i>	<i>Value (m)</i>
Inner Radius	R_i	0.60
Outer Radius	R_o	0.66
Width	t	1.00
Height	h	0.06

The curved plate is subjected to a pure bending moment (M) of 100 Nm/m, in a direction that tends to apply a compressive bending moment in the outer half cross section of the curved beam, and a tensile bending moment in the inner half cross section (see Figure 6-2).

The calculated radial (σ_{33}) and tangential (σ_{22}) stresses according to Eqs (6-1) and (6-2), for 12 evenly distributed radial locations (5mm between two consecutive locations) across the curved beam thickness are summarised in Table 6-3, and presented in Figure 6-3.

Table 6-3 Radial and tangential stresses from exact solution obtained at different radial location (from inner to outer every 5mm) (in SI units).

<i>Point</i>	<i>Radial Position (m)</i>	<i>Radial Stress σ_{33} (Pa)</i>	<i>Tangential Stress σ_{22} (Pa)</i>
12	0.60500	1.30E+03	1.42E+05
11	0.61000	2.33E+03	1.12E+05
10	0.61500	3.10E+03	8.26E+04
9	0.62000	3.62E+03	5.37E+04
8	0.62500	3.91E+03	2.53E+04
7	0.63000	3.97E+03	-2.64E+03
6	0.63500	3.81E+03	-3.02E+04
5	0.64000	3.44E+03	-5.72E+04
4	0.64500	2.86E+03	-8.39E+04
3	0.65000	2.09E+03	-1.10E+05
2	0.65500	1.14E+03	-1.36E+05
1	0.66000	0.00E+00	-1.62E+05

According to these results, all radial stresses across the beam (σ_{33}) are found positive (tensile), with a parabolic distribution, and a maximum value of 3.97 kPa in the beam mid-plane section. The tangential stresses (σ_{22}) however, are found positive (tension) across the inner half section from the beam mid-plane, while the outer half section is under compression, in agreement with the direction of application of the bending moment.

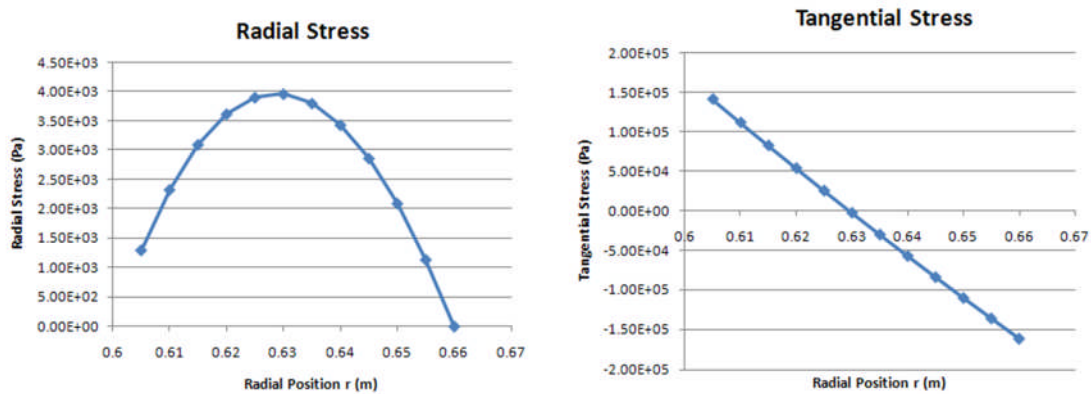


Figure 6-3 Analytic radial (σ_{33}) and tangential (σ_{22}) stresses (Pa) across the thickness of a curved beam under applied out-of-plane bending moment $M=100$ Nm/m.

6.1.2 FE Analysis

The previous analytic radial (σ_{33}) and tangential stress (σ_{22}) are now intended to be reproduced by performing a FEA of an equivalent laminated curved, made of a 12 orthotropic plies of carbon fibre-epoxy resin, with all plies at 0° .

The curve plate was created making use of two different layered solid element formulations (8 and 20 nodes). Different modelling strategies were evaluated, modifying the number of layered elements through the thickness, in order to evaluate the effects that, not only the element formulation, but also the modelling technique has on the accuracy of the results.

A summary of the ANSYS element formulations and the different modelling strategies used is summarised below:

- *Solids:* SOLID46 & SOLID185 (8-node layered solid element), SOLID186 & SOLID191 (20-node layered solid element).
- *Modelling Strategy:* 1, 2, 3, 4 layered elements through the thickness; and 1 element per layer with both element formulations.

A general description of these layered elements can be found in Section 4.3.2.

Following, a description of the plate FE model generation is presented.

6.1.2.1 Model Description

The laminated material properties are summarised in the following table (the material properties are the same as the ones used in Section 5.1):

Table 6-4 2D orthotropic material properties (in SI units).

<i>Elastic Constant</i>	<i>Definition</i>	<i>Value</i>
E_1 (Pa)	Young's modulus in the fibre direction	1.81E+11
E_2 (Pa)	Young's modulus in the transverse direction	1.03E+10
ν_{12}	Major Poisson's ratio	0.28
G_{12} (Pa)	Shear modulus	7.17E+09

The laminate definition is described below:

Table 6-5 Laminate definition.

<i>Laminate Parameters</i>	<i>Value</i>
Total number of plies	12
Ply thickness (m)	5.00E-03
Total Ply Thickness (m)	0.06
Stacking Sequence	[0/0/0/0/0/0] _s



Figure 6-4 Iso view of the curved plate and the material axes directions. Source: Nguyen, 2010.

Figure 6-4 depicts the material axes orientation, where the fibre direction is along the plate width, the transverse fibre direction is defined along the tangential direction, and the normal direction (radial) is defined according to the right hand rule.

6.1.2.2 Geometry

A semicircular curved beam model was created; its geometry definition was determined by the modelling strategy adopted. The curved plate is modelled as a single volume, for the case of having only one layered element through the thickness. When more than one layered element is going to be used, a series of volumes stacked on top of each other need to be modelled (Figure 6-5 and Figure 6-6) (the justification to this approach is given in Section 4.2).

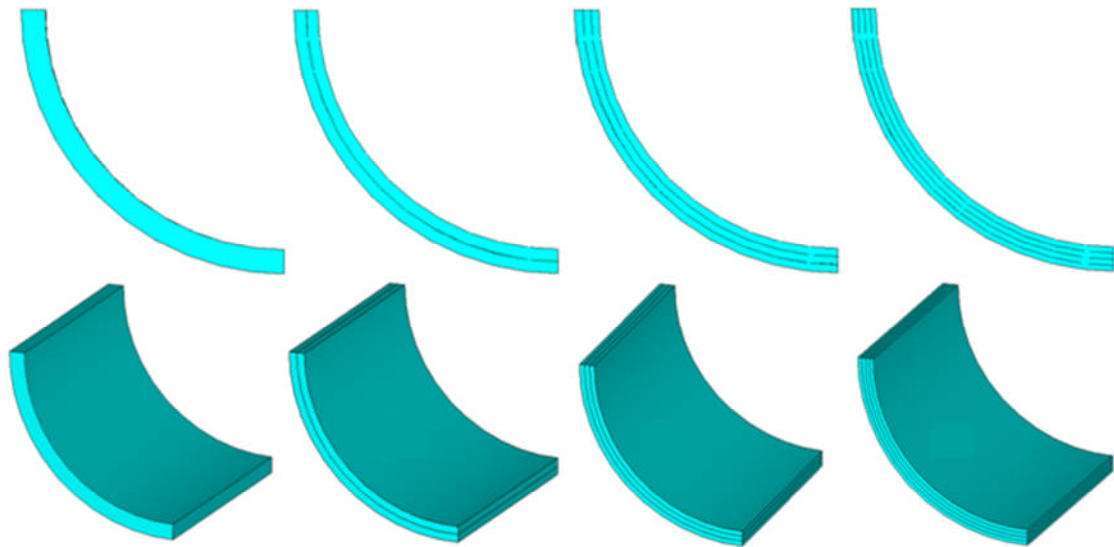


Figure 6-5 Curved plate geometry model. Geometry is defined different for each model: 1 element through the thickness (l) to four elements through the thickness (r).

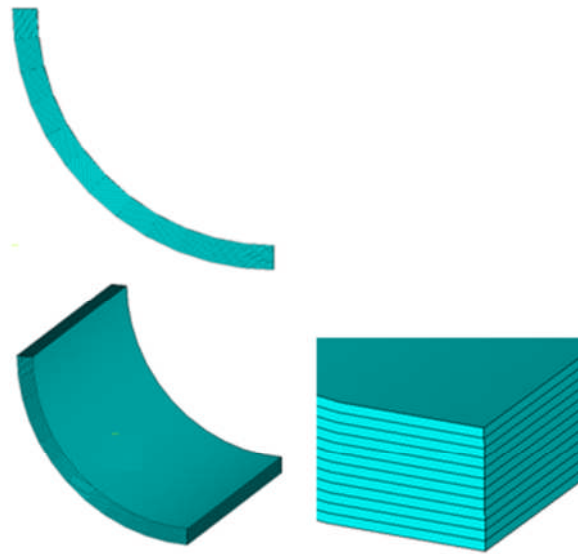


Figure 6-6 Curved plate geometry model. Geometry is defined with 12 volumes to be meshed with one solid element per ply.

6.1.2.3 Mesh

All five models have the same in-plane mesh, with 24 elements in the width direction and 30 elements in the circumferential direction.

The number of elements in the radial direction though, is again determined by the modelling strategy.

6.1.2.4 Element coordinate system

By default, the layer coordinate system in ANSYS is parallel to the element coordinate system. The ESYS command should be used in this case in order to re-orientate the element coordinate system of the model the laminate as required, i.e., with the fibre direction along the width and with the matrix defined in the tangential direction:

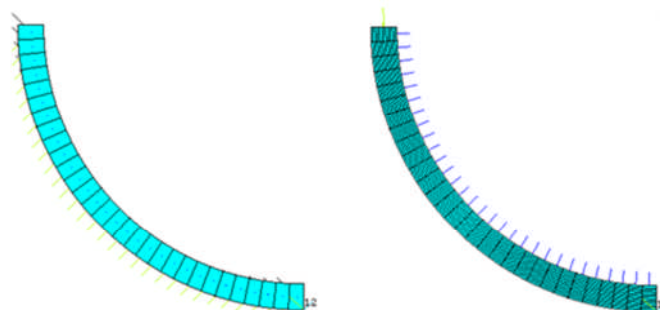


Figure 6-7 Reorientation of the elements coordinate system, ESYS. Initial ESYS orientation (l), modified ESYS orientation (r).

The ANSYS code required for this operation (according to the defined geometry) is:

```

/VSCALE,,2                ! Double size of symbols, like element CS
/PSYMB,ESYS,1            ! Turn on element coordinate system symbols

CSYS,0
LOCAL,12,,a+h,,t,,,90,   ! Define a Cartesian local system
CLOCAL,12,,,,,-45,       ! and modify its orientation as required
ESYS,12                  ! Sets the element coordinate system
                          ! attribute pointer to the previously defined
                          ! coordinate system

VMESH,ALL                ! Mesh all volumes
ESLV,S                   ! Select all elements
EORIENT,LYSL,NEGZ        ! Recreate SOLID191 elements, as desired
EPlot

```

6.1.2.5 Boundary conditions

The two boundary conditions applied are defined in the global coordinate system.

Symmetries in geometry, laminate definition and load applied, allow to fully restrain all nodes at one end of the curved beam.

```

CSYS,0                    ! Global Cartesian coordinate system

NSEL,S,LOC,Y,a+h         ! Select the nodes at the top end
D,ALL,ALL                ! Fully-clamped

```

A pure bending moment of $M=100 \text{ Nm/m}$ was applied at the free end. Its direction of application is defined so as when applied the inner cross section is under tension, and the outer cross section is under compression.

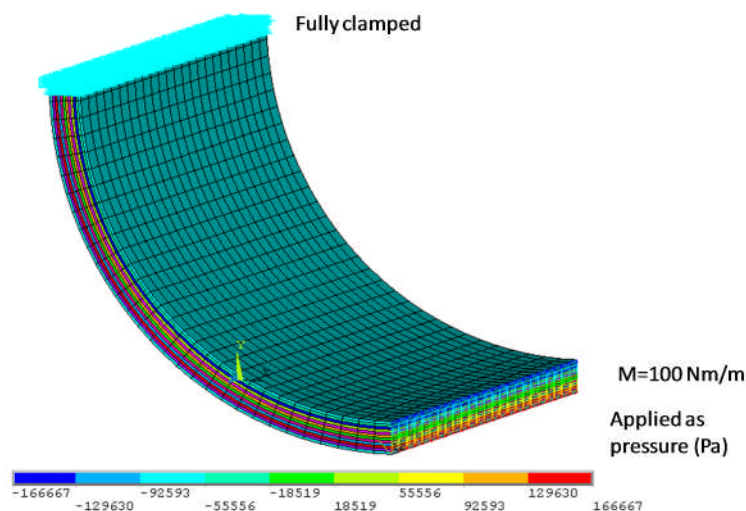


Figure 6-8 BCs applied on the curved beam modelled with one solid element per layer. Bending moment applied as a linear varying pressure over the end section.

6.1.3 Results

The results are requested at the bottom nodes of each ply (according to the z axis of the element coordinate system), for the nodes located in the middle of the curved plate.

ANSYS calculate the results in the integration points and then they are extrapolated to the nodes. Nodal results or element results are the only type of results to be requested in ANSYS.

Following, a comparison between all layered solid element formulations considered and the exact analytic solution for the five modelling strategies is presented.

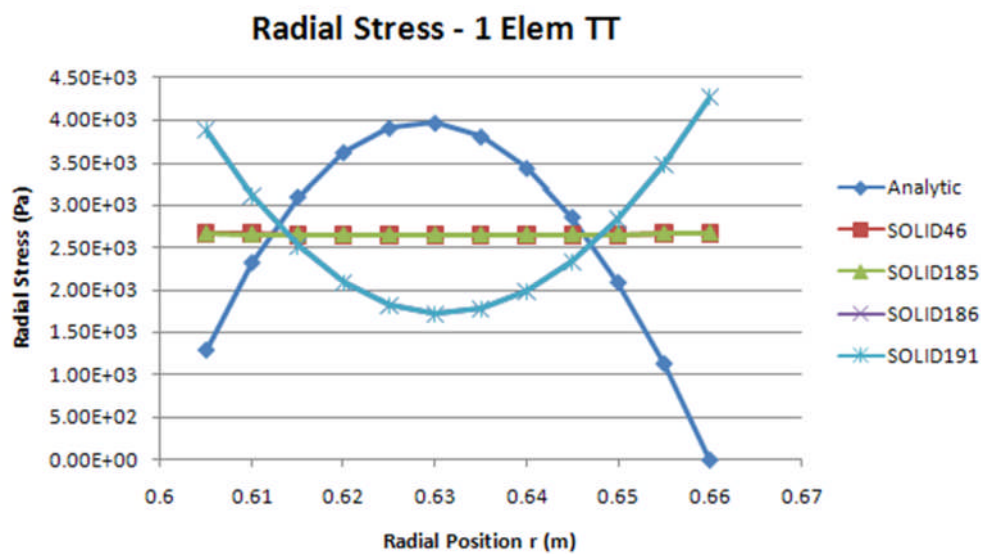


Figure 6-9 Comparison of radial stress (σ_{33}) (Pa) across the curved plate thickness (m). One layered solid element through the thickness with 12 plies (at 0°). Curved plated (0.06 m thick) under $M=100\text{Nm/m}$.

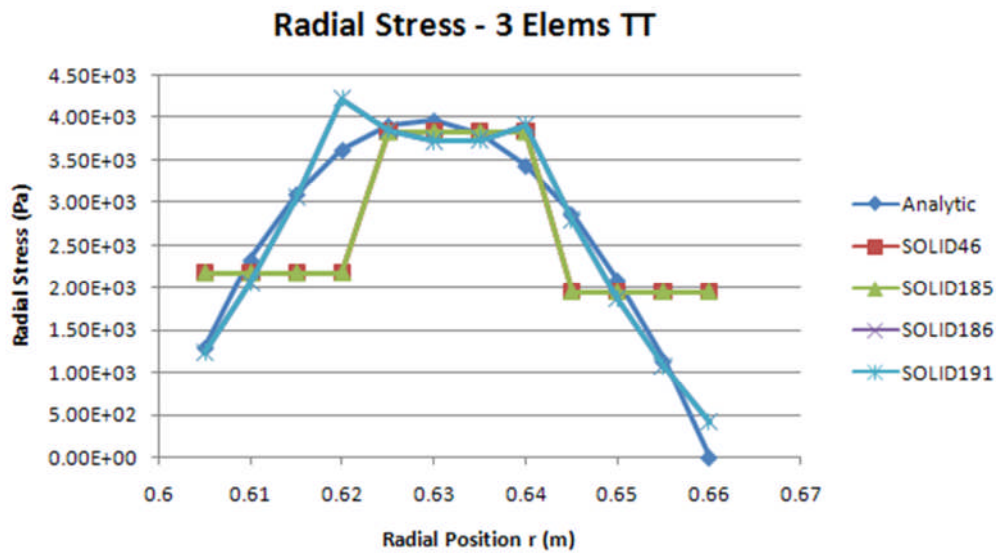


Figure 6-10 Comparison of radial stress (σ_{33}) (Pa) across the curved plate thickness (m). Three layered solid element through the thickness with 4 layers per element (12 layers in total at 0°). Curved plated (0.06 m thick) under $M=100\text{Nm/m}$.

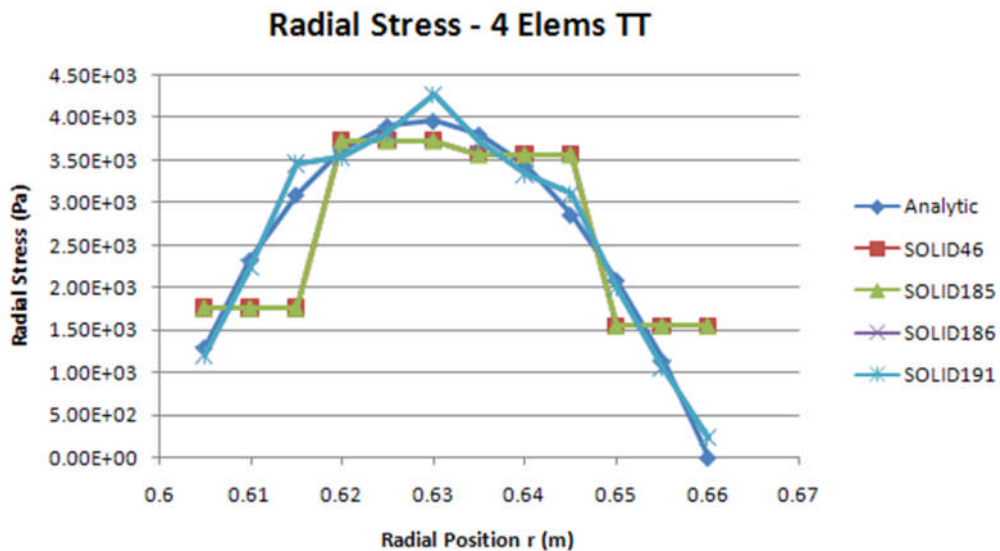


Figure 6-11 Comparison of radial stress (σ_{33}) (Pa) across the curved plate thickness (m). Four layered solid element through the thickness with 3 layers per element (12 in total at 0°). Curved plated (0.06 m thick) under $M=100\text{Nm/m}$.

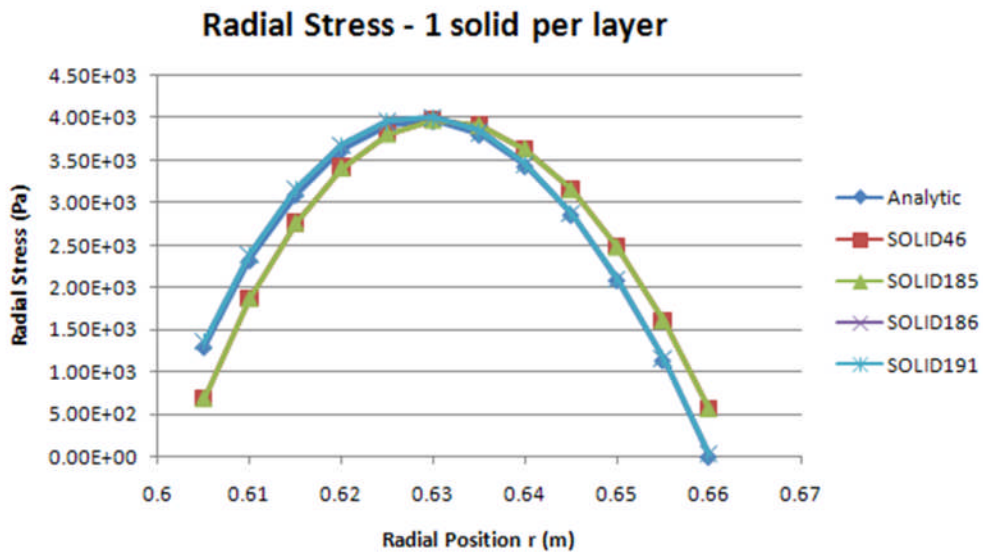


Figure 6-12 Comparison of radial stress (σ_{33}) (Pa) across the curved plate thickness (m). One solid element per layer (12 layers in total at 0°). Curved plated (0.06 m thick) under $M=100\text{Nm/m}$.

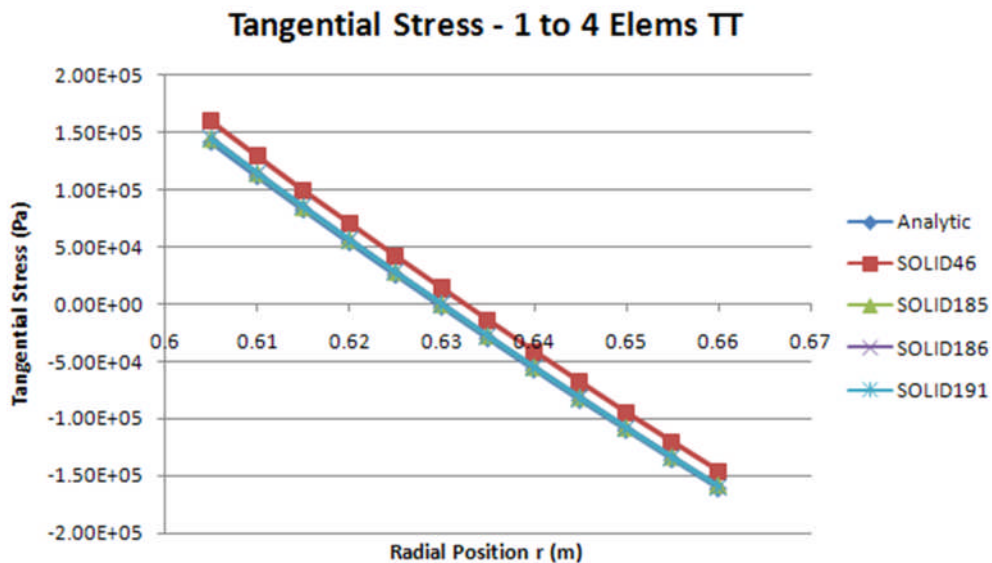


Figure 6-13 Comparison of tangential stress (σ_{22}) (Pa) across the curved plate thickness (m). Results represent the behaviour of four different cases, 1 to 4 layered solid elements through the thickness (12 layers in total at 0°). Curved plated (0.06 m thick) under $M=100\text{Nm/m}$.

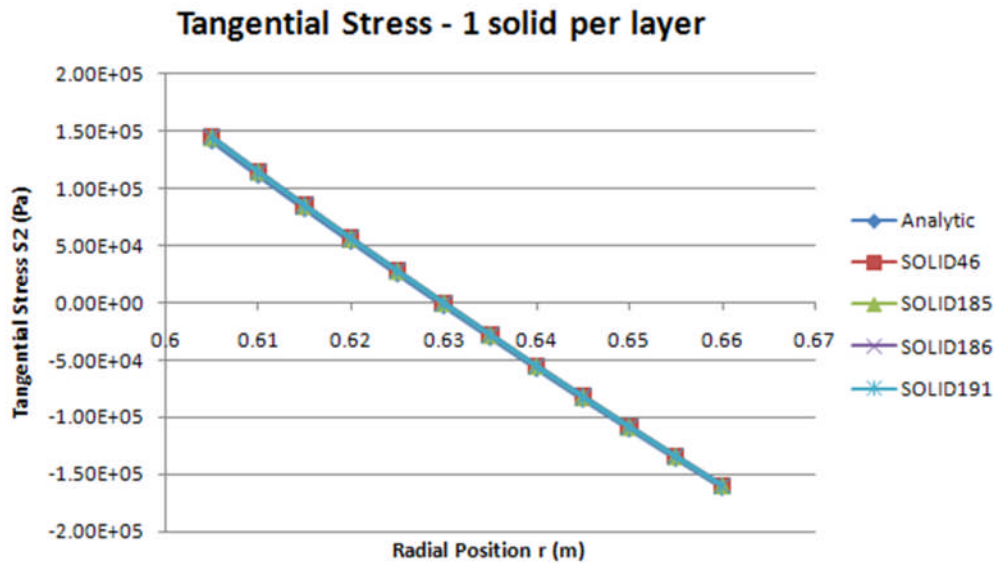


Figure 6-14 Comparison of tangential stress (σ_{22}) (Pa) across the curved plate thickness (m). 1 solid element per layer(12 layers in total at 0°). Curved plated (0.06 m thick) under $M=100\text{Nm/m}$.

Regardless of the element formulation, and modelling strategy, both under integrated layered solid elements, SOLID46 and SOLID185 (8 node layered solid) provide the same radial stress results (σ_{33}), and the same conclusion applies to the 20-node solid elements (SOLID186 and SOLID191). The first two tune the material properties in the transverse direction, allowing constant radial stress value σ_{33} across each element thickness, which does not reproduce the parabolic distribution expected, especially for the case of having just one layered element through the thickness (the trend is improved though, according to the layers of elements stacked). The best results are obtained when using one element per layer, although with certain offset with respect to the analytic solution. This fact could be caused by the slight inaccuracy in the through thickness integration when requesting, as in this case, through-thickness results in elements with non-parallel end layered faces (ANSYS help manual).

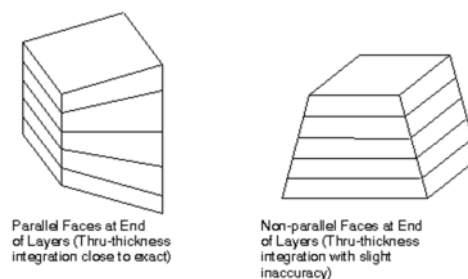


Figure 6-15 Level of through thickness integration accuracy based on the element shape. Source: ANSYS help manual.

In the case of SOLID186 or SOLID191 (20 node layered solid), the radial stress σ_{33} is best represented when using one solid element per layer. One layered solid through the thickness gives the opposite trend, providing a result which is not yet fully understood. Furthermore, radial stress discontinuities between stacked layered elements occur. This effect is softened though as the number of layered solid elements through the thickness increases.

Regarding the tangential stress σ_{22} , all element formulations, regardless of the modelling strategy used, give the same result, which coincide with the analytical one, except for the case of SOLID46, which has the same trend that the analytical result, but with a certain offset. However, for the case of having one element through the thickness, all element formulation give the exact solution.

The computational cost of the analyses performed is measured for all modelling strategies, which is directly related with the number of DOF of the FEM. Figure 6-16 represents then the number of nodes required to build the curved plate FEM for each modelling strategies and element type, with 1 to 4 layered solid elements through the thickness, or with 1 solid element per ply, and for each element formulation (SOLID46 & SOLID185 (8-nodes) and SOLID186 & SOLID191 (20-nodes)).

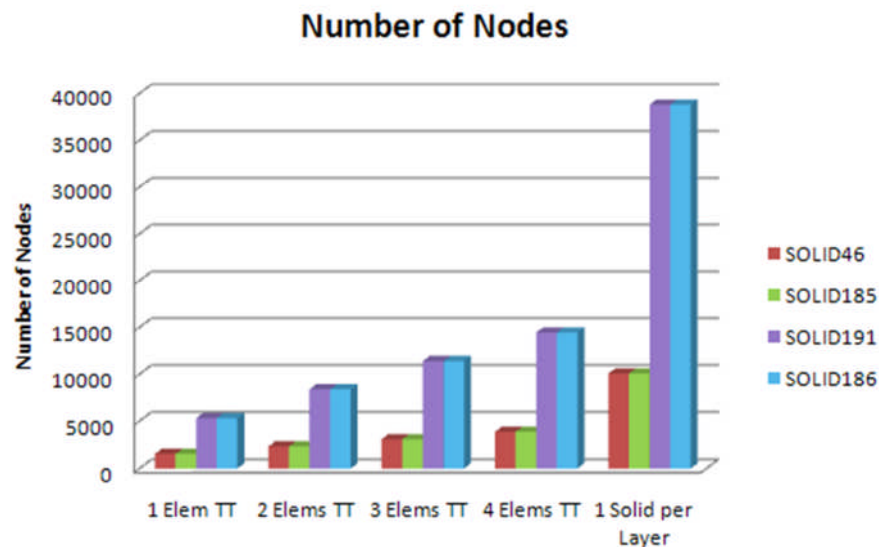


Figure 6-16 Number of nodes in the curved plate FEM. Different modelling strategies, with 1 to 4 layered solid elements through the thickness or 1 solid element per ply.

Executing the analyses in a PC with a processor of the following characteristics:

Computer: Intel(R) Core(TM)2 CPU T7200 @ 2.00GHz 997 MHz, 2.00 GB of RAM

Figure 6-17 Processor characteristics.

The CPU time required to complete each FEA is (every strategy and element formulation) is shown in Figure 6-18.

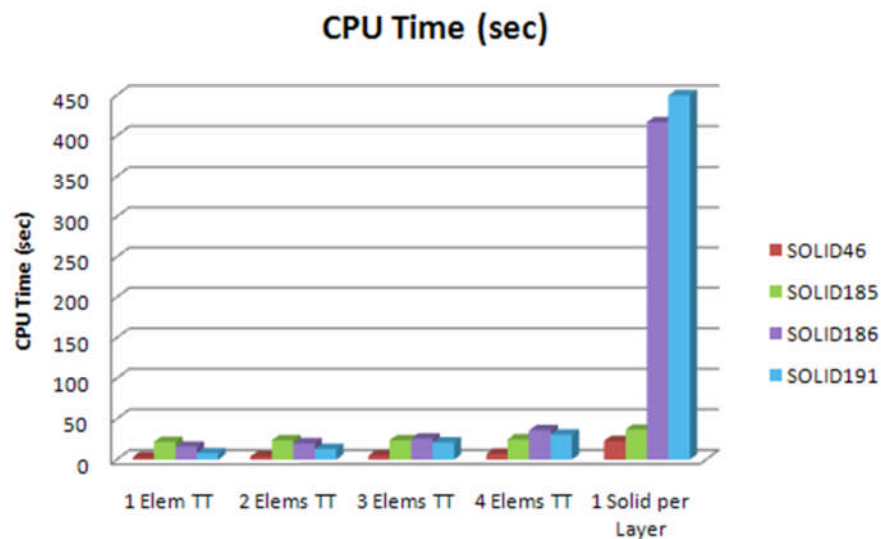


Figure 6-18 CPU time (seconds) required to run a single analysis of curved plate under bending. 5 different modelling strategies with 1 to 4 layered solid elements through the thickness or 1 solid element per ply.

The computational cost of under integrated layered solid elements (SOLID46 and SOLID185) is barely affected by the modelling strategy. However, when using SOLID186 or SOLID191 (20-node solid element), the CPU time increases enormously when, instead of using layered solid elements with various layers per element (all of these modelling strategies with similar computational cost), the model is defined with one solid per layer.

6.1.4 Conclusions

Regardless of the element formulation, the accuracy of the radial stress distribution is directly related with the number of integration points through the thickness (number of elements through the thickness). Both under integrated solid elements (SOLID46 and SOLID185) seem to give the same radial stress results (σ_{33}), and the same conclusion applies to the 20-node solid elements (SOLID186 and SOLID191). Effectively,

SOLID185 and SOLID186 are improved and more user friendly formulations than SOLID46 and SOLID191, respectively.

Radial stress σ_{33} is best represented when using one solid element per layer with a 20-node element (SOLID186 or SOLID191), although it is computationally very expensive. The best compromise between accuracy and CPU time is obtained when using four layered elements through the thickness (3 layers per element).

On the other hand, SOLID46 and SOLID185 tune the material properties in the through thickness direction, not delivering the desired parabolic distribution, as σ_{33} presents a constant radial stress value across each element thickness.

Regardless of the number of layered elements through the thickness, the tangential stress achieved with SOLID185, SOLID186 and SOLID191 give the exact solution.

6.2 3-Points bending test

Delamination is a frequent failure mode which affects laminated composites structural performance (Barbero, 2008). The interface between layers debonds due to crack propagations because of the lower matrix strength (section 3.4.1). There are two possible approaches to design a structure against delamination failure. In a strength analysis, the calculated interlaminar shear stresses (associated with bending applications) are compared with the interlaminar allowable properties obtained by means of experimental test (three-point bending shear test on a short-beam (Matthews et al., 2000; Swanson et al., 1997)). By contrary, in the fracture mechanics approach, it is assumed an initial crack line, which will propagate according to three different modes (opening, in-plane shear, out-of-plane shear).

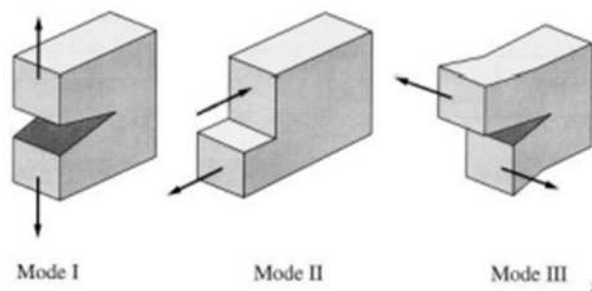


Figure 6-19 Crack propagations modes according to the fracture mechanics approach. Source: Swanson et al., 1997.

A FE analysis of a 3-point bending test was carried out using ANSYS. Results were verified against available numerical results obtained by FE analysis performed with MSC MARC/MENTAL and experimental test results (Czichon et al., 2011). The aim is to represent an accurate shear stress distribution through the thickness by using an appropriate layered element formulation, and a flexible parametric model definition.

6.2.1 Settings and assumptions

The tests were carried out in a 30 mm thick specimen (and 60 mm thick specimen, not considered in this paper) made of non-crimped-fabric (NCF) with two different configurations. The dimensions of the specimens were determined in order to have through thickness delamination due to shear stress τ_{31} . The Biax configuration is made of 120 plies with a ply thickness of 0.25mm and the following stacking sequence $[0/90/-45/45]_s$. The Quadrax configuration is made of 240 plies with a ply thickness of 240 plies and the following stacking sequence $[0/90/-45/45]_s$ (where the s subscript represents an eight plies symmetric laminate).

Non-crimped fabrics are a type of through-thickness reinforced laminates which provide properties between UD and woven reinforcement, representing also a meaningful economic benefit by reducing the plies count, with fibres arranged in a more optimal disposition (Baker et al., 2004) (Figure 6-20). The current NCF production machines are only able to manufacture fabrics with a maximum of 8 layers, and the 0° plies must be placed on an outer layer (Tong et al., 2002).

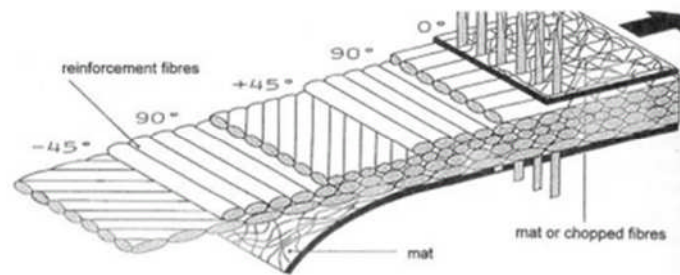


Figure 6-20 Non-Crimped Fabric. Source: Baker et al., 2004.

Following, a summary of all specimen dimensions, laminate definition and material properties (all in SI units) used in the paper are presented in the following tables:

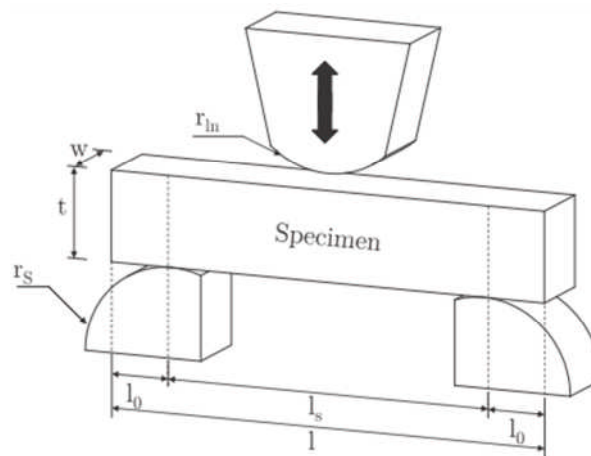


Figure 6-21 Simply supported beam dimensions. Source: Czichon et al., 2011.

Table 6-6 Specimen dimensions. Source: Czichon et al., 2011.

<i>Description</i>	<i>Symbol</i>	<i>30 mm thick sample</i>
Thickness	t (mm)	30
Width	w (mm)	$\frac{5}{6}t$ (25)
Length	l (mm)	5t (150)
Support distance	l_s (mm)	4t
Support radius	r_s (mm)	30
Loading nose radius	r_{in} (mm)	30

Table 6-7 Laminate definition. Source: Czichon et al., 2011.

<i>Description</i>	<i>Symbol</i>	<i>Biax configuration</i>	<i>Quadrax configuration</i>
Thickness	t (mm)	30	30
Ply thickness	t_{ply} (mm)	0.25	0.125
Number of plies	N	120	240
Lay up		$[(0/90/-45/45)_s]_{15}$ (15 layers of eight plies)	$[(-45/0/45/90)_s]_{30}$ (30 layers of eight plies)

Table 6-8 3D material properties (in SI units). Source: Czichon et al., 2011.

E_{11} (MPa)	E_{22} (MPa)	E_{33} (MPa)	G_{12} (MPa)	G_{13} (MPa)	G_{23} (MPa)	ν_{12}	ν_{13}	ν_{23}
136,000	9400	6580	3100	3100	3100	0.3	0.3	0.3

Table 6-9 Strength properties (in SI units). Source: Czichon et al., 2011.

S_{1t} (MPa)	S_{1c} (MPa)	S_{2t} (MPa)	S_{2c} (MPa)	S_{3t} (MPa)	S_{3c} (MPa)	S_{12} (MPa)	S_{13} (MPa)	S_{23} (MPa)
1970	990	67	240	67	240	62	62	62

Delamination failure is the primary failure mode presented in the specimen due to the transverse shear stress distribution. φ_c designates the position of the crack from the bottom surface.

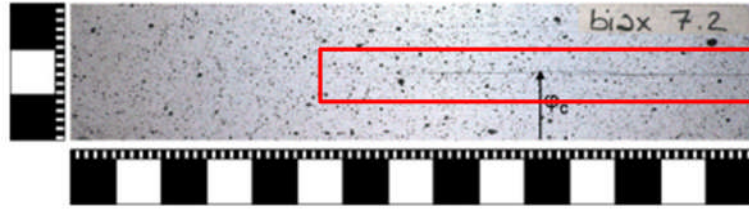


Figure 6-22 Delamination on a sample specimen ($F_{\text{crit,Biax}} = 43 \text{ kN}$). Source: Czichon et al., 2011.

Test specimens failed at about one third of the thickness from the bottom of the specimen ($\varphi_c \approx 10 \text{ mm}$ approximately), when applying a load of $F_{\text{crit,Biax}} = 43 \text{ kN}$.

Table 6-10 Crack position (measured from the bottom of the specimen) for several tests. Source: Czichon et al., 2011.

<i>Biax (t=30 mm) Sample number</i>	<i>Crack position φ_c (mm)</i>	<i>Quadrax (t=30 mm) Sample number</i>	<i>Crack position φ_c (mm)</i>
1.1	11	1.1	n.a.
1.2	14	1.2	n.a.
1.3	10	1.3	8
2.1	12	2.1	7
2.2	13	2.2	12
2.3	16	2.3	12
3.1	n.a.	3.1	10
3.2	11	3.2	n.a.
Average	~12		~10

6.2.2 Analytic solution

For comparison purposes, the shear stress distribution across the thickness (coordinate z), at a cross section located between the load application and the support, for an isotropic beam, with a cross sectional area of $A = tw$ can be determined with Eq (6-4) (Czichon. et al., 2011):

$$\tau_{13} = \frac{F_{test}}{2I_z}(tz - z^2) \quad (6-4)$$

with $0 < z < t$ (mm)

$$I_z = \frac{tw^3}{12} \quad (6-5)$$

Where:

- F_{test} is the load applied on the loading nose
- I_z is the second moment of area of a rectangular cross section
- t, w are the height and width of a square section.

The expressions above are calculated for the following input values.

Table 6-11 Input parameters. Source: Czichon et al., 2011.

<i>Parameter</i>	<i>Symbol</i>	<i>Value</i>
Thickness	t (mm)	30
Width	w (mm)	25
Second moment of area	I (mm ⁴)	39062.5
Applied load	F _{crit,Biax} (kN)	43

The shear stress distribution across the isotropic beam at the centre section (where load is introduced), and at a section located between the load application and the support is presented in Table 6-12.

Table 6-12 Analytic shear stress distribution τ_{13} across the thickness of an isotropic beam.

Thickness z (mm)	τ_{13} at Centre section (MPa)	τ_{13} at an offset section (MPa)
0	0.000	0.000
2	30.822	10.750
4	57.242	19.964
6	79.258	27.643
8	96.870	33.786
10	110.080	38.393
12	118.886	41.464
14	123.290	43.000
16	123.290	43.000
18	118.886	41.464
20	110.080	38.393
22	96.870	33.786
24	79.258	27.643
26	57.242	19.964
28	30.822	10.750
30	0.000	0.000

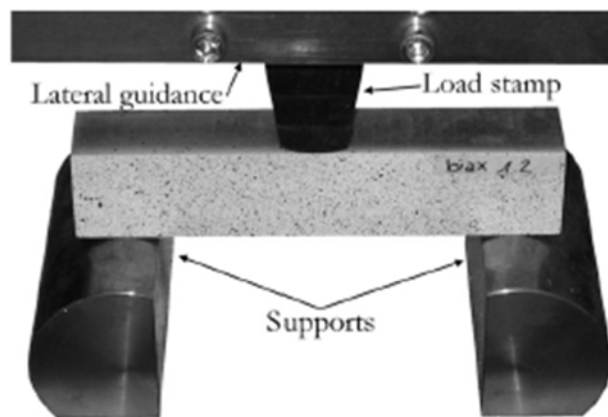
The maximum value of $\tau_{13} = 43\text{MPa}$ was taken as the apparent shear strength for the experimental failure load applied ($F_{\text{crit,Biax}}=43\text{ kN}$) (Czichon et al., 2011). Thus, the analytic results obtained in the section where the load was introduced, were scaled down to present a maximum shear stress value of 43 MPa at the specimen mid-plane (across the thickness). The resulting shear stress distribution is presented in the third column of Table 6-12.

6.2.3 FE Analysis

The relevant characteristics of the 3-point bending FEM created using layered solid elements are summarised in Table 6-13, these are presented alongside Czichon's FEM description. The main difference between both FEMs is that for the present analysis a 20-node layered solid element (SOLID191 - ANSYS) was used, instead of the 8-node layered solid element (Element 149 – MARC/MENTAT) used by Czichon et al., 2011.

Table 6-13 FEM comparison (between Czichon et al., 2011, and author's).

<i>MSC MARC/MENTAT (Czichon et al.)</i>	<i>ANSYS</i>
8-node layered solid elements (Elem 149)	20-node layered solid element (SOLID191)
8 plies per layered element (NCF)	
15 Elements (Biax) or 30 Elements (Quadrax) through the thickness	
Quarter Symmetry	
$F_{crit}=43$ kN	

**Figure 6-23 3-points bending experimental test setup. Source: Czichon et al., 2011.**

A capture of the 3-point bending FEM with 15 layered elements through the thickness is depicted in Figure 6-24. Rigid to flexible contact pairs have been defined between the loading nose and the top surface of the specimen (with a pilot node in which the load was applied), and between the support and the bottom surface of the specimen.

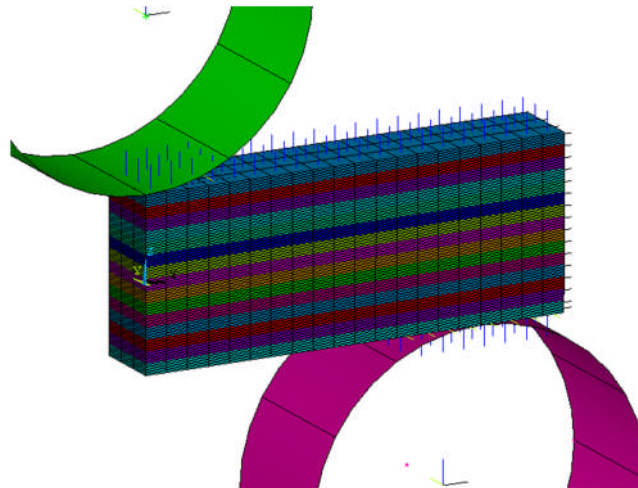


Figure 6-24 3-points bending FEM. UTL component with 15 layers of elements (SOLID191 20-node layered solid elements), under $F_{\text{crit, Biax}}=43\text{kN}$.

The ANSYS input file of the 3-point bending FEA is available in Appendix F.

6.2.4 Results

A capture of the transverse shear stress distribution (in Pa) across the specimen thickness for the Biax configuration is shown in Figure 6-25.

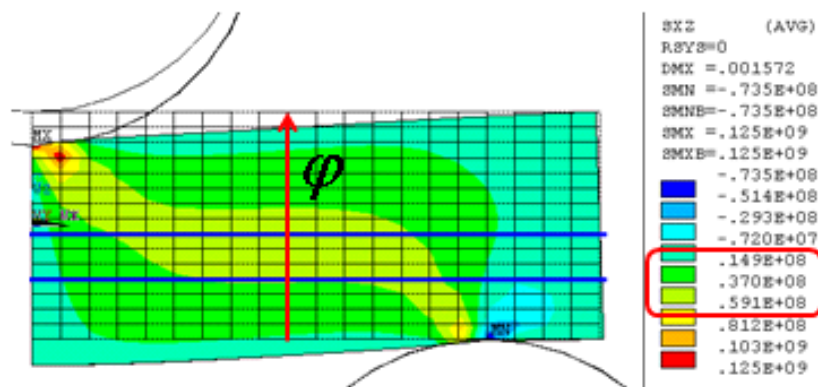


Figure 6-25 Transverse shear stress distribution (Pa) across the thickness, for a 30 mm specimen at 43 kN.

Plotting the same result in a localized number of plies (33 to 80, by using the command ESEL,S,REAL,,5,10) (Figure 6-26), it has been observed that the maximum τ_{13} is achieved at ply 56, which means that for the Biax configuration (ply thickness of 0.25mm) the specimen fails at 14mm from the bottom, demonstrating good agreement with the crack position from the bottom of the specimen obtained in the experimental tests (Table 6-10).

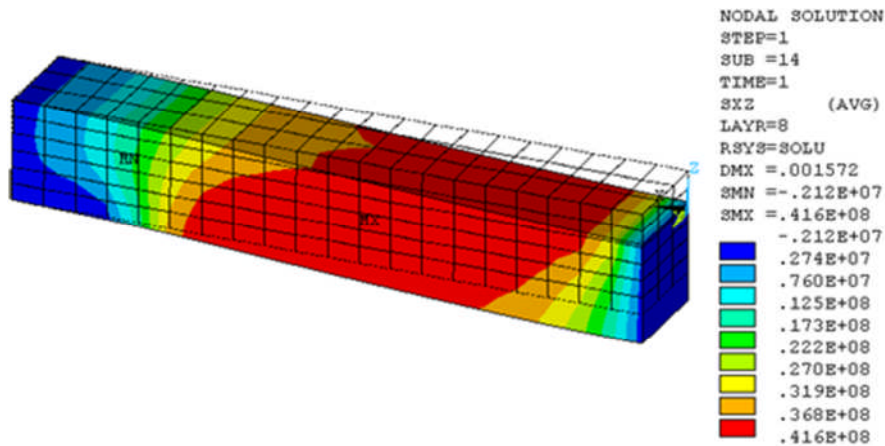


Figure 6-26 Transverse shear stress distribution (Pa) for layers 33 to 80, for a 30 mm specimen at 43 kN.

The transverse shear stress was requested at the specimen edge (where the largest interlaminar shear stresses are generated) at the location shown in Figure 6-27.

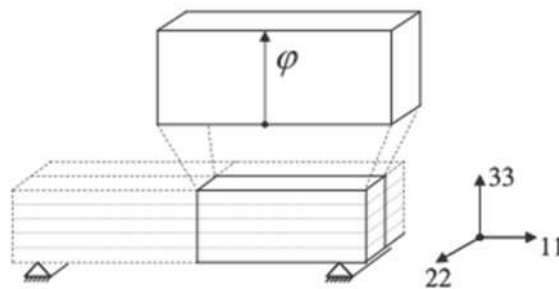


Figure 6-27 Location of the section where τ_{13} requested (outer surface along the transverse direction). Source: Czichon et al., 2011.

The nodal transverse shear stress results were requested at the bottom of each layer for every layered solid element across the thickness in the abovementioned location.

The shear stress distribution was not only compared with the MARC / MENTAT results (8-node layered solid elements) (Czichon et al, 2011), but also with the analytical shear stress distribution over the thickness (z) for an isotropic beam with square cross section (Table 6-12).

Figure 6-28 presents the results comparison of the transverse shear stresses between the results available in literature (Czichon et al., 2011), and the obtained with ANSYS (using 20-node layered solid element).

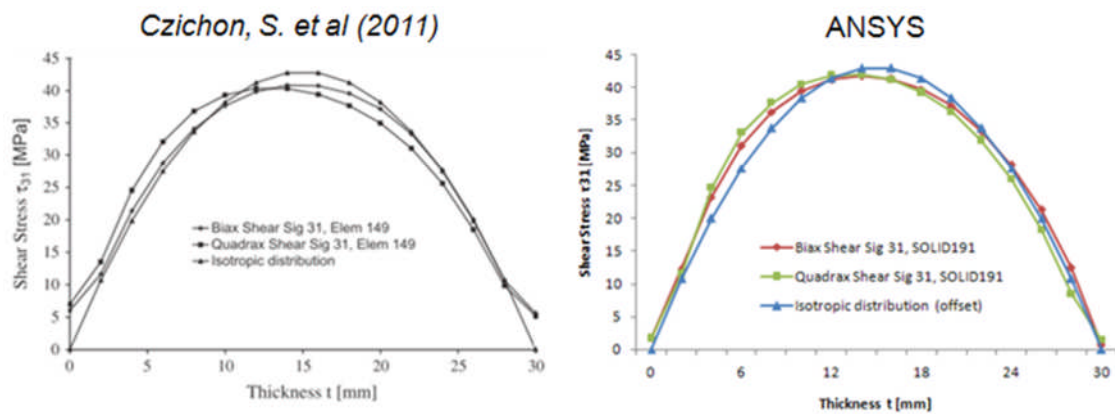


Figure 6-28 Transverse shear stress (τ_{13}) distribution comparison (MPa), for a 30mm specimen at 43 kN. Source (left): Czichon et al, 2011.

A good agreement between both results has been achieved, and the maximum transverse shear stress level has been obtained with reasonable accuracy.

Transverse shear stress results obtained when the specimen is modelled with two solid elements per layer (Biax) are shown in Figure 6-29 (Czichon et al., 2011). Comparison with the layered solid element results shown in Figure 6-28, only indicates deviations on a ply level. However, as justified by Czichon et al., the level of accuracy of the results achieved with layered solids is accurate enough, as delamination failure is expected to occur in the region that presents the highest shear stress. For this reason, the verification of the results shown in Figure 6-29 was not justified for the present research, which intention is to justify the benefits, in terms of low computational cost, of using layered brick elements.

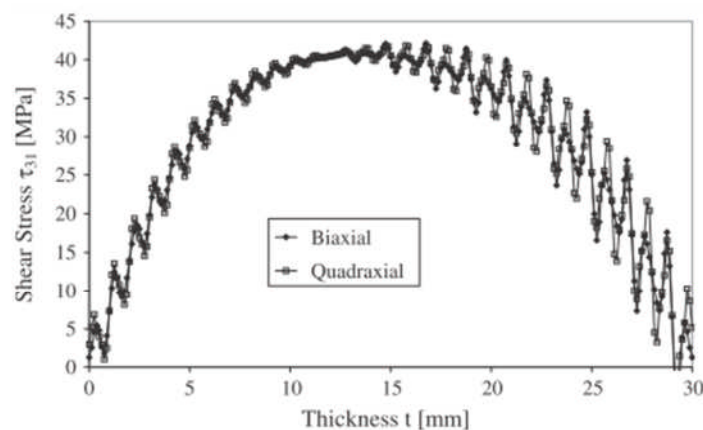


Figure 6-29 Transverse shear stress (τ_{13}) distribution (MPa), for a 30mm specimen at 43 kN. Two solid elements per ply (Biax). Source: Czichon et al., 2011.

Figure 6-30 represents the element result of the interlaminar shear stress across the thickness, superimposed with the nodal results (which are the same as the ones presented in Figure 6-28, but without editing) of the transverse shear stress (in MPa). The element results present a more regular distribution, although both results account for the same maximum stress value. Also, at an element level, the interlaminar shear stresses present a slight discontinuity at the interface between elements.

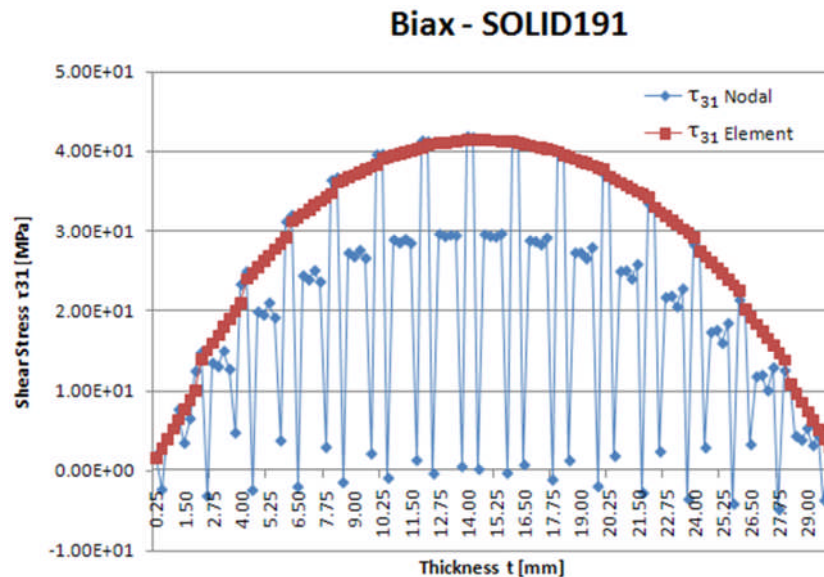


Figure 6-30 Nodal / Element (averaged) transverse shear stress (τ_{13}) distribution (MPa), for a 30mm specimen at 43 kN. 15 stacked SOLID191 (Biax).

6.2.5 Conclusions

SOLID191 (20 nodes) has proved to be a quite accurate and effective layered element formulation for predicting the interlaminar shear stresses in UTL composite applications (a 30 mm thick specimen has been considered).

The transverse shear stress distribution τ_{13} , computed with this formulation, and its maximum stress level present a good agreement with the analytical and experimental test results obtained by EADS IW (Czichon et al., 2011), using MARC layered solid element formulation (ELEM149 with 8 nodes).

Comparison of transverse stress results obtained with layered solid elements and when using two solid elements per layer, only indicates deviations on a ply level. However, as justified by Czichon et al., the level of accuracy of the results achieved with layered solid is accurate enough, as delamination failure is expected to occur in the region that presents the highest shear stress.

7 UTL Composites: Design Exploration

7.1 FE-Based optimisation methodology

7.1.1 Introduction

Structural design engineers' ultimate goal is to achieve the best component design, measured in terms of its performance. Depending on the type of application the component performance can be evaluated either by the component maximum stiffness (as for the case of this research) or by its minimum weight, considering in both cases certain strength limits.

Component design is traditionally based on experience. According to this procedure a list of certification and design requirements are initially identified for a certain application and then a design(s) that comply with those requirements is proposed. In a second stage, a series of design modifications are evaluated, which may lead to an improved design or may determined that the design obtained in the first place was the best solution.

As mentioned in Section 1.2.1.2 the design of UTL composites is traditionally based on the application of the *black metal* approach, which relies on design experience with metallic components, and which may not efficiently evaluate alternative designs that may significantly improve the component performance.

Mathematical optimisation has revealed as a powerful tool for the design of structural components. It is a systematic method that may assist engineers in the component design process, in order to determine the maximum or minimum performance objective function subjected to multiple constraints.

7.1.2 Composite design optimisation

Section 1.1 already introduced the main benefits of composite materials. Beyond the weight reduction advantage, the use of composite materials in structural applications provides great design flexibility, as the change in laminate configuration and material properties, which can be defined as design variables, directly affects the stiffness of the component. This fact represents a great advantage in terms of design problem formulation, as the performance of the component can be optimised, considering the certification and design requirements, by tailoring not only the component dimension, but also the laminate stiffness properties (Gürdal et al., 1999).

However, the optimisation of composite material components is a task that has to be considered carefully. There are still failure and material mechanisms which are not fully understood, being some of them even under investigation. Furthermore, a practical application of the composite design optimisation should consider the interaction between design and the manufacturing concepts. In the past, due to the limitation on

the optimisation algorithms available, the performance optimisation analysis of composite laminate in terms of ply orientation considered only continuous design variables, which led to impractical stacking sequences. Also, due to the manufacturing constraints, only few laminate configurations are evaluated, which may neglect some other viable configurations that would provide a better component performance (Gürdal et al., 1999).

The introduction of UTL composites in the design of aerospace primary structures represents a great opportunity to develop new design methodologies that can be used to improve these components performance.

7.1.3 Smearred properties vs individual ply definition approach

For determining the best modelling approach to tackle the FE based optimisation of UTL various concepts already mentioned in the previous chapters are going to be discussed.

According to what has been presented in Section 3.6, the use of layered solid elements (with HSOT) for the modellisation of UTL composite structures provides an accurate and efficient transverse shear stress distribution through the structure thickness. As already considered in the structural analysis of the short beam example in Section 6.2, the laminate is going to be divided into a series of sublaminates, represented by layered solid elements of the same thickness. The way in which the laminate configuration is defined for these elements is going to determine somehow the optimisation approach.

The behaviour of a laminated composite structure is determined by its layered configuration, which can be evaluated by means of the stiffness matrices coefficients (A, B, D, H) of the constitutive equation (Section 3.3.4.1), being [H] the transverse shear stiffness matrix. In ANSYS, there are two methods available to define the behaviour of a composite laminate (Section 4.4):

- By considering the equivalent homogeneous smeared properties of the laminate, specifying the constitutive matrices coefficients (available for SOLID46 (8-node solid element)) (macro-scale level analysis).
- By means of the individual definition of the ply properties alongside with the laminate stacking sequence (meso-scale level analysis).

Based on the previous information presented, the benefits and disadvantages of this two modelling approaches, in terms of performing a subsequent performance optimisation, are going to be evaluated.

7.1.3.1 Layered configuration definition

For the case of having an unknown laminate stacking sequence, or for laminates with a large number of different plies, this option represents an alternative form of defining an

accurate laminate stiffness, avoiding the tedious process of input a great amount of data. In this case the laminate is defined by an equivalent smeared homogeneous properties so, regardless of the number of plies the laminate might be made of, the only information needed to characterise the component behaviour are the constitutive matrices coefficients, which could eventually be defined by few lamination parameters (Section 3.5.4).

This laminate definition has been used in a two-level decomposition approach for optimising the performance of anisotropic panels with T-shape stiffeners (Herencia et al., 2008). The first step implied the determination of the optimum specimen thickness and lamination parameters of a superlamina, characterised by homogeneous smeared properties. The design variables (both, laminate thickness and lamination parameters), defined as continuous parameters, were optimised by means of numerical techniques (gradient base) that are less computationally expensive than the non-linear exploratory methods (Genetic Algorithms). As a result, the percentages of each ply orientation within the lamina were determined by the optimum lamination parameter, but the optimum stacking sequence was not yet known. At this stage no stress results at a ply level can be requested, as the change in lamina material properties is not specified, but only the component displacement, or the buckling and vibrations modes. A second GA optimisation was required then to calculate an optimum laminate stacking sequence which stiffness behaviour was similar to the one obtained in the first optimisation analysis. A fitness function was created to evaluate the differences between both laminates.

Also, in order to determine the transverse shear resultants $\{Q\}$ in the abovementioned optimisation analysis, a shear correction coefficient $K(z)$ was considered for assuming a transverse shear stresses variation across the plate thickness (to fulfil the boundary condition).

SOLID46 (8-node) is the only layered solid element available in ANSYS that enables a layered configuration definition by means of the constitutive matrices (see Appendix 8.2.8.2J.2). The analysis done with this element in Section 6.1, has determined that the element tunes the material properties in the transverse direction, allowing constant radial stress value σ_{33} through the thickness, which does not reproduce the through thickness distribution expected.

The lack of accuracy of the SOLID46 for out-of-plane results and the fact that no shear correction coefficient $K(z)$ is provided in the ANSYS help manual for assuming a transverse shear stresses variation across the plate thickness, makes impossible to characterise the a stack up of sublaminates with smeared homogeneous properties in order to achieve an accurate transverse shear stress prediction.

Thus, as already considered in all analyses presented in this document, the laminates are defined at a ply level. This requires a LSS description, specifying the angle of each

lamina with respect to the laminate x-axis (global coordinates), which are the design variables to be evaluated in an optimisation analysis. Due to the discrete nature of the ply angles a non-linear optimisation would be required to obtain the optimum LSS, which may be a very expensive and cumbersome analysis.

7.1.4 FE-Based optimisation methodology

Design methodology presented here is based on similar frameworks available in literature (Chen et al., 2000; Monroy et al., 2008; Belegundu et al., 2008; ALTAIR HyperWorks v9.0 Help Manual). It can be used in the early stages of the design process, where a large number of design alternatives are available and need to be compared and evaluated.

It is based on creating a record of databases obtained from the finite element analysis simulations performed on the model, for different combinations of all previously determined design variables.

The stored results will be explored in order to determine possible design drivers of the model and for these key drivers obtained optimise then the model according to certain design criteria. The final goal is to identify the list of all possible optimum designs that meet the original design targets or specifications.

A schematic description of a generic FE-based optimisation methodology is presented below. Robust design has not been considered within the scheme.

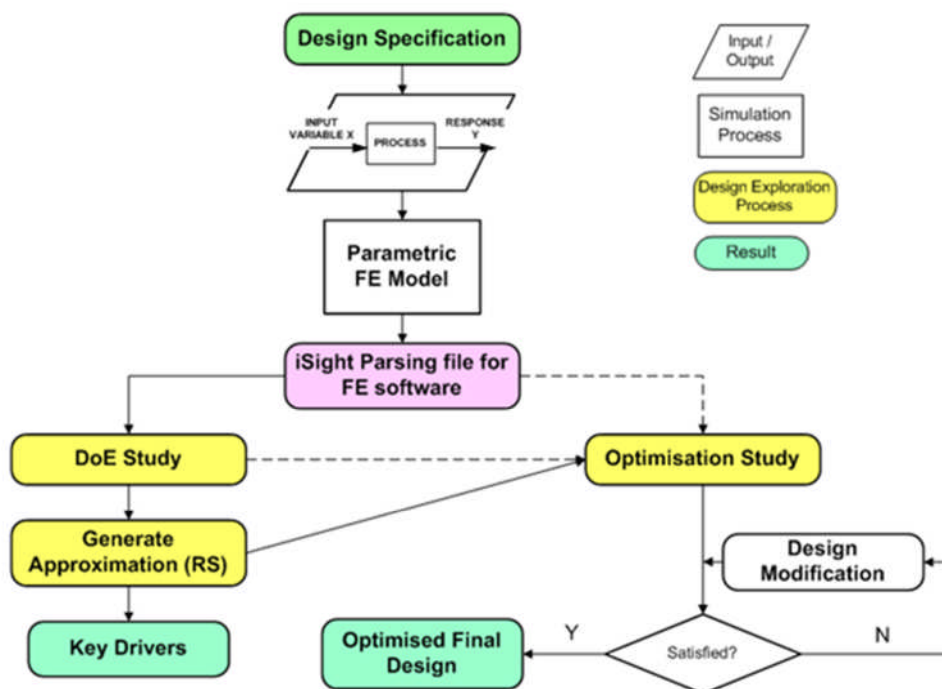


Figure 7-1 Schematic description of a generic FE-based optimisation methodology.

7.1.5 Framework requirements and simulation tools

The key points considered when designing the framework are the following:

- *Commercial tools:* The purpose was to use commercial tools, as the framework is intended for industry applications. Initially, the type of analyses to perform are linear static, but for future applications the FEA may require full non linear capabilities (material, geometric and contact), as well as capabilities to account for a wide range of different analyses types, i.e. dynamic, thermal, coupled fields, etc. ANSYS is a multidisciplinary FE code proposed for this framework.
- *Robust and flexible parametric definition of FE models:* In order to account for a broad design space exploration of the structure a parametric definition of the model is required. ANSYS enables a parametric definition of the FEA by means of the Ansys Parametric Design Language (APDL).
- *Layered structural solid elements:* As described in Section 4.2, ANSYS offers various layered element formulations, including layered solid elements (both 8-node and 20-node solid elements), that enables not only to account for the 3D stress state that characterise UTL applications, but also to reduce the computational cost associated with this type of analysis.
- *Data base management:* Due to the large amount not only of input design variables required to characterise an UTL components, but also of results generated, it has been regarded as vital to consider tools that enables an accurate data exchange among all modules. ISIGHT is a data base management tool with design exploration and optimisation capabilities that furthermore, has a commercial ANSYS add-on.

A summary of the simulation tools used in the proposed optimisation methodology framework is presented in **Error! Reference source not found..**

Table 7-1 Simulation tools.

<i>Architecture Component</i>	<i>Vendor</i>	<i>Software Name</i>
FE Prepost + FE Solver	ANSYS Inc.	ANSYS v11 (classic)
Design Exploration and Optimisation	SIMULIA	I-Sight FD +ANSYS add-on

The commercial design optimisation and data management system finally selected is ISIGHT (by Simulia), which is designed not only for the integration and precise data management among different simulation codes (including ANSYS by means of a

commercialised add-on), but also for the design space exploration and optimisation analysis based on the interdigitation strategy (Koch et al., 1990) (Figure 7-2).

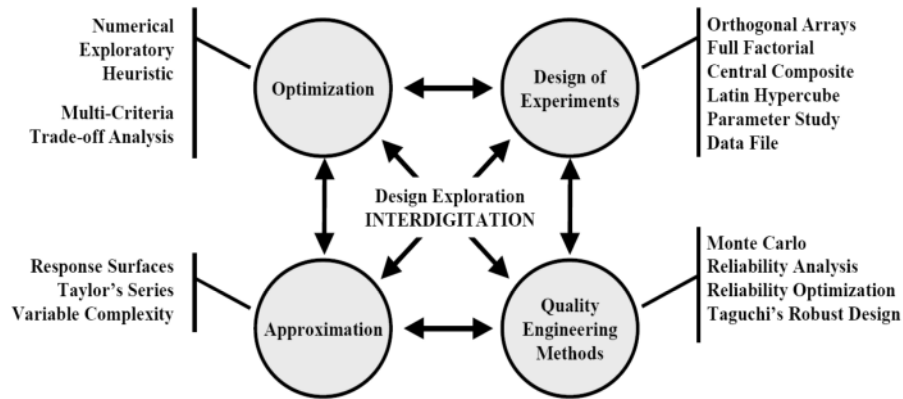


Figure 7-2 Design exploration interdigitation. Source: Koch et al., 2002.

The use of this flexible tool enables to evaluate different design alternatives and identify the optimum solution in a more efficient manner, with effects in the preliminary design time reduction and product reliability.

Following, a general description of the main modules that configure the framework is presented.

7.1.6 Main Modules

7.1.6.1 Setup Study

This module of the methodology can be considered its core. An ANSYS parametric finite element model of the UTL component needs to be created. This input text file should contain a parametric definition of the FEA, including both, the input and output variables required in the subsequent design exploration and/or optimisation analyses.

The main input parameters considered are the following:

- Design variables: stacking sequence (ply orientation), which are discrete variables.
- Other possible design variables are:
 - Geometric entities of the laminated structure (see **Error! Reference source not found.**). These are defined as continuous design variables.

The main output parameters considered are the following:

- Objective function: Maximum vertical (out-of-plane) displacement u_z (as a measure of the component stiffness)

- Possible strength constraints
 - Maximum transverse shear stress τ_{13} per ply, extracted in the free-edge.

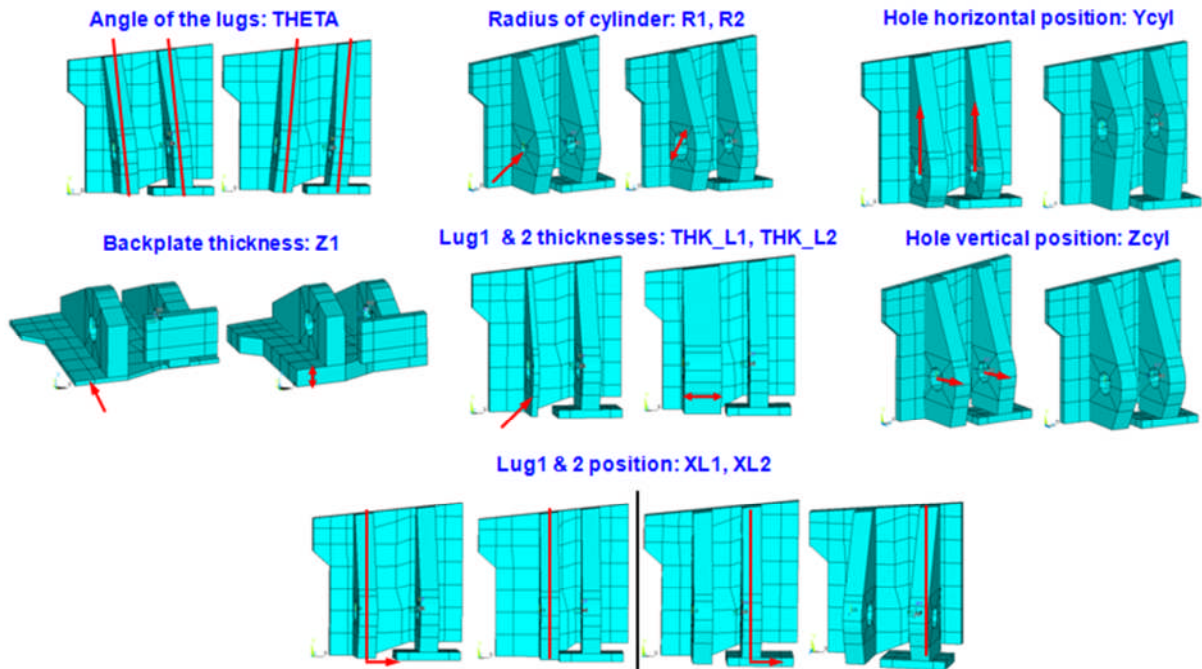


Figure 7-3 Design space exploration of a parametric MLG SSF geometric model.

A detail description of how to create a parametric FEM of a laminated structure is presented in Chapter 4.

7.1.6.2 Design of Experiments

It is a set of statistical techniques which provide a systematic way to get as much information as possible from a design space, based on the results obtained from the performed experiments. Thus, it is particularly useful when tackling with new problems for which no much information about the design space is available. A model is repeatedly run through a simulation in order to study the effects that multiple input design variable have over the response of one or more output parameters.

A DOE analysis is normally used to identify among all potential design variables the factors that influence the most the output response (key drives), as well as the meaningful parameter interactions (Montgomery, 1996). It assists in the design space exploration and in the identification of a possible optimum design. Moreover, it creates a data set which could be used for the generation of a response surface approximation for a subsequent approximation-based optimisation (Myers and Montgomery, 1995; Kodiyalam et al, 1998).

There are many DOE techniques available in the literature. An exhaustive review and recommendations in the use of some of these techniques is given by Simpson et al (2001).

The DOE techniques available in ISIGHT are introduced in the following table.

Table 7-2 DOE techniques provided in ISIGHT. Source: Koch et al., 2002.

EXPERIMENT	DESCRIPTION
Orthogonal Arrays	Taguchi designs; Fractional factorial designs, with fractional subset carefully selected to maintain orthogonality of factors and certain interactions
Central Composite	5-level design: 2-level full-factorial augmented with a center point and two additional star points for each factor, located on the factor axes
Latin Hypercube	Number of levels for each factor equal to number of points, with random combinations
Full-Factorial	Specify any number of levels for each factor and study all combinations of all factors at all levels.
Parameter Study	Factors studied independently (One factor at a time approach – all other factors held fixed while one varied)
Data File	User defined DOE matrix, specified as file from which to read in data points to analyze.

Full factorial technique evaluates all combinations of all factors at all levels specified, resulting in an accurate, yet expensive estimation of the factors and the interaction effects. The Parameter study evaluates the effects of one factor by leaving the others at their base level; it could be useful when interactions are negligible. Taguchi's orthogonal arrays offer a systematic and efficient manner to explore the design space (Taguchi and Konishi, 1987). Latin hypercube represents an efficient design space sampling, as it is uniformly divided for each factor, and a specific number of level are then randomly combined (each level of a factor is studied only once). An improved Optimal latin hypercube technique is also available. Central composite design is normally used to generate data for a RS modelling. (Myers and Montgomery, 1995). Finally the data file technique allows to evaluate a user define DOE matrix.

7.1.6.3 Approximation Method: Response Surface Method

The cost expenses of running high-fidelity simulation analyses could be enormous when evaluating different design options, thus alternative solutions for avoiding this drawback have been proposed. Approximation methods represent a trade-off between accuracy and computational cost efficiency when exploring the design space in preliminary design studies.

After performing the DOE studies determined, the model responses obtained can be computed and described as a mathematical expression of its parameters in order to approximate the true response. The algebraic or numerical function used to represent the approximate model response is called surrogate model or response surface.

Response surface technology is a polynomial-based modelling technique (16.888/ESD.77 Multidisciplinary system design optimization, 2004. MIT) which grade of approximation depends on the number of designs (levels) used to generate the response surface. The number of levels determines the polynomial order, which directly affects the computational cost of the study.

Once a surrogate model has been created it can be invoked to observe how a new design variable vector (with small variations) affects the model response, without the need of running the whole analysis again. This approximation method represents though a substantial computational cost saving.

It is also more computational effective to generate a surrogate model before developing an optimisation study, as is not expensive as using its own solver. It is most likely that the results obtained from both methods differ, but the optimal design vector obtained by performing the optimisation study using the response surface could be used for a new optimisation using the solver. Objective functions and constraints can be also approximated.

No response surface method is going to be applied in the design exploration of UTL composites presented in this document, although it might be required in future work.

7.1.6.4 Optimisation

ISIGHT offers great flexibility for tackling different optimisation problems, with capabilities to deal with design variables of different nature (continuous, discrete, integer and mixed variables), linear and non-linear constraints, and to perform multidisciplinary design optimisation analysis and decomposition problems (Colmenares, 2009).

There are 13 design optimisation algorithms in ISIGHT (Table 7-3) classified in three main categories (Figure 7-4), numerical algorithms (gradient-based), exploratory algorithms (global-search), and heuristic algorithms (knowledge-based), which can be applied independently or combined in the most suitable manner for each kind of problem. For instance, by using a genetic algorithm for an initial global search of the design space for determining regions where the local minimum could be located, followed by a gradient-based algorithm for refining the search in order to identify the optimum solution (Colmenares, 2009).

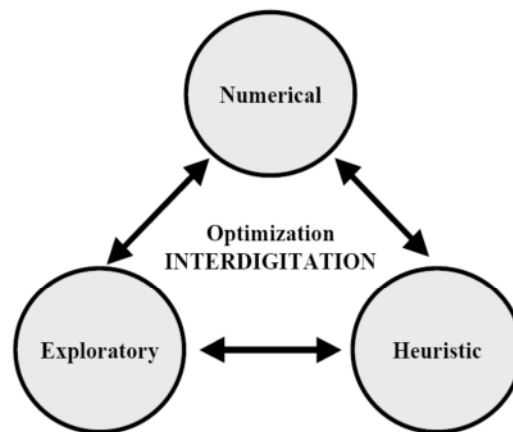


Figure 7-4 Optimisation techniques available in ISIGHT. Source: Koch et al., 2002.

Table 7-3 Optimisation techniques implemented in ISIGHT. Source: Koch et al., 2002.

TYPE		TECHNIQUE
Numerical	1	Method of Feasible Directions - CONMIN [*]
	2	Modified Method of Feasible Directions (MMFD) [*] - ADS
	3	Sequential Linear Programming (SLP) [*] - ADS
	4	Exterior Penalty [*] - ADS
	5	Sequential Quadratic Programming (SQP) - DONLP [*]
	6	Sequential Quadratic Programming (SQP) - NLPQL [*]
	7	Mixed Integer Optimization - MOST, Tseng (1996)
	8	Hooke-Jeeves Direct Search Method [*]
	9	Successive Approximation Method (LPSOLVE) [*]
Exploratory	1	Genetic Algorithm [*]
	2	Genetic Algorithm with Bulk Evaluation
	3	Simulated Annealing [*]
Heuristic	1	Directed Heuristic Search (DHS - U.S. Patent No. 6,086,617)

^{*} For reference, see: <http://www-unix.mcs.anl.gov/otc/Guide/faq/nonlinear-programming-faq.html#Q4>

No optimisation techniques are going to be applied in the design exploration of UTL composites presented in this document, although they might be required in future work. For a more detailed description of the design optimisation techniques available in ISIGHT refer to Koch et al. (2002) or the ISIGHT help manual.

7.1.7 Scope of application

Despite a general description of the FE-based optimisation methodology framework has been presented (Sections 7.1.4 and 7.1.6), for the design exploration purposes of this research the DOE module is the only one that is going to be considered for the analysis, although future analysis may require the use of all capabilities of the framework.

The problem description, for which the design exploration methodology considered in this research can be applied to, is stated below:

- *Objective function*: maximise the UTL composite structure stiffness
- *Design variables*: stacking sequence (discrete variables)
- *Constraints*: strength limits (in order to avoid the through thickness delamination)

The main key points to be considered for the correct application of this methodology are:

- The design exploration methodology (DOE) only applies at this stage to constant thickness laminated composites.
- In order to reduce the computational cost of the analysis, the laminate has to be divided into sublaminates, which are represented with layered solid elements of the same thickness (SOLID191 for what has been concluded in Section 6.2.5).
- All sublaminates will have the same stacking sequence (although as a future work different stacking sequences for each sublaminate may be considered).
- The layered configuration assigned to the layered solid element is defined at a ply level.
- For practicality purposes, only four possible ply orientations are going to be considered, 0/90/±45 (discrete design variables).
- For reducing significantly the number of analyses to be evaluated, manufacturing design rules are applied, for discarding those stacking sequences that imprint unfavourable coupling effects (constitutive stiffness matrix).
- For the strength analysis, the main in-plane failure modes described in Section 3.3.3 are the only ones considered at this stage.
- The through thickness strength analysis is the method adopted to determine delamination failure mechanism in the laminate (UTL composite components primary mode of failure), by which the calculated interlaminar shear stresses (associated with bending applications) are compared with the interlaminar allowable properties obtained by means of experimental test.
- Delamination failure is going to be evaluated in terms of the maximum transverse shear stresses through the laminate thickness, which are requested

at the laminate free-edge; according to what has been discussed in Section 3.4.1 and Section 6.2.5.

- Ply drop-off is ignored (considered as future work, Section 8.2.5).

7.1.8 Stacking sequence design exploration

One of the main difficulties of the optimisation analysis of laminate ply orientations, when they are considered as continuous design variables with values ranging between 0° and 90° , is that the solution may result impractical from the manufacturing point of view. For that reason, design variables with discrete nature are required, with plies that can only have orientation values of 0° , 90° and $\pm 45^\circ$. As a consequence, the stacking sequence optimisation is normally an integer non-linear mathematical programming problem. Gürdal et al. (1999) propose several approaches to tackle this kind of analysis, none of them applied for the stacking sequence optimisation of UTL composites. In this section, an alternative, more efficient and yet simpler DOE technique will be used to explore the design of constant thickness UTL composite structures with discrete ply orientation definition, in order to determine the stacking sequence that provides the best component performance out of a series of feasible and practical stacking sequences.

Considering that one of such components may account for over a hundred layers in some cases, for the main four layer orientations typically considered (determined by manufacturing limitations) ($0/\pm 45/90$), the number of possible stacking sequences to evaluate would make the analysis unfeasible (i.e. full factorial analysis $L^n=4^{100}$).

The number of laminate configurations to compare can be reduced significantly by using manufacturing design rules, which furthermore discards the cases that would imprint unfavourable mechanical properties to the component under investigation. Only symmetric or mid symmetric laminates are considered, for not having undesirable bending-extension coupling (Section 3.3.4.1).

A design exploration methodology for UTL composites with constant thickness is proposed in order to determine, for a certain component, which laminate stacking sequence gives the best mechanical performance.

7.1.8.1 Stacking sequence: Methodology

The design exploration methodology proposed for the stacking sequence exploration (Figure 7-5) is based in a generic FE-based design optimisation methodology (Figure 7-1).

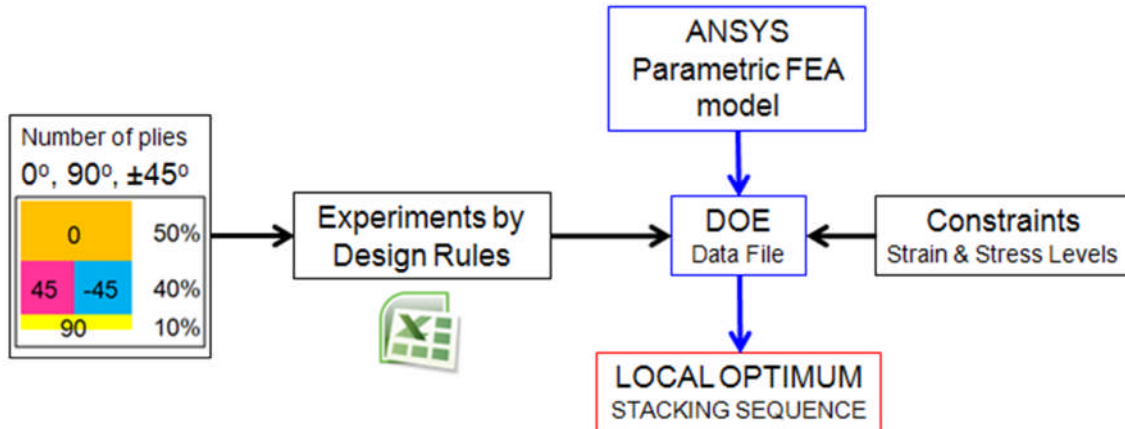


Figure 7-5 Stacking sequence design exploration methodology.

Various stacking sequences obtained after applying the heuristic design on a laminate with a certain number of plies are evaluated for a laminated structure, in order to determine which configuration is the best in terms of stiffness (measured by the minimum vertical displacement) and performance (measured by the maximum transverse shear stress). The comparison is carried out by means of a DOE technique, using a matrix of experiments defined by all feasible stacking sequences. As a result, a ply orientation local optimisation is performed, due to the discrete nature of the input variables.

The core of the analysis is defined by a parametric FE model of a UTL component (or assembly).

The UTL component is modelled as a collection of a fixed number of sub-assemblies or laminates across the thickness. These sub-assemblies can be stacked independently from one another in order to represent the required mechanical properties of the whole laminate. In addition, this type of approach could be extended in the future to consider shuffling within each sub-assembly, which would be dependent upon the constraints of the manufacturing process chosen. As Cranfield did not have access to this level of detail, a fixed sub-assembly approach was initially adopted to test the robustness of the proposed modelling and optimisation methodology.

For this analysis, all sub-assemblies (laminates) are defined with the same stacking sequence. The layers orientations (of half the laminate due to symmetry) are the input variables (factors). For each variable only four orientations (levels) are considered, i.e. 0,±45,90.

The matrix of experiments defining all feasible stacking sequences for a laminate with certain number of plies is generated using the VBA Excel spreadsheet shown in Figure 7-6.

Half of the total number of plies, which includes the mid layer for a mid symmetric laminate, is the main input parameter required to generate the feasible matrix of experiments (referred to as Nplies/2 in the spreadsheet).

The first step would be to create a full factorial set of experiments. It is recommended not to use a factor bigger than 6 (input number of plies), as the number of experiments to generate would be computationally very expensive ($\text{Levels}^{\text{factors}}$). Once those are generated, each design rule can be applied independently, which would determine the final number of experiments to evaluate.

Each row represents a stacking sequence (of half of the laminate). The total number of rows is the total number of experiments to be run in a DOE.

Figure 7-6 Manufacturing design rules spreadsheet.

The spreadsheet shows the following data and rules:

Total Thickness	0.05
tply	5.00E-03
NDV	5
Nlevels	4
NExp	1024

Ply Percentage Matrix:

50	40	10
0	45	90

Design Rules: Full Factorial, +/-45 @ top & bot, Ply Blocking 1, Ply Blocking Mid Plane, Ply Percentage, Progressive Sequence, Balanced, Compress Rows.

Text Box Content:

- Total Thickness & Ply Percentage ==>> **VALUES TO CHANGE!!!**
- tply = ply thickness (Fixed value)
- Nlevels = 4 --> [0 45 -45 90] (values that each ply can have)
- NDV = Half number of plies (half due to symmetry): **COLUMNS**
- NExp = Number of Experiments: **ROWS**

Formulas:

$$\frac{Nplies}{2} = \frac{Total_Thickness}{2 \times tply}$$

$$NExp = levels^{Factors} = levels^{NDVs} = levels^{Nplies}$$

Note: 10 plies → 5 plies (Symm)
Nexp=Lⁿ=4⁵=1024
Reduced to 8

Figure 7-6 Manufacturing design rules spreadsheet.

The design rules applied in the Excel spreadsheet are listed below:

- 0, 90, ±45 are the only considered angles.
- Mid symmetric or mid-plane symmetric stacking sequence, for avoiding the bending-extension coupling ($[B]=0$).
- Ply blocking: no more than four plies of the same orientation stacked together plies, to minimise interlaminar shear stresses at particular locations of the structures (holes, free edges, discontinuities, etc).
- For thin laminate application it is recommended to use ±45 at extreme outer top and bottom surfaces ($z = \pm t/2$), for improving the load transfer capacity in joints,

for enhancing the buckling resistance, and for better impact resistance (Rothwell, A., 2007).

- No more than $\pm 45^\circ$ between two consecutive UD plies.
- Balanced stacking sequence, to avoid the coupling effects between in-plane forces and in in-plane shear strains (Section 3.3.4.1).
- Stacking sequences considered have at least 10% of each orientation, to avoid in-plane loading in the transverse fibre direction.
- Stacking sequences considered have a certain percentage of each ply orientation (0/ ± 45 /90) per laminate. For thin laminate aerospace applications it is common practice to apply 50/40/10. Thus, this has been the percentage applied in the present case. Experimental test results should determine the accuracy this assumption for the case of UTL applications. As future work these percentages could be defined as additional design variables, for a further design space exploration.

The VBA subroutines of all design rules created are presented in Appendix H.

7.1.9 Conclusions

In this section, mathematical optimisation has been proposed as a natural method to be applied to composite structural design, and to UTL composite components design in particular. The fact that composite structure stiffness can be tailored by modifying the laminate and material properties influences the way in which the design problem is formulated. The best design performance can be achieved then by considering the laminate properties and the geometric component definition in the optimisation analysis.

A general standard, flexible and expandable FE-based optimisation framework has been presented, which considers the design exploration and optimisation of a wide range of design alternatives in order to identify the optimum solution. ISIGHT and ANSYS are the simulations tools finally chosen for the optimisation framework, as they comply with a series of requirements proposed. Also, a general description of the main framework modules has been done.

Within the presented framework, a design exploration methodology is proposed for the effective design exploration and local optimisation of constant thickness UTL, in terms of the laminate stacking sequence, which considers layered solid element formulation (SOLID191) for reducing the computational cost of the analysis, laminate configuration defined at a ply level, and manufacturing design rules to ensure the practicality of the solution, and which also reduces significantly the number of analysis to be evaluated.

The scope of application of the methodology for the type of analysis considered in this research has been clearly defined.

7.2 Stacking sequence: Case study

The UTL component under 3-point bending test analysed in Section 6.2 is going to be explored for improvement. The Biax configuration (NCF) used in that case is going to be compared against various stacking sequences to determine which one gives the best performance behaviour.

7.2.1 Settings and assumptions

The current NCF production machines are only able to manufacture fabrics with a maximum of 8 layers, and the 0° plies must be placed on an outer layer (Tong et al, (2002)). According to this restriction, for the following analysis the final matrix of experiments considered consisted of 25 possible stacking sequences (Table 7-4). Only the ply percentage design rule was applied, and the final stacking sequences selected were those that have a 0° orientation at extreme outer top and bottom surfaces of each sub-assembly.

Table 7-4 Matrix of experiments.

<i>Number</i>	<i>Stacking sequence</i>
Biax Baseline	[0 90 -45 45] _s
2	[0 0 45 90] _s
3	[0 0 -45 90] _s
4	[0 0 90 45] _s
5	[0 0 90 -45] _s
6	[0 45 0 90] _s
7	[0 45 45 90] _s
8	[0 45 -45 90] _s
9	[0 45 90 0] _s
10	[0 45 90 45] _s
11	[0 45 90 -45] _s
12	[0 -45 0 90] _s
13	[0 -45 45 90] _s
14	[0 -45 -45 90] _s
15	[0 -45 90 0] _s
16	[0 -45 90 45] _s
17	[0 -45 90 -45] _s
18	[0 90 0 45] _s
19	[0 90 0 -45] _s
20	[0 90 45 0] _s
21	[0 90 45 45] _s
22	[0 90 45 -45] _s
23	[0 90 -45 0] _s
24	[0 90 -45 45] _s
25	[0 90 -45 -45] _s

The ANSYS parametric FE model to analyse, material properties and critical load applied are the same as the one used in Section 6.2 (Figure 6-24).

The main output parameters considered are the following:

- Maximum vertical displacement u_z (as a measure of the component stiffness)
- Maximum transverse shear stress τ_{13} per ply, extracted in the free-edge location illustrated in Figure 6-27.

Also, as a measure of a possible secondary in-plane failure, other output parameters were considered:

- Number of plies failed (Tsai-Wu failure criteria)
- Averaged Tsai-Wu strength ratio
- Maximum Tsai-Wu strength ratio

7.2.2 Results

The data management system and optimisation commercial tool called ISIGHT, was used to perform a DOE of the 3-point bending FEA for all stacking sequences proposed. The results obtained are presented in Table 7-5.

Table 7-5 DOE results.

<i>Number</i>	<i>Stacking Sequence</i>	<i>Max u_z (mm)</i>	<i>Max τ_{13} (MPa)</i>	<i>Plies Failed</i>	<i>Averaged TWSR</i>	<i>Max TWSR</i>
Biax Baseline	[0 90 -45 45] _s	-1.57	41.8	18	1.31	1.95
2	[0 0 45 90] _s	-1.40	41.7	17	1.37	1.94
3	[0 0 -45 90] _s	-1.41	39.2	18	1.35	1.97
4	[0 0 90 45] _s	-1.41	41.7	18	1.35	1.96
5	[0 0 90 -45] _s	-1.41	39.2	17	1.37	1.96
6	[0 45 0 90] _s	-1.41	41.7	15	1.39	1.88
7	[0 45 45 90] _s	-1.63	45.0	21	1.29	2.09
8	[0 45 -45 90] _s	-1.57	43.2	17	1.38	2.23
9	[0 45 90 0] _s	-1.41	41.7	16	1.35	1.87
10	[0 45 90 45] _s	-1.63	45.0	20	1.30	2.11
11	[0 45 90 -45] _s	-1.57	43.8	18	1.36	2.17
12	[0 -45 0 90] _s	-1.41	39.3	15	1.39	1.94
13	[0 -45 45 90] _s	-1.57	42.0	15	1.36	2.06
14	[0 -45 -45 90] _s	-1.64	38.7	23	1.34	2.20
15	[0 -45 90 0] _s	-1.41	39.3	16	1.35	1.91
16	[0 -45 90 45] _s	-1.57	42.1	18	1.35	2.02
17	[0 -45 90 -45] _s	-1.64	38.7	23	1.33	2.16
18	[0 90 0 45] _s	-1.41	41.7	15	1.38	1.93
19	[0 90 0 -45] _s	-1.41	39.1	16	1.36	1.92
20	[0 90 45 0] _s	-1.41	41.8	16	1.35	1.91
21	[0 90 45 45] _s	-1.63	45.0	20	1.30	2.13
22	[0 90 45 -45] _s	-1.57	43.1	18	1.31	1.99
23	[0 90 -45 0] _s	-1.41	39.1	16	1.35	1.89
24	[0 90 -45 45] _s	-1.57	41.8	18	1.31	1.95
25	[0 90 -45 -45] _s	-1.64	38.9	23	1.32	2.13

A selection of some laminate configurations from the Table 7-5 were represented in Pareto front diagrams for comparing purposes. In Figure 7-7 maximum vertical displacement is compared against maximum shear stress. The baseline design is highlighted and an arrow points towards laminates which present stiffer behaviour and yet lower maximum shear stress values, as desirable.

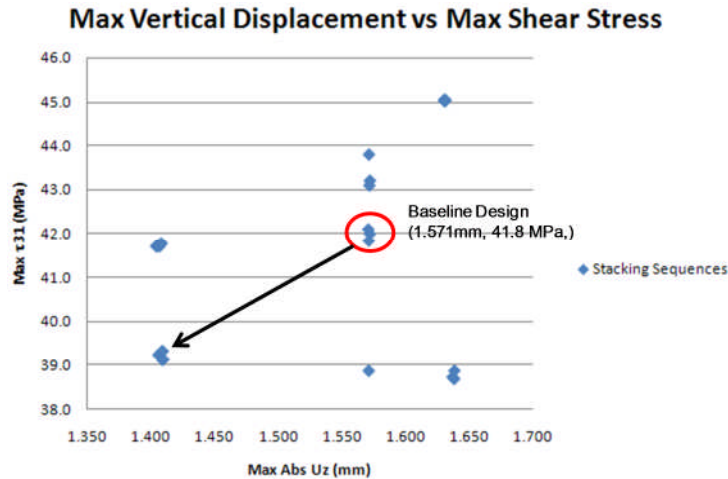


Figure 7-7 Maximum vertical displacement (mm) vs maximum shear stress (MPa).

In Figure 7-8 maximum shear stress is compared against maximum number of plies failed according to Tsai-Wu failure criterion. The baseline design is highlighted and the arrow points towards a laminate which presents lower maximum shear stress value and a lower number of plies in-plane failed (considering it as a secondary mode of failure).

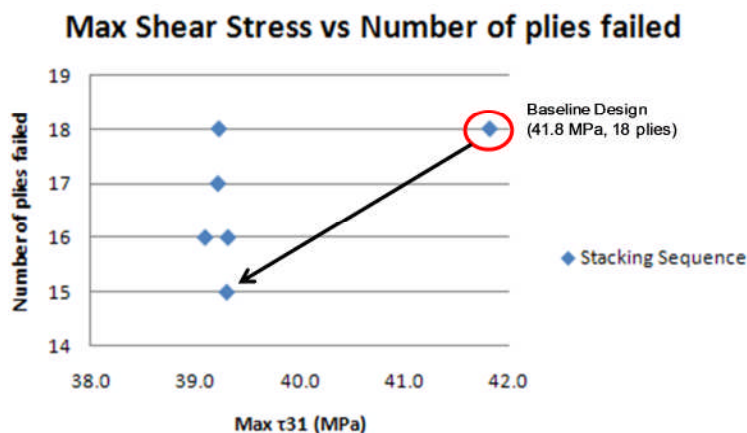


Figure 7-8 Maximum shear stress (MPa) vs maximum number of plies failed (in-plane).

From all 25 laminate configurations compared it has been found several which may have a better performance than the baseline design. Table 7-6 presents a comparison between the baseline Biax configuration and the configuration which shows the best performance; not only being stiffer and with a lower maximum shear stress value, but with lower number of plies in-plane failed.

Table 7-6 Performance comparison between the baseline Biax configuration and an improved configuration.

Number	Stacking Sequence	Max u_z (mm)	Max τ_{13} (MPa)	Plies Failed	Averaged TWSR	Max TWSR
Biax Baseline	[0 90 -45 45] _s	-1.57	41.8	18	1.31	1.95
19 (Improved)	[0 90 0 -45] _s	-1.41	39.1	16	1.36	1.92

7.2.3 Conclusions

The FE based design exploration methodology proposed is applied for the performance optimisation of the 30 mm thick short-beam under three points bending test analysed in Section 6.2 (that is regarded as the baseline model), in order to determine which laminate stacking sequence from a series of configurations considered gives the best mechanical performance (measured in terms of its vertical displacement (stiffness) and maximum shear stress value (responsible of through thickness delamination failure)).

The component was modelled as a stack up of a fixed number of sub-assemblies or laminates across the thickness, all of these defined with the same stacking sequence. As abovementioned layers orientations (of half the laminate due to symmetry) were the only input variables defined.

The Biax configuration (NCF) introduced in Section 6.2 was compared against various stacking sequences to determine which one gives the best performance behaviour.

Due to NCF manufacturing limitations, the final stacking sequences generated were within those that had a 0° orientation at extreme outer top and bottom surfaces of each sub-assembly (as other heuristic design rules were also applied).

The analysis has identified other possible configurations that may have a better performance than the baseline (Biax), considering only the maximum transverse shear stress values as directly responsible for the delamination failure. However, these improved designs may present as a secondary mode of failure a higher number of plies failed or a higher failure index (in-plane failure). Considering then the limited number of test results evaluated, it was not possible to compare the overall benefits of the alternative configurations, and additional tests are required. However, this was not the objective of this study.

Tsai-Wu failure criterion was considered in this case as an additional parameter to evaluate a possible secondary failure. Maximum stress failure criterion, which is a more

conservative criterion, is better predicted by layered element formulation (according to what was presented in Section 5.5), and should be evaluated also for future analysis.

The design space exploration has provided an initial framework that represents a powerful tool to evaluate the performance for a broad number of laminate feasible configurations.

8 Conclusions and Future Work

8.1 Conclusions

“Black metal” approach is the current method employed to design UTL components, which may neglects one of the main drivers of composite materials, by which the component stiffness matrix can be tailored and optimised in order to deliver the best performance.

On the other hand, Ultra Thick Laminates (UTL) require a 3D stress state characterisation, in order to predict the out-of-plane delamination failure, associated with transverse shear stresses and interlaminar stresses at the laminate free edge. Thus, an accurate determination of the transverse shear stresses is of paramount importance in order to design a fail-safe component.

For the reasons above stated the overall objective of this work is to address the following research questions:

- To assess the functionality, advantages and limitations of different layered solid elements that are available in commercial Finite Element codes, applied to the mechanical response prediction of UTL composite components (thicknesses up to 30 mm are considered).
- To perform a design exploration and optimisation of constant thickness UTL composite component in terms of the orientation of a varying and repeatable stacking sequence of an eight ply Non-Crimped Fabric, in order to assess the design implications on performance.

In order to achieve these objectives a standard, flexible and expandable FE based optimisation methodology for UTL composite components that can explore a broad design space, enabling to evaluate different layup configuration, a wider range of bracket geometric layouts and dimensions, and various laminate stacking sequences and material properties, was proposed.

Following, a series of activities undertaken for successfully achieve the research objectives are presented.

8.1.1 Plate deformations due to transverse shear

Section 3 provided a general description of the main theories developed for modelling laminated composite plates, some of them implemented in the element formulation of most of the commercial FE codes; focusing on their suitability and limitations for accurately represent the through thickness shear effects, as delamination failure mechanisms of thick laminated plates are highly influenced by them.

CLT and FSDT do not allow an accurate description of the transverse shear stresses for the case of thick and moderately thick laminated plates. However, a reasonable representation of their behaviour can be obtained by the HSDT, currently adopted by several layered solid elements.

The layerwise theory is also unable to accurately define transverse shear stresses despite it allows their interlaminar continuity at the plies interface.

An accurate computation of transverse shear stresses can only be achieved then by adopting 3D equilibrium equations, using one or various solid elements per layer for describing the laminate behaviour, with the associated penalty in computational cost due to the large number of variables considered (directly related to the number of layers), which makes this approach impractical for engineering applications.

8.1.2 FEA of UTL composite components

The methodology proposed is based on FE analysis of thick laminates. Section 4 gives an overview of the main characteristics of FE analysis of laminated composite, particularised for this kind of structures. Depending on the level of post-processing sought, possible modelling strategies were presented, and meso-scale approach was proposed for this research, as the through thickness stress, the main variable for evaluating delamination, is required at a ply level.

The use of layered solid elements was justified, providing benefits in terms of accuracy and efficiency of the analysis of thick laminates, which requires the division of the laminate into sublaminates (normally defined by a repeated stack up), each one of them represented by a layer of elements of the same thickness.

ANSYS was the multidisciplinary FEA commercial tool used in this research, and its election was based on the fact of having parametric model definition capabilities, by means of the Ansys Parametric Design Language. It also offers several layered solid formulations, and licences were available in the School of Engineering at Cranfield University.

The analysis steps involved in a laminated structure FE Analysis are particularised for ANSYS. A general description of the layered element formulations available (for theoretical description of various element formulations refer to 8.2.8.2Appendix J).

Best parametric modelling and post-processing practice are given, including the layered configuration definition, element coordinate system transformation (defining the laminate coordinate system), and the available 3D failure criteria definition.

Special emphasis is given to solid modelling generation and postprocessing, and to discuss the limitations of ply drop off for solids elements applications, which finally have not been considered in this study.

Some practical recommendation for the pre and postprocessing of thick laminate FE models are given

- Different real constants (element attribute) should be applied to each layer of solid elements of the laminate in order to select a particular layer, for postprocessing purposes.
- When modelling laminated components with complex topology, the geometry generated for an FEA should account for the manufacturing constrains (see Figure 8-1), as well as the element coordinate system definition ESYS.

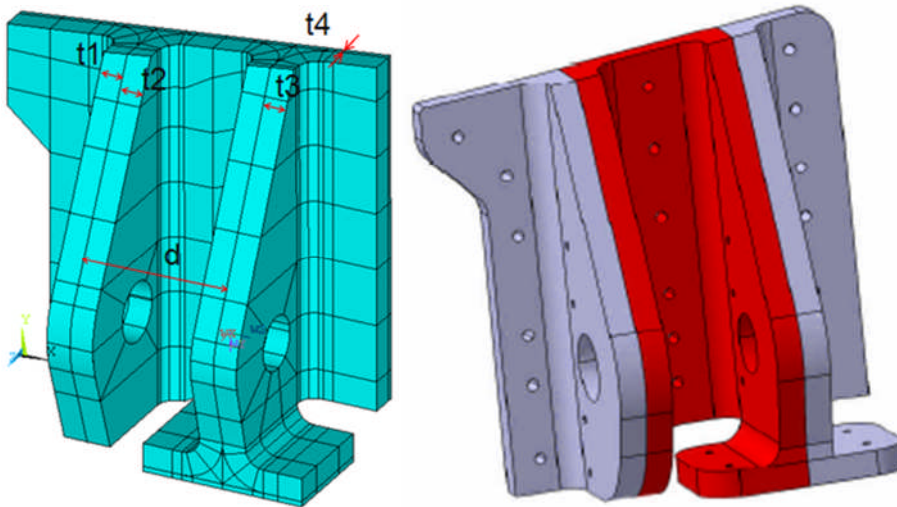


Figure 8-1 Parametric MLG SSF FE model (only geometry shown), alongside with available geometric design variables (l). CAD model (r). Source (r): Siemetzki et al., 2007.

- Parametric model generation enables a flexible definition of the design space, and the possibility to evaluate multiple design variables (geometric entities, layer orientation, material properties, etc).

8.1.3 Case studies for thin and thick composite components

In Section 5 a series of FE analysis with thin laminates were carried out in order to get practical experience with ANSYS, as a previous step before tackling the UTL composite structural analysis. Different layered element formulations were benchmarked against analytical results obtained from CLT analysis performed on a particular configuration of a laminated plate under in-plane and out-of-plane load cases, by comparing several in-plane results (ultimately the ply failure index for Tsai-Wu and Maximum stress criteria).

For the case of layered solid formulations, different modelling strategies were also evaluated, modifying the number of layered elements through the thickness for a fixed number of plies; in order to evaluate the effects that, not only the element formulation,

but also the modelling technique has an impact on the accuracy of the results at a layer in-plane level.

This analysis has helped also to develop the author skills for creating and postprocessing parametric models using the Ansys Parametric Design Language, which could represent a wide range of different laminate configurations, with the idea of using such capability in future applications.

The plate was modelled with layered shell elements (4 and 8 nodes), layered solid elements (8 and 20 nodes), and intermediate layered solid-shell formulation (8 nodes), defining all laminates at a ply level, and not by using smeared properties.

All layered shell formulations give a very good agreement with the analytical results, for both, in-plane and out-of-plane. The only deviations are found in the under integrated formulation (SHELL181) when in-plane shear is applied.

The higher deviation values obtained for layered solid formulations demonstrate that, in general, they are not suited for thin applications, although in some cases they have a very good agreement with the analytical results (as for the case of in-plane shear load).

For Maximum stress criterion, which has shown to be a more conservative failure criterion than Tsai-Wu's, its ply failure indices are more accurately predicted by layered solid formulations than Tsai-Wu failure indices. For the latter, most layered solid formulations overestimate the failure index for the plies defined in the direction where load is applied, presenting up to 10% of deviation in some cases.

The results obtained for SOLID191 modelled with one element per ply showed more variability at a ply level than the rest of the formulations, and considering the deviations obtained for this element formulation for all different modelling strategies thicker applications are required to extract more solid conclusions.

For a fixed number of plies and a fixed plate thickness, as the number of layered elements through the thickness is increased their aspect ratio is distorted, possibly affecting the quality of the results. For this reason a mesh sensitivity analysis was carried out. Results are presented in Appendix C. Various meshes were compared (14x14, 28x28, 50x50). From the results obtained it can be concluded that in-plane failure indexes results are not really mesh dependent, for the element size considered.

In Section 6.1 Ansys layered solid element formulations were extended to consider more complex examples, such as a moderately thick curved plate under pure bending moment (to which an analytical solution is available), which could partially represent a simplified model of one half of the main side stay fitting flange. This natural extension to the complexity of the problem provided another opportunity to assess the applicability of layered solid formulations for analysing and predicting the mechanical response of UTL components.

The results shown that regardless of the element formulation, the accuracy of the radial stress distribution is directly related with the number of integration points through the thickness (number of elements through the thickness). Both under integrated solid elements (SOLID46 and SOLID185) seem to give the same radial stress results (σ_{33}), and the same conclusion applies to the 20-node solid elements (SOLID186 and SOLID191). Effectively, SOLID185 and SOLID186 are improved and more user friendly formulations than SOLID46 and SOLID191, respectively.

SOLID186 has full non-linear capabilities. Despite that, for linear elastic applications, as the ones analysed in this thesis, the results provided by both formulations are pretty similar. For the present case SOLID191 has been the formulation used in the majority of the applications, but for future applications SOLID186 is recommended.

SOLID46 and SOLID185 formulations (8 node layered solid) tune the material properties in the transverse direction, allowing constant radial stress value σ_{33} through the thickness under bending moment. Thus, the use of this layered element type is not recommended for bending applications. In case it is required to be used, radial stress results are improved as the number of element through the thickness increases (although only trends can be accounted).

Radial stress σ_{33} is best represented when using one solid element per layer with a 20-node element (SOLID186 or SOLID191), although it is computationally very expensive. The best compromise between accuracy and CPU time is obtained when using four layered elements through the thickness (3 layers per element).

Regardless of the number of layered elements through the thickness, the tangential stress achieved with SOLID185, SOLID186 and SOLID191 give the exact solution.

The computational cost associated with the modelling strategy chosen was evaluated. It became evident that the cost of using of one solid element per ply thickness will make unaffordable the analysis of complex structures, thus the use of layered solid elements is justified.

In Section 6.2 a FE analysis of a 3-point bending test was carried out using ANSYS. Results were verified against available numerical results obtained by FE analysis performed with MSC MARC/MENTAL and experimental test results (Czichon et al., 2011). The aim was to represent an accurate shear stress distribution through the thickness by using an appropriate layered element formulation, and a flexible parametric model definition.

SOLID191 (20 nodes) has proved to be a quite accurate and effective layered element formulation for predicting the interlaminar shear stresses in UTL composite applications (a 30 mm thick specimen has been considered).

The transverse shear stress distribution τ_{13} , computed with this formulation, and its maximum stress level present a good agreement with the analytical and experimental

test results obtained by EADS IW (Czichon et al., 2011), using MARC layered solid element formulation (ELEM149 with 8 nodes).

Comparison of transverse stress results obtained with layered solid elements and when using two solid elements per layer, only indicates deviations on a ply level. However, as justified by Czichon et al. (2011), the level of accuracy of the results achieved with layered solid is accurate enough, as delamination failure is expected to occur in the region that presents the highest shear stress.

8.1.4 Design exploration methodology

A general standard, flexible and expandable FE-based optimisation framework has been presented, which considers the design exploration and optimisation of a wide range of design alternatives in order to identify the optimum solution. ISIGHT and ANSYS are the simulations tools finally chosen for the optimisation framework, as they comply with a series of requirements proposed. Also, a general description of the main framework modules has been done.

The proposed framework is particularised for the effective design exploration (DOE) of constant thickness UTL, in terms of the laminate stacking sequence (discrete design variables), which considers layered solid element formulation (SOLID191 or SOLID186, 20-node layered solid elements) for reducing the computational cost of the analysis, and which according to what was concluded in Section 6.2.5, provide an accurate yet efficient mean to compute the maximum shear stress value at the component free edge, at which through thickness delamination failure may occur. Laminate configuration defined at a ply level, and manufacturing design rules to ensure the practicality of the solution, and which also reduces significantly the number of analysis to be evaluated.

Delamination failure mechanism in UTL structures is predicted via a through thickness strength analysis, and ply drop-off is not considered.

The scope of application of the methodology for the type of analysis considered in this research has been clearly defined (Section 7.1.7).

8.1.5 Design exploration methodology: case study

The FE based design exploration methodology proposed is applied for the performance optimisation of the 30 mm thick short-beam under three points bending test analysed in Section 6.2 (that is regarded as the baseline model), in order to determine which laminate stacking sequence from a series of configurations considered gives the best mechanical performance (measured in terms of its vertical displacement (stiffness) and maximum shear stress value (responsible of through thickness delamination failure)).

Due to NCF manufacturing limitations, the final stacking sequences generated were within those that had a 0° orientation at extreme outer top and bottom surfaces of each sub-assembly (as other heuristic design rules were also applied).

The analysis has identified other possible configurations that may have a better performance than the baseline (Biax), considering only the maximum transverse shear stress values as directly responsible for the delamination failure. However, these improved designs may present as a secondary mode of failure a higher number of plies failed or a higher failure index (in-plane failure). Considering then the limited number of test results evaluated, it was not possible to compare the overall benefits of the alternative configurations, and additional tests are required. However, this was not the objective of this study.

Tsai-Wu failure criterion was considered in this case as an additional parameter to evaluate a possible secondary failure. Maximum stress failure criterion, which is a more conservative criterion, is better predicted by layered element formulation (according to what was presented in Section 5.5), and should be evaluated also for future analysis.

The design space exploration has provided an initial framework that represents a powerful tool to evaluate the performance for a broad number of laminate feasible configurations.

The proposed methodology could be applied for the design exploration of more complex UTL components, such as the MLG SSB. Not only considering the sublaminated layers orientation as design variables, but also different material properties, geometric entities of the bracket (as presented in **Error! Reference source not found.**). This detailed FE model could be analysed alongside a coarse definition of the whole wing assembly, in order to evaluate and improve its effects in performance more accurately.

8.2 Recommendations for Future Work

8.2.1 Layered solid element orientation analysis

Making use of the proposed methodology, the relative orientation of the sub-assemblies can be assessed, for a fixed stacking sequence for all sub-assemblies. The research objectives in this case are the following:

- Layered solid element orientation optimisation: Considering the manufacturing constraints within a block of eight plies (according to NCF), it offers a mean to improve the design, considering that there is no restriction in the way two consecutive laminates, with Biax configuration, are stacked together.
- Robustness: Assessing the impact of the input parameters on the output parameters, as well as identifying significant parameter interactions.

Making use of the previous 3-points bending test of the UTL test, for the Biax configuration specimen, the design variables considered would be for this analysis the layered solid element orientation. Only half the elements are considered due to symmetry (ThetaR1 to ThetaR7) and the mid sub-assembly would have its element coordinate system at 0 degrees. The FEA models are already created (See the input file shown in Appendix I).

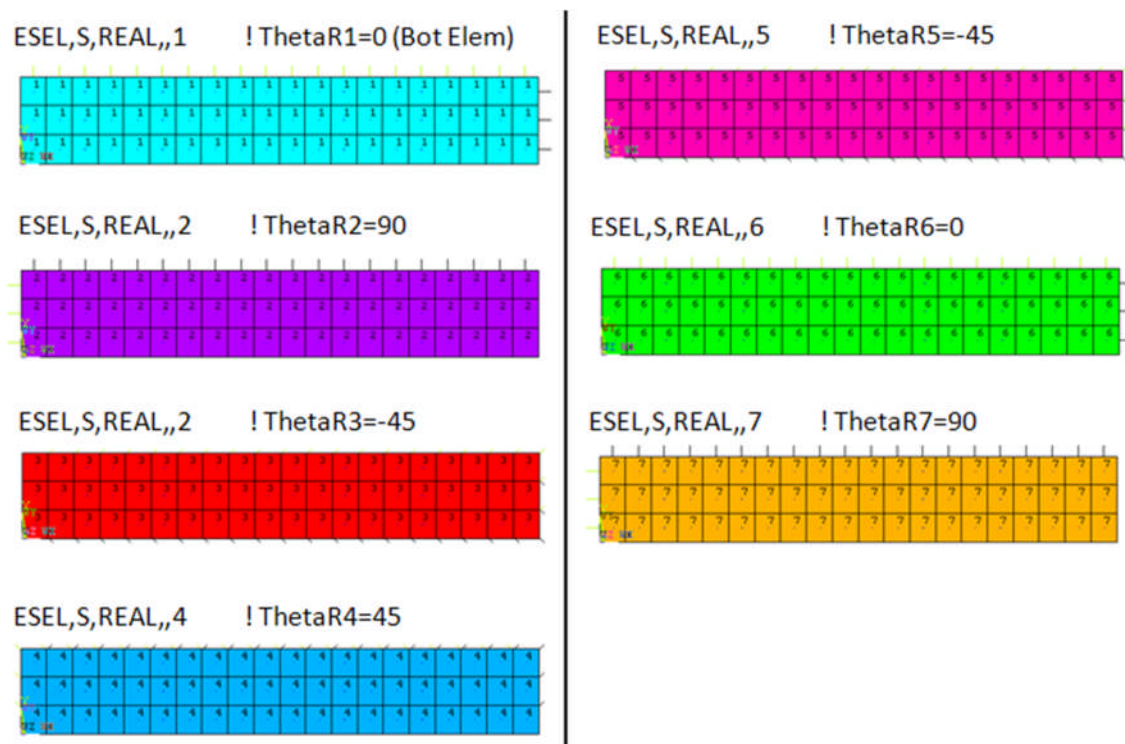


Figure 8-2 Element coordinate system of half of the laminate elements. Design variables.

8.2.2 3D analytical results

There are few sources available in literature that provide exact 3D elasticity solutions for thick laminated composite plates (Pagano, 1970, and Savoia and Reddy, 1992). More recently, some authors presented efficient approaches to accurately describe through thickness behaviour, demonstrating their accuracy by comparison with results from these references (Kulikov and Plotnikova, 2011), as well as with FSDT and HSDT (Bhar and Satsangi, 2011). Try to reproduce and verify the exact through thickness elasticity solutions available in literature with the ANSYS layered solid formulations.

8.2.3 Geometric design variables

Extend the scope of application of the proposed design optimisation methodology in order to consider not only the stacking sequence optimisation of UTL composites, but also to include continuous geometric design variables. Simple examples for which analytical or experimental information is available should be chosen. The analysis should evaluate and discuss the benefits or limitations of selecting different optimisation approaches. For instance, the proposed optimisation can be accounted as a two step process, in which the stacking sequence optimisation is carried out in the first place, according to the design exploration methodology presented in this report, followed by the continuous geometric design variables optimisation using non-linear numerical optimisation techniques. Alternatively, all discrete and continuous design variables can be evaluated at the same time, which would require the use of GAs.

8.2.4 Experimental test validation

Perform an experimental test validation of the 3-point bending short beam FEA for some of the laminate configurations presented in Section 7.2.2 that showed the best performance (for instance, $[0\ 90\ 0\ -45]_s$). Also, for validation purposes carry out experimental tests for the sub-assemblies orientation analysis that predict the best laminate performance (Section 8.2.1).

8.2.5 Ply drop off

Section 4.4.3 discussed the main difficulties associated with the modellisation of ply drop-off in thick laminates. The inability to use solid layered formulations in the regions of the model representing the ply drop-off pocket force to find other alternatives. In this respect, the implementation of 3D layerwise element (Zinno and Barbero, 1994), capable of representing a variable number of layers and thicknesses should be investigated (Section 3.5.3 and Section 4.4.3). The results obtained will have direct impact in future weight optimisation studies of thick laminates.

8.2.6 User defined failure criteria

A source in literature features (Czichon et al., 2011) presents results of a multiscale approach using non linear material model with a progressive failure model and an implemented interactive failure model, to be considered in the failure analysis of UTL. Investigate the possibility of specify user-written failure criteria via the ANSYS user subroutines USRFC1 through USRFC6. These subroutines should be linked with the ANSYS program beforehand; refer to the Advanced Analysis Techniques Guide (ANSYS help manual) for a brief description of user-programmable.

8.2.7 Edge effects: Stress concentration due to bolts

Make use of the capabilities offered by the design exploration methodology framework proposed to evaluate the stress concentration of moderate and UTL composites due to pretension bolts, in order to improve the laminate performance. Experimental validation will be required.

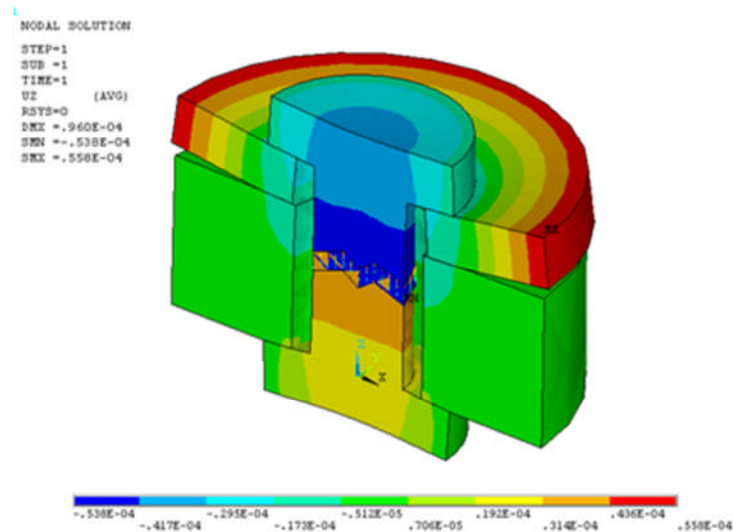


Figure 8-3 Vertical displacement u_z (m) of a metallic plate due to pretension bolts.

8.2.8 Weight Optimisation methodology of UTL composites

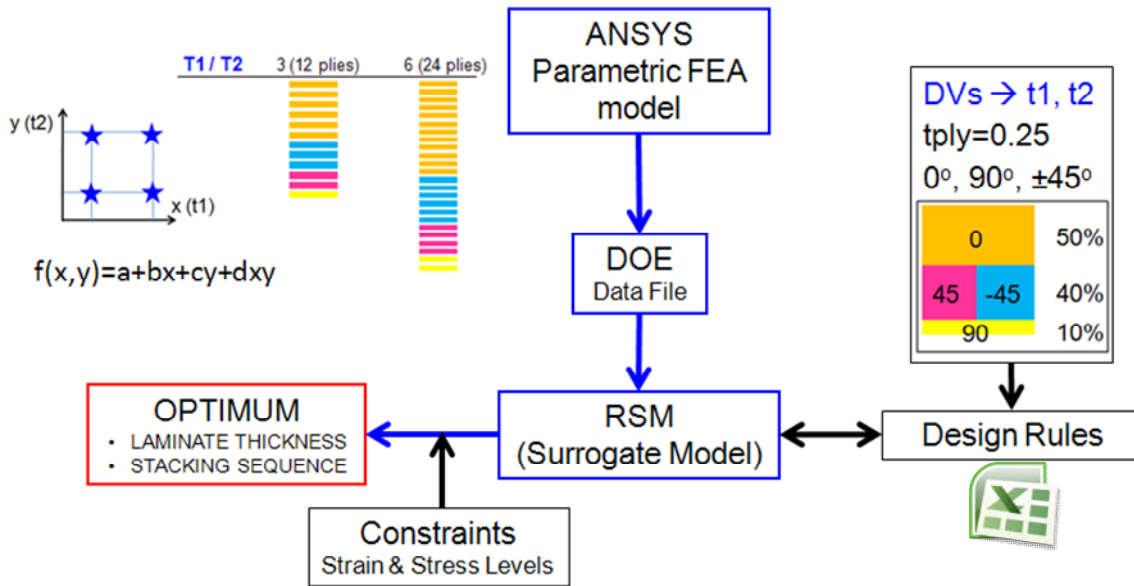


Figure 8-4 Proposed weight optimisation methodology for UTL composites.

Regarding the weight optimisation methodology of UTL composites, the proposed approaches are based in the FE-based optimisation methodology (Section **Error! Reference source not found.**).

There are many unknowns at this stage, so the procedures presented here can be only considered as a guide. Also, the problems that can be faced when performing a weight optimisation are:

- Difficulties associated with validation / verification of results.
- The difficulties associated with representing ply drop off when considering layered solid elements (Section 4.4.3). Thus, the approaches introduced, as a first guess, do not take ply drop off into account.

8.2.8.1 Approach 1: Constant number of plies per sub-assembly

In this case, the baseline composite structure is created with a fixed number of plies (8 plies, for instance) per sub-assembly (layered solid element), and a fixed stacking sequence configuration for all sub-assemblies. Various stacked sub-assemblies through the thickness are required to improve accuracy, as justified in Section 6.1.

The design variables are then, the number of brick elements through the thickness. Future optimisation studies may account as well for geometric entities.

Proposed case study: Reinforced Curved Plate

The proposed case study is based in the curved plate analysis presented in Section 6.1, in which an additional plate has been added as reinforcement to improve the through thickness behaviour.

Optimisation set up:

- Parameters: Number of plies per sub-assembly (NPlies) and plies orientations (Theta1 to Theta4)
- DVs: Number of sub-assemblies per plate (N_Brick1 for the bottom plate, N_Brick2 for the top plate)
- Constraints: Through thickness failure index (determined by the interlaminar allowable strength)
- Objective function: minimum weight
- The normal stress σ_{33} can be used for verification purposes by using a reinforced curved plate with orthotropic plies at 0° , as the analytic solution for an isotropic beam is known (see Section 6.1).

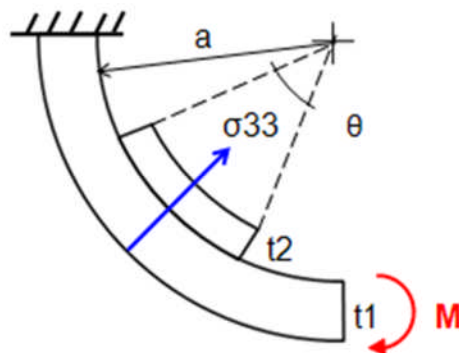


Figure 8-5 Schematic representation of a reinforced thick curved plate under pure bending moment.



Figure 8-6 Reinforce curved plate geometry, with various sub-assemblies across the thickness.

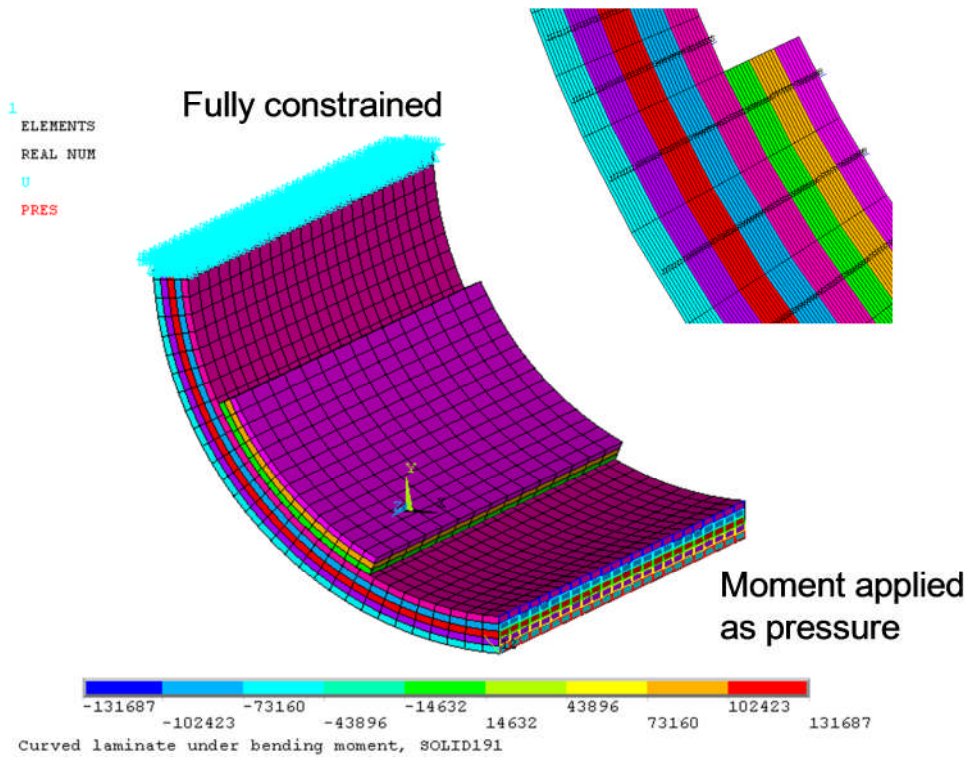


Figure 8-7 Reinforce curved plate FE model, with various layered solid elements across the thickness.

8.2.8.2 Approach 2: Constant number of subassemblies through the thickness

In this second case, the baseline composite structure is created with a fixed number of sub-assemblies through the thickness. Various stacked sub-assemblies through the thickness are required to improve accuracy, as justified in Section 6.1.

The design variables are then, the number of plies per subassembly. Future optimisation studies may account as well for geometric entities.

Proposed case study: Reinforced Curved Plate

Optimisation set up:

- Parameters: Constant number of brick through the thickness.
- DVs: Number of plies per sub-assembly (NPlies1 for the bottom plate subassemblies, NPlies2 for the top plate subassemblies)
- Constraints: Through thickness failure index (determined by the interlaminar allowable strength)
- Objective function: minimum weight
- The normal stress σ_{33} can be used for verification purposes by using a reinforced curved plate with orthotropic plies at 0° , as the analytic solution for an isotropic beam is known (see Section 6.1).

REFERENCES

1. Abbey, T. (2010). Composites e-learning course EL 009 v1.0. NAFEMS.
2. Agarwal, B.D., Broutman, L.J. and Chandrashekhara, K. (2006). Analysis and performance of fiber composites. 3rd edition. John Wiley & Sons, Inc., Hoboken, New Jersey, US.
3. ALTAIR HyperWorks v10.0 Help Manual.
4. ANSYS 11.0 Help Manual & ANSYS Workbench 11.0 Help Manual
5. Assler, H. (2006). Design of aircraft structures under special consideration of NDT. 9th European Conference on NDT., September 25th – 29th, 2006. Berlin, Germany.
6. Barbero E.J. (1999). Introduction to composite materials design. Taylor and Francis Ltd. London, England.
7. Barbero, E.J. (2008). Finite element analysis of composite materials. CRC Press.
8. Barker, R.M., Lin, F.T., Dana, J.R. (1972). Three-dimensional finite-element analysis of laminated composites. Computers & structures, Vol. 2, pp. 1013-1029. Pergamon Press.
9. Baker, A., Dutton, S. and Kelly D. (2004). Composite materials for aircraft structures. AIAA Education Series. Reston, Virginia, USA.
10. Belegundu, A.D., Argod, V., Rajan, S.D., and Krishnan, K. (2008). Shape optimization of panels subject to blast loading modeled with LS-DYNA. 49th AIAA/ASME/ASCE/AHS/ASC Structures, Structural Dynamics, and Materials. 7th - 10th April 2008, Schaumburg, IL. AIAA 2008-2285.
11. Bhar, A., and Satsangi, S.K. (2011). Accurate transverse stress evaluation in composite/sandwich thick laminates using a C⁰ HSDT and a novel post-processing technique. European Journal of Mechanics A/Solids 30, 46-53. Elsevier Science Ltd.
12. Chedid, M.M. (2009). Optimisation of composite materials using a multilevel decomposition approach. MSc Thesis. Cranfield University. Cranfield.
13. Chen, W., Fu, W., Biggers, S.B., and Latour, R.A. (2000). An affordable approach for robust design of thick laminated composite structure. Optimization and engineering, 1, 305-322.
14. Cho M.H., and Parmerter RR. (1993). AIAA J 31(7): 1299.
15. Coley D.A. (1999). An introduction to genetic algorithms for scientist and engineers. World Scientific, Singapore.
16. Colmenares Quintero, R.F. (2009). Techno-economic and environmental risk assessment of innovative propulsion systems for short-range civil aircraft. PhD Thesis. Cranfield University. Cranfield.
17. Conti, P. and Cella, A. (1992). An optimal design of multilayered laminates based on finite element stress analysis. Composite Material Technology, ASME vol. 45, pp. 205–212.

18. Czichon, S., Zimmermann, K., Middendorf, P., Vogler, M., Rolfes, R. (2011). Three-dimensional stress and progressive failure analysis of ultra thick laminates and experimental validation. *Composite Structures* 93, 1394-1403.
19. Diedrich, A. 2004. Air transport systems cost and weight analysis.
20. Fu, W. (1998). Design optimisation of laminated composite femoral component for hip joint arthroplasty. PhD thesis. Clemson University. Clemson.
21. Fu, W., Biggers, S.B. Jr., and Latour, R:A. Jr. (1998) Design optimisation of a laminated composite femoral component for hip joint arthroplasty. *Journal of Thermoplastic Composite Materials* vol. 11, no. 2, pp. 99-112.
22. Fukunaga, H. and Vanderplaats, G.N. (1991). Stiffness optimization of orthotropic laminated composites using lamination parameters. *AIAA J* 29:641–646.
23. Ghiasi, H., Pasini D., and Lessard L. (2009) Pareto frontier for simultaneous structural and manufacturing optimization of a composite part. *Struct. Multidisc. Optim.*, Doi:10.1007/s00158-009-0366-4.
24. Goldberg, D.E. (1989). Genetic algorithms in search, optimization and machine learning. Addison-Wesley Longman, Reading, MA.
25. Gürdal, Z., Haftka, R.T. and Hajela, P. (1999). Design and optimisation of laminated composite materials. John Wiley & Sons. New York, USA.
26. Haftka, R.T., and Walsh, J.L. (1992). Stacking sequence optimization for buckling of laminated plates by integer programming. *AIAA J* 30:814–819.
27. Herencia, J.E., Weaver, P.M., and Friswell, M.I. (2007). Optimisation of anisotropic composite panels with T-shaped stiffeners including transverse shear effects and out-of-plane loading. *Struc. Multidisc Opt.*
28. Herencia, J.E., and Weaver, P.M. (2008). Optimization of anisotropic composite panels with T-shaped stiffeners including transverse shear effects and out-of-plane loading. *Structural Multidisciplinary Optimization*. Springer-Verlag.
29. Jones, R.M. (1999). Mechanics of composite materials. Virginia Polytechnic University and State University. Blacksburg, Virginia.
30. Kaufmann, M. (2008). Cost/Weight optimization of aircraft structures. Licentiate Thesis. Stockholm, Sweden.
31. Khandan, R., Noroozi, S., Sewell, P., Vinney, J. (2012). The development of laminated composite plate theories: a review. *Journal of Material Science* 47: 5901-5910.
32. Koch, P.N., Evans, J.P. and Powell, D. (2002). Interdigitation for Effective Design Space Exploration using i-SIGHT. *Journal of Structural and Multidisciplinary Optimization*, 23 (2).
33. Kodiyalam, S., Su Lin, J. and Wujek, B.A. (1998). Design of Experiments Based Response Surface Models for Design Optimization. 39th AIAA/ASME/ASCE/AHS/ASC Structures, Structural Dynamics and Materials Conference, Long Beach, CA, 2718-2727.
34. Kollár, L.P. and Springer, G.S. (2003). Mechanics of composite structures. Cambridge University Press.

35. Kuhlmann, G., and Rolfes, R. (2004). A hierarchic 3D finite element for laminated composites. *International Journal for Numerical Methods in Engineering*. 61:96-116.
36. Kulikov, G.M. and Plotnikova, S.V. (2012). Exact 3D stress analysis of laminated composite plates by sampling surfaces method. *Composite Structures* 94, 3654-3663. Elsevier Science Ltd.
37. Le Riche, R., Haftka, R.T. (1993). Optimization of laminate stacking sequence for buckling load maximization by genetic algorithm. *AIAA J* 31:951–956.
38. Mahmood, A. (2007). Design and analysis of landing gear for composite aircraft. MSc AVD Thesis. Cranfield University. Cranfield.
39. Marsden, W. and Irving, D.J. (2002). How to analyse composites. NAFEMS.
40. Matthews, F.L., Davies, G.A.O., Hitchings, D., and Soutis, C. (2000). Finite element modelling of composite materials and structures. Cambridge. Woodhead publishing limited.
41. Monroy Aceves, C., Skordos, A.A., and Sutcliffe, M.P.F. (2008). Design selection methodology for composite structures. *Materials and design* 29, 418-426. Elsevier.
42. Montgomery, D.C. (1996). *Design and Analysis of Experiments*, New York, John Wiley & Sons.
43. Myers, R.H. and Montgomery, D.C. (1995). *Response Surface Methodology: Process and Product Optimization Using Designed Experiments*, New York, John Wiley & Sons.
44. Nagendra, S., Haftka, R.T., Gürdal, Z. (1992). Stacking sequence optimization of simple supported laminates with stability and strain constraints. *AIAA J* 30:2132–2137.
45. Nguyen, T. (2010). Effects of curvature on the stresses of a curved laminated beams subjected to bending. MSc in Mechanical Engineering. University of Texas at Arlington. US.
46. Pagano, N.J. (1970). Exact solutions for rectangular bidirectional composites and sandwich plates. *Journal of Composite Materials* 4, 20-34.
47. Park, C.H., Lee, W.I., Han, W.S. and Vautrin, A. (2003). Weight minimization of composite laminated plates with multiple constraints. *Composite science and technology* 63. 1015-1026.
48. Pipes, R. B. and Pagano, N. J. (1970). Interlaminar stresses in composite laminates under uniform axial extension. *J. Composite Materials* 4, 538-544.
49. Savoia, M., Reddy, J.N. (1992). A variational approach to three-dimensional elasticity solutions of laminated composite plates. *ASME Journal of Applied Mechanics* 59, S166-S175.
50. Schmit, L.A., and Farshi, B. (1973). Optimum laminate design for strength and stiffness. *Inter J Numer Methods Eng* 7: 519–536.
51. Schmit, L.A., and Farshi, B. (1977). Optimum design of laminated fiber composite plates. *Int J Numer Methods Eng* 11:623–640.

52. Siemetzki, M.A., Zimmermann, K. et al. (2007). ALCAS SS/F 'B' Maturity Report (Official version). CTO/IW-SP-2007-93 Technical Report. EADS Innovation Works.
53. Simpson, T.W., Peplinski, J.D., Koch, P.N., Allen, J.K. (2001). Metamodels for computer-based engineering design: Survey and recommendations. *Engineering with computers* 17: 129-150. Springer-Verlag London Limited.
54. Smith, B. (2003). The Boeing 777. *Journal of Advanced Materials and Processes*.
55. Sobieszczanski-Sobieski, J., James, B.B., and Dovi, A.R. (1985). Structural optimization by multilevel decomposition. *AIAA Journal* vol. 23, no. 11, pp. 1775–1782.
56. Swanson S. (1997). *Introduction to design and analysis with advanced composite materials*. Prentice-Hall.
57. Taguchi, G. and Konishi, S. (1987). *Orthogonal Arrays and Linear Graphs*. American Supplier Institute, Dearborn, USA.
58. Tsai, S.W., and Pagano, N.J. (1968). *Composite materials workshop*. Technomic, Stamford, CT, pp 233–253.
59. Tsai, S.W., and Hahn, H.T. (1980). *Introduction to composite materials*. Technomic, Stamford, CT.
60. Thuis, H.G.S.J. (1999). Development of a composite torque link for helicopter landing gear applications. National Aerospace Laboratory NLR. NLR-TP-99026.
61. Tong, L., Mouritz, A.P., Bannister, M.K. (2002). *3D fibre reinforced polymer composites*. Elsevier Science Ltd. Oxford, UK.
62. Toporov, V.V., Jones, R., Willment, T., and Funnell, M. (2005). Weight and manufacturability optimization of composite aircraft components based on a genetic algorithm. 6th World congress of structural and multidisciplinary optimization. 30th May – 3rd June 2005. Rio de Janeiro, Brazil.
63. Ugural A.C. and Fenster S.K. (2003). *Advanced strength and applied elasticity* 4th ed., Pearson Education, Inc.
64. Venkataraman, S. and Haftka, R.T. (2002). Structural optimisation: What has Moore's law done for us? *American Institute of Aeronautics and Astronautics AIAA-2002-1342*.
65. Venkateswaran, S. and Sundararajan, K. Bolt modeling wizard in ANSYS. TATA Consultancy Services, Chennai, India.
66. Watkins, R.I., and Morris, A.J. (1987). A multicriteria objective function optimization scheme for laminated composites for use in multilevel structural optimization schemes. *Computer Methods in Applied Mechanics and Engineering* vol. 60, pp. 233–251.
67. Watson, G. (2007). ALCAS – Advanced Low-Cost Aircraft Structures. EU 7th Turkey Forum: National Launch Conference. 12th-13th February 2007. Ankara, Turkey.
68. Zhang, X., Wang, S. and Zhang, Y. (2010) Stress and failure analysis of laminated composites based on layerwise B-spline finite strip method. *Composite Structures* 92 (2010) 3020-3030. Elsevier Science Ltd.

69. Zinno, R. and Barbero, E.J. (1994). A three-dimensional layer-wise constant shear element for general anisotropic shell-type structures. *International Journal for Numerical Methods in Engineering*, Vol. 37, 2445-2470.

BIBLIOGRAPHY

1. ALCAS website. <http://alcas.twisoftware.com/> (Accessed September 2008).
2. Almeida, F.S., Awruch, A.M. (2009). Design optimization of composite laminated structures using genetic algorithms and finite element analysis. *Composite Structures* 88, 443-454. Elsevier.
3. Ashby, M.F., Bréchet, Y.J.M., Cebon, D., and Salvo, L. (2004). Selection strategy for materials and processes. *Materials and design* 25, 51-67.
4. Bader, M.G. (1996). Material selection, preliminary design and sizing for composite laminates. *Composites Part A* 27A, 65-70. Elsevier.
5. Barkanov, E., Gluhih, S., Ozolins, O., Eglitis, E., Almeida, F., Bowering, M.C., and Watson, G. Optimal weight design of composite lateral wing upper covers.
6. Bendsoe M.P., and Stolpe, M. (2008). PLATO-N: Developing specialized methods for aeronautics structural design applications. EngOpt – International Conference on Engineering Optimization. 1st-5th June 2008. Rio de Janeiro, Brazil.
7. Chatiri, M., Güll, T., and Matzenmiller, A. (2009). An assessment of the new LS-DYNA layered solid element: basics, patch simulation and its potential for thick composite structure analysis. 7th European LS-DYNA conference.
8. Chedid, M. (2009). Optimisation of composite materials using multilevel decomposition approach. MSc Thesis by Research. Cranfield University.
9. Chen, T.Y., Lin, C.Y. (2000). Determination of optimum design spaces for topology optimization. *Finite elements in analysis and design* 36, 1-16.
10. Conceição António, C.A., Torres Marques, A., and Soeiro, A.S. (1995). Optimization of laminated composite structures using a bilateral strategy. *Composite structures* 33, 193-200. Elsevier.
11. Crisfield, M.A. (1992). A review of contact and friction in Finite Element Analysis. NAFEMS.
12. Davidson, B., Roy, U., and Ludden, C. (1999). An expert system for the design and analysis of composite structures. *IIE Transactions* 31, 303-312.
13. Ferguson, R. (2004). Large scale composite testing at Airbus Filton Site. 2nd International conference on composites testing and model identification. 21st September 2004.
14. Giunta, A.A., Wojtkiewicz, S.F. and Eldred, M.S. (2003). Overview of modern design of experiments methods for computational simulations. AIAA 2003-0649.
15. Hammer, V.B., Bendsoe, M.P., Lipton, R., and Pedersen, P. (1997). Parametrization in laminate design for optimal compliance. *International Journal Solids Structures* Vol. 34, No. 4, pp. 415-434.

16. Herencia, J.E., Weaver, P.M., and Friswell, M.I. (2007). Optimization of long anisotropic laminated fiber composite panels with T-shaped stiffeners. *AIAA Journal*. Vol. 45, No. 10.
17. Jakiela, M.J., Chapman, C., Duda, J., Adewuya, A., and Saitou, K. (2000). Continuum structural topology design with genetic algorithms. *Computer Methods in Applied Mechanics and Engineering* 186, 339-356.
18. Jansson, N., Wakeman, W.D., Manson, J.-A.E. (2007). Optimization of hybrid thermoplastic composite structures using surrogate models and genetic algorithms. *Composite Structures* 80, 21-31.
19. Johansen, L., Lund, E. (2009). Optimization of laminated composite structures using delamination criteria and hierarchical models. *Struct Multidisc Optim*, 38:357-375.
20. Kant, T., Swaminathan, K. (2000). Estimation of transverse/interlaminar stresses in laminated composites – a selective review and survey of current developments. *Composite structures* 49, 65-75.
21. Kim, J.S., Kim, C.G., and Hong, C.S. (1999). Knowledge-based expert system for optimal stacking sequence design of composite structures. *Journal of composite materials* 33; 1244.
22. Kim, J.S. (2007). Development of a user-friendly expert system for composite laminate design. *Composite Structures* 79, 76-83. Elsevier.
23. Kim, J.Y., Hong, C.S. (1991). Three-dimensional finite element analysis of interlaminar stresses in thick composite laminates. *Computers and structures* Vol. 40, No. 6, pp. 1395-1404.
24. Konter, A. (2000). How to undertake contact and friction analysis. *NAFEMS*
25. Krog, L., Tucker, A., and Rollema, G. (2002). Application of topology, sizing and shape optimization methods to optimal design of aircraft components. *Altair Engineering*.
26. Krog, L., Tucker, A., Kemp, M., and Boyd, R. (2004). Topology optimization of aircraft wing box ribs. 10th AIAA/ISSMO Multidisciplinary Analysis and Optimization Conference. 30th August – 1st September 2004. Albany, New York.
27. Kwon, Y.W., and Akin, J.E. (1987). Analysis of layered composite plates using a high-order deformation theory. *Computers and structures* Vol. 27, No 5, pp. 619-623.
28. Leiva, J.P., Watson, B.C., and Kosaka, I. (1999). Modern structural optimization concepts applied to topology optimization. *AIAA-99-1388*.
29. Luo, Z., Yang, J., and Chen, L. (2006). A new procedure for aerodynamic missile designs using topological optimization approach of continuum structures. *Aerospace Science and Technology* 10, 364-373.
30. Menzel, S., Dr. T. Fuhrmann, Beuermann, S., and Dr. B. Wiedemann. Optimization of a composite B-pillar. Volkswagen and Altair.
31. Montgomery, J. Methods for modelling bolts in the bolted joint. Siemens Westinghouse Power Corporation, Orlando, FL.

32. Mottershead, J.E. (1993). Finite Element Analysis of contact and friction – A survey. NAFEMS
33. Muc, A., and Gurba, W. (2001). Genetic Algorithms and finite element analysis in optimization of composite structures. *Composite Structures* 54, 275-281.
34. Muc, A. (2005). Optimization of multilayered composite structures with randomly distributed mechanical properties. *Mechanics of composite materials*, Vol. 41, No. 6.
35. Oh, J.H., Kim, J.K., Lee, D.G., and Jeong, K.S. (1999). Interlaminar shear behaviour of thick carbon/epoxy composite materials. *Journal of Composite Materials* 33, 2080.
36. Pagano, N.J., and Hatfield, S.J. (1972). Elastic behaviour of multilayered bidirectional composites.
37. Paluch, B., Grédiac, M., Faye, A. (2008). Combining a finite element programme and a genetic algorithm to optimize composite structures with variable thickness. *Composite structures* 83, 284-294.
38. Panteny, S. (2007). Lighter, stronger and cheaper. *Material World* 15(3), 28-31.
39. Park, C.H., Lee, W.I., Han, W.S., and Vautrin, A. (2003). Weight minimization of composite laminated plates with multiple constraints. *Composites Science and Technology* 63, 1015-1026.
40. Park, C.H., Lee, W.I., Han, W.S., and Vautrin, A. (2005). Multiconstraint optimization of composite structures manufactured by Resin Transfer Molding process. *Journal of Composite Materials* 39; 347.
41. Poloni, C., Pediroda, V., Clarich, A., and Steven, G. (2002). The use of Design of Experiments (DOE) and Response Surface Analysis (RSA) in PSO.
42. Rohwer, K., Rolfes, R. (1998). Calculating 3D stresses in layered composite plates and shells. *Mechanics of composite materials*, Vol. 34, No. 4.
43. Rolfes, R., Noor, A.K., and Spar, H. (1998). Evaluation of transverse thermal stresses in composite plates based on first-order shear deformation theory. *Computer Methods in Applied Mechanics and Engineering* 167, 355-368. Elsevier.
44. Rozvay, G.I.N. (2001). Aims, scope, methods, history and unified terminology of computer-aided topology optimization in structural mechanics. *Struct Multidisc Optim* 21, 90-108. Springer-Verlag.
45. Schramm, U., and Zhou, M. (2006). Recent developments in the commercial implementation of topology optimization. *IUTAM Symposium on Topological Design Optimization of Structures, Machines and Materials: Status and Perspectives*, 239-248. Springer, Netherlands.
46. Siemetzki, M., Zimmermann, K., Filsinger, J., Strachauer, F., Miletic, A., Tursun, G., Phipps, D., Watson, G., and Giles, D. (2008). Main landing gear fitting in CFRP. *International SAMPE Symposium and Exhibition*, Vol. 52.
47. Stockwell, A.E. (1995). A verification procedure for MSC/NASTRAN Finite Element Models. NASA Contractor Report 4675.

48. Sun, C.T., and Li, S. (1988). Three-Dimensional effective elastic constants for thick laminates. *Journal of Composite Materials* Vol. 22, No. 7, 629-639.
49. Sun, E.Q. Shear locking and Hourglassing in MSC Nastran, ABAQUS, and ANSYS.
50. Taig, I.C. (1992). Finite Element Analysis of composite materials. NAFEMS.
51. Thuis, H.G.S.J. (1999). Development of a composite torque link for helicopter landing gear applications. NLR-TP-99026. National Aerospace Laboratory NLR.
52. Thuis, H.G.S.J, Wiggeraad, J.F.M. and Vries, H.P.J. (2004). Composite landing gear components made with Resin Transfer Moulding (RTM). National Aerospace Laboratory NLR. NLR-TP-2004-122.
53. Thuis, H.G.S.J. (2004). Composite landing gear components for aerospace applications. National Aerospace Laboratory NLR. ICAS 2004. 24th International Congress of the Aeronautical Sciences.
54. Thuis, H.G.S.J. (2004). The development of composite landing gear components for aerospace applications. National Aerospace Laboratory NLR. NLR-TP-2004-141.
55. Todoroki, A., and Ishikawa, T. (2004). Design of experiments for stacking sequence optimizations with genetic algorithm using response surface approximation. *Composite structures* 64, 349-357. Elsevier.
56. Toporov, V.V., Schramm, U., Sahai, A., Jones, R.D., Zeguer, T. (2005). Design optimization and stochastic analysis based on the moving least squares method. 6th World Congresses of Structural and Multidisciplinary Optimization., 30th May – 3rd June 2005. Rio de Janeiro, Brazil.
57. Tsai, S.W., Hahn H.T. (1980). Introduction to composite materials. Technomic, Stamford, CT.
58. Watson, G. (2005). ALCAS technical report – WP1.2 MLG attachment loading. Reference ALCAS/01/00074/WP125. AIRBUS. 23rd Nov 2005.
59. Weaver, P.M: (2002). Designing composite structures: lay-up selection. *Proc Instn Mech Engrs Vol 216 Part G: J Aerospace Engineering*.
60. Wu, C.P., Kuo, H.C. (1993). An interlaminar stress mixed finite element method for the analysis of thick laminated composite plates. *Composite structures* 24, 29-42.
61. Zhou, M., Pagaldipti, N., Thomas, H.L. and Shyy, Y.K. (2004). An integrated approach to topology, sizing and shape optimization. *Structural Multidisciplinary Optimization* 26, 308-317.
62. Zhou, M., Shyy, Y.K., and Thomas, H.L. (2001). Checkerboard and minimum member size control in topology optimization. *Struct Multidisc Optim* 21, 152-158. Springer-Verlag.
63. Zimmermann, K. Robust design/stress 2nd generation composite aero structures. Development of the Side Stay Fitting. EADS IW TCC-3.

Appendix A Laminate strength analysis

1. Determine the [ABD] matrix

$$Q_{11} = \frac{E_1}{1 - \nu_{12}\nu_{21}} \quad (\text{A-1})$$

$$Q_{22} = \frac{E_2}{1 - \nu_{12}\nu_{21}} \quad (\text{A-2})$$

$$Q_{12} = Q_{21} = \frac{\nu_{12}E_2}{1 - \nu_{12}\nu_{21}} \quad (\text{A-3})$$

$$Q_{66} = G_{12} \quad (\text{A-4})$$

$$\begin{bmatrix} U_1 \\ U_2 \\ U_3 \\ U_4 \\ U_5 \end{bmatrix} = \frac{1}{8} \begin{bmatrix} 3 & 2 & 3 & 4 \\ 4 & 0 & -4 & 0 \\ 1 & -2 & 1 & -4 \\ 1 & -6 & 1 & -4 \\ 1 & -2 & 1 & 4 \end{bmatrix} \begin{bmatrix} Q_{11} \\ Q_{12} \\ Q_{22} \\ Q_{66} \end{bmatrix} \quad (\text{A-5})$$

$$\begin{Bmatrix} \bar{Q}_{11} \\ \bar{Q}_{22} \\ \bar{Q}_{12} \\ \bar{Q}_{66} \\ \bar{Q}_{16} \\ \bar{Q}_{26} \end{Bmatrix} = \begin{bmatrix} U_1 & \cos 2\theta & \cos 4\theta \\ U_1 & -\cos 2\theta & \cos 4\theta \\ U_4 & & -\cos 4\theta \\ U_5 & & -\cos 4\theta \\ & \frac{1}{2} \sin 2\theta & \sin 4\theta \\ & \frac{1}{2} \sin 2\theta & -\sin 4\theta \end{bmatrix} \begin{Bmatrix} 1 \\ R_1 \\ R_2 \end{Bmatrix} \quad (\text{A-6})$$

$$R_1 = \pm U_2$$

$$R_2 = \pm U_3$$

$$[A] = \sum_1^n (z_k - z_{k-1}) [\bar{Q}]_k \quad (\text{A-7})$$

$$[B] = -\frac{1}{2} \sum_1^n (z_k^2 - z_{k-1}^2) [\bar{Q}]_k \quad (\text{A-8})$$

$$[D] = \frac{1}{3} \sum_1^n (z_k^3 - z_{k-1}^3) [\bar{Q}]_k \quad (\text{A-9})$$

$$[A] = \begin{bmatrix} A_{11} & A_{12} & A_{16} \\ A_{12} & A_{22} & A_{26} \\ A_{16} & A_{26} & A_{66} \end{bmatrix} \quad (\text{A-10})$$

$$[B] = \begin{bmatrix} B_{11} & B_{12} & B_{16} \\ B_{12} & B_{22} & B_{26} \\ B_{16} & B_{26} & B_{66} \end{bmatrix} \quad (\text{A-11})$$

$$[D] = \begin{bmatrix} D_{11} & D_{12} & D_{16} \\ D_{12} & D_{22} & D_{26} \\ D_{16} & D_{26} & D_{66} \end{bmatrix} \quad (\text{A-12})$$

2. Calculate the [ABD] matrix inverse, [abd]
3. Calculate the mid-plane strains in the laminate, from:

$$\{\varepsilon_{x-y}^0, k_{x-y}\} = [abd]\{N, M\} \quad (\text{A-13})$$

4. Work out the total strain for each ply

$$\{\varepsilon_{x-y}\} = \{\varepsilon_{x-y}^0\} + z \cdot \{k_{x-y}\} \quad (\text{A-14})$$

5. And then transform it to the principal material axes by

$$\{\varepsilon_{1-2}\} = [T_\varepsilon]\{\varepsilon_{x-y}\} \quad (\text{A-15})$$

$$\begin{Bmatrix} \varepsilon_1 \\ \varepsilon_2 \\ \gamma_{12} \end{Bmatrix} = \begin{bmatrix} m^2 & n^2 & -mn \\ n^2 & m^2 & mn \\ 2mn & -2mn & m^2 - n^2 \end{bmatrix} \begin{Bmatrix} \varepsilon_x \\ \varepsilon_y \\ \gamma_{xy} \end{Bmatrix} \quad (\text{A-16})$$

6. Calculate the stresses in the layer coordinate system for each ply

$$\begin{Bmatrix} \sigma_1 \\ \sigma_2 \\ \tau_{12} \end{Bmatrix} = \begin{bmatrix} Q_{11} & Q_{12} & \\ Q_{21} & Q_{22} & \\ & & Q_{66} \end{bmatrix} \begin{Bmatrix} \varepsilon_1 \\ \varepsilon_2 \\ \gamma_{12} \end{Bmatrix} \quad (\text{A-17})$$

7. Apply the desired failure criteria for a ply strength evaluation (Tsai-Wu).

$$FI = \sigma_1 \left[\frac{1}{X_T} - \frac{1}{X_C} \right] + \sigma_2 \left[\frac{1}{Y_T} - \frac{1}{Y_C} \right] + \frac{\sigma_1^2}{X_T X_C} + \frac{\sigma_2^2}{Y_T Y_C} + \frac{\tau_{12}^2}{S^2} + 2F_{12}\sigma_1\sigma_2 \quad (\text{A-18})$$

$$F_{12} = 0$$

$$2F_{12}\sigma_1\sigma_2 = 0$$

Appendix B ANSYS parametric input file

01-SHELL99_Nx_Shuff_complete.txt

The following input file represent a $1 \times 1 \text{m}^2$ thin plate subjected to in-plane load Nx.

```
FINISH
/CLEAR, NOSTART

/TITLE, Guo's Example - 22.1 (SHELL99)

! All dimensions in m, kg, sec --> N, Pa

!=====
! PARAMETERS DEFINITION

! Laminate
Nplies=14! Total number of plies
tply=5e-3! Ply thickness

! Plies' orientations (half symmetry)
Theta1=45
Theta2=0
Theta3=0
Theta4=0
Theta5=0
Theta6=45
Theta7=90

! Dimensions
L=1                ! 1 m
t=Nplies*tply

! Strength (Pa)
Xt=1500e6          ! 1500 MPa
Xc=1500e6          ! 1500 MPa
Yt=40e6            ! 40 MPa
Yc=246e6           ! 246 MPa
S12=68e6           ! 68 MPa

! Load
Nx=1000            ! N/m
Ny=1000            ! N/m

!=====
! ET & MATERIAL PROPERTIES DEFINITION
```

```

/PREP7

ET,1,SHELL99,,,,,,,,,1      ! 8 NODE LAYERED SHELL

KEYOPT,1,2,0                ! Constant thickness layer input
                             ! (250 layers maximum)
KEYOPT,1,3,0                ! Basic element printout
KEYOPT,1,5,2                ! Both strain and stress will be used
KEYOPT,1,6,4                ! print the layer solution at the corner nodes
                             ! for all layers
KEYOPT,1,8,1                ! Store data for all layers
KEYOPT,1,9,0                ! Evaluate at midthickness of each layer
!KEYOPT,1,10,               ! Nodes located at midsurface
KEYOPT,1,11,0

! Laminate definition→ by means of real constant set
R,1,Nplies,1                ! Nplies=total number of plies; Symmetric Stacking
RMORE
RMORE,1,Theta1,tply,1,Theta2,tply      ! RMORE,MAT1,THETA1,TK1,MAT2,THETA2,TK2
RMORE,1,Theta3,tply,1,Theta4,tply
RMORE,1,Theta5,tply,1,Theta6,tply
RMORE,1,Theta7,tply

MP,EX,1,181E9               ! ORTHOTROPIC MATERIAL PROPERTIES
MP,EY,1,10.3E9
MP,EZ,1,10.3E9             ! EZ=EY ASSUMED
MP,GXY,1,7.17E9
MP,GYZ,1,7.17E9
MP,GXZ,1,7.17E9
MP,PRXY,1,0.28             ! MAJOR POISSONS RATIO
MP,PRYZ,1,0.28             ! MAJOR POISSONS RATIO
MP,PRXZ,1,0.28             ! MAJOR POISSONS RATIO

!=====
! GEOMETRY GENERATION

K,1                          ! Corner Keypoints ofplate
K,2,L
K,3,L,L
K,4,,L
A,1,2,3,4! Area (plate) joining Keypoints

!=====
! MESH GENERATION

/ESHAPE,1                   ! view layers comprising laminate
/VSCALE,,2                  ! double size of symbols, like element CS
/PSYMB,ESYS,1              ! turn on element coordinate system symbols
/DEVICE,VECTOR,0           ! elements shown in render style

ESIZE,,12                   ! 12X12 MESH USING half SYMMETRY
AMESH,1! Mesh the area

```

```

!LAYPLOT,1          ! Displays the layer stacking sequence for element 1
!/GROPTS,VIEW,1

!=====
! BOUNDARY CONDITIONS

! Supports
NSEL,S,LOC,X,0! Select nodes at X=0
DSYM,SYMM,X! Restrain translation in 1, and rotations in 5, 6

NSEL,S,LOC,X,0
NSEL,R,LOC,Y,L/2
D,ALL,ALL! Fix node in (0,L/2,0) in all directions

ALLSEL,ALL

! in-plane load application NX
LSEL,S,LOC,X,L
SFL,ALL,PRES,-Nx! surface loads on X=L. Negative sign → tension

/PSF,PRES,NORM,2,0,1! Display the applied pressure as arrows

SBCTRAN! Transfers solid model loads and BCs to the FE model
ALLSEL,ALL
EPLOT

!=====
! FC

TB,FAIL,1,1          ! TB, FAIL, material number, 1 temperature
TBTEMP,,CRIT
TBDATA,3,1          ! Include the Tsai-Wu strength index
TBDATA,2,1
TBTEMP,0
TBDATA,10,Xt,-Xc,Yt,-Yc, 10e13,          ! stresses XT, XC, YT, YC, ZT, ZC
TBDATA,16,S12,10e13,10e13          ! shear stresses XY, YZ (large number),
                                     ! XZ (large number)
TBDATA,19,0,0,0          ! coupling coefficients
!TBLIST,ALL,1          ! Lists the data tables

OUTPR,NSOL,1
OUTPR,RSOL,1

FINISH

!=====
! SOLUTION
!=====

/SOLU
SOLVE

```

```

FINISH

!=====
!=====
! POSTPROCESSING
!=====
!=====

/POST1

/DSCALE,,0          ! Scale displacements automatically
/GRAPHICS,FULL

RSYS,0              ! Global Cartesian coordinate system (default)

!=====
! Max total displacement (abs)

NSORT,U,SUM         ! Sort nodal displ (vector sum) in descending order
*GET,USUM,SORT,,MAX ! retrieve the maximum total displacement
*SET,USUM,USUM
*STAT,USUM

!=====
! Max Z displacement (abs)

NSORT,U,Z,,1       ! Sort Z nodal displ (absolute value) in descending order
*GET,UZ_MAX,SORT,,MAX ! retrieve the maximum absolute Z displacement
*SET,MaxUZ,UZ_MAX
*STAT,MaxUZ

!=====
!=====

ETABLE,ERASE
ETABLE,TX,SMISC,1   ! Element total in-plane forces per unit length
                   ! (in element coordinates)

ETABLE,TY,SMISC,2
ETABLE,TXY,SMISC,3

ETABLE,MX,SMISC,4   ! Element total moments per unit length (in element
                   ! coordinates)

ETABLE,MY,SMISC,5
ETABLE,MXY,SMISC,6

ETABLE,NX,SMISC,7   ! Out-of-plane element X and Y shear forces
ETABLE,NY,SMISC,8

!=====

! Extract maximum values of the element total in-plane forces per unit length
! (in element coordinates) (TX, TY, TXY)

```

```

!TX - 1000 N/m and the rest =0
ESORT,ETAB,TX          ! Sorts the element table (descending)
*GET,TX_MAX,SORT,,MAX  ! Maximum TX value
*GET,E_TX_MAX,SORT,,IMAX ! Element number where TX maximum value occurs
*SET,TX_MAX,TX_MAX
*STAT,TX_MAX
*SET,E_TX_MAX,E_TX_MAX
*STAT,E_TX_MAX

!TY
ESORT,ETAB,TY          ! Sorts the element table (descending)
*GET,TY_MAX,SORT,,MAX  ! Maximum TY value
*GET,E_TY_MAX,SORT,,IMAX ! Element number where TY maximum value occurs
*SET,TY_MAX,TY_MAX
*STAT,TY_MAX
*SET,E_TY_MAX,E_TY_MAX
*STAT,E_TY_MAX

!TXY
ESORT,ETAB,TXY          ! Sorts the element table (descending)
*GET,TXY_MAX,SORT,,MAX  ! Maximum TXY value
*GET,E_TXY_MAX,SORT,,IMAX ! Element number where TXY maximumvalue occurs
*SET,TXY_MAX,TXY_MAX
*STAT,TXY_MAX
*SET,E_TXY_MAX,E_TXY_MAX
*STAT,E_TXY_MAX

!=====

! Extract maximum values for the element total moments per unit length
! (in element coordinates) (MX, MY, MXY)
!MX
ESORT,ETAB,MX          ! Sorts the element table (descending)
*GET,MX_MAX,SORT,,MAX  ! Maximum MX value
*GET,E_MX_MAX,SORT,,IMAX ! Element number where MX maximum value occurs
*SET,MX_MAX,MX_MAX
*STAT,MX_MAX
*SET,E_MX_MAX,E_MX_MAX
*STAT,E_MX_MAX

!MY
ESORT,ETAB,MY          ! Sorts the element table (descending)
*GET,MY_MAX,SORT,,MAX  ! Maximum MY value
*GET,E_MY_MAX,SORT,,IMAX ! Element number where MY maximum value occurs
*SET,MY_MAX,MY_MAX
*STAT,MY_MAX
*SET,E_MY_MAX,E_MY_MAX
*STAT,E_MY_MAX

!MXY
ESORT,ETAB,MXY          ! Sorts the element table (descending)
*GET,MXY_MAX,SORT,,MAX  ! Maximum MXY value

```

```

*GET,E_MXY_MAX, SORT, , IMAX ! Element number where MXY maximum value occurs
*SET,MXY_MAX,MXY_MAX
*STAT,MXY_MAX
*SET,E_MXY_MAX,E_MXY_MAX
*STAT,E_MXY_MAX

!=====

! Extract maximum values of the out-of-plane element X and Y shear forces
!NX
ESORT,ETAB,NX ! Sorts the element table (descending)
*GET,NX_MAX, SORT, , MAX ! Maximum NX value
*GET,E_NX_MAX, SORT, , IMAX ! Element number where NX maximum value occurs
*SET,NX_MAX,NX_MAX
*STAT,NX_MAX
*SET,E_NX_MAX,E_NX_MAX
*STAT,E_NX_MAX

!NY
ESORT,ETAB,NY ! Sorts the element table (descending)
*GET,NY_MAX, SORT, , MAX ! Maximum NY value
*GET,E_NY_MAX, SORT, , IMAX ! Element number where NY maximum value occurs
*SET,NY_MAX,NY_MAX
*STAT,NY_MAX
*SET,E_NY_MAX,E_NY_MAX
*STAT,E_NY_MAX

!=====
! Strains in global coord system EPELX,EPELY,EPELXY (@ centre node) -
! Nodal Results
!=====

RSYS,0 ! Global Cartesian coordinate system (default)

SHELL, TOP ! Top of shell element
NSEL,S,LOC,X,L/2
NSEL,R,LOC,Y,L/2
*GET, Centre_Node, NODE, , NUM, MAX ! Centre_Node (L/2,L/2,0)

*DO, II, 1, NPlies, 1 ! for all layers
/GO
LAYER, II ! element layer for which data are to be processed
! PRNSOL, EPELX_%II%, COMP
*GET, EPELX_%II%, NODE, Centre_Node, EPEL, X ! EPELX
*SET, EPELX_%II%, EPELX_%II%
*STAT, EPELX_%II%

*GET, EPELY_%II%, NODE, Centre_Node, EPEL, Y ! EPELY
*SET, EPELY_%II%, EPELY_%II%
*STAT, EPELY_%II%

*GET, EPELXY_%II%, NODE, Centre_Node, EPEL, XY ! EPELXY

```

```

*SET,EPELXY_%II%,EPELXY_%II%
*STAT,EPELXY_%II%
*ENDDO

!=====
! Strains in layer coord system EPEL1,EPEL2,EPEL12 (@ centre node) -
! Nodal Results
!=====

RSYS,LSYS                ! Layer coordinate system

*DO,II,1,Nplies,1       ! for all layers
/GO
LAYER,II                ! element layer for which data are to be processed
*GET,EPEL1_%II%,NODE,Centre_Node,EPEL,X           ! EPEL1
*SET,EPEL1_%II%,EPEL1_%II%
*STAT,EPEL1_%II%

*GET,EPEL2_%II%,NODE,Centre_Node,EPEL,Y           ! EPEL2
*SET,EPEL2_%II%,EPEL2_%II%
*STAT,EPEL2_%II%

*GET,EPEL12_%II%,NODE,Centre_Node,EPEL,XY        ! EPEL12
*SET,EPEL12_%II%,EPEL12_%II%
*STAT,EPEL12_%II%
*ENDDO

!=====
! Stress in layer coord system S1,S2,S12 (@ centre node) - Nodal Results
!=====

RSYS,LSYS                ! Layer coordinate system

*DO,II,1,Nplies,1       ! for all layers
/GO
LAYER,II                ! element layer for which data are to be processed
*GET,S1_%II%,NODE,Centre_Node,S,X                 ! S1
*SET,S1_%II%,S1_%II%
*STAT,S1_%II%

*GET,S2_%II%,NODE,Centre_Node,S,Y                 ! S2
*SET,S2_%II%,S2_%II%
*STAT,S2_%II%

*GET,S12_%II%,NODE,Centre_Node,S,XY               ! S12
*SET,S12_%II%,S12_%II%
*STAT,S12_%II%
*ENDDO

ALLSEL,ALL

!=====

```

```

!=====
! FC
!=====
!=====

RSYS,LSYS                ! Layer coordinate system

! NOTE: If you don't want the failure stress or strain to be checked in
! a particular direction, specify a large number in that direction
FC,1,S,XTEN,  Xt
FC,1,S,XCMP, -Xc
FC,1,S,YTEN,  Yt
FC,1,S,YCMP, -Yc
FC,1,S,ZTEN, 10e13      ! Z value set to a large number
FC,1,S,XY   ,  S12
FC,1,S,YZ   , 10e13      ! YZ value set to a large number
FC,1,S,XZ   , 10e13      ! XZ value set to a large number
FC,1,S,XYCP,  0
FC,1,S,YZCP,  0
FC,1,S,XZCP,  0
!FCLIST

!=====

SHELL, TOP
NL=Nplies
*DO, II, 1, NL          ! for all layers
  /GO
  LAYER, II
  *GET, SMAXF_%II%, NODE, Centre_Node, S, MAXF      ! MAXF: Maximum stress FC
  *SET, SMAXF_%II%, SMAXF_%II%
  *STAT, SMAXF_%II%

  *GET, STWSI_%II%, NODE, Centre_Node, S, TWSI      ! TWSI: Tsai-Wu strength FC
  *SET, STWSI_%II%, STWSI_%II%
  *STAT, STWSI_%II%

  *GET, STWSR_%II%, NODE, Centre_Node, S, TWSR      ! TWSR: Inverse of Tsai-Wu
  ! strength ratio index FC
  *SET, STWSR_%II%, STWSR_%II%
  *STAT, STWSR_%II%

*ENDDO

!=====
!=====
! FAIL: Failure criteria.

RSYS,LSYS      ! Layer coordinate system
LAYER,FCMAX    ! Processes the layer with the largest failure criteria
               ! (SHELL99, SOLID46, SOLID191)

```

```

!PRESOL,FCMX      ! Maximum FC over the entire element. Components:
! Layer number where the maximum occurs (LAY), name of the maximum FC,
! and value of the maximum FC (VAL)

!PLESOL,FAIL,MAX  ! Maximum of all FC defined at the current location
!PLESOL,FAIL,SMAX ! Maximum stress FC
!PLESOL,FAIL,TWSI ! Tsai-Wu Strength Index FC
!PLESOL,FAIL,TWSR ! Inverse of Tsai-Wu strength ratio index FC
!PLESOL,FCMX,LAY  ! Layer number where the maximum of all FC over the
! entire element occurs
!PLESOL,FCMX,FC   ! Number of the maximum FC over the entire element:
! 2-EMAX, 3-SMAX, 4-TWSI, 5-TWSR
!PLESOL,FCMX,VAL  ! Value of the maximum FC over the entire element

!*GET,FCMAX_elem_1,ELEM,1,NMISC,1

ETABLE,ERASE
ETABLE,FCMAX,NMISC,1      ! FC values and maximum at each integration point
ETABLE,VALUE,NMISC,2     ! Maximum value for this criterion
ETABLE,LN,NMISC,3        ! Layer number where maximum occurs
ETABLE,ILMAX,NMISC,4     ! Maximum ILSS (occurs between LN1 and LN2)
ETABLE,LN1,NMISC,5       ! Layer numbers which define location ILMAX
ETABLE,LN2,NMISC,6       ! Layer numbers which define location ILMAX

!PRETAB,GRP1
!PRETAB,FCMAX            ! etc, with the rest of the output variables

!=====

! FCMAX (MAX)
ESORT,ETAB,FCMAX         ! Sorts the element table
*GET,FCMAX,SORT,,MAX
*GET,E_FCMAX,SORT,,IMAX  ! Element number where maximum value occurs
*SET,FCMAX,FCMAX
*SET,E_FCMAX,E_FCMAX
*STAT,FCMAX

! FCMAX (@ CENTRE)
*GET,FCMAX_ctr,ELEM,79,ETAB,FCMAX ! CHANGE element number if wanted!!!
*SET,FCMAX_ctr,FCMAX_ctr
*STAT,FCMAX_ctr

!=====

! VALUE (MAX)
ESORT,ETAB,VALUE        ! Sorts the element table
*GET,VALUE,SORT,,MAX
*GET,E_VALUE,SORT,,IMAX ! Element number where maximum value occurs
*SET,VALUE,VALUE
*SET,E_VALUE,E_VALUE
*STAT,VALUE

```

```

! VALUE (@ CENTRE)
*GET,VALUE_ctr,ELEM,79,ETAB,VALUE ! CHANGE element number if wanted!!!
*SET,VALUE_ctr,VALUE_ctr
*STAT,VALUE_ctr

!=====

! LN (MAX)
ESORT,ETAB,LN ! Sorts the element table
*GET,LN,SORT,,MAX
*GET,E_LN,SORT,,IMAX ! Element number where maximum value occurs
*SET,LN,LN
*SET,E_LN,E_LN
*STAT,LN

! LN (@ CENTRE)
*GET,LN_ctr,ELEM,79,ETAB,LN ! CHANGE element number if wanted!!!
*SET,LN_ctr,LN_ctr
*STAT,LN_ctr

!=====

!ILANG: Angle of interlaminar shear stress vector (measured from the element
! x-axis towards the element y-axis in degrees)
!ILSUM: Interlaminar shear stress vector sum

NL=Nplies
*DO,II,1,NL,1 ! for all layers
/GO
ETABLE,ERASE
ETABLE,FCMAX_%II%,NMISC,(2*(NL+II))+7
ETABLE,VALUE_%II%,NMISC,(2*(NL+II))+8

! Maximum value and element where it occurs

ESORT,ETAB,FCMAX_%II% ! Sorts the element table
*GET,FCMAX_%II%_MAX,SORT,,MAX
*GET,E_FCMAX_%II%_MAX,SORT,,IMAX ! Element number where maximum value
! occurs
*SET,FCMAX_%II%_MAX,FCMAX_%II%_MAX
*SET,E_FCMAX_%II%_MAX,E_FCMAX_%II%_MAX
*STAT,FCMAX_%II%_MAX

ESORT,ETAB,VALUE_%II% ! Sorts the element table
*GET,VALUE_%II%_MAX,SORT,,MAX
*GET,E_VALUE_%II%_MAX,SORT,,IMAX ! Element number where maximum value
! occurs
*SET,VALUE_%II%_MAX,VALUE_%II%_MAX
*SET,E_VALUE_%II%_MAX,E_VALUE_%II%_MAX
*STAT,VALUE_%II%_MAX

*ENDDO

```


Appendix C Mesh Refinement

This section is complementary to the *Element Formulation vs CLT* analysis presented in Section 5. As some of the results diverged significantly from the analytic values, a series of mesh sensitivity analyses have been carried out in order to determine the influence that the mesh size has ultimately on the in-plane failure index of a thin laminate.

These experiments use the same settings and assumptions that the ones already presented in Section 5, in which a 1x1 m² thin laminate plate, with 14 plies, is subjected to five different load cases (in-plane and out-of-plane loads). A series of FE models were created with different layered element formulation and the results were compared against the values obtained using Classic Lamination Theory for thin laminates.

For the present case, only two layered solid element formulations are going to be evaluated, as all layered shell element formulations seemed to have good agreement with theory:

- SOLID46: 8-node layered solid element
- SOLID191: 20-node layered solid element

And only two loading cases are used:

- Nx: in-plane axial load per unit length (in tension)
- Mx: out-of-plane bending moment per unit length

The following subsections present the mesh size used and the results obtained.

C.1 Mesh size

Initially, the same mesh of 12 by 12 elements was used for all element formulations. For the solid models various modelling strategies were used, ranging from using one layered element through the thickness to making use of only one element per ply. The fact of discretizing the mesh in the through thickness direction modifies the aspect ratio of the elements, which has a direct effect on the quality of the results. Find below the aspect ratio expression; remember that the best results are obtained with aspect ratio values close to one.

$$\text{Aspect Ratio} = \frac{\text{maximum edge length}}{\text{minimum edge length}} \quad (\text{C-1})$$

For the present case, a laminate plate with 14 plies with a ply thickness of 5 mm, the total plate thickness is:

$$t = N_{plies} \times t_{ply} = 14 \times 5 \times 10^{-3} = 0.07 \text{ m}$$

Following, element size dimensions are calculated in order to have an aspect ratio of one in every modelling strategy. The element size in this case is:

$$\text{Element size} = \frac{\text{edge length}}{\text{Number of elements}} \quad \text{(C-2)}$$

12x12 elements Plate

$$\text{Element size} = \frac{1}{12} = 0.0833$$

$$\text{Aspect Ratio} = \frac{0.0833}{0.07} = 1.19$$

14x14 elements Plate

Having a mesh of 14 x 14 with 1 element through the thickness improves the aspect ratio value:

$$\text{Element size} = \frac{1}{14} = 0.0714$$

$$\text{Aspect Ratio} = \frac{0.0714}{0.07} = 1.02$$

2 Elements through the thickness → 28x28 elements Plate

In case of having two layered solid elements through the thickness, each one accounting for seven layers, the element thickness in this case is:

$$t = N_{plies} \times t_{ply} = 7 \times 5 \times 10^{-3} = 0.035 \text{ m}$$

A mesh of 28 x 28 x 2 is the one to be used in this case:

$$\text{Element size} = \frac{1}{28} = 0.0357$$

$$\text{Aspect Ratio} = \frac{0.0357}{0.035} = 1.02$$

3 Elements through the thickness → 50x50 elements Plate

In case of having three layered solid elements through the thickness, the following layers distribution has been used:

Bottom layer of elements → 7 plies each element

Mid layer of elements → 4 plies each element

Top layer of elements → 3 plies each element

Calculation of the aspect ratio for the mid layer of elements:

Element thickness (4 plies): $t = N_{plies} \times t_{ply} = 4 \times 5e - 3 = 0.02 \text{ m}$

$$\text{Element size} = \frac{1}{50} = 0.02$$

$$\text{Aspect Ratio} = \frac{0.02}{0.02} = 1.00$$

C.2 Results

Maximum Stress Failure per Ply (Nx)

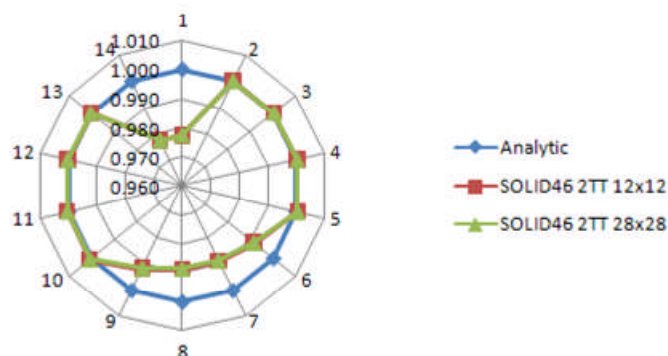


Figure C-1 Maximum Stress Failure Index per ply comparison. Thin plate under in-plane load $N_x=1000 \text{ N/m}$.

Maximum Stress Failure per Ply (Nx)

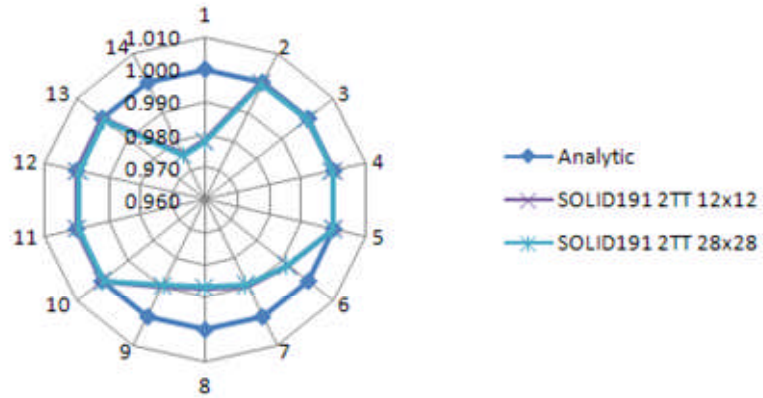


Figure C-2 Maximum Stress Failure Index per ply comparison. Thin plate under in-plane load $N_x=1000$ N/m.

Tsai-Wu Failure Index per Ply (Nx)

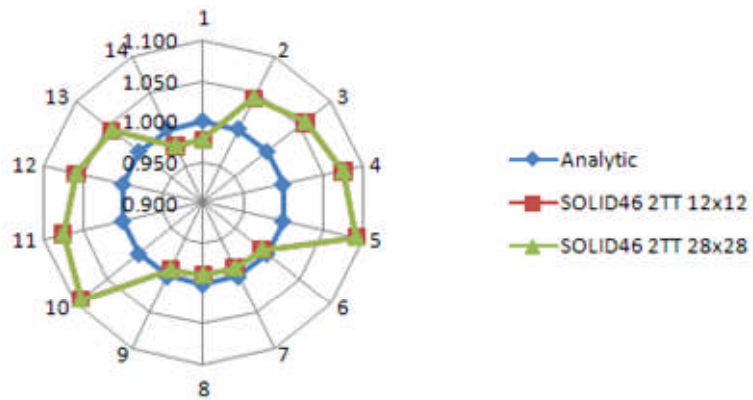


Figure C-3 Tsai-Wu Failure Index per ply comparison. Thin plate under in-plane load $N_x=1000$ N/m.

Tsai-Wu Failure Index per Ply (Nx)

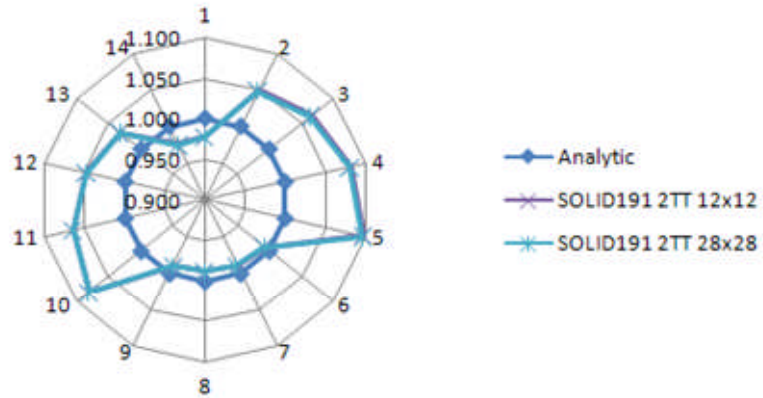


Figure C-4 Tsai-Wu Failure Index per ply comparison. Thin plate under in-plane load $N_x=1000$ N/m.

Maximum Stress Failure per Ply (Nx)

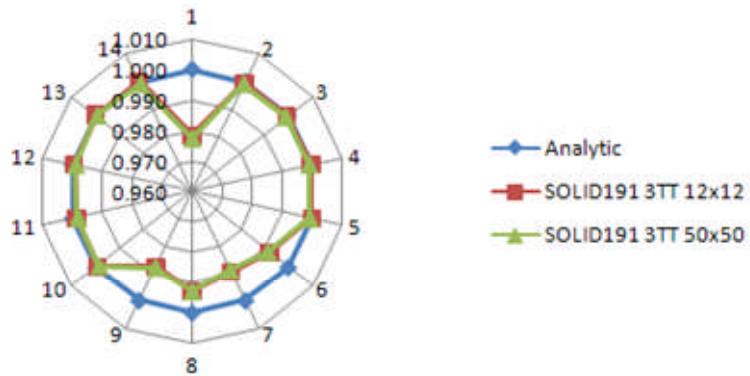


Figure C-5 Maximum Stress Failure Index per ply comparison. Thin plate under in-plane load $N_x=1000$ N/m.

Tsai-Wu Failure Index per Ply (N_x)

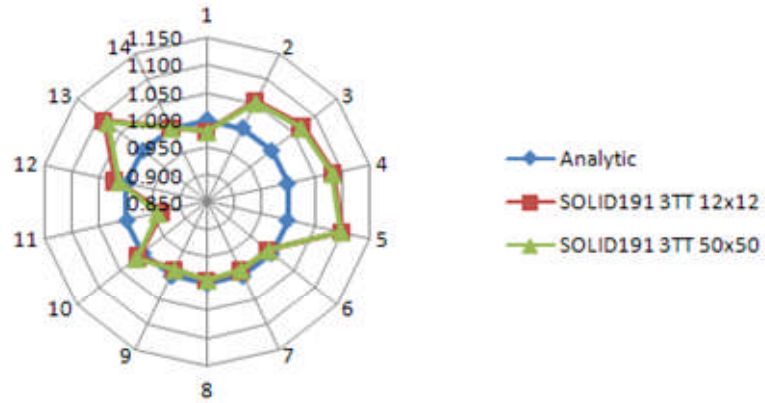


Figure C-6 Tsai-Wu Failure Index per ply comparison. Thin plate under in-plane load $N_x=1000$ N/m.

Maximum Stress Failure per Ply (M_x)

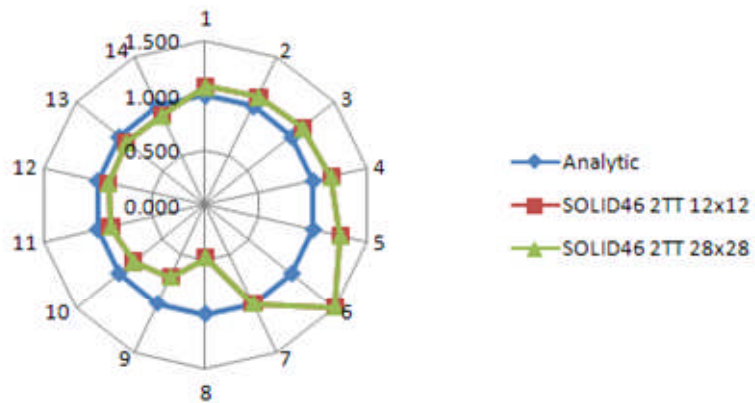


Figure C-7 Maximum Stress Failure Index per ply comparison. Thin plate under out-of-plane load $M_x=1000$ Nm/m.

Maximum Stress Failure per Ply (Mx)

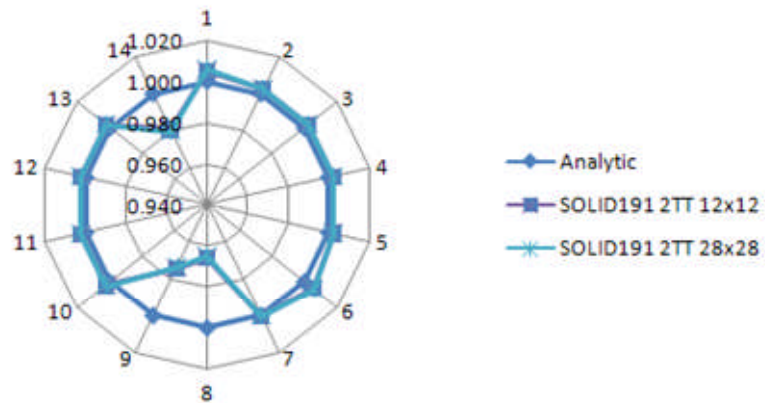


Figure C-8 Maximum Stress Failure Index per ply comparison. Thin plate under out-of-plane load $M_x=1000$ Nm/m.

Tsai-Wu Failure Index per Ply (Mx)

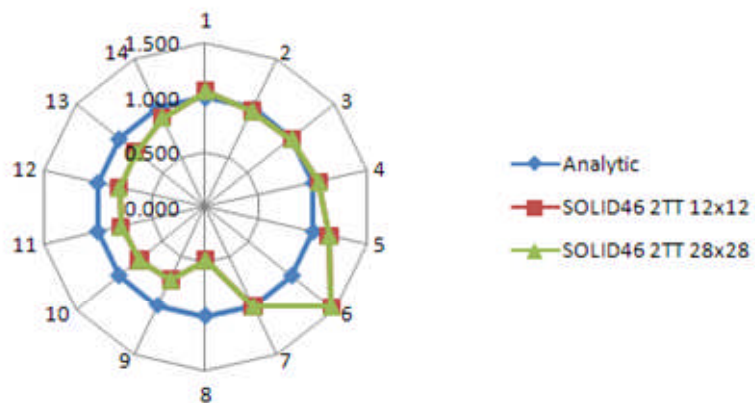


Figure C-9 Tsai-Wu Failure Index per ply comparison. Thin plate under out-of-plane load $M_x=1000$ Nm/m.

Tsai-Wu Failure Index per Ply (Mx)

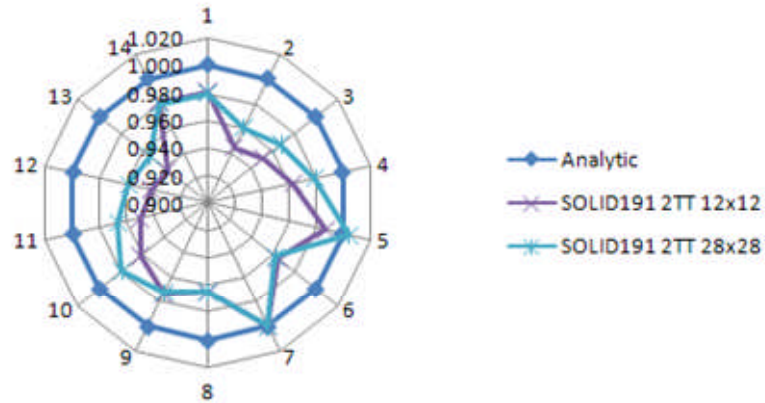


Figure C-10 Tsai-Wu Failure Index per ply comparison. Thin plate under out-of-plane load $M_x=1000$ Nm/m.

Maximum Stress Failure per Ply (Mx)

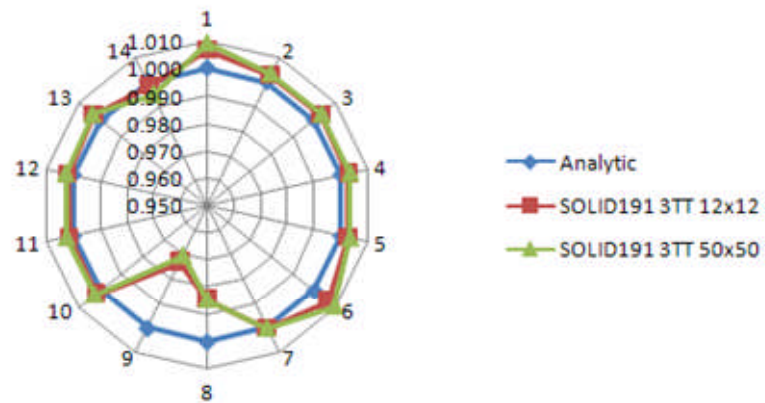


Figure C-11 Maximum Stress Failure Index per ply comparison. Thin plate under out-of-plane load $M_x=1000$ Nm/m.

Tsai-Wu Failure Index per Ply (Mx)

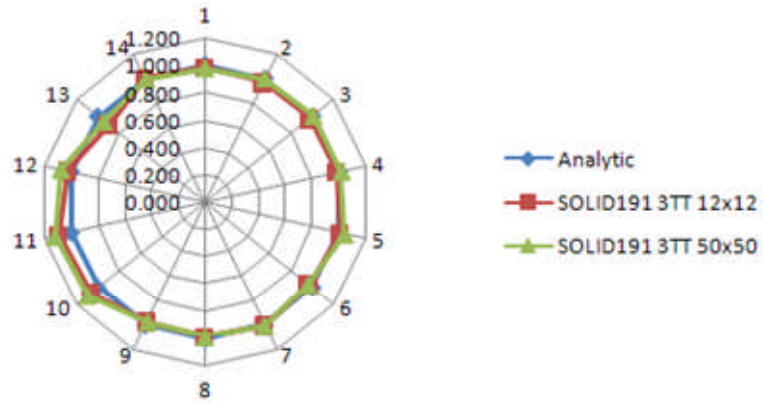


Figure C-12 Tsai-Wu Failure Index per ply comparison. Thin plate under out-of-plane load $M_x=1000$ Nm/m.

Appendix D ANSYS parametric input file

Curved_Plate_SOLID191_Shuff_Opt_4_elems_TT.txt

Explain about this model

```
fini
/clear                ! Clears the database

/TITLE, Curved laminate under bending moment, SOLID191
! All dimensions in m, kg, sec --> N, Pa (SI units)

!=====
! PARAMETERS DEFINITION

! Laminate
Nplies=12! Total number of plies
tply=5e-3          ! ply thickness

! Plies orientations 1 (bottom) to 12 (top). Half symmetry
Theta1=0
Theta2=0
Theta3=0
Theta4=0
Theta5=0
Theta6=0
Theta7=Theta6
Theta8=Theta5
Theta9=Theta4
Theta10=Theta3
Theta11=Theta2
Theta12=Theta1

! Dimensions
a=0.6              ! Inner radius a=Ri
b=a+(Nplies*tply) ! Outer radius b=Ro
t=1                ! width
h=b-a              ! Laminate thickness

! load - pure bending moment
M=100              ! 100 Nm/m

! Material Properties
E11=181E9          ! 2D ORTHOTROPIC MATERIAL PROPERTIES
E22=10.3E9
E33=E22
```

```

G12=7.17E9
G23=7.17E9
G13=G12
v12=0.28          ! MAJOR POISSONS RATIO
v23=0.28          ! MAJOR POISSONS RATIO
v13=v12

! Strength (Pa)
Xt=1500e6          ! 1500 MPa
Xc=1500e6          ! 1500 MPa
Yt=40e6           ! 40 MPa
Yc=246e6          ! 246 MPa
S12=68e6          ! 68 MPa

!=====
! GEOMETRY GENERATION

/PREP7

! Create 4 cylindrical volumes
! CYL4, XCENTER, YCENTER, RAD1, THETA1, RAD2, THETA2, DEPTH
CYL4, a+h, a+h, a+(3*h/4), -180, a+h, -90, t          ! bottom
CYL4, a+h, a+h, a+h/2, -180, a+(3*h/4), -90, t
CYL4, a+h, a+h, a+h/4, -180, a+h/2, -90, t
CYL4, a+h, a+h, a, -180, a+h/4, -90, t              ! top

NUMMRG, KP

!=====
! ET & MATERIAL PROPERTIES DEFINITION

! Material definition
MP, ex, 1, E11
MP, ey, 1, E22
MP, ez, 1, E33
MP, prxy, 1, v12
MP, prxz, 1, v13
MP, pryz, 1, v23
MP, gxy, 1, G12
MP, gyz, 1, G23
MP, gxz, 1, G13

ET, 1, SOLID191, , , , , , 1          ! 20 NODE LAYERED SOLID

KEYOPT, 1, 2, 0          ! Constant thickness layer input (100 layers)
KEYOPT, 1, 3, 0          ! Use material properties as given
KEYOPT, 1, 5, 3          ! Print results, including FC, at layer top
                          ! and bottom 4 integration points and averages
KEYOPT, 1, 8, 1          ! Store data for all layers
!KEYOPT, 1, 10, 1       ! Print summary of all the FC

! Create 4 sets of real constants for the laminate definition with 3 plies per

```

```

! set. (from bottom to top)
R,1,Nplies/4,          ! Nplies/4=3 plies (bottom)
RMORE
*DO,II,1,Nplies/4,2
  RMORE,1,Theta%II%,tply,1,Theta%II+1%,tply  ! RMORE,MAT1,THETA1,TK1,MAT2,etc
*ENDDO

R,2,Nplies/4,          ! Nplies/4=3 plies
RMORE
*DO,II,(Nplies/4)+1,Nplies/2,2
  RMORE,1,Theta%II%,tply,1,Theta%II+1%,tply
*ENDDO

R,3,Nplies/4,          ! Nplies/4=3 plies
RMORE
*DO,II,(Nplies/2)+1,(3*Nplies/4),2
  RMORE,1,Theta%II%,tply,1,Theta%II+1%,tply
*ENDDO

R,4,Nplies/4,          ! Nplies/4=3 plies (top)
RMORE
*DO,II,(3*Nplies/4)+1,Nplies,2
  RMORE,1,Theta%II%,tply,1,Theta%II+1%,tply
*ENDDO

! Associate each real constant set with each volume (from bottom to top)
VSEL,S,VOLU,,1! Select Volume 1 (bottom)
      ! Associates element attributes with the selected, unmeshed volumes
VATT,1,1,1! VATT,MAT,REAL,TYPE,ESYS

VSEL,S,VOLU,,2
VATT,1,2,1

VSEL,S,VOLU,,3
VATT,1,3,1

VSEL,S,VOLU,,4! Select Volume 4 (top)
VATT,1,4,1

ALLSEL,ALL

!=====
! MESH GENERATION

/ESHAPE,1          ! view layers comprising laminate
/VSCALE,,2        ! double size of symbols, like element CS
/PSYMB,ESYS,1    ! turn on element coordinate system symbols
/DEVICE,VECTOR,0  ! elements shown in render style

! define a cylindrical local system to assign number of elements in each
! direction
LOCAL,11,1,a+h,a+h,,180,,

```

```

! 1 layered element through the thickness (for each volume → 4 in total)
LSEL,S,LOC,Y,0
LSEL,A,LOC,Y,90
LSEL,U,LOC,Z,t/2
LESIZE,ALL,,1

! 30 elements in the radial direction
LSEL,S,LOC,X,a
LSEL,A,LOC,X,a+(h/2)
LSEL,A,LOC,X,b
LSEL,U,LOC,Y,0
LSEL,U,LOC,Y,90
LESIZE,ALL,,30

! 24 elements in width
LSEL,S,LOC,X,a
LSEL,A,LOC,X,a+(h/2)
LSEL,A,LOC,X,b
LSEL,U,LOC,Z,0
LSEL,U,LOC,Z,t
LESIZE,ALL,,24

ALLSEL,ALL

/PNUM,REAL,1! Real constant set colors on volumes
VPLOT

! Mesh and re-orientate all elements' coordinate system
CSYS,0
LOCAL,12,,a+h,,t,,90, ! define a Cartesian local system
CLOCAL,12,,,,,-45,! re-orientate the local system
ESYS,12! Element coordinate system attribute defined by CS 12
VMESH,ALL! Mesh all volumes
ESLV,S! select all elements
EORIENT,LYSL,NEGZ ! SOLID191 elements - Reorientation
EPLLOT

ALLSEL,ALL
EPLLOT

! Displays the layer stacking sequence for layered elements (for each real
! constant → for each layer of elements)
!LAYPLOT,1
!LAYPLOT,193
!LAYPLOT,385
/GROPTS,VIEW,1

!=====
! BOUNDARY CONDITIONS

CSYS,0

```

```

! Support
NSEL,S,LOC,Y,a+h
D,ALL,ALL           ! Top end - built in

ALLSEL,ALL

!=====

! MZ →Refer to Appendix-Pressure due to Bending Moment
SLOPE=12*M/(h**3)
SFGRAD,PRES,0,Y,0,-SLOPE      ! Gradient (slope) for surface loads
NSEL,S,LOC,X,a+h
SF,ALL,PRES,6*M/(h**2)       ! surface loads on nodes

ALLSEL,ALL
EPLLOT

FINISH

!=====
! SOLUTION
!=====

/SOLU

SOLVE

FINISH

!=====
! POSTPROCESSING
!=====

/POST1

/DSCALE,,0           ! Scale displacements automatically
/GRAPHICS,FULL

RSYS,0               ! Global Cartesian coordinate system (default)

!=====
! Max total displacement (abs)

NSORT,U,SUM          ! Sort nodal displ (vector sum) in descending order
*GET,USUM,SORT,,MAX  ! retrieve the maximum total displacement
*SET,USUM,USUM
*STAT,USUM

!=====

```

```

! Max Z displacement (abs)

NSORT,U,Z,,1      ! Sort Z nodal displ (absolute value) in descending order
*GET,UZ_MAX, SORT,,MAX      ! retrieve the maximum absolute Z displacement
*SET,MaxUZ,UZ_MAX
*STAT,MaxUZ

!=====
! Stress in layer coord system S1,S2,S12 (@ centre bottom node) -
! Nodal Results
!=====

CSYS,11
NSEL,S,LOC,Z,t/2
NSEL,R,LOC,Y,45,
NSEL,R,LOC,X,b
*GET,Ctr_Nd_elem1,NODE,,NUM,MAX ! centre-bottom node (R0=0.66)→ plies 1 to 3

NSEL,S,LOC,Z,t/2
NSEL,R,LOC,Y,45,
NSEL,R,LOC,X,b-h/4
*GET,Ctr_Nd_elem2,NODE,,NUM,MAX ! centre-bottom node → plies 4 to 6

NSEL,S,LOC,Z,t/2
NSEL,R,LOC,Y,45,
NSEL,R,LOC,X,b-h/2
*GET,Ctr_Nd_elem3,NODE,,NUM,MAX! centre-bottom node → plies 7 to 9

NSEL,S,LOC,Z,t/2
NSEL,R,LOC,Y,45,
NSEL,R,LOC,X,b-(3*h/4)
*GET,Ctr_Nd_elem4,NODE,,NUM,MAX ! centre-bottom node → plies 10 to 12

ALLSEL,ALL

RSYS,LSYS          ! Layer coordinate system

*DO,JJ,1,4,1      ! Real constant
/GO

ESEL,S,REAL,,JJ! Select each layer of elements (by real constant)

*DO,II,1+3*(JJ-1),3*JJ,1
/GO
*IF,JJ,EQ,1,THEN
  LAYER,II
*ELSEIF,JJ,EQ,2,THEN
  LAYER,II-3
*ELSEIF,JJ,EQ,3,THEN
  LAYER,II-6
*ELSE
  LAYER,II-9

```

```

*ENDIF
*GET,S1_%II%,NODE,Ctr_Nd_elem%JJ%,S,X           ! S1
*SET,S1_%II%,S1_%II%
*STAT,S1_%II%

*GET,S2_%II%,NODE,Ctr_Nd_elem%JJ%,S,Y           ! S2
*SET,S2_%II%,S2_%II%
*STAT,S2_%II%

*GET,S3_%II%,NODE,Ctr_Nd_elem%JJ%,S,Z           ! S3
*SET,S3_%II%,S3_%II%
*STAT,S3_%II%

*GET,S12_%II%,NODE,Ctr_Nd_elem%JJ%,S,XY         ! S12
*SET,S12_%II%,S12_%II%
*STAT,S12_%II%

*GET,S13_%II%,NODE,Ctr_Nd_elem%JJ%,S,XZ         ! S13
*SET,S13_%II%,S13_%II%
*STAT,S13_%II%

*GET,S23_%II%,NODE,Ctr_Nd_elem%JJ%,S,YZ         ! S23
*SET,S23_%II%,S23_%II%
*STAT,S23_%II%
*ENDDO

ALLSEL,ALL

*ENDDO

ALLSEL,ALL

```

Appendix E Pressure due to Bending Moment

Some of the loads applied in the ANSYS FE solid models throughout this research (curve plate under bending, 3-point bending test) have been defined as gradient (slope) loads on surface, by means of the SFGRAD command. The mathematical justification of the load values used as arguments in the abovementioned command is presented below.

E.1 Linearly varying surface load on a surface

Consider a pure bending moment M applied on a plane square section of a beam. If the bending moment direction of application is the one shown on the figure, for instance, the section above the axis would be under compression, while the bottom section would be under tension.

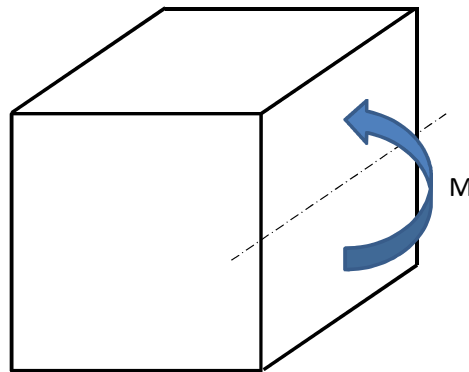


Figure E-1 Schematic representation of a bending moment applied on a plane section.

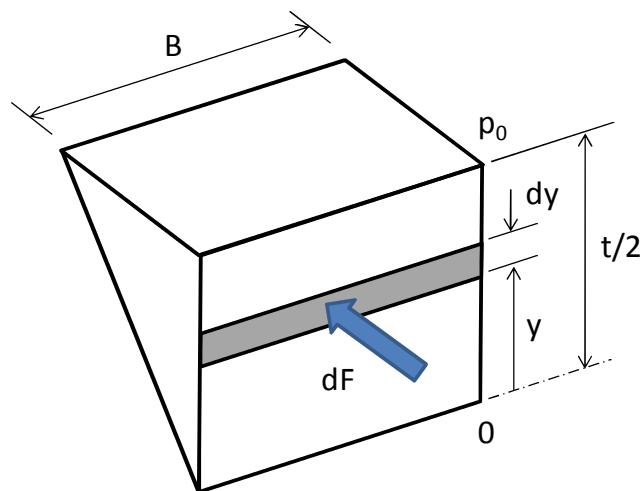


Figure E-2 Schematic representation of a linearly varying surface load on a surface.

Isolating the section under compression (top), the force applied to the plane surface, due to the bending moment, can be obtained according to the schematic representation shown in Figure E-2, in which the magnitude of the force depends on its distance of application to the axis. The pressure applied on the surface at a distance y from the axis is:

$$p = \frac{y}{t/2} p_0 \quad (\text{E-1})$$

Where p_0 is the maximum pressure applied at a thickness $t/2$.

The origin of y coordinate is at the middle of the section

- If $y = \frac{t}{2} \rightarrow p = p_0$ (maximum value)
- If $y = 0 \rightarrow p = 0$

The differential force applied in the differential area of dimensions Bdy is:

$$dF = (pdy)B = Bpdy \quad (\text{E-2})$$

The differential bending moment applied is then:

$$dM = ydF = y(Bpdy) = \left(\frac{y}{t/2} p_0 \right) B y dy \quad (\text{E-3})$$

$$dM = \left(\frac{p_0 B y^2}{t/2} \right) dy \quad (\text{E-4})$$

Integrating:

$$M = 2 \int_0^{t/2} \frac{p_0 B y^2}{t/2} dy \quad (\text{E-5})$$

Where the 2 in front of the integral is due to the 2 sides added (top and bottom sections).

$$M = 4 \int_0^{t/2} \frac{p_0 B}{t} y^2 dy = 4 \frac{p_0 B}{t} \left[\frac{y^3}{3} \right]_0^{t/2} = \frac{4 p_0 B}{3 t} \left(\frac{t^3}{8} \right) \quad (\text{E-6})$$

The total moment applied is then:

$$M = \frac{1}{6} p_0 B t^2 \quad (\text{E-7})$$

From which the maximum pressure applied can be obtained:

$$p_0 = \frac{6}{t^2} \left(\frac{M}{B} \right) \quad (\text{E-8})$$

Where M/B is the moment applied per unit length (moment per meter (M_x)). As the values of the pressure p at $y = 0$ and $y = t/2$ are known, the following expression can be obtained:

$$p = p_0 - \frac{12}{t^3} \left(\frac{M}{B} \right) \left(y + \frac{t}{2} \right) \quad (\text{E-9})$$

$$p = \frac{6}{t^2} \left(\frac{M}{B} \right) - \frac{12}{t^3} \left(\frac{M}{B} \right) \left(y + \frac{t}{2} \right) \quad (\text{E-10})$$

The pressure values then, at a different sections' locations are:

$$\text{If } y = \frac{t}{2}$$

$$p = -\frac{6}{t^2} \left(\frac{M}{B} \right) \quad (\text{E-11})$$

$$\text{If } y = 0 \rightarrow p = 0$$

$$\text{If } y = -\frac{t}{2}$$

$$p = \frac{6}{t^2} \left(\frac{M}{B} \right) \quad (\text{E-12})$$

Appendix F 3 Point bending test

F.1 ANSYS parametric input file

3PB_SOLID191_Biax_15_Elems_TT_30mm_QS_finer.txt

```
FINISH
/CLEAR, NOSTART

/TITLE, 3 Points Bending - Quarter Symmetry (SOLID191 (Biax) - 15 layered
solid elements through thickness)

! All dimensions in m, kg, sec --> N, Pa

!=====
! PARAMETERS DEFINITION

! Laminate
Nplies=8! Number of plies per layer of elements (Biax)
tply=0.25e-3! Ply thickness
t_Brick=Nplies*tply      ! Brick thickness
N_Brick=15              ! Number of bricks through thickness (15)
NpliesT=N_Brick*Nplies  ! Total number of plies (120)

! Biax configuration - ply orientation
Theta1=0
Theta2=90
Theta3=-45
Theta4=45
!====Symmetry====
Theta5=Theta4
Theta6=Theta3
Theta7=Theta2
Theta8=Theta1

! Dimensions
t=NpliesT*tply          ! 30 mm
LT=5*t                 ! (l) specimen length - 150 mm
L=4*t                  ! Outer span
b=5*t/6                ! Width - 25 mm
R2=30e-3               ! Support radius
R1=30e-3               ! Pusher radius

Surf_edit=t
Surf_edit1=1e-3

! Strength (Pa)
```

```

Xt=1970e6           ! 1970 MPa
Xc=990e6           ! 990 MPa
Yt=67e6            ! 67 MPa
Yc=240e6           ! 240 MPa
Zt=67e6            ! 67 MPa
Zc=240e6           ! 240 MPa
S12=62e6           ! 62 MPa
S13=62e6           ! 62 MPa
S23=62e6           ! 62 MPa

! Load
F=43000/4           ! N (divided by 4 due to quarter symmetry)

!=====
! GEOMETRY GENERATION

/PREP7

! Create a longitudinal transverse section of the specimen
WPCSYS,,0
WPROTA,,90
CSWPLA,11,0

*DO,II,0,t-t_Brick,t_Brick! 15 rectangular areas
  RECTNG,0,LT/2,II-(t/2),II-(t/2)+t_Brick
*ENDDO

LSEL,S,LOC,X,,
LSEL,A,LOC,X,LT/2,
LESIZE,ALL,,1! 1 element through the thickness in each area

ALLSEL,ALL

VEXT,ALL,,,,,-b/2! Create the specimen extruding the transverse section

NUMMRG,KP

VPLLOT

! Edit the volume (split in three volumes) to define contact regions
WPLANE,,Surf_edit/2,-Surf_edit1,-Surf_edit1-(t/2),(Surf_edit/2)+Surf_edit1,-
Surf_edit1,-Surf_edit1-(t/2),(Surf_edit/2),,-Surf_edit1-(t/2)
WPROTA,,,-90
VSBW,ALL
WPOFFS,,,-Surf_edit
VSBW,ALL

CSYS,0

! Create area components with the contact regions of the specimen
ASEL,S,LOC,X,0,Surf_edit/2
ASEL,R,LOC,Z,t/2

```

```

CM,CONTACT_SURFACE_Pusher,AREA

ASEL,S,LOC,X,2*Surf_edit,LT/2      !3*Surf_edit
ASEL,R,LOC,Z,-t/2
CMSEL,U,CONTACT_SURFACE_Pusher
CM,CONTACT_SURFACE_Right,AREA

ALLSEL,ALL
CM,Composite_Specimen,VOLU

! supports
WPLANE,,(L/2),,-R2-(t/2),(L/2)+1,,-R2-(t/2),(L/2),1,-R2-(t/2)
WPROTA,,-90      ! Rotates the WP right hand rule:
                 ! WPROTA,THXY,THYZ,THZX (DV's)
CSYS,4           ! Activates the previously defined WP
                 ! create the Right hand side cylinder
CYLIND,,R2,,b    ! Create the support as a cylinder

CMSEL,U,Composite_Specimen
CM,Right_Support,VOLU
ASEL,S,EXT
ASEL,U,LOC,Z,0
ASEL,U,LOC,Z,b
CM,TARGET_SURFACE_Right,AREA      ! Create area component of the support target

! pusher
WPOFFS,-L/2,-(R2+t+R1)
CYLIND,,R1,,b      ! Create the pusher as a cylinder

CMSEL,U,Right_Support
CM,Pusher,VOLU
ASEL,S,EXT
ASEL,U,LOC,Z,0
ASEL,U,LOC,Z,b
CM,TARGET_SURFACE_Pusher,AREA      ! Create area component of the pusher target

ALLSEL,ALL

CSYS,0

!=====
! ET & MATERIAL PROPERTIES DEFINITION

MP,EX,1,136E9      ! ORTHOTROPIC MATERIAL PROPERTIES
MP,EY,1,9.4E9
MP,EZ,1,6.58E9     ! EZ=EY ASSUMED
MP,GXY,1,3.1E9
MP,GYZ,1,3.1E9
MP,GXZ,1,3.1E9
MP,PRXY,1,0.3     ! MAJOR POISSONS RATIO
MP,PRYZ,1,0.3     ! MAJOR POISSONS RATIO
MP,PRXZ,1,0.3     ! MAJOR POISSONS RATIO

```

```

ET,1,SOLID191,,,,,,,,,1      ! 20 NODE LAYERED SOLID

KEYOPT,1,2,0                ! Constant thickness layer input (100 layers)
KEYOPT,1,3,0                ! Use material properties as given
KEYOPT,1,5,3                ! Print results, including FC, at layer top
                             ! and bottom 4 integration points and averages
KEYOPT,1,8,1                ! Store data for all layers
KEYOPT,1,10,1               ! Print summary of all the FC

! Create the real constant sets with the laminate definition
*DO,II,1,N_Brick
  R,II,Nplies,1              ! N_Brick (15) real constant set
  RMORE
  *DO,JJ,1,Nplies,2
    RMORE,1,Theta%JJ%,tply,1,Theta%JJ+1%,tply      ! RMORE,MAT1,THETA1,TK1
  *ENDDO
*ENDDO

! Associate each real constant set with each volume (from bottom to top)
JJ=0
*DO,II,0,t-t_Brick,t_Brick
  !Reall=1+JJ
  VSEL,S,LOC,X,0,LT/2
  VSEL,R,LOC,Z,II-(t/2),II-(t/2)+t_Brick
  VATT,1,JJ+1,1              ! VATT,MAT,REAL,TYPE,ESYS
  ALLSEL,ALL
  JJ=1+JJ
*ENDDO

/PNUM,REAL,1! Real constant set colors on volumes
VPLOT

ALLSEL,ALL

!=====
! MESH GENERATION

/ESHAPE,1                    ! view layers comprising laminate
/VSCALE,,2                  ! double size of symbols, like element CS
/PSYMB,ESYS,1              ! turn on element coordinate system symbols
/DEVICE,VECTOR,0           ! elements shown in render style

! Number of elements per line - Element size definition
! Length
LSEL,S,LINE,,282,311,29
LESIZE,ALL,,10

LSEL,S,LINE,,233
LESIZE,ALL,,5

! Width

```

```

LSEL,S,LOC,Y,b/4
LESIZE,ALL,,4

! Mesh specimen and re-orientate elements
WPCSYS,0
CSWPLA,12,0! Create a local coordinate system at the origin
ESYS,12! Element coordinate system attribute defined by CS 12
MSHKEY,1! Use mapped meshing
CMSEL,S,Composite_Specimen! select the specimen component
VMESH,ALL! Mesh specimen
ESLV,S
EORIENT,LYSL,NEGZ          ! SOLID191 elements - Reorientation
EPLLOT

!LAYPLOT,1! Displays the layer stacking sequence for element 1
!/GROPTS,VIEW,1

NUMMRG,NODE
NUMMRG,ELEM

!=====
! CONTACT PAIR 1 - BOTTOM SPECIMEN-RIGHT SUPPORT

MP,MU,2,0.1          ! MU= Coefficient of Friction (unitless)
R,16
ET,2,170            ! TARGE170 - 3D Target Segment
ET,3,174            ! CONTAL74 - 3D 8-Node Surface-to-Surface Contact
KEYOPT,2,1,1        ! High order elements (used by AMESH and LMESH
                    ! only) <-- VITAL for this analysis, otherwise ERROR!!!
KEYOPT,2,2,0        ! Automatically constrained by ANSYS
KEYOPT,3,2,0        ! Contact algorithm: Augmented Lagrangian (default)
KEYOPT,3,4,2 ! On nodal point - normal to target surface -->
                    ! for a rigid surface constraint
KEYOPT,3,5,1        ! Close gap with auto CNOF
KEYOPT,3,7,0        ! Element level time incrementation control: No control
KEYOPT,3,9,2        ! Include both initial geometrical penetration or
                    ! gap and offset, but with ramped effects
KEYOPT,3,10,0

! R1,R2,FKN,FTOLN,ICONT,PINB
! PMAX,PMIN,TAUMAX,CNOF,FKOP,FKT
! FKN=Normal penalty stiffness factor
RMODIF,16,3,0.1     ! FKN = Normal penalty stiffness factor
!RMODIF,16,5,4e-5   ! ICONT = Initial contact closure
RMODIF,16,10,0.! CNOF = Contact surface offset
RMODIF,16,12,0. ! FKT = Tangent penalty stiffness factor

! Generate the target surface
CMSEL,S,TARGET_SURFACE_Right
MAT,2
REAL,16
TYPE,2

```

```

AMESH,ALL

ALLSEL,ALL
EPLLOT

! Generate the contact surface
CMSEL,S,CONTACT_SURFACE_Right
TYPE,3
NSLA,S,1
ESLN,S,0
ESURF

ALLSEL,ALL
EPLLOT

!-----
! CONTACT PAIR 2 - TOP SPECIMEN-PUSHER

MP,MU,4,0.1      ! MU= Coefficient of Friction (unitless)
R,17
ET,4,170        ! TARGE170 - 3D Target Segment
ET,5,174        ! CONTA174 - 3D 8-Node Surface-to-Surface Contact
KEYOPT,4,1,1    ! High order elements (used by AMESH and LMESH commands
                ! only) <-- VITAL for this analysis, otherwise ERROR!!
KEYOPT,4,2,0    ! Automatically constrained by ANSYS
KEYOPT,5,2,0    ! Contact algorithm: Augmented Lagrangian (default)
KEYOPT,5,4,0    ! Location of contact detection point: On Gauss
                ! point (for general cases)
KEYOPT,5,5,1    ! Close gap with auto CNOF
KEYOPT,5,7,0    ! Element level time increment control: No control
KEYOPT,5,9,2    ! Include both initial geometrical penetration or
                ! gap and offset, but with ramped effects
KEYOPT,5,10,0

! R1,R2,FKN,FTOLN,ICONT,PINB
! PMAX,PMIN,TAUMAX,CNOF,FKOP,FKT
! FKN=Normal penalty stiffness factor
RMODIF,17,3,0.1 ! FKN = Normal penalty stiffness factor
!RMODIF,17,5,3e-5 ! ICONT = Initial contact closure
RMODIF,17,10,0. ! CNOF = Contact surface offset
RMODIF,17,12,0. ! FKT = Tangent penalty stiffness factor

! Generate the target surface
CMSEL,S,TARGET_SURFACE_Pusher
MAT,4
REAL,17
TYPE,4
AMESH,ALL

ALLSEL,ALL
EPLLOT

```

```

! Create a pilot node
CSYS,0
K,,,,R1+(t/2)
*GET,KP_F,KP,0,NUM,MAXD
KMESH,KP_F          ! ELIST to see the pilot node definition
*GET,Node_F,NODE,0,NUM,MAXD

! Generate the contact surface
CMSEL,S,CONTACT_SURFACE_Pusher
TYPE,5
NSLA,S,1
ESLN,S,0
ESURF

ALLSEL,ALL
EPLLOT

!=====
! BOUNDARY CONDITIONS

! Symmetry
ASEL,S,LOC,Y,0
ASEL,R,LOC,Z,-t/2,t/2
DA,ALL,UY! Translation in Y in specimen areas at Y=0

ASEL,S,LOC,X,0
ASEL,R,LOC,Z,-t/2,t/2
CMSEL,U,TARGET_SURFACE_Pusher
DA,ALL,UX! Translation in X in specimen areas at X=0

! Nodal load application
NSEL,S,NODE,,Node_F
F,ALL,FZ,-F

ALLSEL,ALL
EPLLOT

SBCTRAN! Transfers loads and BCs to FE model

!=====
! FC

TB,FAIL,1,1          ! TB, FAIL, material number, 1 temperature
TBTEMP,,CRIT
TBDATA,3,2          ! Include the inverse of the Tsai-Wu strength ratio
!TBDATA,2,1
TBTEMP,0
TBDATA,10,Xt,-Xc,Yt,-Yc,Zt,-Zc      ! stresses XT, XC, YT, YC, ZT, ZC
TBDATA,16,S12,S23,S13      ! shear stresses XY, YZ (large number),
                             ! XZ (large number)
TBDATA,19,0,0,0      ! coupling coefficients
!TBLIST,ALL,1      ! Lists the data tables

```

```

OUTPR,NSOL,1
OUTPR,RSOL,1

FINISH

!=====
!=====
! SOLUTION
!=====
!=====

/SOLU

ANTYPE,0           ! Perform a static analysis
!NLGEOM,1          ! Includes large-deflection (large rotation) effects
                   ! or large strain effects, according to the element type
SOLC,ON,ON,INCP    ! Turn on solution control with ability to use
                   ! contact time prediction

EQSL,SPARSE,,,,,1
RESC,,NONE         ! Do not keep any restart files
CNTR,PRINT,1       ! print out contact info and also make no initial
                   ! contact an error
NLDIAG,CONT,ITER   ! print out contact info each equilibrium iteration
/NOPR
/GOPR
AUTOTS,ON          ! Use automatic time stepping

NSUBST,50,10000,10! NSUBST,NSBSTP,NSBMX,NSEMN
!TIME,10           ! maximum load applied
OUTRES,ERASE
OUTRES,ALL,ALL

SOLVE

FINISH

!=====
!=====
! POSTPROCESSING
!=====
!=====

/POST1

/DSCALE,,0         ! Scale displacements automatically
/GRAPHICS,FULL

!/EXPAND,4,POLAR,HALF,,90! Expansion of the FE model display
!/REPLOT

! Select the specimen elements (Element type 1)

```

```

ESEL,S,TYPE,,1

PLNSOL,U,Z,1           ! Plot nodal UZ displacement

PLNSOL,S,Z,1           ! Plot nodal SZ

!=====
! Max total displacement (abs)

NSORT,U,SUM            ! Sort nodal displ (vector sum) in descending order
*GET,USUM,SORT,,MAX    ! retrieve the maximum total displacement
*SET,USUM,USUM
*STAT,USUM

!=====
! Max Z displacement (abs)

NSORT,U,Z,,1          ! Sort Z nodal displ (absolute value) in descending order
*GET,UZ_MAX,SORT,,MAX  ! retrieve the maximum absolute Z displacement
*SET,MaxUZ,UZ_MAX
*STAT,MaxUZ

!=====
!=====

! Get maximum SXZ for plies located at 5-7 layer of elements
RSYS,LSYS
!LAYER,8
ESEL,S,REAL,,5,7
NSORT,S,XZ
*GET,Node_Max_SXZ,SORT,,IMAX
RSYS,0                ! Global Cartesian coordinate system (default)
*GET,X_Node_Max_SXZ,NODE,Node_Max_SXZ,LOC,X
*SET,X_Node_Max_SXZ,X_Node_Max_SXZ
!PRNSOL,S,COMP        ! ordered by descending SXZ

!=====
!=====

! for S13
*DO,II,1,N_Brick
  NSEL,S,LOC,X,X_Node_Max_SXZ
  NSEL,R,LOC,Y,b/2
  NSEL,R,LOC,Z,-t/2+(II*t_Brick)
  *GET,Node_Max_SXZ_Real%II%,NODE,,NUM,MAX

  ALLSEL,ALL
*ENDDO

ALLSEL,ALL

!=====

```

```

! Stress in layer coord system S13 (@ Max S13 values layer 8-Real,6) -
! Nodal Results
!=====

RSYS,LSYS                ! Layer coordinate system

*DO,JJ,1,N_Brick,1      ! Real constant
/GO

ESEL,S,REAL,,JJ

*DO,II,Nplies*(JJ-1)+1,Nplies*JJ,1    ! for all layers
/GO
*IF,JJ,EQ,1,THEN
  LAYER,II
*ELSE
  LAYER,II-Nplies*(JJ-1)
*ENDIF

*GET,S13_%II%,NODE,Node_Max_SXZ_Real%JJ%,S,XZ      ! S13
*SET,S13_%II%,S13_%II%
*STAT,S13_%II%

*ENDDO

ALLSEL,ALL

*ENDDO

ALLSEL,ALL

!=====
!=====
! Interlaminar shear stresses (ILSXZ, ILSYZ, ILSUM, ILANG)

!RSYS,SOLU                ! For element quantities, these are the element
coordinate system for each element

!ESEL,S,ELEM,,7          ! CHANGE element number if wanted!!!!!!!!!!!!!!
!*GET,Elem1,ELEM,,NUM,MAX

!ALLSEL,ALL

!ESEL,S,ELEM,,43        ! CHANGE element number if wanted!!!!!!!!!!!!!!
!*GET,Elem2,ELEM,,NUM,MAX

!...
! 15 elements to extract the ILSXZ
!...

!ALLSEL,ALL

```

```

!*DO,JJ,1,N_Brick,1      ! Real constant
! /GO

! ESEL,S,REAL,,JJ

! bottom of layer i
! *DO,II,Nplies*(JJ-1)+1,Nplies*JJ,1 ! for all layers
! /GO
! *IF,JJ,EQ,1,THEN
!     KK=II
!     LAYER,KK
! *ELSE
!     KK=II-Nplies*(JJ-1)
!     LAYER,KK
! *ENDIF

! ETABLE,ERASE
! ETABLE,ILSXZ_%II%,SMISC,(2*KK)-1      ! interlaminar (transverse) SXZ
shear stress
!PRETAB,GRP1

! MAXIMUM VALUE AND ELEMENT WHERE IT OCCURS

! ESORT,ETAB,ILSXZ_%II%      ! Sorts the element table
! *GET,ILSXZ_%II%_MAX,SORT,,MAX
! *GET,E_ILSXZ_%II%_MAX,SORT,,IMAX      ! Element number where maximum
value occurs
! *SET,ILSXZ_%II%_MAX,ILSXZ_%II%_MAX
! *SET,E_ILSXZ_%II%_MAX,E_ILSXZ_%II%_MAX
! *STAT,ILSXZ_%II%_MAX

! IL STRESS VALUES AT CENTRE ELEMENT

! *GET,ILSXZ_ctr_%II%,ELEM,Elem%JJ%,ETAB,ILSXZ_%II%
! *SET,ILSXZ_ctr_%II%,ILSXZ_ctr_%II%
! *STAT,ILSXZ_ctr_%II%

! *ENDDO

! ALLSEL,ALL

!*ENDDO

!ALLSEL,ALL

!=====
!=====
! FC
!=====
!=====

RSYS,LSYS

```

```

! NOTE: If you don't want the failure stress or strain to be checked in
! a particular direction, specify a large number in that direction
FC,1,S,XTEN, Xt
FC,1,S,XCMP, -Xc
FC,1,S,YTEN, Yt
FC,1,S,YCMP, -Yc
FC,1,S,ZTEN, Zt          ! Z value set to a large number
FC,1,S,ZCMP, -Zc
FC,1,S,XY  , S12
FC,1,S,YZ  , S23          ! YZ value set to a large number
FC,1,S,XZ  , S13          ! XZ value set to a large number
FC,1,S,XYCP, 0
FC,1,S,YZCP, 0
FC,1,S,XZCP, 0
!FCLIST

!=====
!=====
! FAIL: Failure criteria

LAYER,FCMAX ! Processes the layer with the largest failure criteria
           ! (SHELL99, SOLID46, SOLID191)

!PRESOL,FCMX ! Maximum FC over the entire element. Components:
! Layer number where the maximum occurs (LAY), name of the maximum FC,
! and value of the maximum FC (VAL)

ETABLE,ERASE
ETABLE,FCMAX,NMISC,1 ! FC values and maximum at each integration point
ETABLE,VALUE,NMISC,2 ! Maximum value for this criterion
ETABLE,LN,NMISC,3 ! Layer number where maximum occurs
ETABLE,ILMAX,NMISC,4 ! Maximum ILSS (occurs between LN1 and LN2)
ETABLE,LN1,NMISC,5 ! Layer numbers which define location ILMAX
ETABLE,LN2,NMISC,6 ! Layer numbers which define location ILMAX

!PRETAB,GRP1
!PRETAB,FCMAX ! etc, with the rest of the output variables

!=====

*DO,II,1,N_Brick,1 ! Real constant
/GO

ESEL,S,REAL,,II

! FCMAX (MAX)
ESORT,ETAB,FCMAX ! Sorts the element table
*GET,FCMAX,SORT,,MAX
*GET,E_FCMAX,SORT,,IMAX ! Element number where maximum value occurs
*SET,FCMAX_R%II%,FCMAX
*SET,E_FCMAX_R%II%,E_FCMAX

```

```

*STAT,FCMAX_R%II%

! VALUE (MAX)
ESORT,ETAB,VALUE ! Sorts the element table
*GET,VALUE,SORT,,MAX
*GET,E_VALUE,SORT,,IMAX ! Element number where maximum value occurs
*SET,VALUE_R%II%,VALUE
*SET,E_VALUE_R%II%,E_VALUE
*STAT,VALUE_R%II%

! LN (MAX)
ESORT,ETAB,LN ! Sorts the element table
*GET,LN,SORT,,MAX
*GET,E_LN,SORT,,IMAX ! Element number where maximum value occurs
*SET,LN_R%II%,LN
*SET,E_LN_R%II%,E_LN
*STAT,LN_R%II%

ALLSEL,ALL

*ENDDO

!=====

!ILANG: Angle of interlaminar shear stress vector (measured from the element
! x-axis towards the element y-axis in degrees)
!ILSUM: Interlaminar shear stress vector sum

*DO,JJ,1,N_Brick,1 ! Real constant
/GO

ESEL,S,REAL,,JJ

*DO,II,Nplies*(JJ-1)+1,Nplies*JJ,1 ! for all layers
/GO
*IF,JJ,EQ,1,THEN
KK=II
LAYER,KK
*ELSE
KK=II-Nplies*(JJ-1)
LAYER,KK
*ENDIF

ETABLE,ERASE
ETABLE,FCMAX_%II%,NMISC,(2*(Nplies+KK))+7
ETABLE,VALUE_%II%,NMISC,(2*(Nplies+KK))+8

! Maximum value and element where it occurs

ESORT,ETAB,FCMAX_%II% ! Sorts the element table
*GET,FCMAX_%II%_MAX,SORT,,MAX
*GET,E_FCMAX_%II%_MAX,SORT,,IMAX ! Element number where maximum

```

```

! value occurs
*SET,FCMAX_%II%_MAX,FCMAX_%II%_MAX
*SET,E_FCMAX_%II%_MAX,E_FCMAX_%II%_MAX
*STAT,FCMAX_%II%_MAX

ESORT,ETAB,VALUE_%II%
! Sorts the element table
*GET,VALUE_%II%_MAX,SORT,,MAX
*GET,E_VALUE_%II%_MAX,SORT,,IMAX
! Element number where maximum
! value occurs

*SET,VALUE_%II%_MAX,VALUE_%II%_MAX
*SET,E_VALUE_%II%_MAX,E_VALUE_%II%_MAX
*STAT,VALUE_%II%_MAX

*ENDDO

ALLSEL,ALL

*ENDDO

SAVE

```

Appendix G First ply failure

The analysis presented in this section is based on Homework 1 exercise proposed at the end of Session 1 of the Composites e-learning course given by NAFEMS (April, 2010).

Its intention is to show how to set up a first ply failure finite element analysis, determining the load at which in-plane failure occurs using the Tsai-Wu failure criteria.

The tests are carried out on a single layer coupon under tension. Some magnitudes, such as the failure load, the in-plane stresses (S_1 , S_2 , S_{12}) and the terms of the Tsai-Wu failure index are plotted against ply angle, and the results are interpreted.

The same exercise could be applied to a failing load due to any other failure criteria, as Maximum Stress or Maximum Strain criteria.

G.1 Settings and assumptions

A schematic representation of the coupon test under axial tension is shown below. Note that the coupon is a single ply specimen with variable orientation from 0° (along the longitudinal X global axis) to 90° (along the transverse Y axis).

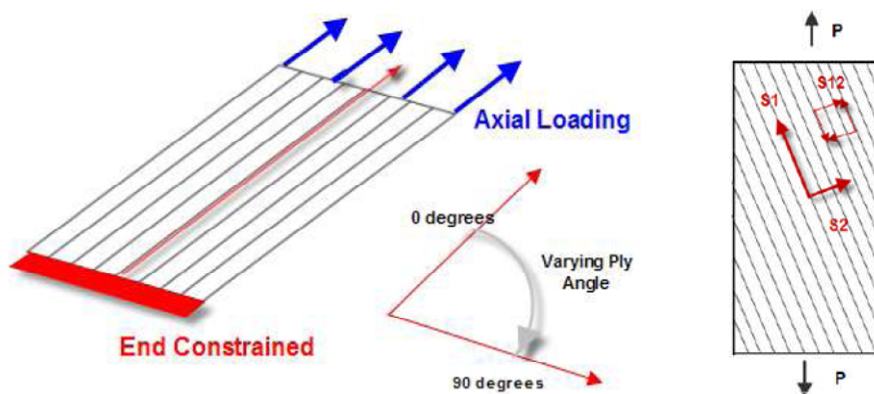


Figure G-1 Schematic description of the analysis. Source: Abbey, 2010.

These are the coupon dimensions in metric units:

Table G-1 Coupon test dimensions. Source: Abbey, 2010.

<i>Length – a (m)</i>	<i>Width – b (m)</i>	<i>Thickness – t (m)</i>	<i>Cross sectional area – A (m²)</i>
0.4	0.08	5.00E-03	4.00E-04

*Note: $A=b \times t$

These are the 2D orthotropic material properties, the stiffness terms E_1 , E_2 , G_{12} , ν_{12} in Pascals:

Table G-2 Material properties.

<i>Elastic Constant</i>	<i>Definition</i>	<i>Value</i>
E_1 (Pa)	Young's modulus in the fibre direction	1.81E+11
E_2 (Pa)	Young's modulus in the transverse direction	1.03E+10
ν_{12}	Poisson's ratio	0.28
G_{12} (Pa)	Shear modulus	7.17E+09

These are the strengths values in Pascals:

Table G-3 Strength values.

<i>Strength</i>	<i>Definition</i>	<i>Value</i>
X_t (Pa)	Strength under tension in the fibre direction	1.50E+09
X_c (Pa)	Strength under compression in the fibre direction	1.50E+09
Y_t (Pa)	Strength under tension in the transverse fibre direction	4.00E+07
Y_c (Pa)	Strength under compression in the transverse fibre direction	2.46E+08
S (Pa)	Shear strength	6.80E+07
F_{12}	Interaction term	0.00

The model presented here was created using 8-node linear layered shell element SHELL99, although the analysis was reproduced, with similar results, with some other layered elements formulations (SHELL181, SHELL281, SOLID46, SOLID186, SOLID191, SOLSH190).

The mesh used was a 20 by 6 elements. The aim was to have a constant stress state, which has shown not to be great mesh dependent.

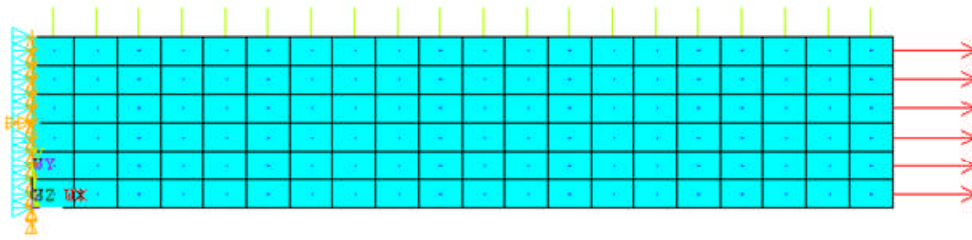


Figure G-2 FE model general view.

Regarding the end constraint, the main idea behind it is to avoid locking in Poisson's ratio. Thus, in case of having that end fully built-in, that will lock in the transverse direction, locking all the strains, which will produce a stress concentration in the transverse direction. Best way to avoid that is to have a roller support that allows transverse direction translation, apart from one central node. A summary of the boundary conditions applied is presented here:

- $X=0 \rightarrow 1, 5, 6 \rightarrow$ Avoiding translation in the X direction and rotation in the complementary directions (Y and Z).
- Centre node (at $X=0 \rightarrow 2, 3, 4 \rightarrow$ Allowing translation in Y except in this centre node. It also constraint that node to translate in Z, and rotate in X.

So when pulling in the X direction, the specimen will stretch in the longitudinal direction and shrink in the transverse direction due to Poisson's ratios effect without locking any strains in Y; that way a constant stress state is achieved.

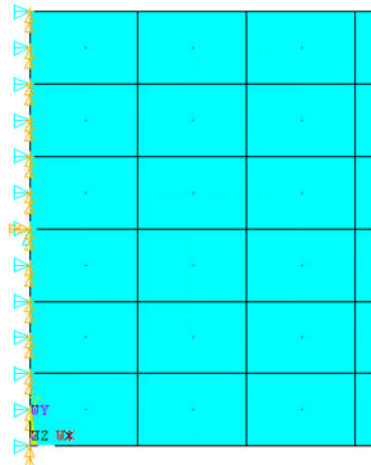


Figure G-3 End constraint applied to avoid locking due to Poisson's ratio.



Figure G-4 Load applied at a middle plane of the shell elements.

Ply end load is applied along the longitudinal direction. The main aim is to find the load that will just fail the coupon. Thus, the load application is an iterative process that requires a parametric factor load definition, initially set to one, and which will increase its value in every iteration. The final load value will be determined by the failure of the coupon.

G.2 Results

Once the model has run, first thing to do is to check that the boundary conditions have been applied successfully. Thus, the in-plane stress S1 is plotted, confirming a constant stress state, as it can be seen in Figure G-5. Furthermore, as the original mesh is overlaid in the model, it can be observed that when the axial load is applied the coupon stretches and shrinks as it is meant to do.

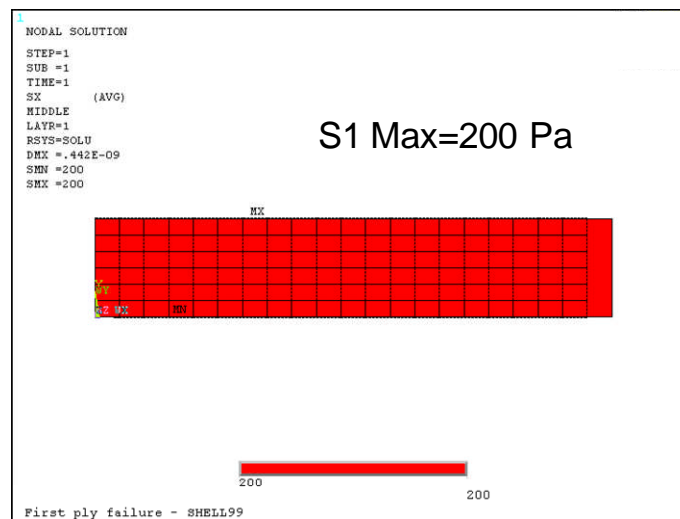


Figure G-5 Constant stress state (in the fibre direction).



Figure G-6 Transverse contraction due to the applied load and the BCs applied.

Next step is to determine the load at which the ply fails, that could be obtained by the strength ratio SR, defined by the following expression:

$$SR = \frac{\text{Allowable stress}}{\text{Applied stress}} \quad (\text{G-1})$$

ANSYS has the output parameter defined as the Tsai-Wu inverse of the “strength ratio”, TWSR, which is also referred to as the Unity Check, UC:

$$UC = \frac{\text{Applied stress}}{\text{Allowable stress}} \quad (\text{G-2})$$

In fact, this factor is the inverse of the required Strength Ratio (SR). Its maximum value shall be less or equal than 1.0 for the ply not to fail.

Figure G-7 represents the Tsai-Wu inverse of the strength ratio (TWSR) for the coupon of a ply angle equal to 0° under a unity axial load, which is constant along the plate. The ANSYS parametric input file, shown in the last subsection of this appendix, enables to obtain the UC value based on the maximum TWSR value.

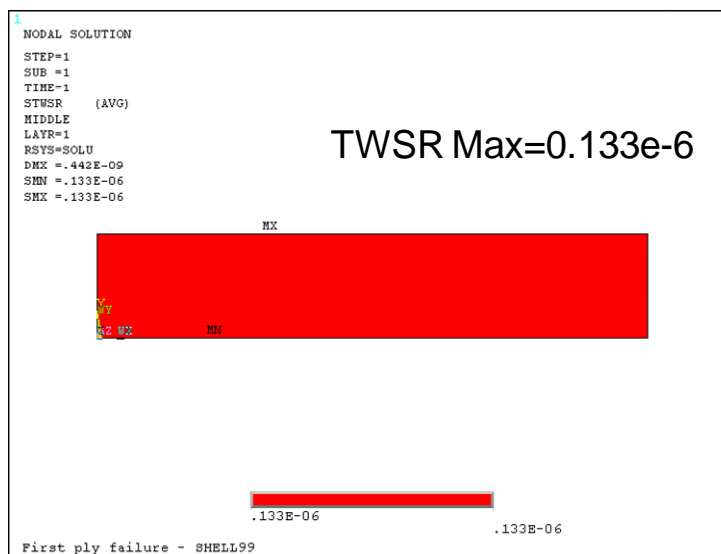


Figure G-7 Inverse of Tsai-Wu strength ratio index failure criterion.

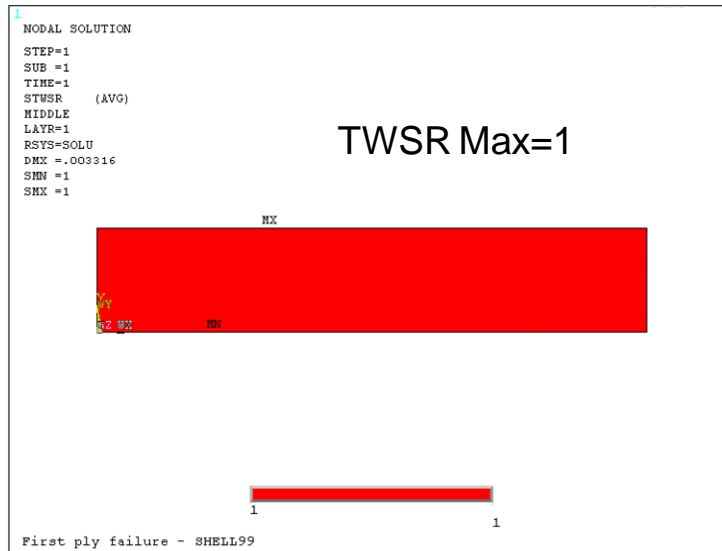


Figure G-10 Inverse of Tsai-Wu strength ratio index failure criterion.

The UC values obtained for all ply angles considered are presented in the following table, alongside with the updated load value per unit with and the total failing load value.

Table G-4 Failing load factor (obtained with ANSYS) and failing load for a range of ply angles.

<i>Theta (deg)</i>	<i>UC=Factor (from ANSYS)</i>	<i>P (N/m)</i>	<i>Total Load (N)</i>
0	7.500E+06	7.500E+06	6.000E+05
10	1.717E+06	1.717E+06	1.374E+05
20	8.047E+05	8.047E+05	6.438E+04
30	5.060E+05	5.060E+05	4.048E+04
40	3.661E+05	3.661E+05	2.929E+04
50	2.896E+05	2.896E+05	2.317E+04
60	2.447E+05	2.447E+05	1.958E+04
70	2.184E+05	2.184E+05	1.747E+04
80	2.044E+05	2.044E+05	1.635E+04
90	2.000E+05	2.000E+05	1.600E+04

*Note: width b = 8 cm

The next plot represents the total tensile failing load against ply angle variation (from 0° to 90°). As it can be seen, the failing load drops dramatically for ply angles between 0-10 degrees, remaining at a minimum level for the rest of the ply angles. Thus, small misalignments between the direction of the load application and the ply angle can have catastrophic consequences for the ply failure.

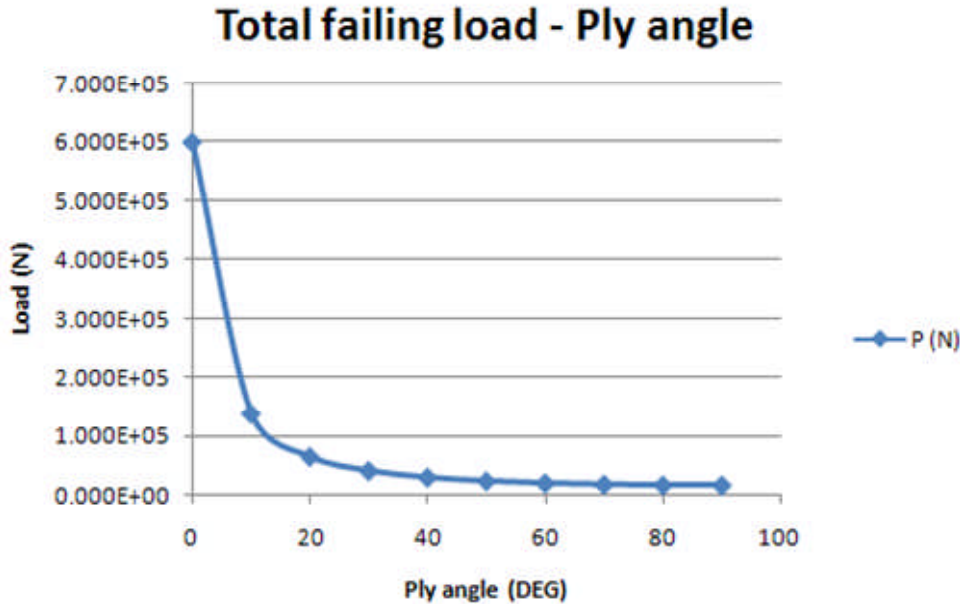


Figure G-11 Total failing load (due to Tsai-Wu failure criteria) against ply angle.

In case of not having access to an FE solver, these are the equations used internally to calculate the in-plane stresses, making use of the failing load, the cross sectional area and the ply angle

$$\sigma_1 = \frac{P}{A} \cos^2\theta \tag{G-3}$$

$$\sigma_2 = \frac{P}{A} \sin^2\theta \tag{G-4}$$

$$\tau_{12} = -\frac{P}{A} \sin\theta \cos\theta \tag{G-5}$$

For the present case the cross sectional area is $A=0.4e-3 \text{ m}^2$. Thus, making use of the equations above the in-plane stresses for the ply angles considered are presented in the following graph.

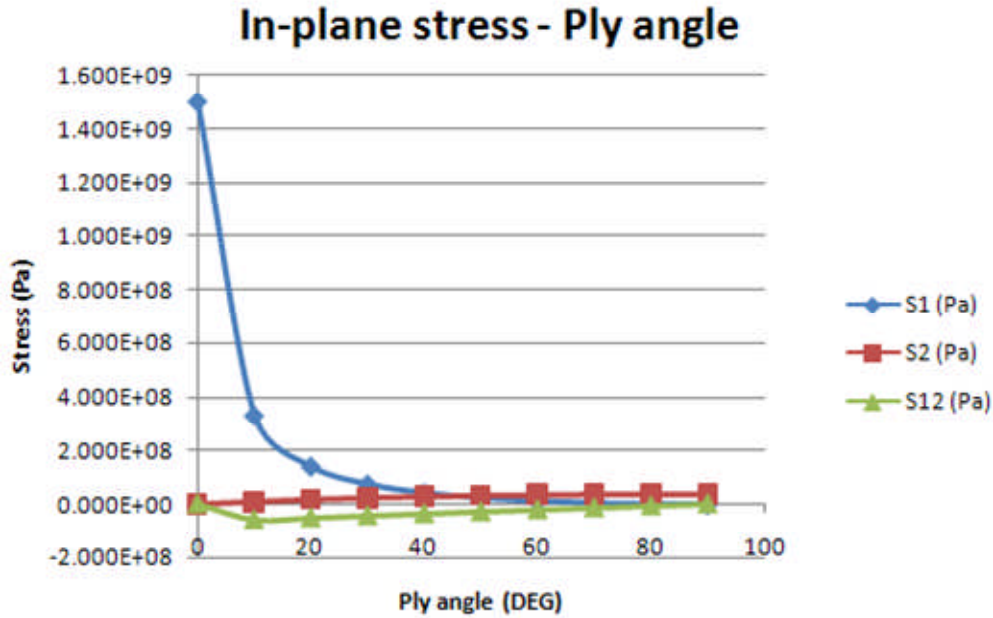


Figure G-12 In-plane stresses (S1, S2, S12) against ply angle.

The coupon is mainly affected by stresses in the fibre direction at low angles (between 0-10 degrees), having a similar distribution to the failing load, reducing though its effects as the ply angle increases. The other to in-plane stresses (transverse direction and shear) are of the order of 10^7 (Pa) for all the ply angle range, being the second one negative.

It is as well possible to represent the variation the Twai-Wu failure index equation terms against the ply angles. Considering that the coupling factor F_{12} is null, no interaction term is accounted in this case.

$$FI = \sigma_1 \left[\frac{1}{X_T} - \frac{1}{X_C} \right] + \sigma_2 \left[\frac{1}{Y_T} - \frac{1}{Y_C} \right] + \frac{\sigma_1^2}{X_T X_C} + \frac{\sigma_2^2}{Y_T Y_C} + \frac{\tau_{12}^2}{S^2} + 2F_{12}\sigma_1\sigma_2 \quad \text{(G-6)}$$

Bear in mind that for the in-plane stress levels calculated, for all ply angles, the Tsai-Wu failure index is close to the unity in all cases. This is expected, as in-plane stresses are calculated based on failing load values.

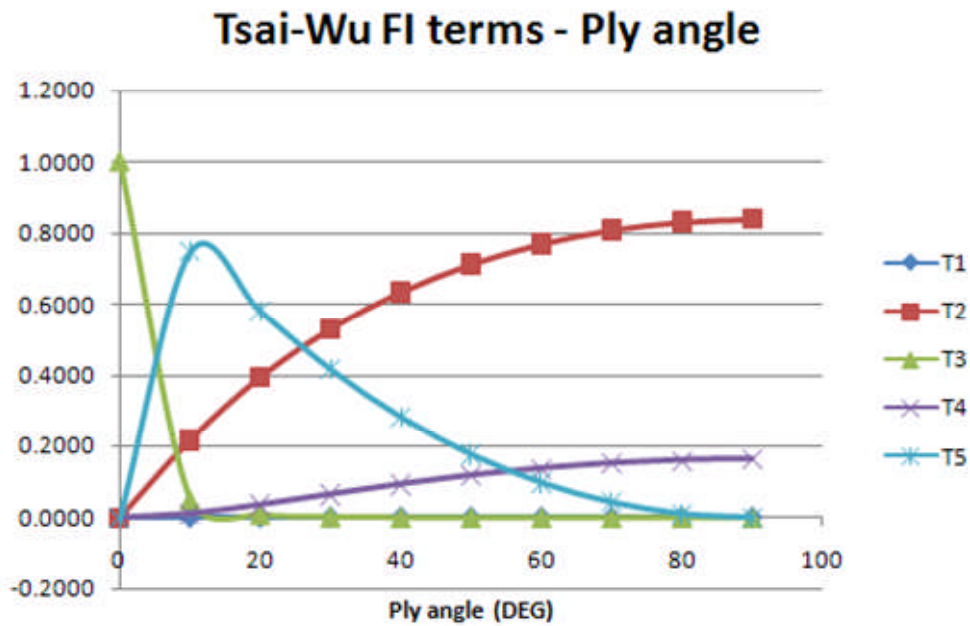


Figure G-13 Tsai-Wu failure index terms against ply angle.

G.2.1 ANSYS parametric input file

```

fini
/clear                ! Clears the database

/TITLE,First ply failure - SHELL99
! All dimensions in m, kg, sec --> N, Pa

!=====
! PARAMETERS DEFINITION

! laminate parameters
tply=5e-3             ! ply thickness
Theta1=0              ! ply angle

! coupon dimensions
a=0.4                 ! length
b=8e-2                ! width
t=tply                ! total thickness

! load
Factor=1
P=1*Factor            ! N/m

! Strength (Pa)
Xt=1500e6             ! 1500 MPa
Xc=1500e6             ! 1500 MPa

```

```

Yt=40e6           ! 40 MPa
Yc=246e6          ! 246 MPa
S12=68e6          ! 68 MPa
S23=S12

! Stiffness (Pa)
E1=181E9
E2=10.3E9
G12=7.17E9
nu12=0.28

!=====
! GEOMETRY GENERATION

/PREP7

RECTNG,0,a,0,b           ! RECTNG,X1,X2,Y1,Y2

!=====
! ET & MATERIAL PROPERTIES DEFINITION

! Material definition - 2D orthotropic
MP,  ex, 1, E1           ! Pa
MP,  ey, 1, E2           ! Pa
MP,  ez, 1, E2           ! Pa
MP,  prxy, 1, nu12       ! unitless
MP,  pryz, 1, nu12       ! unitless
MP,  prxz, 1, nu12       ! unitless
MP,  gxy, 1, G12         ! Pa
MP,  gyz, 1, G12         ! Pa
MP,  gxz, 1, G12         ! Pa

ET,1,SHELL99,,,,,,1     ! 8 NODE LAYERED SHELL

KEYOPT,1,2,0            ! Constant thickness layer input (250 layers maximum)
KEYOPT,1,3,0            ! Basic element printout
KEYOPT,1,5,2            ! Both strain and stress will be used
KEYOPT,1,6,4            ! print the layer solution at the corner nodes for all
layers
KEYOPT,1,8,1            ! Store data for all layers
KEYOPT,1,9,0            ! Evaluate at midthickness of each layer
!KEYOPT,1,10,
KEYOPT,1,11,0           ! Nodes located at midsurface

! Laminate definition - only 1 ply laminate
R,1,1,1                ! Nplies=1 (2nd) --> total number of plies;
                        ! Symmetric Stacking

RMORE
RMORE,1,Theta1,tply     ! RMORE,MAT,THETA,TK

!=====

```

```

! MESH GENERATION

/ESHape,1           ! view layers comprising laminate
/VSCALE,,2         ! double size of symbols, like element CS
/PSYMB,ESYS,1     ! turn on element coordinate system symbols
/DEVICE,VECTOR,0  ! elements shown in render style

LESize,1,,,20     ! 20 elements in the longitudinal direction
LESize,4,,,6      ! 6 elements in the transverse direction
MSHKEY,1          ! Use mapped meshing

AMESH,ALL         ! Mesh area

!LAYPLOT,1        ! layer stacking sequence for layered element 1
!/GROPTS,VIEW,1

!=====
! BOUNDARY CONDITIONS

! Support
NSEL,S,LOC,X,0    ! Select nodes at X=0
DSYM,SYMM,X      ! Restrain translation in 1, and rotations in 5, 6
ALLSEL,ALL

NSEL,S,LOC,X,0
NSEL,R,LOC,Y,b/2
D,ALL,UY,,,,UZ,ROTX ! Fix node in (0,b/2,0) in all directions
ALLSEL,ALL

! load P
LSEL,S,LOC,X,a
SFL,ALL,PRES,-P  ! surface loads on X=a. Negative sign → tension
/PSF,PRES,NORM,2,0,1 ! Display the applied pressure as arrows

ALLSEL,ALL
EPLOT

SBCTRAN          ! Transfers solid model loads and BCs to the FEM

!=====
! SOLUTION
!=====

/SOLU

SOLVE

FINISH

!=====
! POSTPROCESSING
!=====

```

```

/POST1

/DSCALE,,0

RSYS,SOLU          ! Layer coordinate system
LAYER,1

SHELL,MID         ! Middle of shell element
PLNSOL,U,X,1,1.0
PLNSOL,S,X,1,1.0  ! S1 for layer coord system

! Failure criteria
! FC and FCLIST commands can be used for any 2-D or 3-D structural
! solid element or any 3-D structural shell element

!=====
!=====

! NOTE: If you don't want the failure stress or strain to be checked in a
! particular direction, specify a large number in that direction
FC,1,S,XTEN, Xt
FC,1,S,XCMP, -Xc
FC,1,S,YTEN, Yt
FC,1,S,YCMP, -Yc
FC,1,S,ZTEN, 10e7      ! Z value set to a large number
FC,1,S,XY  , S12
FC,1,S,YZ  , S23
FC,1,S,XZ  , 10e7      ! XZ value set to a large number
FC,1,S,XYCP, 0
FC,1,S,YZCP, 0
FC,1,S,XZCP, 0
! FCLIST
!PRNSOL,S,FAIL      ! Maximum Stress, Tsai-Wu Strength Index, and inverse of
! Tsai-Wu Strength Ratio Index Failure Criteria

!PRNSOL,FAIL

!=====

! FAIL: Failure criteria. Components listed: Maximum of all failure criteria
! defined at current node (MAX), maximum strain (EMAX), maximum stress (SMAX),
! Tsai-Wu Strength Index (TWSI), inverse of Tsai-Wu Strength Ratio Index
! (TWSR), and any user-defined failure friteria (USR1 through USR6).

!PLNSOL,S,MAXF,0,1.0      ! Maximum Stress Failure Criteria
!PLNSOL,S,TWSI,0,1.0      ! Tsai-Wu Strength Index Failure Criterion
PLNSOL,S,TWSR,0,1.0      ! Inverse of Tsai-Wu Strength Ratio Index Failure
Criterion

*GET,Max_TWSR,PLNSOL,0,MAX ! Maximum value of item in last contour display

```

```

!=====
! FACTOR=UC=1/MAX(TWSR) --> FACTOR=UC=1/Max_TWSR
!=====

ALLSEL,ALL

NSLE,S,CORNER          ! Tensions are not calculated in the mid side nodes!
*GET,NMAX,NODE,,NUM,MAX ! max number of nodes

!=====

! TWSR: Inverse of Tsai-Wu strength ratio index failure criterion
Max_STWSR=0
N_Max_STWSR=0
I_node=0
*DO,II,1,NMAX
  !/go          ! To plot all do cycle
  I_node=NDNEXT(II-1)
  *GET,Max_STWSR_ini,NODE,I_node,S,TWSR
  *IF,Max_STWSR,LT,Max_STWSR_ini,THEN
    Max_STWSR=Max_STWSR_ini          ! Stores the minimum TWSR
    N_Max_STWSR=I_node              ! N_Min_STWSR stores the node for which TWSR is
                                   ! minimum
  *ENDIF
*ENDDO

*SET,Max_STWSR_xx,Max_STWSR
*SET,UC,1/Max_STWSR_xx
*SET,N_Max_STWSR_xx,N_Max_STWSR
*STAT,UC          ! Factor = unity check. Should be smaller than 1 (< 1)

```

Appendix H Design Rules

The current section presents the visual basic code developed in the Design Rules Excel spreadsheet, which is used to create a matrix of experiments required for a ply orientation exploration analyses.

A *Full Factorial* matrix of experiments needs to be created initially, then the design rules can be applied independently. As every time a design rule is applied certain number of experiments are deleted, and optional *Compress Rows* macro is also created in order to compress the experiments' matrix, which could be applied either after applying each design rule or at the end.

For more information about the input parameters in the spreadsheet, and a general description of the design rules refer to Section 7.1.8.1.

H.1 Design Rules – Visual Basic Code

H.1.1 Full Factorial

This code defines the full factorial matrix of experiments of n Design Variables with L levels (Levelsⁿ).

```
Sub Full_Factorial()

Dim NDV As Integer, NLevels As Integer
Dim NExp As Long

    NDV = Range("C5").Value           ' Number of DVs --> Number of plies
    NLevels = 4                       ' Number of levels: 0 45 -45 90
    NExp = NLevels ^ (Range("C5").Value) ' Nlevels**NDV --> Number of
                                        ' experiments l**n (levels**factors)

Dim V(4) As Integer                 ' 4=NLevels
    V(0) = 0
    V(1) = 45
    V(2) = -45
    V(3) = 90

Dim II As Integer
Dim JJ As Long
Dim KK As Long
Dim x As Integer, F_offs As Integer, C_offs As Integer
Dim F As Long

    F_offs = 22                       ' Row offset
    C_offs = 1                         ' Column offset
For II = 1 To NDV                     ' DVs-->columns
    F = 1                               ' F=Filas --> Row number
```

```

x = 0
For JJ = 1 To NLevels ^ II
For KK = 1 To NLevels ^ (NDV - II)
    Cells(F + F_offs, II + C_offs).Value = V(x)
    F = F + 1
Next KK
If x = NLevels Then
    x = 1
Else
    x = x + 1
End If
Next JJ
Next II
'
End Sub

```

Example

Table H-1 Matrix of experiments of 3 variables with 3 levels.

RUN	DV1	DV2	DV3
1	0	0	0
2	0	0	1
3	0	0	2
4	0	1	0
5	0	1	1
6	0	1	2
7	0	2	0
8	0	2	1
9	0	2	2
10	1	0	0
11	1	0	1
12	1	0	2
13	1	1	0
14	1	1	1
15	1	1	2
16	1	2	0
17	1	2	1
18	1	2	2
19	2	0	0
20	2	0	1
21	2	0	2
22	2	1	0
23	2	1	1
24	2	1	2
25	2	2	0
26	2	2	1
27	2	2	2

Considering that the number of experiments in a full factorial matrix, with n Design Variables and L levels, is:

$$L^n \quad \text{(H-1)}$$

and defining as “Block” a subdivision of a column containing the maximum number of equal levels per variable. The following relation is defined

$$\frac{\text{Number of Experiments}}{\text{Number of Experiments per Block}} = \text{Number of Blocks per Column}$$

$$\frac{l^n}{l^{n-i}} = l^i$$

In this example:

Number of Design Variables n=3

Number of Levels per variable = 3 → (0,1,2) (possible values that each DV can have)

Number of Experiments = Levels^{DVs} = Levels^{factors} = Levelsⁿ

→ Number of Experiments = 3³ = 27 Experiments

Number of experiments per block in each column (i) = Levelsⁿ⁻ⁱ

- 1st column → i=1 → Number of experiments per block in column 1 = 3³⁻¹ = 9
- 2nd column → i=2 → Number of experiments per block in column 2 = 3³⁻² = 3
- 3rd column → i=3 → Number of experiments per block in column 3 = 3³⁻³ = 1

Number of blocks in each column (i) = Levelsⁱ

- 1st column → i=1 → Number of blocks in column 1 = 3¹ = 3
- 2nd column → i=2 → Number of blocks in column 2 = 3² = 9
- 3rd column → i=3 → Number of blocks in column 3 = 3³ = 27

Simplified Pseudo-code:

```
DO II = 1 To NDV                ! DVs → columns
    Row = 1
    DO JJ = 1 To NLevelsii      ! Number of blocks per column
        DO KK = 1 To NLevels(NDV-II) ! Number of experiments per block (for
            ! each column)
                Cells(Row, II).Value = V(x)    ! Fill in each cell with the level value
            Row = Row + 1
        ENDDO
    ENDDO
ENDDO
```

H.1.2 Delete Empty Rows

This code enables to delete the empty rows, compressing the matrix of experiments.

```
Sub CompressRow()
'
' DeleteRow Macro
'
Dim LastRow As Long
Dim r As Long
Dim Counter As Long
Dim F_offs As Integer

F_offs = 22                ' Row offset
Application.ScreenUpdating = False
LastRow = ActiveSheet.UsedRange.Rows.Count + _
    ActiveSheet.UsedRange.Rows(1).Row - 1
For r = LastRow To (F_offs + 1) Step -1    ' Row = 7 --> data start
                                            ' from this row
If Application.WorksheetFunction.CountA(Rows(r)) = 0 Then
    Rows(r).Delete
    Counter = Counter + 1
End If
Next r
Application.ScreenUpdating = True
MsgBox Counter & " Empty rows were deleted."
'
```

```
End Sub
```

H.1.3 +/- 45 in Top and Bottom

The laminate should have +/- 45 degree plies at top and bottom.

```
Sub top_Bot()  
  
Dim NDV As Integer, NLevels As Integer, NExp As Long, F_offs As Integer  
  
    NDV = Range("C5").Value           ' Number of DVs --> Number of plies  
    NLevels = 4                       ' Number of levels: 0 45 -45 90  
    NExp = NLevels ^ (Range("C5").Value) ' Nlevels**NDV --> Number of  
                                        ' experiments l**n (levels**factors)  
    F_offs = 22                       ' Row offset  
  
Dim V(4) As Integer                   ' 4=NLevels  
    V(0) = 0  
    V(1) = 45  
    V(2) = -45  
    V(3) = 90  
  
Dim II As Long  
  
' If the first column (1st ply) is different from +/-45 → delete that column  
For II = 1 To NExp  
If Cells(II + F_offs, 2) = V(0) Then  
    Cells(II + F_offs, 2).EntireRow.ClearContents  
ElseIf Cells(II + F_offs, 2) = V(3) Then  
    Cells(II + F_offs, 2).EntireRow.ClearContents  
End If  
Next II  
'  
End Sub
```

Simplified Pseudo-Code:

```
DO II = 1 To NExp  
IF Cells(II,1) = 0 or Cells(II,1) = 90 THEN  
    Delete row  
ENDIF  
ENDDO
```

H.1.4 Ply Blocking

No more than 4 plies with the same orientation should be stacked together.

```
Sub PlyBlocking()

Dim NDV As Integer, NLevels As Integer, NExp As Long

    NDV = Range("C5").Value           ' Number of DVs --> Number of plies
    NLevels = 4                       ' Number of levels: 0 45 -45 90
    NExp = NLevels ^ (Range("C5").Value) ' Nlevels**NDV --> Number of
                                        ' experiments l**n (levels**factors)

Dim V(4) As Integer                 ' 4=NLevels
    V(0) = 0
    V(1) = 45
    V(2) = -45
    V(3) = 90

Dim II As Long
Dim JJ As Integer
Dim KK As Integer
Dim x As Integer, F As Integer, F_offs As Integer, C_offs As Integer
Dim n0 As Integer, n45 As Integer, n_45 As Integer, n90 As Integer

    F_offs = 22                       ' Row offset
    C_offs = 1                         ' Column offset
    ' For each experiment count the number of plies with the same orientation
    ' stacked together
For II = 1 To NExp
    n0 = 0
    n45 = 0
    n_45 = 0
    n90 = 0
For JJ = 1 To NDV
If Cells(II + F_offs, JJ + C_offs) = V(0) Then
    n0 = n0 + 1
ElseIf Cells(II + F_offs, JJ + C_offs) = V(1) Then
    n45 = n45 + 1
ElseIf Cells(II + F_offs, JJ + C_offs) = V(2) Then
    n_45 = n_45 + 1
ElseIf Cells(II + F_offs, JJ + C_offs) = V(3) Then
    n90 = n90 + 1
End If
Next JJ
    ' Delete the rows with more than 4 plies in the same orientation
If n0 > 4 Then
    Cells(II + F_offs, 2).EntireRow.ClearContents
ElseIf n45 > 4 Then
    Cells(II + F_offs, 2).EntireRow.ClearContents
ElseIf n_45 > 4 Then
    Cells(II + F_offs, 2).EntireRow.ClearContents
```

```

ElseIf n90 > 4 Then
    Cells(II + F_offs, 2).EntireRow.ClearContents
End If
Next II
'
End Sub

```

H.1.5 Mid Plane Ply Blocking

No more than 2 plies with the same orientation stacked together in the midplane (due to symmetry they are 4 in total).

```

Sub PlyBlocking_MidPlane()

Dim NDV As Integer, NLevels As Integer, NExp As Long

NDV = Range("C5").Value           ' Number of DVs --> Number of plies
NLevels = 4                       ' Number of levels: 0 45 -45 90
NExp = NLevels ^ (Range("C5").Value) ' Nlevels**NDV --> Number of
                                     ' experiments l*n (levels**factors)

Dim V(4) As Integer               ' 4=NLevels
V(0) = 0
V(1) = 45
V(2) = -45
V(3) = 90

Dim II As Long
Dim JJ As Integer
Dim KK As Integer
Dim x As Integer, F As Integer, F_offs As Integer, C_offs As Integer
Dim n0 As Integer, n45 As Integer, n_45 As Integer, n90 As Integer

F_offs = 22                       ' Row offset
C_offs = 1                         ' Column offset
' For each experiment count the number of plies with the same orientation
' stacked together in the 3 last rows (3 last plies of the half symmetry
' laminate)
For II = 1 To NExp
    n0 = 0
    n45 = 0
    n_45 = 0
    n90 = 0
    For JJ = NDV - 2 To NDV        ' loop in the last 3 rows (plies)
        If Cells(II + F_offs, JJ + C_offs) = V(0) Then
            n0 = n0 + 1
        ElseIf Cells(II + F_offs, JJ + C_offs) = V(1) Then
            n45 = n45 + 1
        ElseIf Cells(II + F_offs, JJ + C_offs) = V(2) Then
            n_45 = n_45 + 1
        '
    Next JJ
Next II

```

```

ElseIf Cells(II + F_offs, JJ + C_offs) = V(3) Then
    n90 = n90 + 1
End If
Next JJ
'Delete the rows with more than 3 plies in the same orientation at the
'end of the half symmetric laminate (6 plies in middle of the laminate)
If n0 = 3 Then
    Cells(II + F_offs, 2).EntireRow.ClearContents
ElseIf n45 = 3 Then
    Cells(II + F_offs, 2).EntireRow.ClearContents
ElseIf n_45 = 3 Then
    Cells(II + F_offs, 2).EntireRow.ClearContents
ElseIf n90 = 3 Then
    Cells(II + F_offs, 2).EntireRow.ClearContents
End If
Next II
'
End Sub

```

H.1.6 Ply Percentage

For aeronautical applications each orientation percentage within the laminate is normally defined as:

[0/+45/90] = [50/40/10]

For fibre at 0°

$$p_0^{min} \leq 50 \leq p_0^{max} \quad \rightarrow \quad 50 - \Delta \leq 50 \leq 50 + \Delta$$

For fibres at +/-45°

$$p_0^{min} \leq 40 \leq p_0^{max} \quad \rightarrow \quad 40 - \Delta \leq 40 \leq 40 + \Delta$$

For fibres at 90°

$$p_0^{min} \leq 10 \leq p_0^{max} \quad \rightarrow \quad 10 - \Delta \leq 10 \leq 10 + \Delta$$

It has been decided that:

$$\Delta = 10$$

```
Sub Ply_Percentage()
```

```
Dim NDV As Integer, NLevels As Integer, NExp As Long
```

```

NDV = Range("C5").Value           ' Number of DVs --> Number of plies
NLevels = 4                       ' Number of levels: 0 45 -45 90
NExp = NLevels ^ (Range("C5").Value) ' Nlevels**NDV --> Number of
                                     ' experiments l**n (levels**factors)

```

```

Dim V(4) As Integer      ' 4=NLevels
    V(0) = 0
    V(1) = 45
    V(2) = -45
    V(3) = 90

Dim II As Long
Dim JJ As Integer
Dim KK As Integer
Dim x As Integer, F As Integer, F_offs As Integer, C_offs As Integer
Dim n0 As Integer, n45 As Integer, n_45 As Integer, n90 As Integer
Dim Percent_0-Allow As Single, Percent_45-Allow As Single, Percent_90-Allow As
Single, Delta As Single
Dim Percent_0 As Single, Percent_45 As Single, Percent_90 As Single

' [0/45/90] --> [50/50/10]
Percent_0-Allow = Range("C8").Value
Percent_45-Allow = Range("D8").Value
Percent_90-Allow = Range("E8").Value
'Delta = Int((1 / NDV) * 100 - Percent_90-Allow) + 1
Delta = 10

F_offs = 22                ' Row offset
C_offs = 1                 ' Column offset

For II = 1 To NExp
    n0 = 0
    n45 = 0
    n_45 = 0
    n90 = 0
For JJ = 1 To NDV
If Cells(II + F_offs, JJ + C_offs) = V(0) Then
    n0 = n0 + 1
ElseIf Cells(II + F_offs, JJ + C_offs) = V(1) Then
    n45 = n45 + 1
ElseIf Cells(II + F_offs, JJ + C_offs) = V(2) Then
    n_45 = n_45 + 1
ElseIf Cells(II + F_offs, JJ + C_offs) = V(3) Then
    n90 = n90 + 1
End If
Next JJ
    Percent_0 = (n0 / NDV) * 100
    Percent_45 = ((n45 + n_45) / NDV) * 100
    Percent_90 = (n90 / NDV) * 100
' 25 <= Percent_0 <= 50
If (Percent_0 < 25) Or (Percent_0 > 50) Then
    Cells(II + F_offs, 2).EntireRow.ClearContents
' 25 <= Percent_45 <= 50
ElseIf (Percent_45 < 25) Or (Percent_45 > 50) Then
    Cells(II + F_offs, 2).EntireRow.ClearContents
' 25 <= Percent_90 <= 25

```

```

ElseIf (Percent_90 < 25) Or (Percent_90 > 25) Then
    Cells(II + F_offs, 2).EntireRow.ClearContents
End If
Next II
'
End Sub

```

H.1.7 Progressive Sequence

The angle difference between two consecutive plies should be no more than 45 degrees.

```

Sub ProgressiveSequence()

Dim NDV As Integer, NLevels As Integer, NExp As Long

NDV = Range("C5").Value           ' Number of DVs --> Number of plies
NLevels = 4                       ' Number of levels: 0 45 -45 90
NExp = NLevels ^ (Range("C5").Value) ' Nlevels**NDV --> Number of
                                     ' experiments l**n (levels**factors)

Dim V(4) As Integer                ' 4=NLevels
V(0) = 0
V(1) = 45
V(2) = -45
V(3) = 90

Dim II As Long
Dim JJ As Integer
Dim KK As Integer
Dim x As Integer, F As Integer, F_offs As Integer, C_offs As Integer

F_offs = 22                        ' Row offset
C_offs = 1                          ' Column offset
..'if the difference in angle between two consecutive plies is 90 → delete
..'the row
For II = 1 To NExp
For JJ = 2 To NDV
If Cells(II + F_offs, JJ + C_offs - 1) = V(0) And Cells(II + F_offs, JJ +
C_offs) = V(3) Then
    Cells(II + F_offs, 2).EntireRow.ClearContents
ElseIf Cells(II + F_offs, JJ + C_offs - 1) = V(3) And Cells(II + F_offs, JJ +
C_offs) = V(0) Then
    Cells(II + F_offs, 2).EntireRow.ClearContents
End If
Next JJ
Next II
'
End Sub

```

H.1.8 Balanced Laminate

The laminate should have the same number of positive and negative plies of the same orientation (+/- 45).

```
Sub Balanced()  
  
Dim NDV As Integer, NLevels As Integer, NExp As Long  
  
NDV = Range("C5").Value           ' Number of DVs --> Number of plies  
NLevels = 4                       ' Number of levels: 0 45 -45 90  
NExp = NLevels ^ (Range("C5").Value) ' Nlevels**NDV --> Number of  
                                     ' experiments l**n (levels**factors)  
  
Dim V(4) As Integer               ' 4=NLevels  
V(0) = 0  
V(1) = 45  
V(2) = -45  
V(3) = 90  
  
Dim II As Long  
Dim JJ As Integer  
Dim KK As Integer  
Dim x As Integer, F As Integer, F_offs As Integer, C_offs As Integer  
Dim n0 As Integer, n45 As Integer, n_45 As Integer, n90 As Integer  
  
F_offs = 22                       ' Row offset  
C_offs = 1                         ' Column offset  
For II = 1 To NExp  
    n45 = 0  
    n_45 = 0  
    For JJ = 1 To NDV  
        If Cells(II + F_offs, JJ + C_offs) = V(1) Then  
            n45 = n45 + 1  
        ElseIf Cells(II + F_offs, JJ + C_offs) = V(2) Then  
            n_45 = n_45 + 1  
        End If  
    Next JJ  
    ' delete the rows with unequal number of positive and negative 45 plies  
    If (n45 <> n_45) Then  
        Cells(II + F_offs, 2).EntireRow.ClearContents  
    End If  
Next II  
'  
End Sub
```

Appendix I Element Orientation

I.1 ANSYS parametric input file

02-Elem_Orient_3PB_SOLID191_15_Elems_TT_failure_edit.txt

```
FINISH
/CLEAR, NOSTART

/TITLE, 3 Points Bending - Quarter Symmetry (SOLID191 (Biax) - 15 layered
solid elements through thickness)

! All dimensions in m, kg, sec --> N, Pa

!=====
! PARAMETERS DEFINITION

! Laminate
Nplies=8! Number of plies per layer of elements (Biax)
tply=0.25e-3! Ply thickness
t_Brick=Nplies*tply ! Brick thickness
N_Brick=15          ! Number of bricks through thickness (15)
NpliesT=N_Brick*Nplies      ! Total number of plies (120)

! Biax configuration - ply orientation
Theta1=0
Theta2=90
Theta3=-45
Theta4=45
!====Symmetry====
Theta5=Theta4
Theta6=Theta3
Theta7=Theta2
Theta8=Theta1

! Element orientation
ThetaR1=0
ThetaR2=0
ThetaR3=0
ThetaR4=0
ThetaR5=0
ThetaR6=0
ThetaR7=0
ThetaR8=0
!====Mid-plane Symmetry====
ThetaR9=ThetaR7
ThetaR10=ThetaR6
ThetaR11=ThetaR5
```

```

ThetaR12=ThetaR4
ThetaR13=ThetaR3
ThetaR14=ThetaR2
ThetaR15=ThetaR1

! Dimensions
t=NpliesT*tply           ! 30 mm
LT=5*t                   ! (l) specimen length - 150 mm
L=4*t                    ! Outer span
b=5*t/6                  ! Width - 25 mm
R2=30e-3                 ! Support radius
R1=30e-3                 ! Pusher radius

Surf_edit=t
Surf_edit1=1e-3

! Strength (Pa)
Xt=1970e6                ! 1970 MPa
Xc=990e6                 ! 990 MPa
Yt=67e6                  ! 67 MPa
Yc=240e6                 ! 240 MPa
Zt=67e6                  ! 67 MPa
Zc=240e6                 ! 240 MPa
S12=62e6                 ! 62 MPa
S13=62e6                 ! 62 MPa
S23=62e6                 ! 62 MPa

! Load
F=43000/4                ! N (divided by 4 due to quarter symmetry)

!=====
! GEOMETRY GENERATION

/PREP7

! Create a longitudinal transverse section of the specimen
WPCSYS,,0
WPROTA,,90
CSWPLA,11,0

*DO,II,0,t-t_Brick,t_Brick! 15 rectangular areas
  RECTNG,0,LT/2,II-(t/2),II-(t/2)+t_Brick
*ENDDO

LSEL,S,LOC,X,,
LSEL,A,LOC,X,LT/2,
LESIZE,ALL,,1! 1 element through the thickness in each area

ALLSEL,ALL

VEXT,ALL,,,,,-b/2! Create the specimen extruding the transverse section

```

```

NUMMRG,KP

VPLOT

! Edit the volume (split in three volumes) to define contact regions
WPLANE,,Surf_edit/2,-Surf_edit1,-Surf_edit1-(t/2),(Surf_edit/2)+Surf_edit1,-
Surf_edit1,-Surf_edit1-(t/2),(Surf_edit/2),,-Surf_edit1-(t/2)
WPROTA,,,-90
VSBW,ALL
WPOFFS,,,-Surf_edit
VSBW,ALL

CSYS,0

! Create area components with the contact regions of the specimen
ASEL,S,LOC,X,0,Surf_edit/2
ASEL,R,LOC,Z,t/2
CM,CONTACT_SURFACE_Pusher,AREA

ASEL,S,LOC,X,2*Surf_edit,LT/2      !3*Surf_edit
ASEL,R,LOC,Z,-t/2
CMSEL,U,CONTACT_SURFACE_Pusher
CM,CONTACT_SURFACE_Right,AREA

ALLSEL,ALL
CM,Composite_Specimen,VOLU

! supports
WPLANE,,(L/2),,-R2-(t/2),(L/2)+1,,-R2-(t/2),(L/2),1,-R2-(t/2)
WPROTA,,,-90      ! Rotates the WP right hand rule:
                  ! WPROTA,THXY,THYZ,THZX (DV's)
CSYS,4      ! Activates the previously defined WP
            ! create the Right hand side cylinder
CYLIND,,R2,,b      ! Create the support as a cylinder

CMSEL,U,Composite_Specimen
CM,Right_Support,VOLU
ASEL,S,EXT
ASEL,U,LOC,Z,0
ASEL,U,LOC,Z,b
CM,TARGET_SURFACE_Right,AREA      ! Create area component of the support target

! pusher
WPOFFS,-L/2,-(R2+t+R1)
CYLIND,,R1,,b      ! Create the pusher as a cylinder

CMSEL,U,Right_Support
CM,Pusher,VOLU
ASEL,S,EXT
ASEL,U,LOC,Z,0
ASEL,U,LOC,Z,b
CM,TARGET_SURFACE_Pusher,AREA      ! Create area component of the pusher target

```

ALLSEL,ALL

CSYS,0

```
!=====
! ET & MATERIAL PROPERTIES DEFINITION

MP,EX,1,136E9           ! ORTHOTROPIC MATERIAL PROPERTIES
MP,EY,1,9.4E9
MP,EZ,1,6.58E9         ! EZ=EY ASSUMED
MP,GXY,1,3.1E9
MP,GYZ,1,3.1E9
MP,GXZ,1,3.1E9
MP,PRXY,1,0.3          ! MAJOR POISSONS RATIO
MP,PRYZ,1,0.3          ! MAJOR POISSONS RATIO
MP,PRXZ,1,0.3          ! MAJOR POISSONS RATIO

ET,1,SOLID191,,,,,,,,1 ! 20 NODE LAYERED SOLID

KEYOPT,1,2,0           ! Constant thickness layer input (100 layers)
KEYOPT,1,3,0           ! Use material properties as given
KEYOPT,1,5,3           ! Print results, including FC, at layer top and
                       ! bottom 4 integration points and averages
KEYOPT,1,8,1           ! Store data for all layers
KEYOPT,1,10,1          ! Print summary of all the FC

! ISIGHT doesn't recognize the Real Constants sets when defined this way
!*DO,II,1,N_Brick
! R,II,Nplies,1        ! Nplies=total number of plies;
                       ! Symmetric Stacking

! RMORE
! *DO,JJ,1,Nplies,2
!   RMORE,1,Theta%JJ%,tply,1,Theta%JJ+1%,tply
! *ENDDO
!*ENDDO

! Create the real constant sets with the laminate definition for all 15
! layers' of elements
R,1,Nplies,1           ! Nplies=total number of plies; Symmetric Stacking
RMORE
*DO,JJ,1,Nplies,2
  RMORE,1,Theta%JJ%,tply,1,Theta%JJ+1%,tply
*ENDDO

R,2,Nplies,1           ! Nplies=total number of plies; Symmetric Stacking
RMORE
*DO,JJ,1,Nplies,2
  RMORE,1,Theta%JJ%,tply,1,Theta%JJ+1%,tply
*ENDDO

R,3,Nplies,1           ! Nplies=total number of plies; Symmetric Stacking
```

```

RMORE
*DO,JJ,1,Nplies,2
  RMORE,1,Theta%JJ%,tply,1,Theta%JJ+1%,tply
*ENDDO

R,4,Nplies,1          ! Nplies=total number of plies; Symmetric Stacking
RMORE
*DO,JJ,1,Nplies,2
  RMORE,1,Theta%JJ%,tply,1,Theta%JJ+1%,tply
*ENDDO

R,5,Nplies,1          ! Nplies=total number of plies; Symmetric Stacking
RMORE
*DO,JJ,1,Nplies,2
  RMORE,1,Theta%JJ%,tply,1,Theta%JJ+1%,tply
*ENDDO

R,6,Nplies,1          ! Nplies=total number of plies; Symmetric Stacking
RMORE
*DO,JJ,1,Nplies,2
  RMORE,1,Theta%JJ%,tply,1,Theta%JJ+1%,tply
*ENDDO

R,7,Nplies,1          ! Nplies=total number of plies; Symmetric Stacking
RMORE
*DO,JJ,1,Nplies,2
  RMORE,1,Theta%JJ%,tply,1,Theta%JJ+1%,tply
*ENDDO

R,8,Nplies,1          ! Nplies=total number of plies; Symmetric Stacking
RMORE
*DO,JJ,1,Nplies,2
  RMORE,1,Theta%JJ%,tply,1,Theta%JJ+1%,tply
*ENDDO

R,9,Nplies,1          ! Nplies=total number of plies; Symmetric Stacking
RMORE
*DO,JJ,1,Nplies,2
  RMORE,1,Theta%JJ%,tply,1,Theta%JJ+1%,tply
*ENDDO

R,10,Nplies,1         ! Nplies=total number of plies; Symmetric Stacking
RMORE
*DO,JJ,1,Nplies,2
  RMORE,1,Theta%JJ%,tply,1,Theta%JJ+1%,tply
*ENDDO

R,11,Nplies,1         ! Nplies=total number of plies; Symmetric Stacking
RMORE
*DO,JJ,1,Nplies,2
  RMORE,1,Theta%JJ%,tply,1,Theta%JJ+1%,tply
*ENDDO

```

```

R,12,Nplies,1          ! Nplies=total number of plies; Symmetric Stacking
RMORE
*DO,JJ,1,Nplies,2
  RMORE,1,Theta%JJ%,tply,1,Theta%JJ+1%,tply
*ENDDO

R,13,Nplies,1          ! Nplies=total number of plies; Symmetric Stacking
RMORE
*DO,JJ,1,Nplies,2
  RMORE,1,Theta%JJ%,tply,1,Theta%JJ+1%,tply
*ENDDO

R,14,Nplies,1          ! Nplies=total number of plies; Symmetric Stacking
RMORE
*DO,JJ,1,Nplies,2
  RMORE,1,Theta%JJ%,tply,1,Theta%JJ+1%,tply
*ENDDO

R,15,Nplies,1          ! Nplies=total number of plies; Symmetric Stacking
RMORE
*DO,JJ,1,Nplies,2
  RMORE,1,Theta%JJ%,tply,1,Theta%JJ+1%,tply
*ENDDO

! Associate each real constant set with each volume (from bottom to top)
JJ=0
*DO,II,0,t-t_Brick,t_Brick
  !Real=1+JJ
  VSEL,S,LOC,X,0,LT/2
  VSEL,R,LOC,Z,II-(t/2),II-(t/2)+t_Brick
  VATT,1,JJ+1,1          ! VATT,MAT,REAL,TYPE,ESYS
  ALLSEL,ALL
  JJ=1+JJ
*ENDDO

/PNUM,REAL,1! Real constant set colors on volumes
VPLOT

ALLSEL,ALL

!=====
! MESH GENERATION

/ESHAPE,1              ! view layers comprising laminate
/VSCALE,,2            ! double size of symbols, like element CS
/PSYMB,ESYS,1        ! turn on element coordinate system symbols
/DEVICE,VECTOR,0     ! elements shown in render style

! Number of elements per line - Element size definition
! Length
LSEL,S,LINE,,282,311,29

```

```

LESIZE,ALL,,8

LSEL,S,LINE,,233
LESIZE,ALL,,4

! Width
LSEL,S,LOC,Y,b/4
LESIZE,ALL,,3

! Mesh specimen and re-orientate elements
! Element rotation (Real constants rotation)
JJ=12
*DO,II,1,N_Brick
  WPCSYS,0
  *IF,II,GT,1,THEN
    WPROTA,-ThetaR%II-1%
  *ENDIF
  WPROTA,ThetaR%II%
  CSWPLA,JJ,0
VSEL,S,REAL,,%II%
  VPLOT
  ESYS,JJ

  MSHKEY,1! Use mapped meshing
  !CMSEL,S,Composite_Specimen
  VMESH,ALL! Mesh specimen
  ESLV,S
  EORIENT,LYSL,NEGZ          ! SOLID191 elements - Reorientation
  EPLOT
  JJ=JJ+1
*ENDDO

ALLSEL,ALL
EPLOT

!LAYPLOT,1
!/GROPTS,VIEW,1

NUMMRG,NODE
NUMMRG,ELEM

!=====
! CONTACT PAIR 1 - BOTTOM SPECIMEN-RIGHT SUPPORT

MP,MU,2,0.1          ! MU= Coefficient of Friction (unitless)
R,16
ET,2,170            ! TARGE170 - 3D Target Segment
ET,3,174            ! CONTA174 - 3D 8-Node Surface-to-Surface Contact
KEYOPT,2,1,1        ! High order elements (used by AMESH and LMESH
                    ! commands only) <- VITAL for this analysis, otherwise ERROR!!!
KEYOPT,2,2,0        ! Automatically constrained by ANSYS
KEYOPT,3,2,0        ! Contact algorithm: Augmented Lagrangian (default)

```

```

KEYOPT,3,4,2      ! On nodal point - normal to target surface -->
                  ! for a rigid surface constraint
KEYOPT,3,5,1      ! Close gap with auto CNOF
KEYOPT,3,7,0      ! Element level time increment control: No control
KEYOPT,3,9,2      ! Include both initial geometrical penetration
                  ! or gap and offset, but with ramped effects
KEYOPT,3,10,0

! R1,R2,FKN,FTOLN,ICONT,PINB
! PMAX,PMIN,TAUMAX,CNOF,FKOP,FKT
! FKN=Normal penalty stiffness factor
RMODIF,16,3,0.1 ! FKN = Normal penalty stiffness factor
!RMODIF,16,5,4e-5 ! ICONT = Initial contact closure
RMODIF,16,10,0. ! CNOF = Contact surface offset
RMODIF,16,12,0. ! FKT = Tangent penalty stiffness factor

! Generate the target surface
CMSEL,S,TARGET_SURFACE_Right
MAT,2
REAL,16
TYPE,2
AMESH,ALL

ALLSEL,ALL
EPLLOT

! Generate the contact surface
CMSEL,S,CONTACT_SURFACE_Right
TYPE,3
NSLA,S,1
ESLN,S,0
ESURF

ALLSEL,ALL
EPLLOT

!=====
! CONTACT PAIR 2 - TOP SPECIMEN-PUSHER

MP,MU,4,0.1      ! MU= Coefficient of Friction (unitless)
R,17
ET,4,170         ! TARGE170 - 3D Target Segment
ET,5,174         ! CONTAL74 - 3D 8-Node Surface-to-Surface Contact
KEYOPT,4,1,1     ! High order elements (used by AMESH and LMESH
                  ! commands only) <-- VITAL for this analysis, otherwise ERROR!!!
KEYOPT,4,2,0     ! Automatically constrained by ANSYS
KEYOPT,5,2,0     ! Contact algorithm: Augmented Lagrangian (default)
KEYOPT,5,4,0     ! Location of contact detection point: On Gauss
                  ! point (for general cases)
KEYOPT,5,5,1     ! Close gap with auto CNOF
KEYOPT,5,7,0     ! Element level time increment control: No control
KEYOPT,5,9,2     ! Include both initial geometrical penetration or

```

```

! gap and offset, but with ramped effects
KEYOPT,5,10,0

! R1,R2,FKN,FTOLN,ICONT,PINB
! PMAX,PMIN,TAUMAX,CNOF,FKOP,FKT
! FKN=Normal penalty stiffness factor
RMODIF,17,3,0.1 ! FKN = Normal penalty stiffness factor
!RMODIF,17,5,3e-5! ICONT = Initial contact closure
RMODIF,17,10,0. ! CNOF = Contact surface offset
RMODIF,17,12,0. ! FKT = Tangent penalty stiffness factor

! Generate the target surface
CMSEL,S,TARGET_SURFACE_Pusher
MAT,4
REAL,17
TYPE,4
AMESH,ALL

ALLSEL,ALL
EPLLOT

! Create a pilot node
CSYS,0
K,, ,R1+(t/2)
*GET,KP_F,KP,0,NUM,MAXD
KMESH,KP_F ! ELIST to see the pilot node definition
*GET,Node_F,NODE,0,NUM,MAXD

! Generate the contact surface
CMSEL,S,CONTACT_SURFACE_Pusher
TYPE,5
NSLA,S,1
ESLN,S,0
ESURF

ALLSEL,ALL
EPLLOT

!=====
! BOUNDARY CONDITIONS

! Symmetry
ASEL,S,LOC,Y,0
ASEL,R,LOC,Z,-t/2,t/2
DA,ALL,UY! Translation in Y in specimen areas at Y=0

ASEL,S,LOC,X,0
ASEL,R,LOC,Z,-t/2,t/2
CMSEL,U,TARGET_SURFACE_Pusher
DA,ALL,UX! Translation in X in specimen areas at X=0

! Nodal load application

```

```

NSEL,S,NODE,,Node_F
F,ALL,FZ,-F

ALLSEL,ALL
EPLLOT

SBCTRAN! Transfers loads and BCs to FE model

!=====
! FC

TB,FAIL,1,1          ! TB, FAIL, material number, 1 temperature
TBTEMP,,CRIT
TBDATA,3,2          ! Include the inverse of the Tsai-Wu strength ratio
!TBDATA,2,1
TBTEMP,0
TBDATA,10,Xt,-Xc,Yt,-Yc,Zt,-Zc      ! stresses XT, XC, YT, YC, ZT, ZC
TBDATA,16,S12,S23,S13              ! shear stresses XY, YZ (large number),
                                   ! XZ (large number)
TBDATA,19,0,0,0                    ! coupling coefficients
!TBLIST,ALL,1                      ! Lists the data tables

OUTPR,NSOL,1
OUTPR,RSOL,1

FINISH

!=====
!=====
! SOLUTION
!=====
!=====

/SOLU

ANTYPE,0              ! Perform a static analysis
!NLGEOM,1            ! Includes large-deflection (large rotation)
                    ! effects or large strain effects, according to the element type
SOLC,ON,ON,INCP      ! Turn on solution control with ability to use
                    ! contact time prediction
EQSL,SPARSE,,,,,1
RESC,,NONE           ! Do not keep any restart files
CNTR,PRINT,1         ! print out contact info and also make no initial
                    ! contact an error
NLDIAG,CONT,ITER     ! print out contact info each equilibrium iteration
/NOPR
/GOPR
AUTOTS,ON            ! Use automatic time stepping

NSUBST,50,10000,10! NSUBST,NSBSTP,NSBMX,NSBMN
!TIME,10             ! maximum load applied
OUTRES,ERASE

```

```
OUTRES,ALL,ALL
SOLVE
```

```
FINISH
```

```
!=====
!=====
! POSTPROCESSING
!=====
!=====
```

```
/POST1
```

```
/DSCALE,,0
/GRAPHICS,FULL
```

```
!/EXPAND,4,POLAR,HALF,,90
!/REPLOT
```

```
ESEL,S,TYPE,,1
```

```
PLNSOL,U,Z,1
```

```
PLNSOL,S,Z,1
```

```
!=====
! Max total displacement (abs)
```

```
NSORT,U,SUM
*GET,USUM, SORT, ,MAX
*SET,USUM,USUM
*STAT,USUM
```

```
!=====
! Max Z displacement (abs)
```

```
NSORT,U,Z,,1
*GET,UZ_MAX, SORT, ,MAX
*SET,MaxUZ,UZ_MAX
*STAT,MaxUZ
```

```
!=====
!=====
```

```
RSYS,LSYS
!LAYER,8
!ESEL,S,REAL,,3,7 ! Assumption: the component is going
! to break in any of these plies!!!
```

```
NSORT,S,XZ
*GET,Node_Max_SXZ, SORT, ,IMAX
*SET,Node_Max_SXZ,Node_Max_SXZ
RSYS,0 ! Global Cartesian coordinate system (default)
```

```

*GET,X_Node_Max_SXZ,NODE,Node_Max_SXZ,LOC,X
*SET,X_Node_Max_SXZ,X_Node_Max_SXZ
!PRNSOL,S,COMP      ! ordered by descending SXZ

!=====
!=====

! for S13
*DO,II,1,N_Brick
  NSEL,S,LOC,X,X_Node_Max_SXZ
NSEL,R,LOC,Y,b/2
NSEL,R,LOC,Z,-t/2+(II*t_Brick)
  *GET,Node_Max_SXZ_Real%II%,NODE,,NUM,MAX

  ALLSEL,ALL
*ENDDO

ALLSEL,ALL

!=====
! Stress in layer coord system S13 (@ Max S13 values) - Nodal Results
!=====

RSYS,LSYS      ! Layer coordinate system

Max_S13=0
Max_S13_Ply=0
*DO,JJ,1,N_Brick,1      ! Real constant
  /GO

  ESEL,S,REAL,,JJ

  *DO,II,Nplies*(JJ-1)+1,Nplies*JJ,1      ! for all layers
    /GO
    *IF,JJ,EQ,1,THEN
      LAYER,II
    *ELSE
      LAYER,II-Nplies*(JJ-1)
    *ENDIF

    *GET,S13_%II%,NODE,Node_Max_SXZ_Real%JJ%,S,XZ      ! S13
    *SET,S13_%II%,S13_%II%

    *IF,Max_S13,LT,S13_%II%,THEN
      Max_S13=S13_%II%
      Max_S13_Ply=II
    *ENDIF

  *ENDDO

ALLSEL,ALL

```

```

*ENDDO

MaxAbs_S13=Max_S13
MaxAbs_S13_Ply=Max_S13_Ply
TT_Failure=Max_S13/40e6

ALLSEL,ALL

!=====
!=====
! FC
!=====
!=====

! NOTE: If you don't want the failure stress or strain to be checked
! in a particular direction, specify a large number in that direction
FC,1,S,XTEN, Xt
FC,1,S,XCMP, -Xc
FC,1,S,YTEN, Yt
FC,1,S,YCMP, -Yc
FC,1,S,ZTEN, Zt          ! Z value set to a large number
FC,1,S,ZCMP, -Zc
FC,1,S,XY  , S12
FC,1,S,YZ  , S23          ! YZ value set to a large number
FC,1,S,XZ  , S13          ! XZ value set to a large number
FC,1,S,XYCP, 0
FC,1,S,YZCP, 0
FC,1,S,XZCP, 0
!FCLIST

!=====
!=====
! FAIL: Failure criteria.

RSYS,LSYS
LAYER,FCMAX          ! Processes the layer with the largest
                    ! failure criteria (SHELL99, SOLID46, SOLID191)

!PRESOL,FCMX        ! Maximum FC over the entire element. Components:
! Layer number where the maximum occurs (LAY), name of the maximum FC,
! and value of the maximum FC (VAL)

ETABLE,ERASE
ETABLE,FCMAX,NMISC,1    ! FC values and maximum at each integration point
ETABLE,VALUE,NMISC,2   ! Maximum value for this criterion
ETABLE,LN,NMISC,3      ! Layer number where maximum occurs
ETABLE,ILMAX,NMISC,4   ! Maximum ILSS (occurs between LN1 and LN2)
ETABLE,LN1,NMISC,5     ! Layer numbers which define location ILMAX
ETABLE,LN2,NMISC,6     ! Layer numbers which define location ILMAX

!PRETAB,GRP1
!PRETAB,FCMAX          ! etc, with the rest of the output variables

```

```

!=====

*DO,II,1,N_Brick,1      ! Real constant
/GO

ESEL,S,REAL,,II

! FCMAX (MAX)
ESORT,ETAB,FCMAX      ! Sorts the element table
*GET,FCMAX,SORT,,MAX
*GET,E_FCMAX,SORT,,IMAX      ! Element number where maximum value occurs
*SET,FCMAX_R%II%,FCMAX
*SET,E_FCMAX_R%II%,E_FCMAX
*STAT,FCMAX_R%II%

! VALUE (MAX)
ESORT,ETAB,VALUE      ! Sorts the element table
*GET,VALUE,SORT,,MAX
*GET,E_VALUE,SORT,,IMAX      ! Element number where maximum value occurs
*SET,VALUE_R%II%,VALUE
*SET,E_VALUE_R%II%,E_VALUE
*STAT,VALUE_R%II%

! LN (MAX)
ESORT,ETAB,LN      ! Sorts the element table
*GET,LN,SORT,,MAX
*GET,E_LN,SORT,,IMAX      ! Element number where maximum value occurs
*SET,LN_R%II%,LN
*SET,E_LN_R%II%,E_LN
*STAT,LN_R%II%

ALLSEL,ALL

*ENDDO

!=====

!ILANG: Angle of interlaminar shear stress vector (measured from the
! element x-axis towards the element y-axis in degrees)
!ILSUM: Interlaminar shear stress vector sum

Failed_Plies_Count=0
Fp=0
*DO,JJ,1,N_Brick,1      ! Real constant
/GO

ESEL,S,REAL,,JJ

*DO,II,Nplies*(JJ-1)+1,Nplies*JJ,1      ! for all layers
/GO
*IF,JJ,EQ,1,THEN

```

```

        KK=II
        LAYER, KK
*ELSE
        KK=II-Nplies*(JJ-1)
        LAYER, KK
*ENDIF

ETABLE, ERASE
ETABLE, FCMAX_%II%, NMISC, (2*(Nplies+KK))+7
ETABLE, VALUE_%II%, NMISC, (2*(Nplies+KK))+8

! Maximum value and element where it occurs

ESORT, ETAB, FCMAX_%II%           ! Sorts the element table
*GET, FCMAX_%II%_MAX, SORT, , MAX
*GET, E_FCMAX_%II%_MAX, SORT, , IMAX           ! Element number where
                                                ! maximum value occurs

*SET, FCMAX_%II%_MAX, FCMAX_%II%_MAX
*SET, E_FCMAX_%II%_MAX, E_FCMAX_%II%_MAX
*STAT, FCMAX_%II%_MAX

ESORT, ETAB, VALUE_%II%           ! Sorts the element table
*GET, VALUE_%II%_MAX, SORT, , MAX
*GET, E_VALUE_%II%_MAX, SORT, , IMAX           ! Element number where
                                                ! maximum value occurs

*SET, VALUE_%II%_MAX, VALUE_%II%_MAX
*SET, E_VALUE_%II%_MAX, E_VALUE_%II%_MAX
*STAT, VALUE_%II%_MAX

*IF, VALUE_%II%_MAX, GT, 1, THEN
    Failed_Plies_Count=Failed_Plies_Count+1
    Fp=Fp+VALUE_%II%_MAX
    !Fp=Fp+1.5** (3*(VALUE_%II%_MAX-1.5))
*ENDIF

*ENDDO

ALLSEL, ALL

*ENDDO

Failed_Plies=Failed_Plies_Count
*IF, Failed_Plies, GT, 1, THEN
    FAIL_Index=Fp/Failed_Plies           ! mean
*ELSE
    FAIL_Index=0
*ENDIF

save

```

Appendix J ANSYS Layered element formulation

Source: All information presented in this section has been directly taken from the ANSYS help manual. However, few modifications have been done in order to have a consistent naming convention with the rest of the document.

J.1 SHELL99 – Linear layered structural shell

Source: ANSYS help manual.

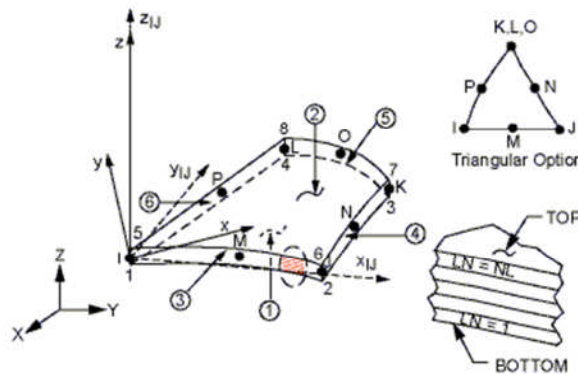


Figure J-1 SHELL99 geometry. Source: ANSYS help manual.

Table J-1 Number of integration points

<i>Matrix</i>	<i>Geometry</i>	<i>Integration points</i>
Stiffness matrix	Quad	In-plane: 2 x 2 Thru-the thickness: 2

Assumptions and restrictions

Normals to the centreplane are assumed to remain straight after deformation, but not necessarily normal to the centreplane.

Each pair of integration points (in the r direction) is assumed to have the same material orientation.

There is no significant stiffness associated with rotation about the element r axis. A nominal value of stiffness is present, however, to prevent free rotation at the node.

Stress-Strain Relationship (same as for SHELL91)

The compliance matrix $[S]_j$ for the layer j is:

$$[S]_j = \begin{bmatrix} BE_{x,j} & B\nu_{xy,j}E_{x,j} & 0 & 0 & 0 & 0 \\ B\nu_{xy,j}E_{x,j} & BE_{y,j} & 0 & 0 & 0 & 0 \\ 0 & 0 & 0 & 0 & 0 & 0 \\ 0 & 0 & 0 & \frac{G_{yz,j}}{f} & 0 & 0 \\ 0 & 0 & 0 & 0 & \frac{G_{xz,j}}{f} & 0 \\ 0 & 0 & 0 & 0 & 0 & G_{xy,j} \end{bmatrix} \quad \text{(J-1)}$$

where:

$$B = \frac{E_{y,j}}{E_{y,j} - (\nu_{xy,j})^2 E_{x,j}}$$

$E_{x,j}$ = Young's modulus in layer x directions of layer j (input as EX on MP command)

$\nu_{xy,j}$ = Poisson's ration in layer x-y plane of layer j (input as NUXY on MP command)

$G_{xy,j}$ = shear modulus in layer x-y plane of layer j (input as GXY on MP command)

$$f = \left\{ \begin{array}{l} 1.2 \\ 1.0 + 0.2 \frac{A}{25t^2} \end{array} \right\}, \text{ whichever is greater}$$

A = element area (in s-t plane)

t = average total thickness

The above definition of f is designed to avoid shear locking. Unlike most other elements, the temperature-dependent material properties are evaluated at each of the in-plane integration points, rather than only at the centroid.

r = normal coordinate, varying from -1.0 (bottom) to +1.0 (top)

The direct input matrix equations (valid for SHELL99 and SOLID46) are not presented as they were not used in the thesis.

J.2 SOLID46 – 3D 8–Node layered structural solid

Source: ANSYS help manual

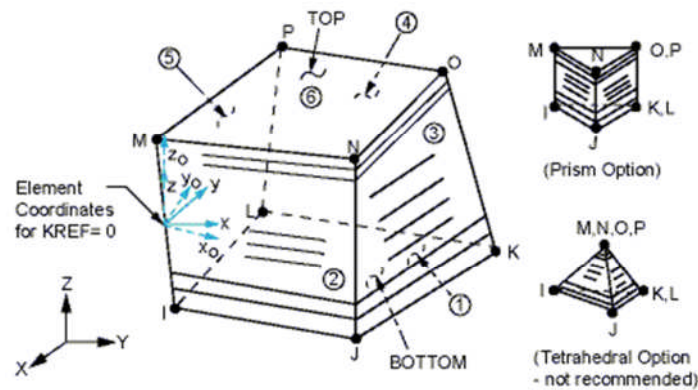


Figure J-2 SOLID46 geometry. Source: ANSYS help manual.

x₀ = Element x-axis if ESYS is not supplied.

x = Element x-axis if ESYS is supplied.

Table J-2 Number of integration points

<i>Matrix</i>	<i>Integration points</i>
Stiffness matrix	2 x 2 x 2

Assumptions and Restrictions

The numerical integration scheme for the thru-thickness effects are identical to that used in SHELL99. This may yield a slight numerical inaccuracy for elements having a significant change of size of layer area in the thru-thickness direction (Figure J-3). The main reason for such discrepancy stems from the approximation of the variation of the determinant of the Jacobian in the thru-thickness direction. The error is usually insignificant. However, users may want to try a patch-test problem to assess accuracy for their particular circumstances.

Unlike shell elements, SOLID46 cannot assume a zero transverse shear stiffness at the top and bottom surfaces of the element. Hence the interlaminar shear stress must be computed without using this assumption, which leads to relatively constant values thru the element.

Offset Geometry

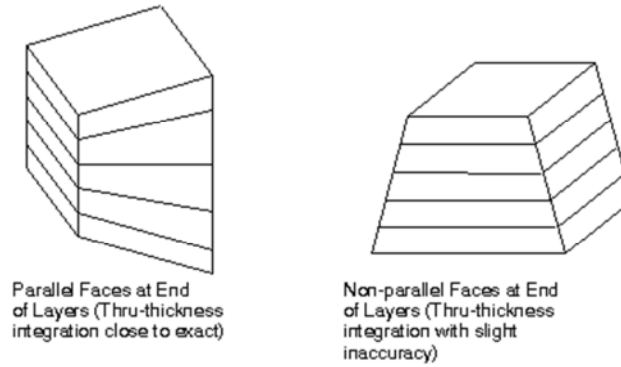


Figure J-3 Level of through thickness integration accuracy based on the element shape. Source: ANSYS help manual.

Stress-strain relationships

For layer j, the strain-stress relationships in the layer coordinate system are

$$\begin{Bmatrix} \epsilon_x \\ \epsilon_y \\ \epsilon_z \\ \gamma_{yz} \\ \gamma_{xz} \\ \gamma_{xy} \end{Bmatrix} = \begin{Bmatrix} \alpha_{x,j}\Delta T \\ \alpha_{y,j}\Delta T \\ \alpha_{z,j}\Delta T \\ 0 \\ 0 \\ 0 \end{Bmatrix} + \begin{bmatrix} \frac{1}{E_{x,j}} & \frac{-\nu_{xy,j}}{E_{y,j}} & \frac{-\nu_{xz,j}}{E_{z,j}} & 0 & 0 & 0 \\ \frac{-\nu_{xy,j}}{E_{y,j}} & \frac{1}{E_{y,j}} & \frac{-\nu_{yz,j}}{E_{z,j}} & 0 & 0 & 0 \\ \frac{-\nu_{xz,j}}{E_{z,j}} & \frac{-\nu_{yz,j}}{E_{z,j}} & \frac{1}{E_{z,j}} & 0 & 0 & 0 \\ 0 & 0 & 0 & \frac{1}{G_{yz,j}} & 0 & 0 \\ 0 & 0 & 0 & 0 & \frac{1}{G_{xz,j}} & 0 \\ 0 & 0 & 0 & 0 & 0 & \frac{1}{G_{xy,j}} \end{bmatrix} \begin{Bmatrix} \sigma_x \\ \sigma_y \\ \sigma_z \\ \tau_{yz} \\ \tau_{xz} \\ \tau_{xy} \end{Bmatrix} \quad (\text{J-2})$$

*Note: The thermal terms are not considered in this thesis.

where:

$\alpha_{x,j}$ = coefficient of thermal expansion of layer j in the layer x-direction (input as ALPX on MP command)

$E_{x,j}$ = Young's modulus of layer j in the layer x -direction (input as EX on MP command)

$G_{xy,j}$ = shear modulus of layer j in layer x - y plane (input as GXY on MP command)

$\nu_{xy,j}$ = Poisson's ratio of layer j in x - y plane (input as NUXY on MP command)

SOLID191 - 3D 20-Node Layered Structural Solid includes the description of the effective material properties and the interlaminar shear stress calculation which also applies to SOLID46.

J.3 SOLID191 – 3D 20–Node layered structural solid

Source: ANSYS help manual

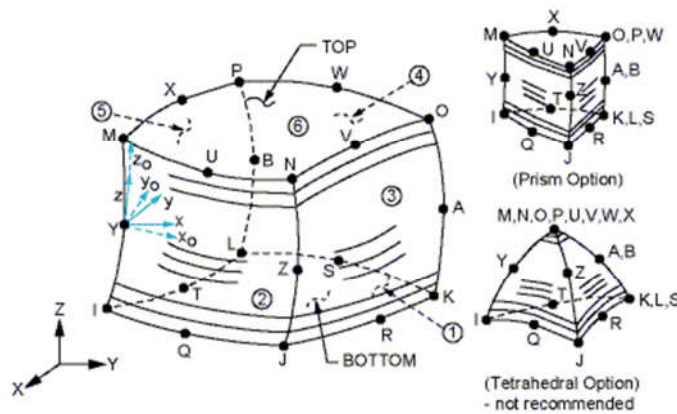


Figure J-4 SOLID191 geometry. Source: ANSYS help manual.

x_0 = Element x -axis if ESYS is not supplied.

x = Element x -axis if ESYS is supplied.

Table J-3 Number of integration points

<i>Matrix</i>	<i>Geometry</i>	<i>Integration points</i>
Stiffness matrix	Brick	In-plane: 2 x 2 Thru-the thickness: 3 for each layer

The use of effective (“eff”) material properties developed below is based on heuristic arguments and numerical experiences rather than on a rigorous theoretical formulation.

The fundamental difficulty is that multilinear displacement fields are attempted to be modelled by a linear (or perhaps quadratic) displacement shape function since the number of DOF per element must be kept to a minimum. A more rigorous solution can always be obtained by using more elements in the thru-the-layer direction. Numerical experimentation across a variety of problems indicates that the techniques used with SOLID46 give reasonable answers in most cases.

To help ensure continuity of stresses between the layers, Eq (J-2) is modified to yield:

$$\begin{Bmatrix} \epsilon_x \\ \epsilon_y \\ \epsilon_z \\ \gamma_{yz} \\ \gamma_{xz} \\ \gamma_{xy} \end{Bmatrix} = \begin{Bmatrix} \alpha_{x,j} \Delta T \\ \alpha_{y,j} \Delta T \\ \alpha_{z,j}^{eff} \Delta T \\ 0 \\ 0 \\ 0 \end{Bmatrix} + \begin{bmatrix} \frac{1}{E_{x,j}} & \frac{-\nu_{xy,j}}{E_{y,j}} & \frac{-\nu_{xz,j}^{eff}}{E_z^{eff}} & 0 & 0 & 0 \\ \frac{-\nu_{xy,j}}{E_{y,j}} & \frac{1}{E_{y,j}} & \frac{-\nu_{yz,j}^{eff}}{E_z^{eff}} & 0 & 0 & 0 \\ \frac{-\nu_{xz,j}^{eff}}{E_z^{eff}} & \frac{-\nu_{yz,j}^{eff}}{E_z^{eff}} & \frac{1}{E_z^{eff}} & 0 & 0 & 0 \\ 0 & 0 & 0 & D_{11,j}^G & D_{21,j}^G & 0 \\ 0 & 0 & 0 & D_{12,j}^G & D_{22,j}^G & 0 \\ 0 & 0 & 0 & 0 & 0 & \frac{1}{G_{xy,j}} \end{bmatrix} \begin{Bmatrix} \sigma_x \\ \sigma_y \\ \sigma_z \\ \tau_{yz} \\ \tau_{xz} \\ \tau_{xy} \end{Bmatrix} \quad (\text{J-3})$$

*Note: The thermal terms are not considered in this thesis.

where:

$$\alpha_{z,j}^{eff} = \frac{\sum_{j=1}^{N_l} t_j \alpha_{z,j}}{t_{TOT}} \quad (\text{Presumes temperatures are fairly uniform within element}) \quad (\text{J-4})$$

$$v_{xz,j}^{eff} = \begin{cases} C & \text{if } C < 0.45 \\ \text{or} & \\ v_{xz,j} & \text{if } C \geq 0.45 \end{cases} \quad (\text{J-5})$$

$$C = v_{xz,j} \frac{E_z^{eff}}{E_{z,j}} \quad (\text{J-6})$$

$$E_z^{eff} = \frac{t_{TOT}}{\sum_{j=1}^{N_l} \frac{t_j}{E_{z,j}}} \quad (\text{J-7})$$

$$[D^G]_j = \begin{bmatrix} D_{11,j}^G & D_{21,j}^G \\ D_{12,j}^G & D_{22,j}^G \end{bmatrix} = ([T]_j^{-1})^T [d^G] [T]_j^{-1} \quad (\text{J-8})$$

= effective inverted shear moduli in layer system

$$[d^G] = \frac{1}{t_{TOT}} \sum_{j=1}^{N_l} t_j [A_l]_j^{-1} = \text{effective inverted shear moduli in element system} \quad (\text{J-9})$$

$$[A_l]_j = [T]_j^T [D_z]_j [T]_j \quad (\text{J-10})$$

$$[T]_j = \text{transformation matrix to convert from layer to element system} \quad (\text{J-11})$$

$$[D_z]_j = \begin{bmatrix} G_{yz,j} & 0 \\ 0 & G_{xz,j} \end{bmatrix} \quad (\text{J-12})$$

t_j = average thickness of layer j

t_{TOT} = average total thickness of element

N_l = number of layers

General Strain and Stress Calculations

The following steps are used to compute strains and stresses at a typical point within layer j:

1. The strain vector $(\epsilon_x \quad \epsilon_y \quad \epsilon_z \quad \gamma_{yz} \quad \gamma_{xz} \quad \gamma_{xy})$ is determined from the displacements and the strain-displacement relationships, evaluated at the point of interest.
2. The strains are converted from element to layer coordinates.
3. The strains are adjusted for thermal effects, with the effective coefficient of thermal expansion in the z-direction being:

$$\alpha_z^{eff} = \frac{\sum_{j=1}^{N_i} t_j \alpha_{z,j}}{t_{TOT}} \quad (\text{J-13})$$

4. The normal strain is then adjusted with.

$$\epsilon'_z = \epsilon_z \frac{E_z^{eff}}{E_{z,j}} \quad (\text{J-14})$$

5. The transverse shear strains are computed by way of the stresses all in the layer coordinate system.

$$\begin{Bmatrix} \sigma_{yz} \\ \sigma_{xz} \end{Bmatrix} = \{D^G\}^{-1} \begin{Bmatrix} \epsilon_{yz} \\ \epsilon_{xz} \end{Bmatrix} \quad (\text{J-15})$$

where:

$\epsilon_{yz}, \epsilon_{xz} =$ shear strains based on strain – displacement relationships

Then,

$$\epsilon'_{yz,j} = \sigma_{yz} / G_{yz,j} \quad (\text{J-16})$$

$$\epsilon'_{xz,j} = \sigma_{xz} / G_{xz,j} \quad (\text{J-17})$$

Where:

$\epsilon'_{yz}, \epsilon'_{xz} =$ shear strains based on continuity of shearing stresses

6. Finally, the strains are converted to stresses by the usual relationship:

$$[\sigma]_j = [S]_j (\{\epsilon\}_j - \{\epsilon^{th}\}_j) \quad (\text{J-18})$$

Where:

$[S]_j$ = compliance matrix used in Eq (J-2).

7. If the element has more than one layer and any layer has $v_{xz,j}^{eff}$ or $v_{yz,j}^{eff}$ exceeding 0.45, the normal stresses are computed based on nodal forces.

Interlaminar Shear Stress Calculation

It may be seen that the interlaminar shear stress will, in general, not be zero at a free surface. This is because the element has no knowledge as to whether or not the top or bottom face is a free surface or if there is another element attached to that face.

There are two methods of calculating interlaminar shear stress: by nodal forces and by evaluating stresses layer-by-layer.

Nodal Forces

The shear stresses over the entire volume are computed to be:

$$\sigma_{xz} = \frac{1}{4} \left[\frac{F_M^x - F_I^x}{A^{I-M}} + \frac{F_N^x - F_J^x}{A^{J-N}} + \frac{F_O^x - F_K^x}{A^{K-O}} + \frac{F_P^x - F_L^x}{A^{L-P}} \right] \quad (\text{J-19})$$

$$\sigma_{yz} = \frac{1}{4} \left[\frac{F_M^y - F_I^y}{A^{I-M}} + \frac{F_N^y - F_J^y}{A^{J-N}} + \frac{F_O^y - F_K^y}{A^{K-O}} + \frac{F_P^y - F_L^y}{A^{L-P}} \right] \quad (\text{J-20})$$

where:

σ_{xz}, σ_{yz} = average transverse shear stress components

F_I^x, F_I^y, etc = forces at node I (etc) parallel to reference plane, with x being parallel to element x direction

A^{I-M}, etc = tributary area for node (evaluated by using the determinant of the Jacobian at the nearest integration point in base plane)

Evaluating Stresses Layer-by-Layer

This option is available only if KEYOPT(2) = 0 or 1 and simply uses the layer shear stresses for the interlaminar stresses. Thus, the interlaminar shear stresses in the element x direction are:

$$\sigma_{xz}^1 = \sigma_{xz} \text{ at bottom of layer I (plane I-J-K-L)}$$

$$\sigma_{xz}^{N_l+1} = \sigma_{xz} \text{ at top of layer NL (plane M-N-O-P)}$$

$$\sigma_{xz}^j = \frac{1}{2}(\sigma_{xz} \text{ at top of layer } j - 1 + \sigma_{xz} \text{ at bottom of layer } j) \text{ where } i < j < N_l$$

The σ_{xz} terms are the shear stresses computed from Eq (J-18), except that the stresses have been converted to element coordinates. The interlaminar shear stresses in the element y-direction are analogous. The components are combined as:

$$\sigma_{il} = \sqrt{(\sigma_{xz})^2 + (\sigma_{yz})^2} \tag{J-21}$$

and the largest value of σ_{il} is output as the maximum interlaminar shear stress.

J.4 SOLID186 – 3D 20–Node layered structural solid

Source: ANSYS help manual

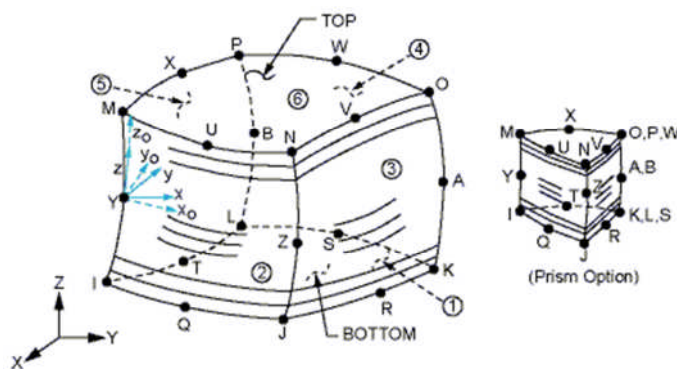


Figure J-5 SOLID186 geometry. Source: ANSYS help manual.

Table J-4 Number of integration points

<i>Matrix</i>	<i>Geometry</i>	<i>Integration points</i>
Stiffness matrix	Brick	In-plane: 2 x 2 Thru-the thickness: <ul style="list-style-type: none">- 2 if no shell section defined (SECxxx)- 1,3,5,7, or 9 per layer if a shell section is defined (SECxxx)
